

THE SECOND
100
IUGS GEOLOGICAL
HERITAGE SITES

“An IUGS Geological Heritage Site is a key place with extraordinary geological elements or processes of the highest scientific relevance, used as a global reference, and/or with a substantial contribution to the development of geological sciences through history.”

First Published in Spain, July 2024

EDITED & PUBLISHED BY IUGS
(International Union of
Geological Sciences)
EMAIL iugs.globalgeosites@igme.es

ISBN: 979-8-218-45558-3
D.L.: LG D 618-2024

DESIGN & LAYOUT BY DOSGES
www.dosges.com

IUGS, Zumaia 2021

INTRODUCTIONS	10	
1 HISTORY OF GEOSCIENCES	16	
101 Arduino's lithostratigraphical sequence of the Agno Valley	22	
102 Cavansham Ferry and Llanstephan Quarries	24	
103 Jurassic Coast: Lyme Regis	26	
104 Metamorphic Barrow Zones in Scottish Highlands	28	
105 Contact metamorphic rocks of Orijärvi	30	
106 Durbuy Anticline	32	
107 Vesuvius volcano	34	
108 Scheibenberg lava flow	36	
109 Montagne Pelée volcano	38	
110 Oligocene Laccoliths and Sedimentary Rock Domes of the Henry Mountains	40	
111 Maruia Falls	42	
112 Mer de Glace	44	
113 Esmark Moraine and Otto Tank's Moraine	46	
114 The Parallel Roads of Glen Roy	48	
2 STRATIGRAPHY AND SEDIMENTOLOGY	50	
115 The Mesoproterozoic Belt-Purcell Supergroup	56	
116 The Ordovician section of the Hällekis Quarry	58	
117 The Ordovician glacial pavements of the Tassili n'Ajjer	60	
118 Carboniferous evolution of The Burren and Cliffs of Moher	62	
119 Permian reef complex of the Guadalupe Mountains	64	
120 Latemar Triassic carbonate platform	66	
121 End-Triassic Flood Basalts at the Old Wife	68	
122 The Jurassic Navajo Sandstone at Coyote Buttes and The Wave	70	
123 The Oligocene-Miocene molassic and rock pinnacles of Meteora	72	
124 Pliocene cyclostratigraphy of Scala dei Turchi	74	
3 PALEONTOLOGY	90	
132 Ediacaran fauna of the Nama Group	96	
133 The Late Devonian fossil-fish Lagerstätte of Miguasha	98	
134 Permian vegetation of the Wuda Fossil Site	100	
135 Triassic Dinosaurs and mammalian reptiles from Ischigualasto	102	
136 Middle Jurassic dinosaur footprints from the Serras de Aire and Candeeiros	104	
137 Dashanpu Middle Jurassic Dinosaur Fossils Site	106	
138 Upper Jurassic Carnegie Quarry Dinosaur Bone Site	108	
139 Early Cretaceous wetland of Las Hoyas	110	
140 Cretaceous Lagerstätten of Cariri Stone	112	
141 The Cretaceous Dinosaur Nesting Grounds of the Willow Creek Anticline	114	
142 Whale Valley, Cetacea and Sirenia Eocene fossils of Wadi Al-Hita	116	
143 The La Venta middle Miocene neotropical biome	118	
144 The modern human fossils of the Kibish Formation	120	
145 The Human Footprints of Acahuainca	122	
4 IGNEOUS AND METAMORPHIC PETROLOGY	124	
146 The larvikite plutonic rocks of the Oslo Rift	130	
147 The Rum Igneous Complex	132	
148 Devils Tower	134	
5 VOLCANOLOGY	146	
154 Deccan Traps	152	
155 Muriwai megapillow lava flows	154	
156 The Pleistocene Al Wahbah dry maar crater	156	
157 El Laco iron lavas	158	
158 Ngorongoro Crater	160	
159 Ruapehu Volcano	162	
160 Parícutin Volcano	164	
161 Heisei Shinzan Lava Dome	166	
162 The Active Hunga Volcano	168	
163 Rotorua's geothermal fields (Ahi-Tupua)	170	
6 TECTONICS	172	
164 The Mid-Atlantic ridge on Reykjanes	178	
165 The evolution of the Andes in Colca Canyon	180	
166 Salt domes and glaciers of the Zagros Fold and Thrust Belt	182	
167 The Patos Shear Zone	184	
168 Esla Unit thrust system	186	
169 Glarus Thrust	188	
170 Monte Perdido massif tectonic structure	190	
171 Brittle structures of the Somerset Coast	192	
172 Surface faulting of a seismic sequence in Mt. Vettore	194	
173 Alpine superposed buckle folds in Aliaga	196	
174 Marine terraces of San Juan de Marcona	198	
7 MINERALOGY	200	
175 The Sar-e-Sang Lapis Lazuli Deposit	206	
176 The Kalahari Manganese Field	208	
177 The Broken Hill Pb-Zn-Ag deposit	210	
178 Mineral site of Mont Saint-Hilaire	212	
179 The Muzo emerald deposit	214	
8 GEOMORPHOLOGY AND ACTIVE GEOLOGICAL PROCESSES	216	
180 Granite landforms of Dartmoor	222	
181 Inverted landscape of a Plio-Pleistocene phreatomagmatic monogenetic volcanic field in the Bakony-Balaton Upland	224	
182 Great Salt Lake	226	
183 Mackenzie Delta	228	
184 Getbol Tidal Flats	230	
185 Fontaine de Vaucluse	232	
186 Wakulla spring	234	
187 Vrelo Bune Spring	236	
188 Mammoth Cave	238	
189 The White Limestone Karst of Cockpit Country	240	
190 Guilin Karst	242	
191 Ha Long Bay-Cat Ba Archipelago	244	
192 Tepuis and quartzite karst of Gran Sabana	246	
193 Fjords and towering sea cliffs of Fiordland	248	
194 Fjords and glaciers in Hornsund and Van Mijenfjorden, Svalbard	250	
195 Vatnajökull	252	
196 Yosemite Valley	254	
9 IMPACT STRUCTURES AND EXTRATERRESTRIAL ROCKS	256	
197 Vredefort Dome	262	
198 Ries Crater	264	
199 Lake Bosumtwi Impact Crater	266	
200 The Barringer Meteorite Crater	268	
REFERENCES AND AUTHORS	270	

Credits

THE SECOND 100 IUGS GEOLOGICAL HERITAGE SITES has been developed as a collaborative endeavor among multiple international organizations and national representatives.

IGCP 731 (2021 – 2024)

THE SECOND 100 IUGS GEOLOGICAL HERITAGE SITES PARTICIPANTS

IUGS COORDINATION

Asier Hilario. Chair, IUGS – International Commission on Geoheritage (IUGS-ICG)

Gonzalo Lozano. Secretariat

Stanley Finney. Secretary General, IUGS

Benjamin Van Wyk de Vries. Chair, IUGS Subcommission on Sites

Juana Vegas. Secretary General, IUGS-ICG

Jianping Zhang. Vice-chair, IUGS-ICG

THE SECOND 100 BOOK EDITORS

Gonzalo Lozano. Geological and Mining Institute of Spain (IGME, CSIC)

Luis Carcavilla. Geological and Mining Institute of Spain (IGME, CSIC)

Stanley Finney. IUGS secretary General. USA

Asier Hilario. Basque Coast UNESCO Global Geopark. Spain.

Juana Vegas. Geological and Mining Institute of Spain (IGME, CSIC)

Benjamin Van Wyk de Vries. Université Clermont Auvergne. France

Jianping Zhang. China University of Geosciences. China

EVALUATORS

Aaron Cavesie. Australia

Adele Bertini. Italy

Alexandru Szakacs. Romania

Alireza Amirkazemi. Iran

Andreas Massanek. Germany

Artur Sá. Portugal

Asfawossen Asrat. Ethiopia

Augusto S. Auler. Brazil

Avi Burg. Israel

Batzl Fischer. United Kingdom

Benjamin Tobin. USA

Benjamin Van Wik de Bries. France

Boris Chako Tchamabe. Mexico

Catherine Mottram. United Kingdom

Christian Chopin. France

Christian Koeberl. Austria

Daniel Aríztegui. Switzerland

Daniel Ballesteros. Spain

David Baratoux. France

David Harper. United Kingdom

David Mogk. USA

Eamon N. Doyle. Ireland

Eiji Ohtani. Japan

Enrique Castellanos. Cuba

Enrique Díaz-Martínez. Spain

Enrique Gómez-Rivas. Spain

Esperanza Fernández. Spain

Ezio Vaccari. Italy

Freya R. George. United Kingdom

Gonzalo D. Veiga. Argentina

Gregory A. Good. USA

Hans-Peter Schertl. Germany

Heather Handley. Netherlands

Hugo Murcia. Colombia

Ilaria Mazzini. Italy

Isabelle Rouget. France

James Crampton. New Zealand

James Day. USA

Jan Urban. Poland

JIN Xiaoichi. China

Joan Martí. Spain

Joana Sanchez. Brazil

José Brilha. Portugal

Juana Vegas. Spain

Karoly Nemeth. Hungary

Khadija El Hariri. Morocco

Kirstin Lemon. United Kingdom

Laia Alegret. Spain

Lars Erikstad. Norway

Laura Giambiagi. Argentina

Lorenzo Gemignani. Italy

Luis Alcalá Martínez. Spain

Luis M. Chiappe. Argentina

Marcela Gómez Pérez. Colombia

Margaret Brocx. Australia

Marissa Betts. Australia

Markus Fiebig. Austria

Martina Kölbl-Ebert. Germany

Mauro Soldati. Italy

Michele Lustriño. Italy

Min ZHU. China

Mónica Sousa. Portugal

Natalia Pardo. Colombia

Nizamettin Kazanci. Turkey

Owen Weller-Gibbs. United Kingdom

Patrick Wyse Jackson. Ireland

Paul Taylor. Australia

Pedro Castiñeira. Spain

Peter Malik. Slovakia

Pierluigi Pieruccini. Italy

Piotr Migoń. Poland

Richard Palin. United Kingdom

Rodolfo Carosi. Italy

Roger Mitchell. United Kingdom

Roger Thomas. USA

Salvatore Iaccarino. Italy

Sebastian Tappe. Germany

Shuzhong Shen. China

Silvia Figueirôa. Brazil

Stanley Finney. USA

Sylvie Crasquin. France

Tatsuo Oji. Japan

Terri Cook. USA

Thijs Van Kolfschoten. Netherlands

Thomas Casadevall. USA

William Birch. Australia

Yves Candela. United Kingdom

Zhang Jianping. China

NATIONAL REPRESENTATIVES

EUROPE

Austria

Bernhard Grasemann. University of Vienna

Belgium

Robert Speijer. KU Leuven University

Cyprus

Efthimios Tsiolakis. Cyprus Geological Survey

France

Nicolas Charles. French Geological Survey (BRGM)

Germany

Heinz-Gerd Röhling. German Geological Society (DGGV)

Iceland

Lovísia Guðrún Ásbjörnsdóttir. Icelandic Institute of Natural History

Ireland

Patrick N. Wyse Jackson. Trinity College Dublin

Italy

Elisa Brustia. Geological Survey of Italy

Lithuania

Jonas Satkunas. Lithuanian Geological Survey

Norway

Kristin Rønnes. Geo Norvegica UGGp

Portugal

Artur Abreu Sá. Arouca UGGp / Universidade de Tras-os-Montes e Alto Douro.

Spain

Luis Carcavilla. Geological and Mining Institute of Spain (IGME, CSIC)

Sweden

Sven Lundqvist. Geological Survey of Sweden

Switzerland

Thomas Buckingham. Swiss Academy of Sciences

Belgium

Christophe Lambiel. University of Lausanne

U.K

Kirstin Lemon. British Geological Survey

AMERICA

Argentina

Fernando Miranda. Servicio Geológico Minero Argentino

Brasil

Joana Sanchez. Federal University of Goias

Bolivia

Wilfredo Ramos Collorana. Universidad Mayor de San Andrés

Canada

Anne-Aurelie Sappin. Geological Survey of Canada

David Sharpe. Geological Survey of Canada

Chile

Manuel Arenas Abarca. Servicio Nacional de Geología y Minería

Colombia

Victoria Elena Corredor Bohórquez. Servicio Geológico Colombiano

Norway

Kristin Rønnes. Geo Norvegica UGGp

Portugal

Sherene Jones Williams. University of West Indies

Mexico

Ricardo Barragan. Universidad Nacional Autónoma de México

Sofia del Pilar Mendoza Castillo. Servicio Geológico Mexicano

Spain

Bilberto Zavala. Instituto Geológico Minero y Metalúrgico de Perú

Peru

South Korea

Daekyo Cheong. Kangwon National University

USA

Stanley Finney. California State University

David Mogk. Montana State University

"IUGS GEOLOGICAL HERITAGE SITES IS A UNIQUE IUGS COLLABORATIVE INITIATIVE TO GIVErecognition TO THOSE SITES ESSENTIAL FOR THE DEVELOPMENT OF GEOLOGICAL SCIENCES WORLDWIDE"

THE SECOND 100 IUGS GEOLOGICAL HERITAGE SITES has been developed thanks to multiple international organizations. Their representatives served as members of the Selection Committee.

On February 6 the final list of 'The Second 100' was approved.

SELECTION COMMITTEE / INTERNATIONAL ORGANIZATIONS

IUGS – International Union of Geological Sciences

Stanley Finney. Secretary General

IUGS – International Commission on Geoheritage (IUGS-ICG)

Asier Hilario. Chair

Juana Vegas. Secretary General

Jianping Zhang. Vice-chair

Benjamin Van Wyk de Vries. Chair, IUGS Subcommission on Sites

Gonzalo Lozano. Secretariat, IUGS Subcommission on Sites

IUGS Commission on the History of Geological Sciences (INHIGEO)

Ezio Angelo Vaccari. Chair

IUGS – International Commission on Stratigraphy (ICS)

David Harper. Chair

International Association of Sedimentologists (IAS)

Daniel Ariztegui. Past-President

International Paleontological Association (IPA)

Sylvie Crasquin. President

The Metamorphic Studies Group (MSG)

Owen Weller-Gibbs. Chair

IUGS Task Group on Igneous Rocks (IUGS-TGIR)

Michele Lustrino. Chair

International association of Volcanology and Chemistry of the Earth's interior (IAVCEI)

Karoly Nemeth. Member

IUGS Commission on Tectonics and Structural Geology (TecTask)

Enrique Gómez Rivas. Chair

Lorenzo Gemignani. Secretary General

International Mineralogical Association (IMA)

Asier Hilario. Chair

Juana Vegas. Secretary General

Jianping Zhang. Vice-chair

Benjamin Van Wyk de Vries. Chair, IUGS Subcommission on Sites

Gonzalo Lozano. Secretariat, IUGS Subcommission on Sites

UNESCO International Research Centre on Karst (IRCK)

Mary Luo Qukan. Chair

International Association of Hydrogeologists (IAH)

David Kreamer. President

Ian Davey. Executive Manager

Impact Cratering Committee (ICC) from The Meteoritical Society

Aaron Cavosie. Chair

International Union for Quaternary Research (INQUA)

Thijs Van Kolfschoten. President

Scientific Committee on Antarctic Research (SCAR)

Enrique Díaz-Martínez. Secretary, SCAR Expert Group on Geoheritage and Geoconservation

Global Geoparks Network (GGN)

Nickolas Zouros. President

ProGEO – International Association for the Conservation of Geological Heritage

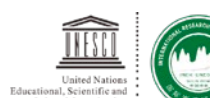
Lars Erikstad. Former-President



SCIENTIFIC PARTNERS:



TecTask



TGIR



SECRETARIAT:



IGCP 731:



Photo: Bernhard Edmaier

The Second 100 IUGS Geological Heritage Sites

The Second 100 IUGS Geological Heritage Sites, as with the First 100, receive IUGS recognition because they are of the highest scientific value. They are the world's best demonstrations of geologic features and processes. They are the sites of fabulous discoveries of the Earth and its history. They are sites that served to develop the science of geology, particularly its early history. They are located worldwide, and they are geologically diverse. Their visibility is greatly enhanced by IUGS recognition. They are attractively illustrated and described in this Book "The Second 100 IUGS Geological Heritage Sites", and they will be promoted further on the website of the International Commission on Geoheritage. www.iugs-geoheritage.org

The Second 100 Geological Heritage Sites are distributed in 53 countries. Some of the sites are classic and known to almost all geologists, but few geologists know most of the sites because of their diverse types and geographic settings. Older geologists know many; young geologists few. The announcement of the "Second 100" and the release of the attractive book at the 37th International Geological Congress in Busan, Republic of Korea on 27 August 2024 will lead to many of the sites becoming known for the first time to large numbers of geologists and the public. Interest in individual sites will increase as will geo-visitors. Many of the "Second 100" are well protected in national parks, geoparks, and natural reserves, but many are not. Recognition and visibility of the "Second 100" by IUGS can lead to their further appreciation, to their use as educational resources, and, most importantly, to their preservation.

Selection of the Second 100 built on the success and the global impact of the First 100. The website with the list of sites has been visited by more than 50.000 geologists from over 190 nations. The process and the procedures evolved for the "Second 100" to include over 400 participants and 16 international organizations that represent well all the disciplines of geological sciences. We thank all of them for their active participation.

For the Second 100, 174 proposed sites from 74 countries were considered. 714 reviews were done by 89 reviewers, who scored and ranked all the sites. The result of the evaluation was discussed and finally approved by 20 voting members of the Selection Committee, which represents the 16 international organizations that participate in this global endeavor. The final selection was ratified by the IUGS Executive Committee on February 21, 2024.

The large number of active participants in this Geological Heritage Sites endeavor reflects an enthusiasm for identifying geologic sites that impress us and captivates us with their geological character and significance. We have studied many of them in our fundamental course work, learned about them from our general interest and inquisitiveness in geological sciences, and visited them on field excursions. We delve into their meaning, their composition and structure, their history, and their ongoing processes. We enjoy being at them and viewing them virtually or, better yet, in person.

There are many more sites of the highest international value that can be considered global references for the geological sciences. This global challenge led by the IUGS is only a representation of most of them. The International Commission on Geoheritage (IUGS) plans to announce the Third 100 IUGS Geological Heritage Sites in 2026, and the Fourth in 2028. We invite you to follow this endeavor at least through 2028.

Stanley Finney
IUGS Secretary General.

Asier Hilario
Chair. IUGS Commission on Geoheritage.



Africa's Contribution to the Second 100 IUGS Geological Heritage Sites

The vast African continent contains many unique and diverse internationally significant geological heritage sites, which substantially contributed to our understanding of the evolution of the Earth and to the development of the geological sciences. Africa's physical geography, its fauna and flora as well as the history, culture and economic mainstay of its population are also strongly tied to its geological heritage. However, proper inventory and scientific valuation of the geoheritage potential of Africa has been limited to few sites. The management and conservation of geoheritage sites in geoparks is at its infancy in the continent, and the local communities are yet to fully benefit from their geoheritage resources.

The identification of the IUGS Geological Heritage sites by the IUGS International Commission on Geoheritage through its flagship IGCP 731 Project is, therefore, a very welcome initiative for Africa for multiple reasons. First, it provides an opportunity to showcase some of the most iconic geological heritage sites of the continent, thereby enhancing their visibility and promoting their preservation, conservation and protection. Second, it encourages several African geoscientists to reassess the geoheritage values of geological sites in their respective countries and regions. Third, the identified and recognized sites could serve as a basis for initiating geopark projects and to enhance geotourism. Finally, many of the geological heritage sites in the continent are closely linked to the traditions and narratives of the respective indigenous populations inhabiting those sites, and their recognition promotes the cultural heritage of these communities.

Following upon the successful completion of its inaugural First 100 IUGS Geological Heritage Sites in 2022, the Second 100 IUGS Geological Heritage Sites showcases another 100 iconic geological heritage sites of high scientific value in this volume. African contribution to the Second 100 is as significant as it was to the First 100. Among the Second 100 geological heritage sites, nine sites are from various parts of Africa including from Algeria and Libya, Egypt, Ethiopia, Ghana, Namibia, Tanzania and South Africa. Some of the most iconic sites from Africa recognized in the Second 100 include the following: the paleontological sites of the Nama Group –one of the most continuous stratigraphic and palaeontological records of the Ediacaran-Cambrian in the World– in Namibia, and the Kibish Formation –home of one of the oldest *Homo sapiens* fossils in the world– in Ethiopia; impact structures of Vredefort Dome –eroded remnant of Earth's largest impact structure– in South Africa and the Lake Bosumtwi impact crater –the youngest well preserved impact structure known on Earth– in Ghana; the volcanological site of the Ngorongoro crater –a uniquely well preserved caldera structure– in Tanzania, and the mineralogical site of the Kalhari Manganese field –world's largest land-based resource of manganese– in South Africa.

Considering Africa's geodiversity, these selected sites are only a few of the multitude of geological heritage sites in the continent. The First 100 and the Second 100 have paved the way for identifying, evaluating and recognizing many more sites from the continent in the future.

Professor Asfawossen Asrat

School of Earth Sciences and
Engineering Botswana International
University of Science and Technology.
Botswana.

School of Earth Sciences
Addis Ababa University. Ethiopia.
IUGS Geological Heritage Sites referee.



The Beauty of Geology

Geology is beautiful, providing an incredible abundance of colours, shapes and structures, primarily created by geological processes within periods of time ranging from seconds to millions of years, without human intervention, and ranging from microscopically small to kilometres in size. It presents countless motifs – often with abstract, graphic and painterly elements – with an amazing aesthetic power!

With my images I like to not only show these fascinating features but also to tell the story behind them - how have they come into being.

Aerial photography is my instrument. From the aerial perspective I can most effectively tell the narrative of a landscape. For instance, when it comes to large structures such as mountain ranges or a chain of volcanic cones on a fissure in the earth's crust, it is much better to shoot them from the air than from the ground.

Bernhard Edmaier

www.bernhard-edmaier.de

Lardana, Pyrenees, Spain

HISTORY OF GEOSCIENCES



Matterhorn, Switzerland

The development of the geosciences through centuries of research reflects a history of ideas and methodology that shows how science works in practise. The historical view provides perspective, distinguishing between the significant and the negligible, of connections, and of continuities as well as contingencies. It documents how undeniable progress of knowledge is won in constant argument with limited data, preconceived ideas, philosophical biases and historical context.

Similar to mapping a given landscape in various scales, for various purposes and in varying detail – always considering the passing of geological time, historians of science map the landscape of human ideas through the centuries. For this, they use documents, but also look into collections and at places, routes and landscapes that have been studied by scholars and scientists throughout the centuries.

Each geological heritage site has its own history of research. Some have been cornerstones for heated debates; others are places where a geological phenomenon was observed for the very first time or where a new methodology has been tested. They can be important in many ways: as a site of scientific “blunder”, from which we take the lesson how ambiguous evidence can be; as a site of constant diligence or of meticulous testing of ideas; or as a site of a rare *Eureka* experience. At any rate, the geosites presented in this section, as well as some others that are included under different thematic chapters within this book, are milestones on the road to modern geoscience.

In the Agno Valley in norther Italy, Giovanni Arduino established his lithostratigraphic theory in four units, which became the basis of modern stratigraphic chronology. At Cavanisham Ferry and Llanstephan in Wales, Roderick Murchison began to establish what later became the Silurian. The Durbuy Anticline in Belgium was part of a larger endeavour of Jean-Baptiste-Julien d'Omalius d'Halloy, who described three rock units that, later became the Silurian, Devonian and Carboniferous. At the Jurassic Coast at Lyme Regis, Mary Anning was the first to collect an iconic fauna of marine reptiles. Non-fossiliferous rocks were notoriously difficult to map and classify. At the Barrow Zones in the Scottish Highlands, George Barrow made the first systematic study of regional metamorphism using mineral assemblages. Pentti Eskola developed a metamorphic facies concept for contact metamorphic rocks at Orijärvi, Finland. The study of glaciers begins with the Mer de Glace in France. Walking the Norwegian mountains, Jens Esmarks and his student Otto Tank discovered evidence of ice ages. The Parallel Roads of Glen Roy in Scotland were later also included in this new Ice Age paradigm. Vesuvius in Italy can be considered as the birthplace of volcanology dating from the description of the 79AD eruption by Pliny the Younger. The 1902 eruption of Montagne Pelée on Martinique alerted society to the dangers of dome collapse and ensuing glowing avalanches. Far from active volcanoes, the nature of volcanoes was hotly debated at Scheibenberg in Germany, which became a cornerstone of Neptunism. Maruia Falls in New Zealand points to the Earth's interior: Seismic data from the earthquake causing the waterfall led Inge Lehmann to postulate the existence of the Inner Earth Core.

Martina Kölbl-Ebert

Ludwig-Maximilians-Universität,
Munich, Germany.

Secretary General, INHIGEO International
Commission on the History of
Geological Sciences – IUGS / IUHPST.
IUGS Geological Heritage Sites referee.

Terri Cook

Laboratory for Atmospheric and Space Physics,
University of Colorado, USA.

ProGeo. International Association for the
conservation of geological heritage.
IUGS Geological Heritage Sites referee.



ARDUINO'S LITHOSTRATIGRAPHICAL SEQUENCE OF THE AGNO VALLEY ITALY

View of the Agno Valley (www.itinerarioenergia.it/).

THE SITE WHERE GIOVANNI ARDUINO ESTABLISHED IN 1758-1760 HIS LITHOSTRATIGRAPHICAL THEORY IN FOUR UNITS, THE BASIS OF MODERN STRATIGRAPHIC CHRONOLOGY.

Giovanni Arduino's study and representation of the lithostratigraphical sequence of the Agno Valley (1758), led to the publication in 1760 (Ell, 2011-2012) of a new theory of sub-division of rocks into four units according to the chronological order of their formation. This classification included mountains - defined as 'Primary' (with a basement of schists and mineral-bearing crystalline rocks; now Paleozoics) 'Sec-

ondary' (stratified limestones with fossils; now Mesozoics) and 'Tertiary' (clays, fossiliferous sandstones and some volcanic material; now Cenozoics) - as well as the most recent terrain of the plains, defined as the 'Fourth unit' (Vaccari, 2006). Arduino's system established the scientific notions of Primary, Secondary and Tertiary strata, and contributed to the later definition of Quaternary (Gibbard, 2019).

SITE 101

GEOLOGICAL PERIOD	Pre-Permian to Quaternary
LOCATION	Vicentinian Alps, Veneto Region, Italy 45°41'32"N 011°16'51"E
MAIN GEOLOGICAL INTEREST	History of geosciences Stratigraphy and sedimentology

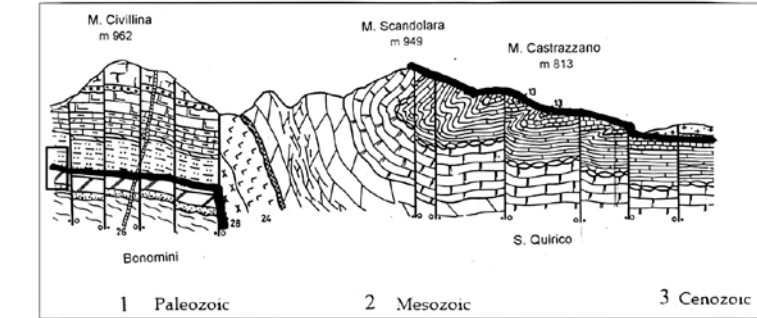
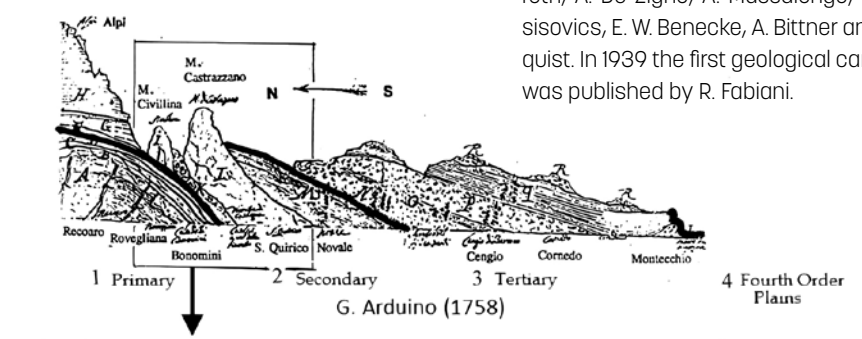


Strata of "biancone" (white limestones of Cretaceous age, Mesozoic), Mt. Castrazzano, Agno Valley; identified by Arduino as secondary "fine-grained limestones". (Photo courtesy of Ezio Vaccari).

Geological Description

The Agno Valley is located in the mountain area of the Venetian Prealps called the "Vicentinian Alps", north-west of Vicenza in north-eastern Italy. Oriented from northwest to southeast following the course of the Agno River, the valley shows a stratigraphic sequence from Paleozoic (Pre-Permian) to Cenozoic (Quaternary) exposed along its length of c. 20 km. In the upper Agno Valley, within the area of Recoaro and at the base of Mt. Spitz and Mt. Civillina, the Pre-Permian metamorphic crystalline basement (quartz-phyllites) of the Southern Alps crops out and is unconformably overlain by Permo-Triassic sedimentary cover of limestones and sandstones, the latter succession also occurring at Scandolara and Castrazzano mountains (Barbieri *et al.*, 1980; De Zanche and Mietto, 1981). In the mid- and lower Agno Valley, from Novale to Montecchio, the outcropping rock units comprising the surrounding mountains decrease in age from Jurassic, Cretaceous to Eocene and Oligocene. Occurrences of volcanics from two magmatic cycles traverse or are intercalated within the stratigraphic sequence: in the Middle Triassic (acid and basic rocks) and in the Paleogene (basaltic rocks).

In the lowest part of the Agno Valley, Holocene gravelly-sandy alluvial deposits lay at the junction with the Po Valley plain.



Arduino's cross-section of the Agno Valley (top) compared to a modern profile of Civillina, Scandolara and Castrazzano mountains (below). Thick black lines indicate Geological Era divisions. (Figures modified by Ezio Vaccari).

G. Barbieri, V. De Zanche, E. Di Lallo, P. Mietto, R. Sedeia (1980).

CAVANSHAM FERRY AND LLANSTEPHAN QUARRIES UNITED KINGDOM



Cavansham Ferry, River Wye, with "grauwacke" bedrock. On 11 July 1831 Murchison ferried across the pool of calmer water, visible upstream, to 'discover' the Silurian.

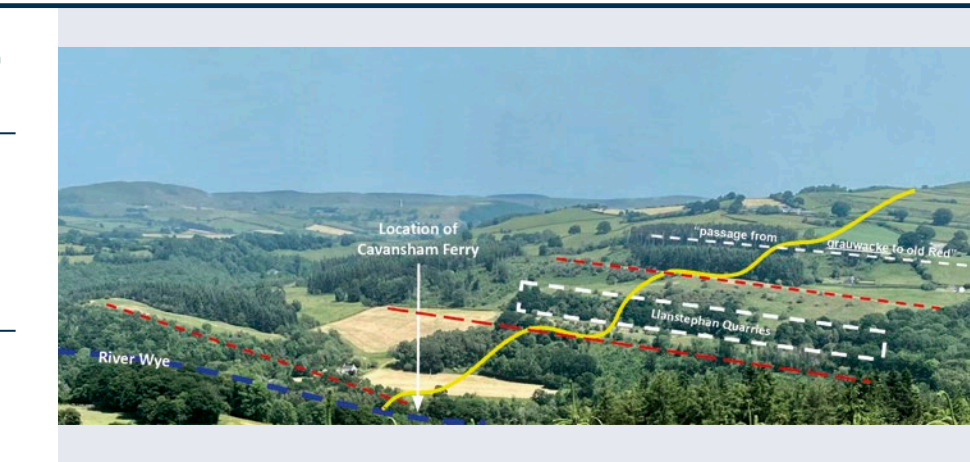
LOCATION OF "THE FIRST TRUE SILURIAN", AS DESIGNATED BY ITS FOUNDER SIR RODERICK IMPEY MURCHISON.

Cavansham Ferry and Llanstephan is an iconic site with international significance for geological heritage as the place the originator of the Silurian, Roderick Impey Murchison, identified as the location where he began to establish what became the Silurian System, labeling it in his notebook "N.B. This was the first true Silurian." Murchison's seminal book, 'The

Silurian System', is of great importance to all students of Lower Palaeozoic geology. This site provides uniquely important context for understanding the motives, approaches, practises and interpretation Murchison employed in founding the Silurian. These outcrops mark an essential stage in the development of modern stratigraphy.

SITE 102

GEOLOGICAL PERIOD	Late Silurian (Ludlow to Pridoli)
LOCATION	Wye Valley, Powys, Wales, United Kingdom 52°04'12"N 003°17'32"W
MAIN GEOLOGICAL INTEREST	History of geosciences Stratigraphy and sedimentology



"Low-terrace shaped ridges of grey rock", Cavansham Ferry to Trewerne Hills. Yellow marks the line of Murchison's section, red dashed lines are ridge crests.

Geological Description

On the right bank of the River Wye, by Trerickett Mill, the "Old Red Sandstone" (Devonian, Pridoli, Moor Cliffs Formation) is "quit" and "Grauwacke slate" (Silurian, Ludlow, Ludfordian) is exposed in the bed of river, and crops out on the left bank as several "low terrace-shaped ridges". This is the first site where Murchison encountered "grey-coloured strata" of "grauwacke" containing fossils he considered "differing from any known in superior deposits". Crossing the river at Cavansham Ferry Murchison "rushed up to those ridges" at Llanstephan Quarries, and to "inexpressible joy found them replete with transition fossils." Upwards, "the strata...

plunges to the east...under the Old Red Sandstone." The archaic geological descriptions quoted here were used by Murchison in his 1831 field notebook No.2. Later, he noted: "The order of succession seen in the left bank of the Wye...first led me to suspect I had met with a district that contained a good part of evidence required to lead to a systematic study of older formations." (Murchison 1839, 5). Retrospectively, Murchison considered this site as the location where he discovered the Silurian, culminating in his establishment of the Silurian System. As such, it provides great insight into Murchison's early fieldwork methods and thinking.

Murchison's section from Wye valley to Trewerne Hills drawn in his notebook, 11th July 1831, with later addition "N.B. This was the first true Silurian".
(© Geological Society of London, reproduced with permission).



Scientific research and tradition

The precise location of Cavansham Ferry was uncertain, with some scholars even doubting its existence, until Hawley (1997) identified this site as 'the first true Silurian' using Murchison's original field notes and systematic inspection of the ground. Since then, the location has been visited by geologists from the both U.K. and worldwide.

JURASSIC COAST: LYME REGIS

UNITED KINGDOM



UNESCO World Heritage Site

Triassic-Jurassic boundary, and overlying Blue Lias, Pinhay Bay, west of Lyme Regis in the Undercliffs National Nature Reserve and Jurassic Coast World Heritage Site.

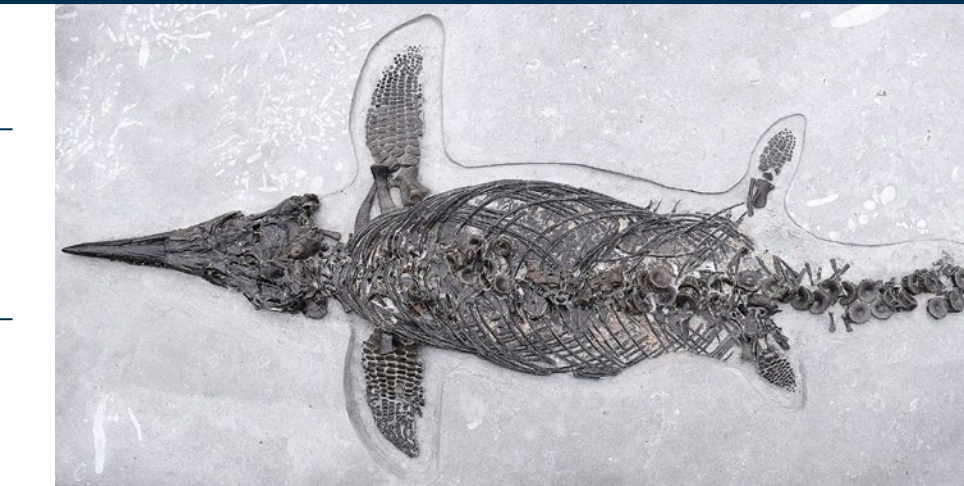
A GLOBALLY UNIQUE NEAR-CONTINUOUS MESOZOIC COASTAL SUCCESSION EXEMPLIFIED BY THE CLASSIC LOWER JURASSIC OF LYME REGIS.

The Jurassic Coast uniquely exposes an almost continuous Mesozoic sequence. It is renowned for its contribution to Earth science with over 300 years of research exemplified by the marine Lower Jurassic of the Lyme Regis area. A prolific source of invertebrate and vertebrate fossils (first collected by Mary Anning and including

many type specimens), this sequence is fundamental to our modern understanding of Lower Jurassic stratigraphy spanning end Triassic (Rhaetian) and Lower Jurassic (Hettangian-Pliensbachian) marine strata, which document environment, climate and sea level change over this interval.

SITE 103

GEOLOGICAL PERIOD	Triassic to Cretaceous
LOCATION	Dorset and East Devon Coast, United Kingdom 50°43'01"N 002°57'01"W
MAIN GEOLOGICAL INTEREST	History of geosciences Stratigraphy and sedimentology



Recent discoveries (Jurassic Coast Collection): exceptionally preserved *Ichthyosaurus communis* from the Blue Lias Formation (found and prepared by Fiann Smithwick).

Geological Description

The Jurassic Coast World Heritage Site exposes an outstanding sedimentary succession displaying 185 million years of the Earth's history - a near-continuous Mesozoic stratigraphical record. This encompasses the transition from terrestrial to marine Triassic (Gallois, 2019) and Jurassic strata, and culminates in the Upper Cretaceous Chalk (Mortimore, 2019) and the iconic Old Harry Rocks.

This coastline provides "one of the finest sections of marine Jurassic rocks anywhere in the world" (Callomon and Cope, 1995) - a statement exemplified by global reference sections in the marine Lower Jurassic at Lyme Regis. This area is noted for its prolific invertebrate (including a near complete Jurassic ammonite zonation) and marine reptile fossil fauna, first collected by Mary Anning (1799-1847). Today, housed in museums the world over, Mary Anning's discoveries included the world's first complete pleiosaur, many complete ichthyosaurs and fossil fish, and the first British pterosaur. She collaborated and corresponded with many contemporary scientists inspiring the world's first

published palaeoecological reconstruction, De la Beche's *Duria antiquior*.

Fundamental to our modern biostratigraphy for the Lower Jurassic (Simms *et al.*, 2004) Lyme Regis remains one of the most readily accessible and studied sources of Lower Jurassic marine fossils in the world (Jurassic Coast Trust, 2021).

Scientific research and tradition

This actively eroding coast has contributed to geoscience for over 300 years, from the earliest collections of Mary Anning and the descriptions of William Buckland and Henry de la Beche. Today the Jurassic Coast is considered by geologists as one of the most significant teaching and research sites in the world.



Mary Anning (1799-1847) with her dog Tray looking eastwards towards Lyme Regis and Golden Cap (Artist unknown, Natural History Museum, London).

METAMORPHIC BARROW ZONES IN SCOTTISH HIGHLANDS UNITED KINGDOM



Field photograph from the Glen Esk region of the Barrow zones, showing steeply-dipping metasedimentary rocks belonging to the chlorite zone.

THE FIRST SYSTEMATIC STUDY OF REGIONAL METAMORPHISM THROUGH ANALYSIS OF INDEX MINERALS IN METAMORPHOSED MUDSTONES.

In the words of Tilley (1925), the Barrow zones represent "the first attempt in the petrological literature to bring precision to the study of regional metamorphism, by laying upon a map zonal lines indicative of varying grades of metamorphism". In essence, Barrow was the first to provide convincing field evidence of a sensitive thermal structure for regional

metamorphism (Evans, 2007). The mineral sequence has become entrenched in the literature as the classic example of intermediate pressure/temperature metamorphism, typically as a consequence of continent-continent collision, and such metamorphism is often referred to as Barrovian-type (e.g. Weller *et al.*, 2013).

SITE 104

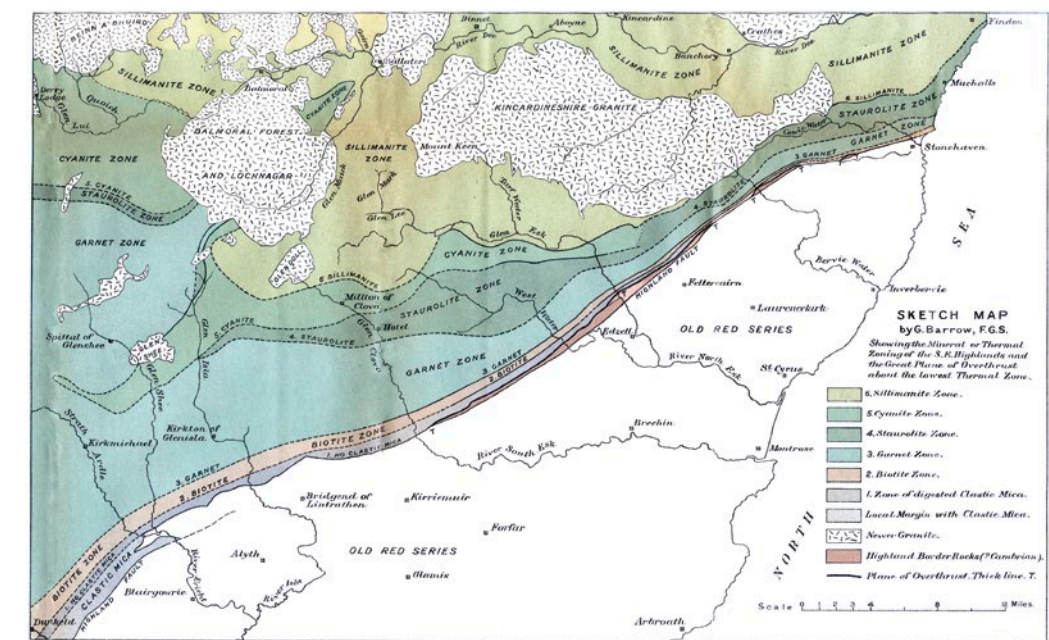
GEOLOGICAL PERIOD	Ordovician
LOCATION	Scottish Highlands, United Kingdom 56°54'00"N 002°48'54"W
MAIN GEOLOGICAL INTEREST	History of geosciences Igneous and Metamorphic petrology



Field photograph from the sillimanite zone, showing sillimanite needles nucleating around garnet grains in a matrix of biotite, muscovite, quartz and feldspar.

Geological Description

The Barrow zones of the Scottish Highlands are located in the southern part of the Grampian Highlands terrane, which is bound to the south by the Highland Boundary Fault. The zones are a series of mineral assemblages in metamorphic mudstones, which start at chlorite grade and are then defined by the sequential first appearance of biotite, garnet, staurolite, kyanite and sillimanite. The zones were first recognised and mapped by British survey geologist George Barrow (Barrow, 1912), and represent increasing metamorphic grade to the northwest away from the Highland Boundary Fault. The metamorphism occurred at c. 470 Ma during the Grampian orogeny, a short-lived tectonometamorphic event involving the collision of the Laurentian margin with the Midland Valley Arc within the longer Caledonian orogeny (Viere *et al.*, 2012). In the type sections of Glen Clova and Glen Esk in the central portion of the Barrow zones, reported metamorphic conditions vary from 500-650 °C and 5-7 kbar in



Index mineral map as first produced by Barrow (1912).

Scientific research and tradition

The Barrow zones are a classic field trip locality, and led to the concept of an isograd (Tilley, 1925) as well as discussions about the timescales of metamorphism (e.g. Viere *et al.*, 2012). Nearly all metamorphic petrology university courses include discussion of the Barrow zones and feature Barrow's original map.

CONTACT METAMORPHIC ROCKS OF ORIJÄRVI FINLAND



Photo from 1908 taken by Pentti Eskola himself during his field work in the Orijärvi area. As Eskola himself stated in his 1914 publication, the image shows: "Folded layers of limestone intercalated with leptite (now fine-grained paragneiss) and amphibolite. Hepolahdenaari, Orijärvi. The photograph was taken from the West." Note the hammer for scale in the photo (GTK, Vanhatkuvat / GTK, old photographs).

STUDY OF THESE ROCKS LED TO THE FOUNDATION OF THE METAMORPHIC FACIES CONCEPT, USED IN NEARLY ALL METAMORPHIC STUDIES.

Eskola (1920) introduced the concept of metamorphic facies to the petrological community as a product of his work on the metamorphic rocks of the Orijärvi region (Eskola, 1915). This work took inspiration from similar studies in Norway by Goldschmidt (1911), and represented a conceptual breakthrough to treat rocks as chemical systems that obeyed the phase rule

and possessed a mineral association as an indication of metamorphic grade (Evans, 2007). The metamorphic facies concept is now one of the central concepts in metamorphic petrology, and the classification provides a common language to discuss metamorphic rocks by specialists and non-specialists alike.

SITE 105

GEOLOGICAL PERIOD	Paleoproterozoic (Orosirian)
LOCATION	Orijärvi, Finland 60°13'00"N 023°32'00"E
MAIN GEOLOGICAL INTEREST	History of geosciences Igneous and Metamorphic petrology



Cordierite gneiss xenolith (20 cm across) in the c. 1.89 Ga Orijärvi granodiorite.

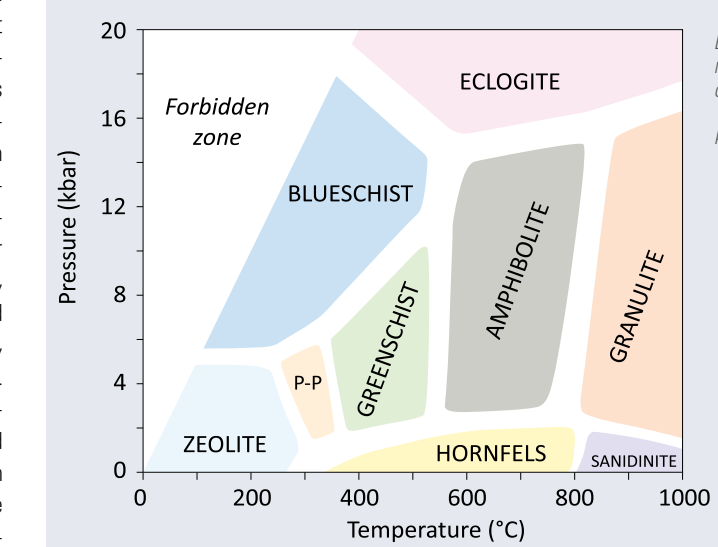
Geological Description

The Orijärvi area forms part of the Southern Svecfennia terrane in southern Finland. This terrane is one of several terranes that were collectively accreted to the Fennoscandian (aka Baltic) shield during the long-lived Svecfennian orogen at c. 1.96–1.77 Ga, during formation of the Nuna (aka Columbia) supercontinent (Kara *et al.*, 2018). Rocks in the Orijärvi area mainly comprise volcanic rocks with sedimentary intercalations and are thought to have formed in an arc rift setting. These rocks were folded and regionally metamorphosed to amphibolite-facies conditions of 3 kbar and 650 °C at c. 1.89–1.88 Ga as part of the Svecfennian orogen (Schneiderman and Tracy, 1991). Synorogenic intrusion of granodiorite caused contact metamorphism at the same or lower pressure-temperature conditions (Eskola, 1915). Metasedimentary rocks are composed dominantly of quartz, feldspar, muscovite, biotite, cordierite, hornblende and garnet. Metavolcanic rocks mainly consist of hornblende, cummingtonite and plagioclase and subordinate biotite and ilmenite. In skarn zones associated with the contact aureole of the granodiorites, cordierite-bearing or-

thoamphibolite gneisses also occur. These chemically-unusual rock types are attributed to both alteration of the protolith prior to regional metamorphism and metasomatism during contact metamorphism (Schneiderman and Tracy, 1991).

Scientific research and tradition

The site has continued to be studied as the associated mineral assemblages are relatively rare (e.g. Schneiderman and Tracy, 1991). However, the main legacy from analysis of metamorphic rocks in Orijärvi is the development of the metamorphic facies concept, which is taught on every metamorphic petrology course in the world.



Example modern-day metamorphic facies diagram.

P-P = prehnite-pumpellyite.

DURBUY ANTICLINE

BELGIUM



UNESCO Global Geopark

The wonderfully exposed Durbuy Anticline in the medieval town of Durbuy was first described in 1807 by the famous Belgian geologist Jean-Baptiste-Julien d'Omalius d'Halloy.

AN ARCHETYPE ANTICLINE DEFINED AS EARLY AS 1807.

The natural cross-section of the Durbuy Anticline represents an archetypal anticline and is a classical site used for the education of geology and geoscience students from Belgium and neighboring countries.

It was scientifically described as early as 1807 and is the subject of one of the

oldest geosite studies in the world, thus serving as a key reference.

Situated within the UNESCO Global Geopark Famenne-Ardenne, the Durbuy Anticline is easily accessible and attracts a broad public. It holds significant local cultural and heritage value and is supported by the town of Durbuy.

GEOLOGICAL PERIOD	Upper Devonian
LOCATION	Durbuy, Province of Luxembourg, Belgium 50°21'13"N 005°27'30"E
MAIN GEOLOGICAL INTEREST	History of geosciences Tectonics

SITE 106



The Anticline is part of the medieval town of Durbuy.

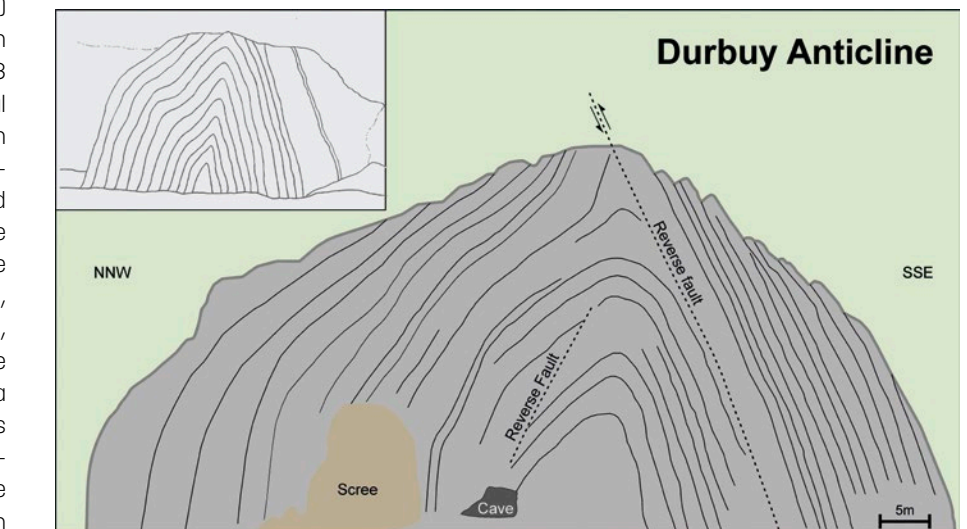
Geological Description

The Durbuy Anticline provides a textbook example of a cross-section through an anticline, widely employed for scientific and educational purposes since the early 19th century. This wonderfully exposed outcrop is also known as l'Anticline d'Omalius after the famous Jean-Baptiste-Julien d'Omalius d'Halloy (the Father of Belgian Geology, known from the clay-mineral halloysite) who described it in 1807. This description was part of a much larger endeavor: in 1813 d'Omalius completed the first geological map of France and bordering areas, which was published only in 1822 due to the political turmoil in western Europe. He divided the northern geological terrains into three parts, which subsequently through the works of Roderick Murchison and others, became well-established as the Silurian, Devonian and Carboniferous. The geosite in the medieval town of Durbuy boasts a base of 90 meters and a height of 37 meters and is composed of about 25 layers of Mid-Frasnian marine limestone of the Philippeville Formation. The slightly faulted anticline is an excellent example of Late Carboniferous Variscan deformation in Europe. The structure

was carved out by the Ourthe River, which originally meandered on a Cenozoic sandy substratum, and is now eroding underlying Devonian formations without distinction of their hardness.

Scientific research and tradition

First described by geologist Jean-Baptiste-Julien d'Omalius d'Halloy (1783-1875) in 1807 and subsequently re-described for a broader audience by Dejonghe and Jumeau (2007), the apex of the anticline is the highest point of the medieval town of Durbuy. It is a common destination for a walk by inhabitants and visitors.



The original sketch of the Durbuy Anticline from the publication by d'Omalius d'Halloy (upper left-hand corner) in comparison with a modern representation.

VESUVIUS VOLCANO

ITALY



UNESCO World Heritage Site

Aerial view of Monte Somma and Vesuvius cone (photo by J.C. Tanguy).

THE BIRTHPLACE OF VOLCANOLOGY, FROM THE DESCRIPTION OF THE 79AD ERUPTION BY PLINY THE YOUNGER UNTIL THE SCIENTIFIC STUDIES IN THE 18TH AND 19TH CENTURIES.

The science of volcanology was born at Vesuvius, with the first description of the phenomena which occurred during an explosive volcanic eruption. This account is included in two letters by Pliny the Younger to Tacitus about the 79AD eruption, which destroyed Herculaneum and Pompei. During the following centuries, the major eruptions of Vesuvius (e.g. 472AD, 1631, 1906, and the last in 1944) were taken as a paradigm for the study of all possible volcanic activity by European scientists. From the 18th century to date, Vesuvius and its crater have been visited by several scholars and considered a natural laboratory for understanding the behavior of an active volcano.

SITE 107

GEOLOGICAL PERIOD	Pleistocene to Holocene
LOCATION	Naples, Campania, Italy 40°49'18"N 014°25'35"E
MAIN GEOLOGICAL INTEREST	History of geosciences Volcanology



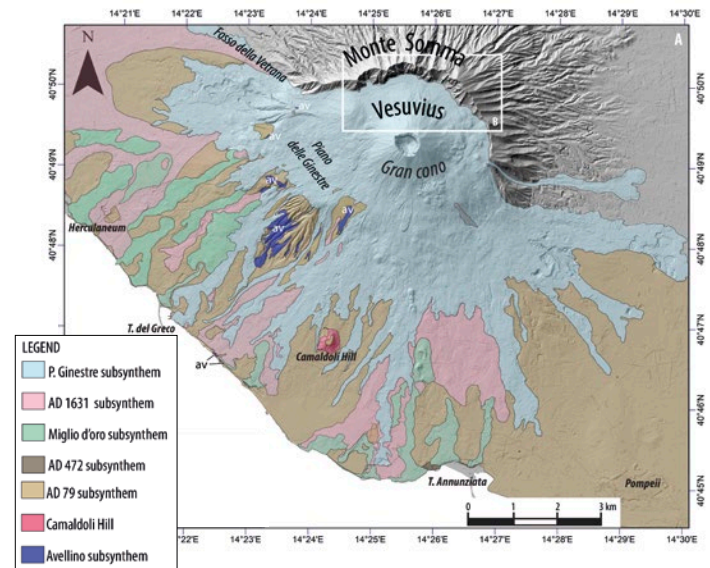
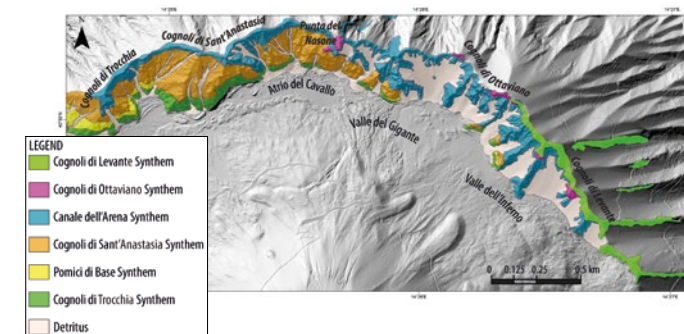
Vesuvius from the Pompeii Forum in a picture of George Sommer (circa 1870).

Geological Description

Volcanic activity at Vesuvius started about 400,000 years ago (Sbrana *et al.*, 2022). Outcropping deposits all belong to the volcanic activity following the Campanian Ignimbrite (about 39,000 years ago). Dated to about 22,000 years ago, the Pomice di Base eruption is the major Plinian eruption that occurred at Vesuvius. Other major explosive eruptions followed, such as the Greenish Pumices Sub-Plinian eruption (about 20,000 years ago), and the Pomice di Mercato Plinian eruption (about 8,900 years ago). Activity during the last 4,000 years can be subdivided into four periods: 1) Proto-Vesuvius, between Plinian eruptions of Pomice di Avellino (about 4,000 years ago) and 79AD; 2) Ancient Vesuvius, between 79AD Plinian eruption (Sigurdsson *et al.*, 1985) and 472AD Sub-Plinian eruption; 3) Medieval Vesuvius, from 472AD Sub-Plinian eruption and

1631 small-scale Plinian eruption (Rosi *et al.*, 1993); 4) Present Vesuvius, between 1631 and 1944 eruptions. Medieval Vesuvius is characterized by lava flows from vents on the slopes of the Vesuvius cone, and of Strombolian and Violent Strombolian scoriae fallout (Principe *et al.*, 2004). During Present Vesuvius period, the volcano passed from effusive and markedly Strombolian activity to episodes of violent Strombolian and Sub-Plinian eruptions with mixed effusive and explosive character (Arrighi *et al.*, 2001). Since the last eruption in 1944, Vesuvius entered a period of eruptive rest.

Main geological units of Vesuvius and Monte Somma volcanoes (map by Claudia Principe).



Scientific research and tradition

Positioned on the outskirts of Naples, Vesuvius has been studied by travellers, scholars, naturalists and scientists, particularly after the devastating eruption of 1631 (Rosi *et al.*, 1993). For centuries volcanologists described volcanoes by comparison with Vesuvius. Consequently, the available documentary record on Vesuvius is one of the best of the world (BIBV database).

SCHEIBENBERG LAVA FLOW

GERMANY



Massive basalt columns at an abandoned quarry at the Scheibenberg. The columns are some 30 meters long. The basalt was quarried until 1936.

AROUND 1790, THE SCHEIBENBERG BECAME A KEY ARGUMENT FOR NEPTUNISM IN THE DISPUTE ABOUT THE ORIGINS OF BASALT FROM WATER OR LAVA.

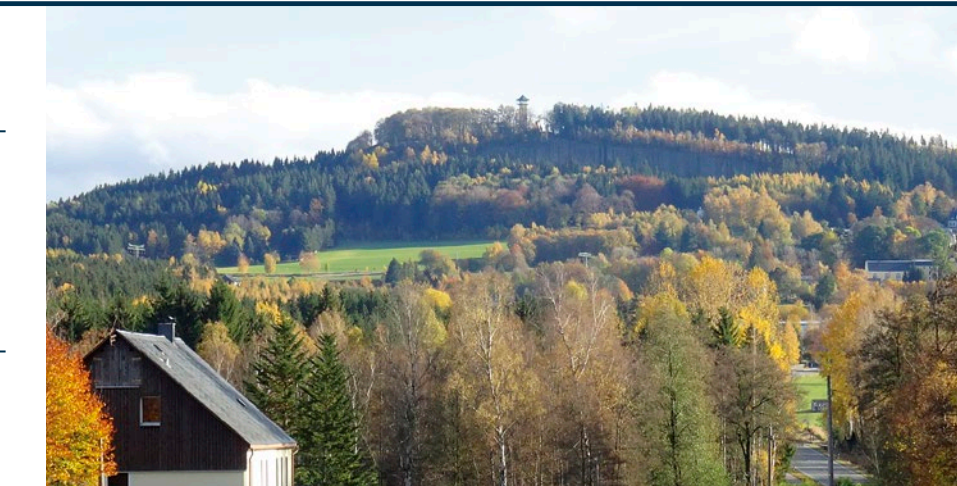
Abraham Gottlob Werner taught at the Mining Academy in Freiberg (Saxony), attracting and inspiring numerous German and foreign students, who spread his geological and mineralogical handicraft, his views and ideas throughout the world.

The assumption of an igneous formation of basalt was already widespread when Werner intervened in the discussion and be-

came the most influential representative of Neptunism. Fieldwork at the Scheibenberg convinced Werner that the underlying sediments graded into columnar basalt. Opposition by Werner's former student Johann C.W. Voigt (1752–1821) triggered a hot dispute in which Leopold von Buch (1774–1853) and Alexander von Humboldt (1769–1859) also intervened.

SITE 108

GEOLOGICAL PERIOD	Oligocene
LOCATION	Erzgebirge, Saxony, Germany 50°32'14"N 012°55'26"E
MAIN GEOLOGICAL INTEREST	History of geosciences



The hill called Scheibenberg in the Saxonian Erzgebirge is the erosional remnant of an Oligocene lava flow.

Geological Description

Extensional tectonics at the Eger Graben (Ohre Graben, Czech Republic) allowed for intraplate volcanism some 32 to 28 Ma ago in the Saxonian Erzgebirge. Nephelinitic lavas poured into pre-existing river valleys and solidified as basalt columns. Subsequent erosion, stronger in the deeply weathered rocks adjacent to the lava flows, led to inversion of the relief. Consequently, the remnants of the lava flows are now preserved as hills topped with basalt columns underlain by the basal breccia of the lava flow, river sediments and crystalline basement.

Around 1790, the origin of basaltoid rocks was hotly debated. Vulcanism – following studies by Guettard (1715–1786) and Desmarest (1725–1815) in Auvergne – postulated a magmatic origin for these rocks.

In contrast Neptunism, represented mainly by Abraham Gottlob Werner (1749–1817), explained the origin of all rocks – with the exception of some recent volcanic products – as chemical or mechanical precipitation from the waters of a primordial ocean that once covered the whole earth and which subsequently retreated to the present ocean basins.

Scientific research and tradition

As the force and scope of erosion was then usually grossly underestimated, the basalt columns at Scheibenberg were interpreted as part of a sedimentary sequence and became a key argument in this dispute.

In spring 1787 Werner visited the Scheibenberg, where he found basalt resting horizontally upon 'wacke', sand, clay and gneiss. This finally convinced him that basalt was precipitated from water and made the Scheibenberg a cornerstone of Neptunism. The controversy even entered popular literature such as Goethe's Faust II.

Photograph from the early 20th century of a quarry at the Scheibenberg showing the sedimentary rocks immediately underneath the basalt columns. (Image: LfUG; <https://www.geologie.sachsen.de/scheibenberg-27293.html>).



MONTAGNE PELÉE VOLCANO

FRANCE



UNESCO World Heritage Site

Montagne Pelée, active volcano in Martinique Island (@ Cyprien Lesage).

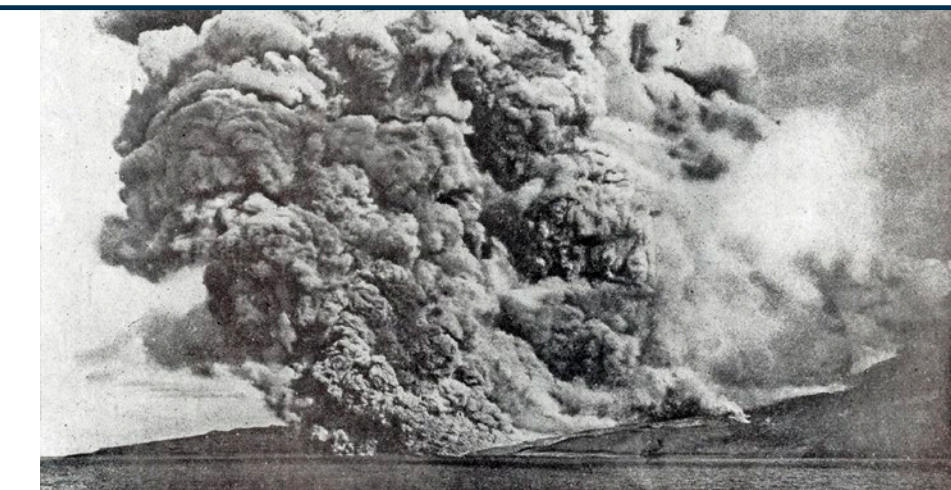
MONTAGNE PELÉE IS THE WORLD REFERENCE VOLCANO FOR THE PELÉAN TYPE ERUPTION, FIRSTLY DESCRIBED BY ALFRED LACROIX IN 1902.

Montagne Pelée is one of the most famous volcanoes worldwide with alternating Plinian and dome-forming eruptions and huge flank-collapse events. Montagne Pelée raised the issue of the explosivity of dome-forming eruptions, especially the May 8, 1902 killer eruption which was the first described as Peléan by Alfred Lacroix (1904) who also introduced the term

"nuée ardente" (pyroclastic flow). This catastrophic eruption paved the way for the creation of the Volcanological and Seismological Observatory of Martinique in 1903, the second in the world after the Vesuvius Observatory in 1841.

SITE 109

GEOLOGICAL PERIOD	Pleistocene to Holocene
LOCATION	Martinique Island, France 14°48'34"N 061°09'59"W
MAIN GEOLOGICAL INTEREST	History of geosciences Volcanology



Nuée ardente (pyroclastic flow) during a Peléan eruption at Montagne Pelée, December 1902
(@ Alfred Lacroix).

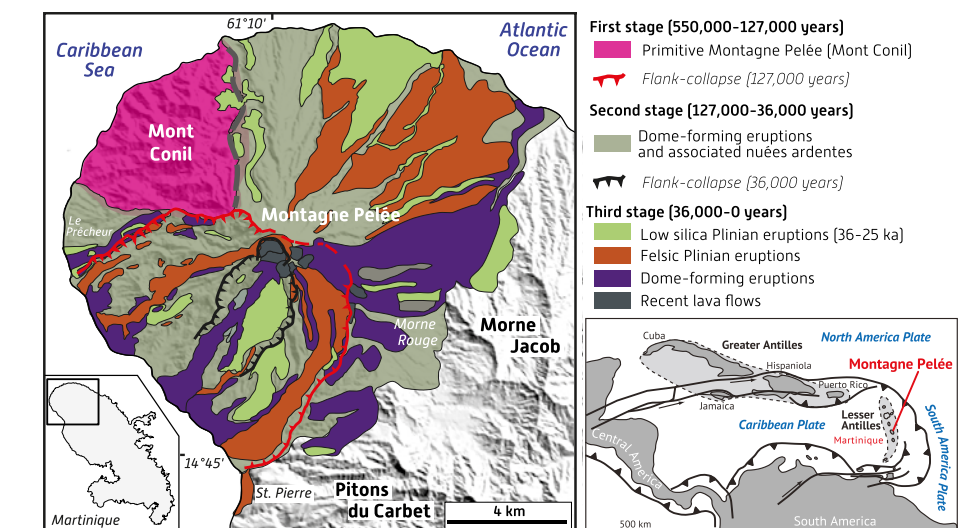
Geological Description

The Montagne Pelée is a typical island-arc calc-alkaline volcano (1397 m high), located in the northern part of Martinique Island. It is one of the most active and dangerous volcanoes in the Lesser Antilles arc. Three main stages are now considered in literature separated by two major flank-collapse events (Le Friant *et al.*, 2003 ; Germa *et al.*, 2015; Boudon and Balcone-Boissard, 2021 and references therein). The first stage of edification (550,000-127,000 years), also called the primitive Montagne Pelée, corresponds to lava flows and lava domes building the Mount Conil and followed by a consequent flank-collapse event. The second stage activity (127,000-36,000 years) is marked by dominant lava dome-forming eruptions and associated concentrated pyroclastic density currents (nuées ardentes). A second flank-collapse initiated the third stage (36,000 years-Today). The volcano activity is largely characterised by alternating Plinian and dome-forming eruptions, primarily involving andesitic magmas. Pyroclastic deposits are dominant compared to massive lavas. The total cumulative erupted volume for Montagne Pelée is estimated at ca. 72

km³ (Germa *et al.*, 2015). The most devastating eruption occurred in 1902 and caused the destruction of the towns of Saint-Pierre and Morne Rouge and the death of 30,000 people (Lacroix, 1904).

Scientific research and tradition

Since Alfred Lacroix (1904), Montagne Pelée has been studied extensively. Land based and offshore studies have been published in numerous scientific papers (see Boudon and Balcone-Boissard (2021) for a review). This geosite is included in the French National Geoheritage Inventory and in the UNESCO World Heritage List.



Geological map of Montagne Pelée (modified from Westercamp *et al.*, 1989).

OLIGOCENE LACCOLITHS AND SEDIMENTARY ROCK DOMES OF THE HENRY MOUNTAINS

UNITED STATES OF AMERICA



The diorite porphyry laccolithic intrusion of Mount Hillers, southern Henry Mountains, Utah, is surrounded by upturned beds of strata and interleaved diorite sills dipping 75°–85°.

THE LACCOLITHIC STRUCTURES IDENTIFIED IN 1875 BY G.K. GILBERT AS IMPORTANT MAGMATIC CONTRIBUTIONS TO TECTONIC PROCESSES OF MOUNTAIN BUILDING.

Mountain building is a seminal research topic of tectonics with great significance for society, providing dramatic landscapes with profound effects on ecosystems, climate, and human activities. The dome-like structures in Triassic to Jurassic sedimentary rocks of the Henry Mountains offer the defining locality (Gilbert, 1877) and one of the best exposures

of laccoliths worldwide. Gilbert's scientific methodology, developed while he investigated these structures, combines field observations with mechanical principles to set the example for those who followed (Pollard and Johnson, 1973; Jackson and Pollard, 1990), but it also provides an educational template for students of structural geology (Pollard and Martel, 2020).

GEOLOGICAL PERIOD	Oligocene
LOCATION	Colorado Plateau, United States of America 37°53'16"N 110°41'51"W
MAIN GEOLOGICAL INTEREST	History of geosciences Tectonics

SITE 110



View of Mount Holmes, where G. K. Gilbert on August 22, 1875 developed the concept of a laccolithic intrusion that lifts and bends overlying strata.

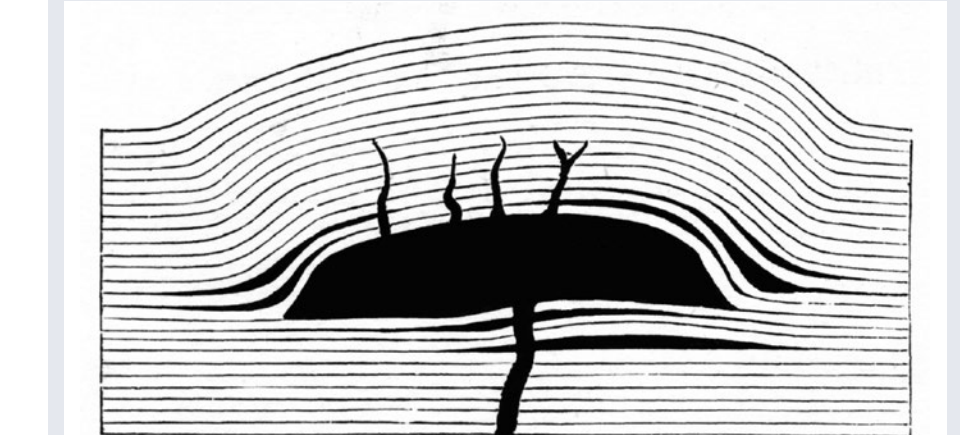
Geological Description

During exploration of the Henry Mountains in 1875, G.K. Gilbert (1843–1918) postulated a process through which magma rose through earth's lithosphere in a dike, spread laterally as a sill, and opened a thick chamber by lifting and bending the overlying strata. He gave these chambers of 'molten rock' the name "laccolite" (now, laccolith) and described associated dikes, uplifted sills, and domed sedimentary strata (Gilbert, 1877; Hunt, 1988). Geological maps of the southern Henry Mountains (Mount Holmes, Mount Ellsworth, and Mount Hillers) show the laccolithic intrusions are circular in plan and formed at similar depths, 3–4 km. The overlying sedimentary rock domes have similar radii, 5–7 km, but their amplitude increases from 1.2 to 1.8 to 2.5 km, respectively. Limb dips steepen from 20° to 50°–55° to 75°–85°, and thus record serial stages in the deformation of strata over the growing laccolithic intrusions (Jackson and Pollard, 1988). The Henry Mountains are the original and now classic examples of magmatic structures building mountains within a broader typology of mountain belts worldwide. Gilbert's investigation exemplifies a scientific meth-

odology that progresses from field observations to idealizations to physical principles to mechanical models to solutions tested using field data (Pollard and Martel, 2020).

Scientific research and tradition

G.K. Gilbert proposed a mechanical model for laccoliths and tested it with field data (Gilbert, 1877). Others followed with computer modeling of faulting and fracturing over laccoliths (Jackson and Pollard, 1988, 1990). Doming over laccoliths is cited as a canonical problem for bending sedimentary strata (Pollard and Martel, 2020).



Gilbert's conceptual model of an ideal laccolith with accompanying sills and dikes, conceived in the Henry Mountains in 1875, published in 1877. Diorite porphyry: black.

MARUIA FALLS

NEW ZEALAND



At Maruia Falls, water cascades over grey sandstone eroding gravel deposits downstream. The boundary between sandstone and gravel may be an older earthquake fault plain. In the area the Alpine Fault coming from the south connects to the Marlborough Fault System.

MURCHISON EARTHQUAKE (1929) CAUSING MARUIA FALLS LED TO THE DISCOVERY OF THE INNER EARTH CORE.

In 1936, the Danish seismologist Inge Lehmann (1888–1993), suggested from the analysis of seismic P-wave data from the 1929 Murchison earthquake, which caused Maruia Falls and which were recorded at seismic stations in Greenland,

that the Earth has an inner core – an important breakthrough in the understanding of the nature of the Earth's interior.

SITE 111

GEOLOGICAL PERIOD	Holocene
LOCATION	Near Murchison, South Island, New Zealand 41°51'36"S 172°15'08"E
MAIN GEOLOGICAL INTEREST	History of geosciences



Inge Lehmann, discoverer of the inner Earth's core, in 1932. (Image courtesy The Royal Library, National Library of Denmark and University of Copenhagen University Library, under a Creative Commons License).

Geological Description

On 17 June 1929, the MS 7.8 Murchison earthquake triggered numerous landslides in the north-western South Island, New Zealand. One of them diverted the course of the Maruia River westward, where it encountered unconsolidated gravel deposits, which it eroded over the years forming a waterfall. At present, its height is about 10 meters. Maruia Falls' significance, however, goes far beyond local geology:

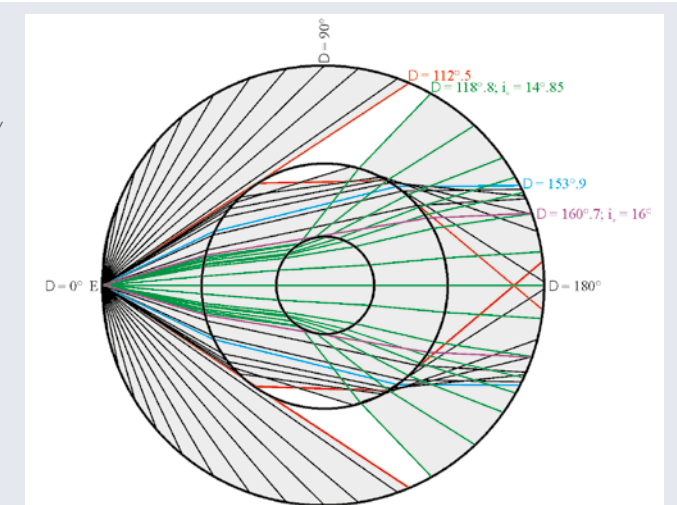
Seismic P waves of large earthquakes travel through the whole Earth. By 1929, it was already known that the Earth had a fluid core, as P waves reached the far side of the globe significantly later than would be expected in a homogeneous globe. Also, the core focused seismic waves acting as a huge lens, creating a shadow zone further out, in which no seismic waves were recorded. In the 1930s, better seismic detectors showed that this shadow zone was not devoid of seismic activity. P-Waves were weak only in terms of surface parallel movements. The vertical movement, however, was quite strong. Explaining seismic activity within the "shadow zone", using data from the Murchison

earthquake, Inge Lehmann postulated the existence of inner Earth's core, which has a higher velocity of seismic waves compared to the outer core.

Scientific research and tradition

Inge Lehmann studied mathematics and science in Copenhagen and Newnham College Cambridge. She worked as a computer at Den Danske Gradmaaling from 1928 onwards being responsible for establishing seismic stations in Denmark and Greenland. She interpreted the institute's seismograms, but also undertook original scientific research. In her 1936 paper P', she postulated the existence of an inner core for the Earth.

Visualisation of Lehmann's simplified earth model: The outer core focuses seismic waves creating a shadow zone, whereas the inner core acts as a diverging lens, shedding seismic energy into the shadow zone (Kölbl-Ebert, 2001).



MER DE GLACE

FRANCE



Mer de Glace, with Mont Blanc summit in the background. The supraglacial debris now completely covers the last two kilometers (Photo: J.-F. Hagenmüller).

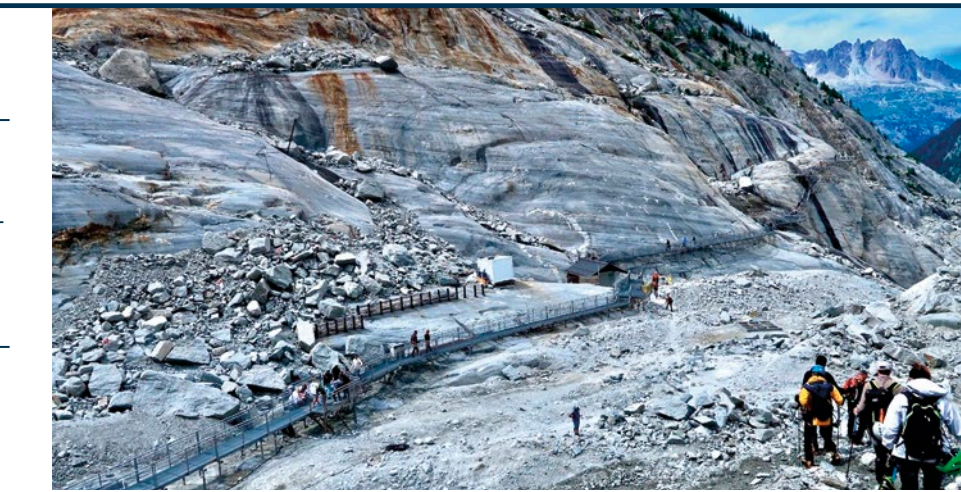
ONE OF THE MOST EMBLEMATIC GLACIERS OF THE WORLD, STUDIED AS EARLY AS THE 18TH CENTURY

The Mer de Glace has been one of the first studied glacier in the world, as early as the 18th Century by de Saussure. Scientific activity has been growing from the 19th century, and Mer de Glace has become nowadays a key place both for the reconstruction of glacier fluctuations during

the Holocene (Le Roy *et al.*, 2015) and the LIA (Nussbaumer and Zumbühl, 2007) and for the assessment of its future dynamics under the current climate change (Vincent *et al.*, 2019; Peyaud *et al.*, 2020). The site is easily accessible to half a million visitors per year since 1909.

SITE 112

GEOLOGICAL PERIOD	Quaternary
LOCATION	Mont-Blanc massif (Western European Alps)/ Auvergne-Rhône-Alpes Region, France 45°54'03"N 006°56'45"E
MAIN GEOLOGICAL INTEREST	History of geosciences Geomorphology and active geological processes



The left side of Mer de Glace valley. The stairs were built to access the man-made ice cave from Montenvers, more than 200 m higher.

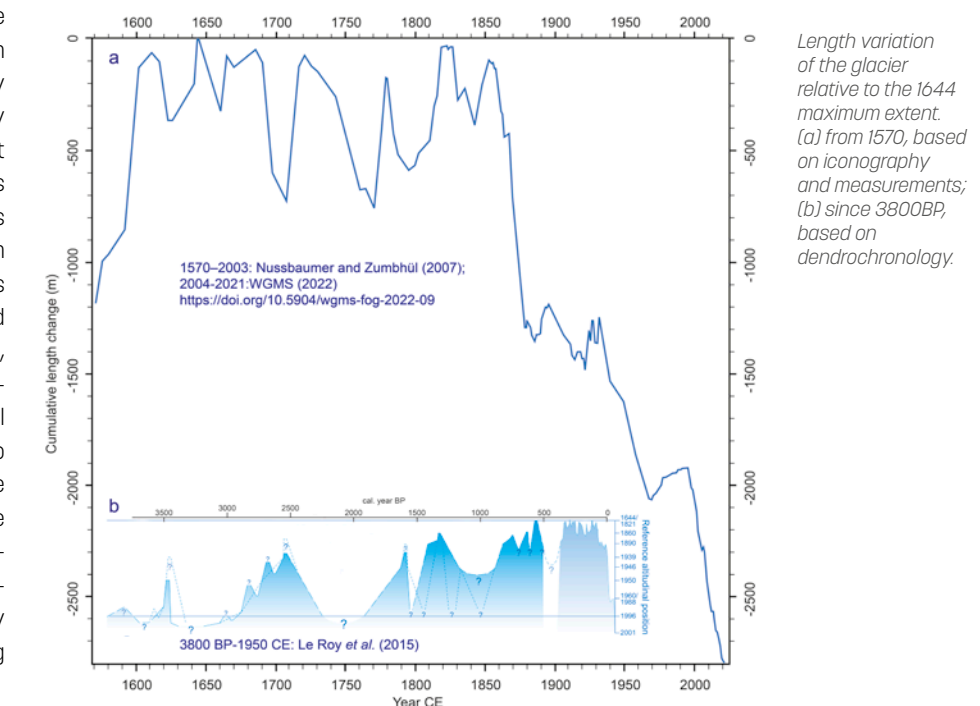
Geological Description

The Mer de Glace is the third largest glacier in the European Alps. It had an area of 28 km² in 2022 including Glacier de Leschaux, its main tributary. It flows from 4205 m asl along 11.5 km, down to 1547 m asl in 2021. Ice thickness ranges from c.300 m where the Tacul and Leschaux Glaciers meet to c.30 m below the Montenvers. Surface ice velocity decreases from 75 to 20 m yr⁻¹, respectively - the ice velocity is maximal (500 m yr⁻¹) at the steep Géant icefall. The Mer de Glace is surrounded by high steep granitic rockwalls culminating at the Aiguille du Midi (3842 m asl), Aiguille Verte (4122 m), and Grandes Jorasses (4208 m). Rockfalls that detached from these permafrost-affected rockwalls, glacially eroded material, and paraglacial reworking of till material from the large lateral moraines have actively supplied debris to the glacier surface since the end of the Little Ice Age (LIA; Deline, 2005). The Mer de Glace front reached the Chamonix valley floor during the second half of the LIA; it then retreated by 2.7 km since 1852 CE, a retreat shortly interrupted by three readvances culminating in 1896, 1931 and 1995.

Scientific research and tradition

Since the 18th century, the Mer de Glace is studied by many scientists, who published a huge literature. A dedicated museum (enlarged for 2026) and scientific and educa-

tional projects have been implemented to promote knowledge of glaciers by a wide audience, in particular as a witness to climate change.



Length variation of the glacier relative to the 1644 maximum extent. (a) from 1570, based on iconography and measurements; (b) since 3800BP, based on dendrochronology.

ESMARK MORaine AND OTTO TANK'S MORaine

NORWAY



1940s aerial view of the Esmark's moraine a few years before the moraine was covered by a pine forest, and the sandur plain, in the foreground. (Widerøe/Hestmark/Djuv).

THE SITES WHERE JENS ESMARK DISCOVERED THE ICE AGE IN 1823.

The comparison of these two moraines, one deposited at the end of the last ice age at sea level where no glaciers are present today and one recently deposited by an extant glacier in the high mountains, made Jens Esmark and his accompanying student Otto Tank, during their fieldwork in 1823, realize that Norway and Northern

Europe had formerly been covered by big glaciers reaching all the way down to sea level, glaciers that had carved out valleys and fjords. The close observation of an extant glacier and its landscape effects thus proved crucial to the discovery of ice ages.

GEOLOGICAL PERIOD	Pleistocene to Holocene
LOCATION	Rogaland and Innlandet counties, Norway Otto Tank: 61°53'37"N 007°26'18"E Esmark: 58°54'14" N 008°08'14"E
MAIN GEOLOGICAL INTEREST	History of geosciences Geomorphology and active geological processes

SITE 113



Otto Tank's moraine in front of Jostedalsbreen 1040 m above sea level, deposited at 'Little Ice Age' maximum ca. 1750. (Hestmark).

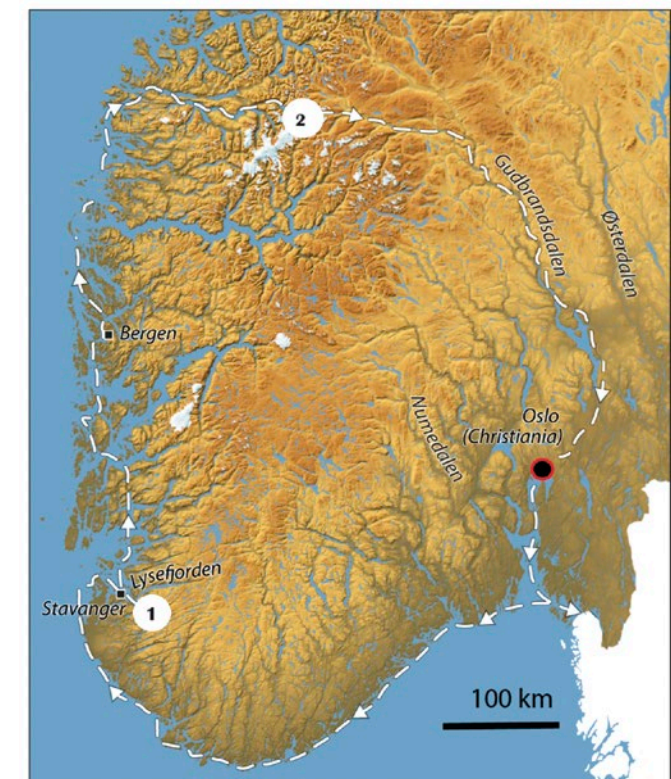
Geological Description

The geomorphological phenomena created by glaciers -moraines, erratic boulders and polished and striated rock surfaces- are the telltale signs of the former presence and greater extension of glaciers in areas where they are today absent. They thus also signal a past colder climate when ice covered a greater part of Earth's surface.

The two moraines are situated transversally in two valleys and mainly differ in size. The Esmark Moraine, deposited at the end of the last ice age close to sea level, is about five times bigger than the Otto Tank Moraine. They both contain a mixture of rock sizes from boulder to clay - a diamictite. Otto Tank's Moraine was deposited by the northern tip of Europe's biggest extant glacier Jostedalsbreen at the culmination of the so-called 'Little Ice Age' around 1750 AD at 1040 m. above sea level in what is today Breheimen national park. In front of both moraines are typical sandur plains where braided glacial rivers once or still flow, depositing the fine bedrock material crushed by the advancing glacier.

Scientific research and tradition

The Esmark moraine was well described by Esmark (1824, 1826) and was been studied by others, e.g. Worsley, 2006. The Otto Tank Moraine was 'rediscovered' by Hestmark in 2008 and published in Hestmark (2017, 2018).



The voyage of discovery 1823. Esmark moraine at site 1 and Otto Tank's Moraine at site 2.

THE PARALLEL ROADS OF GLEN ROY

UK



Classic view of the Parallel Roads of Glen Roy looking northwards from the Viewpoint area. The shorelines are at altitudes of 260m, 325m and 350m. (Photo: CC by 3.0 - Richard Crowe https://commons.wikimedia.org/wiki/File:Parallel_Roads.JPG).

AN ICONIC SUITE OF GLACIAL LAKE SHORELINES THAT UNDERPINNED THE DEVELOPMENT OF THE GLACIAL THEORY IN THE 19TH CENTURY.

The Parallel Roads were fundamental in the development of the Glacial Theory (Agassiz, 1840). They provided convincing evidence for the former existence of glaciers in an area where none exist today, thus refuting the then-prevailing marine submergence theory of Darwin, Lyell and others, although Darwin later recognised his error and subsequently accepted the glacial interpretation (Rudwick, 2017). Since this pivotal contribution, research on the landforms, sediments and chronology of the area has played a major role in understanding the complexity, rapidity and trajectory of landscape evolution and environmental change at the end of the last glaciation (Palmer and Lowe, 2017).

SITE 114

GEOLOGICAL PERIOD	Pleistocene
LOCATION	Lochaber, Scotland, United Kingdom 56°55'40"N 004°47'54"W
MAIN GEOLOGICAL INTEREST	History of geosciences Geomorphology and active geological processes



The Parallel Roads form three distinctive benches along the flanks of Glen Roy.

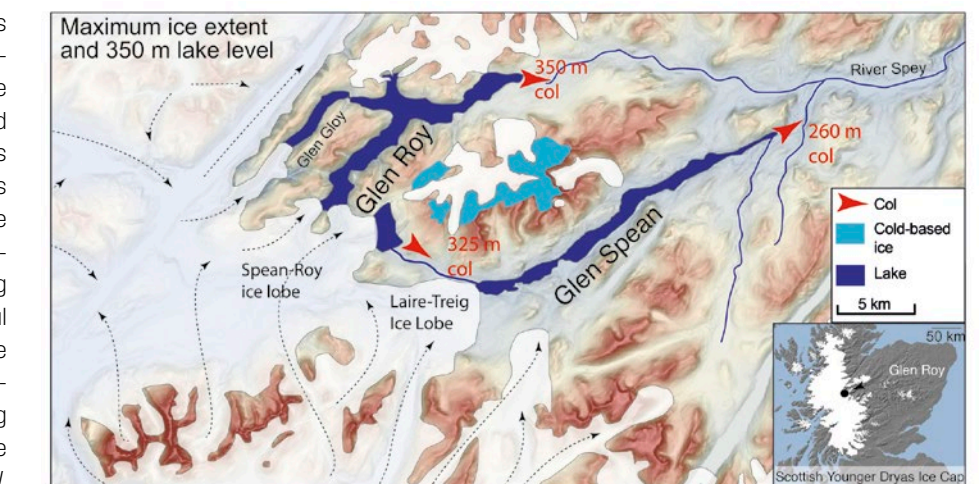
Geological Description

The landscape of the Western Grampian Highlands is dominated by the effects of geomorphological processes that operated during the Quaternary and especially during the Loch Lomond Stade (~Younger Dryas, ~12.9–11.7 ka) (Palmer and Lowe, 2017; Palmer, 2021). Particular highlights are three shorelines ('Parallel Roads') present along the flanks of Glen Roy at altitudes of 260m, 325m and 350m. Louis Agassiz visited Glen Roy in 1840 and, from comparison with similar landforms around modern glaciers in Switzerland, concluded that the Parallel Roads represent the shorelines of former ice-dammed lakes and not, as previously believed (e.g. by Charles Darwin and Charles Lyell), marine shorelines formed during a great submergence. The shorelines demonstrate that glaciers formerly existed in Scotland, providing compelling evidence for Agassiz' theory of continental glaciation during a geologically recent Ice Age. The surface levels of the lakes were determined by those of overspill cols. Building on seminal work by J.B. Sissons during the 1970s and 1980s (Sissons, 2017), Palmer *et al.* (2020) developed a varve chronology which indicates that the lakes existed for 515 years

between ~12.1 ka and ~11.6 ka. The area is a flagship geoheritage locality within the Great Britain Geological Conservation Review (Brazier *et al.*, 2017).

Scientific research and tradition

Glen Roy and Glen Spean have stimulated geological debate from the early-nineteenth century to the present day (Palmer and Lowe, 2017; Rudwick, 2017). They remain a research focus through analysis of annually resolved lake-sediment (varve) records to understand glacier dynamics at decadal scales using high-precision chronologies (Palmer *et al.*, 2020).



Glacier limits and the 350m ice-dammed lake in Glen Roy and Glen Spean. The lake levels were controlled by the altitudes of overspill cols.

2

STRATIGRAPHY AND SEDIMENTOLOGY

SITE 115 - SITE 130



Photo: Bernhard Edmaier

Stratigraphy is the branch of geology concerned with studying sedimentary strata and their chronological relationships. It involves analysing the distribution, deposition, and age of sedimentary strata to understand Earth's history and the processes shaping its surface. **Sedimentology** focuses on sediments and sedimentary rocks – their origin, structure, and depositional process.

Stratigraphy and **sedimentology** are crucial for reconstructing past environments, understanding geological events, and correlating stratigraphic successions, which are essential for defining the geological time scale, which are essential for defining geological time scales. Additionally, they are fundamental in assessing past climate changes, sea-level fluctuations, and the impact of human activities on geological processes and they host economically resources of oil, gas, coal, and minerals. They serve as aquifers of groundwater and provide massive amount of non-economic materials such as sand, gravel, and limestone.

The historical evolution of stratigraphy began in the 17th century with Nicolaus Steno's principles of superposition, original horizontality, and lateral continuity. In the 18th century, James Hutton introduced the concept of deep time and recognized the significance of unconformities. These principles laid the groundwork for understanding how sedimentary layers are deposited over time. The 19th century saw significant advances, in particular of biostratigraphy to correlate and date strata, thanks to scientists like William Smith. Sedimentology emerged as a distinct field in the mid-20th century, with modern theories and techniques emphasizing sediment transport and deposition processes.

Technological innovations and interdisciplinary approaches drive advancements in **stratigraphy** and **sedimentology**, including artificial intelligence through machine and deep learning. High-resolution imaging, geochemical analysis, and computer modelling have enhanced the precision and scope of research. Integration with palaeontology, geochronology, and geophysics has led to a more comprehensive understanding of Earth's history. Researchers increasingly focus on sedimentary records to predict future geological and environmental scenarios, addressing contemporary challenges like climate change and resource management.

The second 100 geological heritage sites include several world-class sites that illustrate singular stratigraphic and sedimentological aspects, from the Precambrian to the present. The Mesoproterozoic Belt-Purcell Supergroup is the oldest, encompassing the thickest sedimentary succession on Earth and capturing pristine Precambrian rocks. Notable Ordovician sites include the Hällekis Quarry with cool to temperate carbonates and the glacial pavements of Tassili n'Ajjer. Two more sites complete the Paleozoic Era: the Carboniferous of The Burren and Cliffs of Moher, exposed in spectacular sea cliffs, and one of the best visible and most accessible reef complexes in the Permian section of the Guadalupe Mountains.

The Mesozoic Era features the Latemar Triassic carbonate platform, the end-Triassic Flood Basalts, and an iconic outcrop of aeolian stratigraphy, the colourfully sculpted Navajo Sandstone landscape, which records the largest erg in geologic history.

The Cenozoic Era includes the Oligocene-Miocene deposits of Meteora, the Scala dei Turchi with Zanclean limestones, the Etosha Pan with Neogene to Pleistocene fossils, and the Racis-ka Pecina Cave with a multi-proxy record of landscape and paleoenvironmental changes. Other sites cover various intervals from the Pliocene to the present, including Kikaijima Island, Shark Bay, the Uyuni salt flat, the Dead Sea, and Lake Salda, a deep alkaline lake that is an excellent analogue for possible ancient life on Mars.

Daniel Ariztegui

Department of Earth Sciences. University of Geneva. Geneva, Switzerland.

Past President. IAS - International Association of Sedimentologists.

IUGS Geological Heritage Sites referee.

Thijs van Kolfschoten

Faculty of Archaeology. Leiden University. Leiden, the Netherlands.

Past President. INQUA - International Union for Quaternary Research.

IUGS Geological Heritage Sites referee.



THE MESOPROTEROZOIC BELT-PURCELL SUPERGROUP

UNITED STATES OF AMERICA AND CANADA



UNESCO World Heritage Site

Majestic view of expansive slopes of Mesoproterozoic sedimentary rock carved by glacial processes still active throughout Waterton-Glacier International Peace Park.

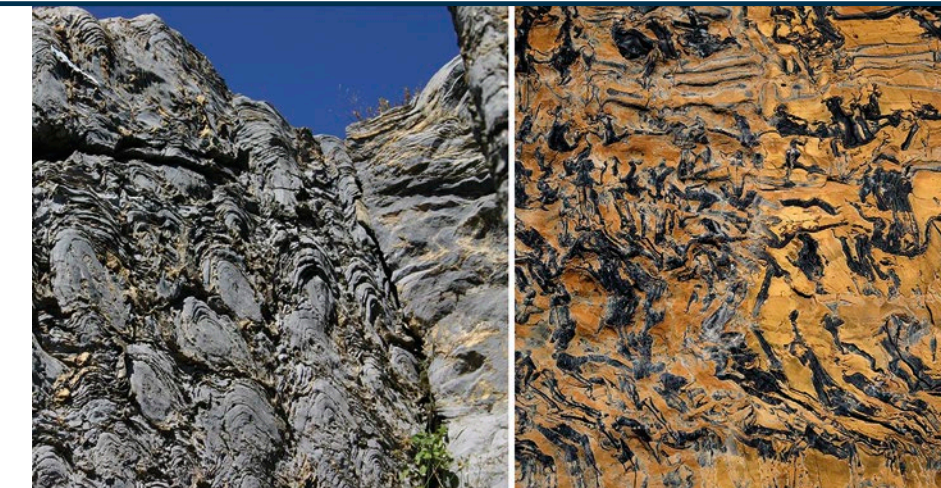
THE THICKEST SEDIMENTARY SUCCESSION ON EARTH CAPTURING PRISTINE PRECAMBRIAN ROCK, SPECTACULARLY EXPOSED BY INTENSIVE GLACIAL CARVING.

The Belt-Purcell Supergroup of western Montana, central and northern Idaho, and southwestern Canada is one of the largest and best studied Mesoproterozoic sedimentary basins in the world. These ancient rocks are relatively undeformed by tectonic forces and undisturbed by plants and animals, resulting in the preservation of pure sedimentary processes,

making them one of the world's finest examples of Precambrian sedimentary rock (Winston and Link, 1993). Intensive glacial erosion of this strata has led to spectacular exposures that have fascinated geologists for over a century. The site is part of Waterton-Glacier International Peace Park UNESCO World Heritage Site.

SITE 115

GEOLOGICAL PERIOD	Mesoproterozoic
LOCATION	Waterton-Glacier International Peace Park, northwestern Montana, USA and southwestern Alberta, Canada 48°57'29"N 113°53'31"W
MAIN GEOLOGICAL INTEREST	History of geosciences Stratigraphy and sedimentology



Beautifully preserved stromatolites of the Siyeh Formation, one of the type localities of the supergroup (left). Textbook example of "molar-tooth" structures, a geologic enigma (right).

Geological Description

The Belt-Purcell Supergroup is an immense package of sedimentary rocks resulting from passive rifting within supercontinent Nuna starting approximately 1.5 billion years ago. This event created a large, intracratonic basin that, during the Mesoproterozoic, filled with up to 11 mi (18 km) of sand, silt, clay, and carbonate sediments resulting in the thickest sedimentary succession on earth (Lonn *et al.*, 2020). Concepts stemming from these rocks not only capture a unique stratigraphic setting, but have implications for other strata of pre-Cambrian age, and the entire Phanerozoic.

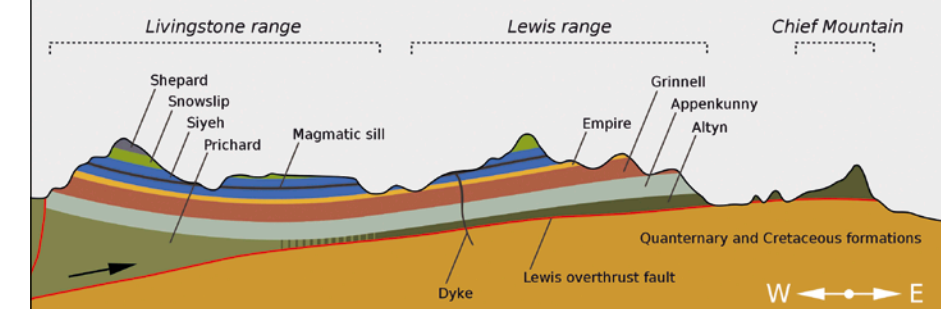
Extensive quaternary glaciation throughout northwestern Montana, USA and southwestern Alberta, CA has resulted in incredible exposures of Precambrian age Belt-Purcell Supergroup in Waterton-Glacier International Peace Park, which, in the Tertiary were displaced eastward onto Cretaceous rocks by the Lewis overthrust fault (Thornberry-Ehrlich, 2004).

The site contains seventeen stratotypes all within the Belt-Purcell Supergroup: two type sections, fourteen type localities, and one

Scientific research and tradition

reference section (Henderson *et al.*, 2020). These stratotypes serve as world-class references for exceptionally preserved sedimentary features like ripples, mud cracks, and crossbedding as well as "molar-tooth" structures, and a variety of stromatolite fossils comprising one of the richest accumulations of Precambrian life in North America (Walcott, 1899). Researchers investigating the complexity within facies are challenging long-held interpretations, leading to continuously evolving conclusions and passionate debates on its origin and depositional environment (Pratt and Rule, 2021).

Cross section of Glacier National Park



Cross section illustrating the vast extent of the Belt-Purcell Supergroup throughout various mountain ranges in Glacier National Park.

THE ORDOVICIAN SECTION OF THE HÄLLEKIS QUARRY SWEDEN



UNESCO Global Geopark

View to the north of the Hällekis Quarry. The succession is approximately 35 meters thick. (Photo: Henrik Theodorsson).

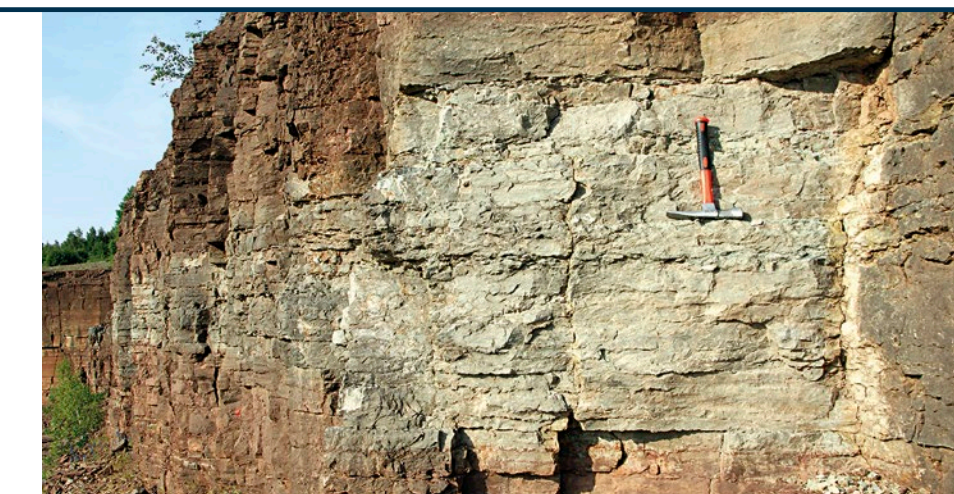
**ONE OF THE MOST COMPLETE,
SPECTACULAR AND MOST
THOROUGHLY DOCUMENTED
SECTIONS OF ORDOVICIAN
COOL TO TEMPERATE WATER
LIMESTONES, GLOBALLY.**

The limestone succession, spanning the Lower–Middle Ordovician boundary, is exceptionally well-exposed and easily accessible, attracting stratigraphers, sedimentologists, paleontologists and geochemists, as well as students from schools and universities. It is a prime example of carbonates formed in an extensive, sediment-starved intracratonic

basin with low net depositional rates. The succession encompasses also the interval that is enriched in extra-terrestrial chromite and has yielded >130 'fossil' meteorites in an active quarry 4 km to the southeast. The quarry is located within a UNESCO Geopark, protected, open as a recreational area, and visited by a large number of tourists every year.

SITE 116

GEOLOGICAL PERIOD	Lower to Middle Ordovician
LOCATION	Kinnekulle, Västergötland, Sweden 58°36'36"N 013°23'37"E
MAIN GEOLOGICAL INTEREST	Stratigraphy and sedimentology Paleontology



The interval with the grey, 1.5-meter-thick 'Täljsten' reflects a prominent sea level drop and is enriched in extraterrestrial chromite grains. (Photo: Anders Lindskog).

Geological Description

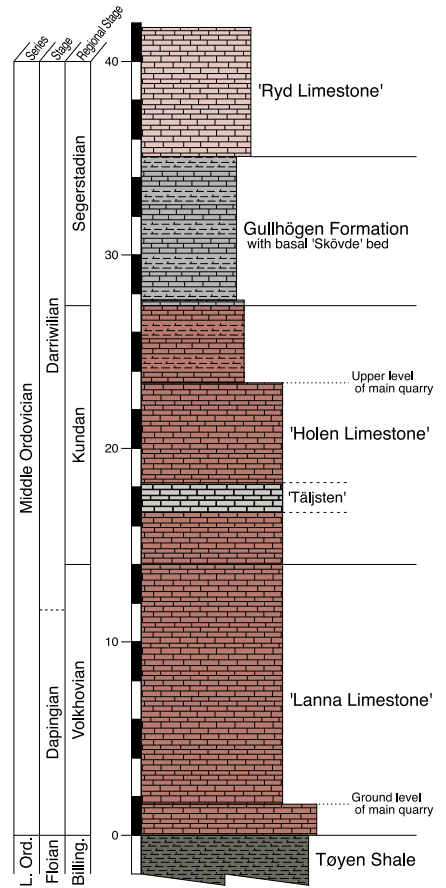
Lower–Middle Ordovician bedded limestones of Sweden have been collectively referred to as the 'orthoceratite limestone'. This world-famous cool to temperate water limestone is widely distributed in Scandinavia, and the table mountain Kinnekulle is regarded as its type area. The 'orthoceratite limestone' here has been the target of numerous focused studies and is among the most thoroughly documented intervals in the Ordovician, both regionally and globally.

The abandoned quarry at Hällekis, Kinnekulle, provides an easily accessible Middle Ordovician succession. The c. 40 m thick succession consists predominantly of 'orthoceratite limestone', often with erosional hardgrounds (Lindskog and Eriksson, 2017; Lindskog *et al.*, 2019). Macrofossils are generally relatively rare, but some beds contain abundant and spectacular accumulations of orthocerite cephalopods and trilobites. Noteworthy is a grey, c. 1.5 m thick unit (the 'Täljsten' or 'carving stone') dominated by in situ preserved specimens of cystoid echinoderms. This interval contains relatively abundant chromite grains with chemical com-

positions that indicate a meteoritic origin. Together with the remarkable occurrence of more than one hundred macroscopic 'fossil' meteorites from the same interval in the Thorsberg quarry to the southeast, this has been linked to an asteroid disruption event in space (Schmitz and Häggström, 2006; Schmitz *et al.*, 2019).

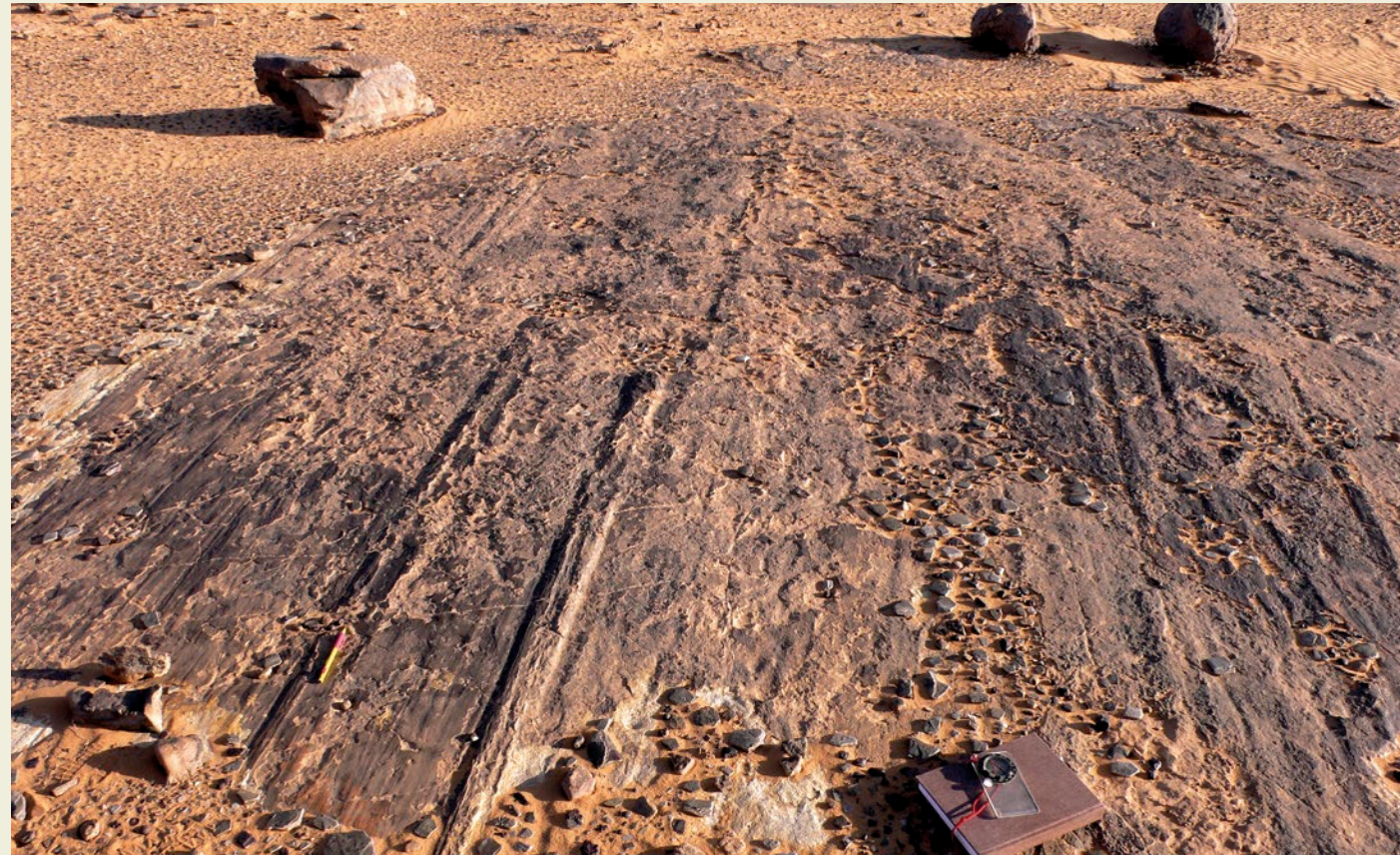
Scientific research and tradition

The 'orthoceratite limestone' has been extensively studied since the mid 1800s. The last three decades have witnessed major efforts to increase our knowledge of the stratigraphy, sedimentology, paleontology, and geochemistry of this limestone interval, and the Hällekis section is significant in understanding the Ordovician world (Streng *et al.*, 2023).



Simplified lithologic succession and stratigraphic units in the Hällekis Quarry. Modified after Streng *et al.* (2023, fig. 13).

THE ORDOVICIAN GLACIAL PAVEMENTS OF THE TASSILI N'AJJER ALGERIA AND LYBIA



UNESCO World Heritage Site

A glacial pavement emerging from the Saharan sands, close to the Algeria-Libya border. It exhibits parallel striae and grooves (ice flowed away from the observer).

SPECTACULAR GLACIAL EROSION SURFACES THAT ALLOW A GLIMPSE OF THE END-ORDOVICIAN ICE STREAMS THAT ONCE CROSSED THE ENTIRE SAHARA.

At the end of the Ordovician, glaciers repeatedly extended over South America, Africa and the Middle East. Meltwater channels, striated pebbles, glaciotectonic fold-and-thrust belts and few tillites have been left behind but the best evidence for an early Paleozoic Ice Age is the stratigraphic superposition of glacial pavements. Recognized from space to field scale, impressive exhumed erosion surfaces are preserved from Mauritania to Chad (Ghienne *et al.*, 2023). In Africa, subsidiary indices occur in Morocco, Ethiopia and South Africa. Together, they highlight past continental-scale ice sheets, which, as in Antarctica today, were drained by ice streams.

SITE 117

GEOLOGICAL PERIOD	Upper Ordovician
LOCATION	Central Sahara, Algeria and Libya 24°55'00"N 010°04'00"E
MAIN GEOLOGICAL INTEREST	Stratigraphy and sedimentology History of geosciences



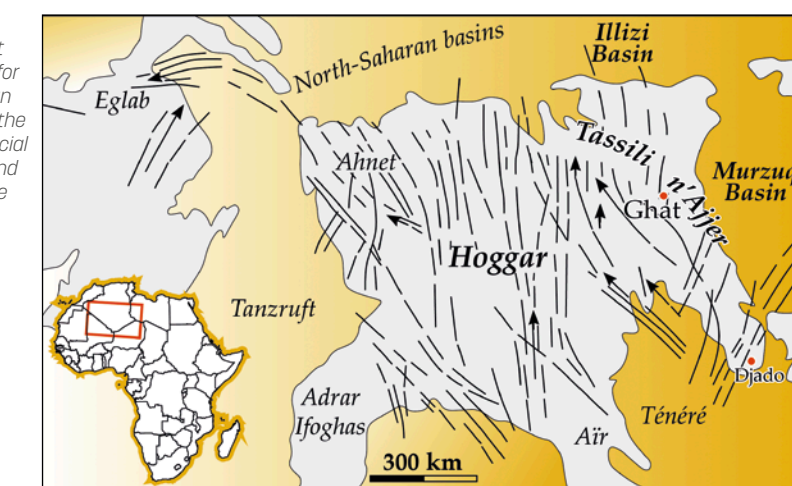
Satellite view of the Tassili n'Ajjer, west of Ghat (SE Algeria – SW Libya). Arrows highlight superposed fields of streamlined bedforms indicative of three ice-streaming events.

Geological Description

The Tassili n'Ajjer is an extensive sandstone plateau gently plunging northeastward into the Illizi (Algeria) and Murzuq (Libya) basins. In its western part wadis have deeply dissected the plateau, and to the east Cenozoic erosion has beautifully exposed stratal surfaces corresponding to paleo-landscapes. From 26°30'N, glacial pavements are identified along the Algerian-Libyan border, as far south as Djado in northern Niger (~700

km). Several surfaces are demonstratively exposed west and south of the town of Ghat, where they constitute 1-10 km-scale corrugations superimposed by subglacial streamlined bedforms best identified on satellite imagery (Moreau *et al.*, 2005). Shear bands are observed in outcrop. They developed in soft sediments –mainly sand–, the substrate of the Ordovician glaciers. Striated and grooved surfaces formed either as intr-

formational shear planes within the subglacial sand, and/or at the ice-sand interface. Sheath folds, sigmoidal fabrics, fluid-escape structures, hydro-schistosity and extensional step fractures (Riedel shears) are additional features linked to subglacial shearing that related to complex sequences of superimposed stages of deformation (Denis *et al.*, 2010). Deformation processes and glacial geomorphology allow us to interpret these streamlined bedforms as the imprints of Ordovician ice streams (Deschamps *et al.*, 2013; Le Heron *et al.*, 2022).



The synoptic map of Beuf *et al.* (1971) gave for the first time an impression of the Ordovician glacial flowlines around and across the Hoggar.

Scientific research and tradition

In the 1960s, a glacial origin was recognized for the Ordovician record throughout the Sahara. Around the Hoggar, the wide distribution of pavements was mapped, promoting the idea of African ice sheets (Beuf *et al.*, 1971). Recently, studies have clarified the chronology and highlighted ice streams, allowing comparison between Paleozoic and Cenozoic glaciations.

CARBONIFEROUS EVOLUTION OF THE BURREN AND CLIFFS OF MOHER IRELAND



UNESCO Global Geopark

The karst landscape of the Mississippian limestone of the Burren.

ONE OF THE MOST COMPLETE SECTIONS WITH MISSISSIPPAN LIMESTONES IN EXCEPTIONAL KARST LANDSCAPES AND PENNSYLVANIAN DELTAICS IN SPECTACULAR SEA CLIFFS.

The Mississippian limestone succession is exceptionally well-exposed and accessible in a dramatic and internationally important karst and biokarst landscape (Best and Wignall, 2016; Gallagher *et al.*, 2006), attracting national and international geologists and geographers. The succeeding Cliffs of Moher siliciclastic basin-fill sequence, spanning the Mississippian-Penn-

sylvanian boundary, is one of the best examples of Palaeozoic deltaic basin-fill successions (Wignall and Best, 2016), exposing syndepositional slumping (Gill, 1979), large growth-fault systems (Wignall and Best, 2004) and condensed sedimentation with biostratigraphically useful fossil ammonoids and conodonts (Hodson and Lewan, 1961; Barham *et al.*, 2015).

GEOLOGICAL PERIOD	Carboniferous (Mississippian to Pennsylvanian)
LOCATION	County Clare, Ireland 53°00'46"N 009°24'05"W
MAIN GEOLOGICAL INTEREST	Stratigraphy and sedimentology Paleontology

SITE 118

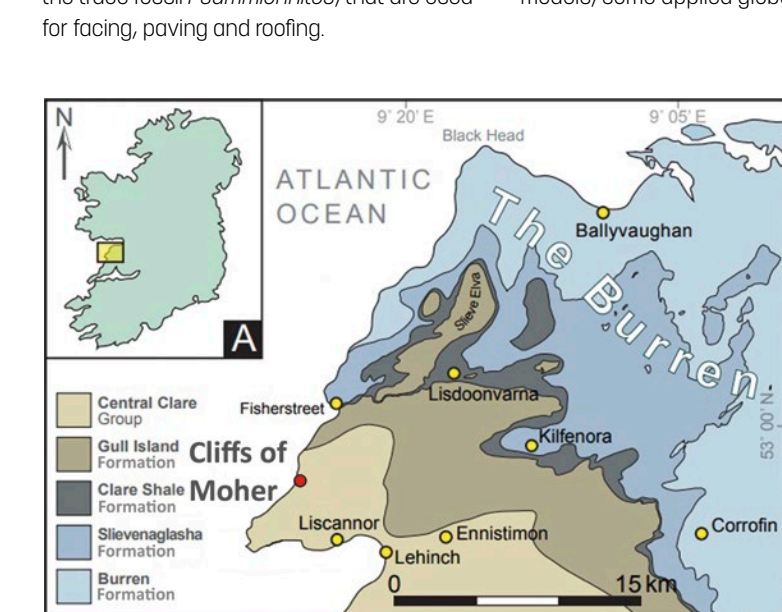


The sedimentary layers of the Cliffs of Moher, County Clare, Ireland.

Geological Description

The Mississippian limestones of the Burren are exposed in an exceptional glacio-karst landscape in extensive exposures. These bioclastic limestones range in age from the Holkerian to Brigantian regional substages of the Viséan, based on foraminferan assemblages. The platform carbonate succession contains cyclic sedimentation patterns with bryozoan, crinoidal, coral, brachiopod and algal communities responding to glacio-eustatic cyclicity. The formations exposed are the Tubber, Burren and Slievenaglasha formations. The Burren Formation contains well-developed palaeokarst horizons.

The Cliffs of Moher expose Pennsylvanian deltaic siliciclastic sedimentation. These units form part of a fine-grained continuous basin-fill sequence recording offshore prodeltaic through prograding delta slope to delta top environments. Thicker, coarser sandstone beds are readily visible as they project slightly and form overhanging ledges. Channels are clearly seen in some sections. The exceptionally large outcrops of the Cliffs of Moher host a growth-fault complex which affects strata up to 60 m in thickness and



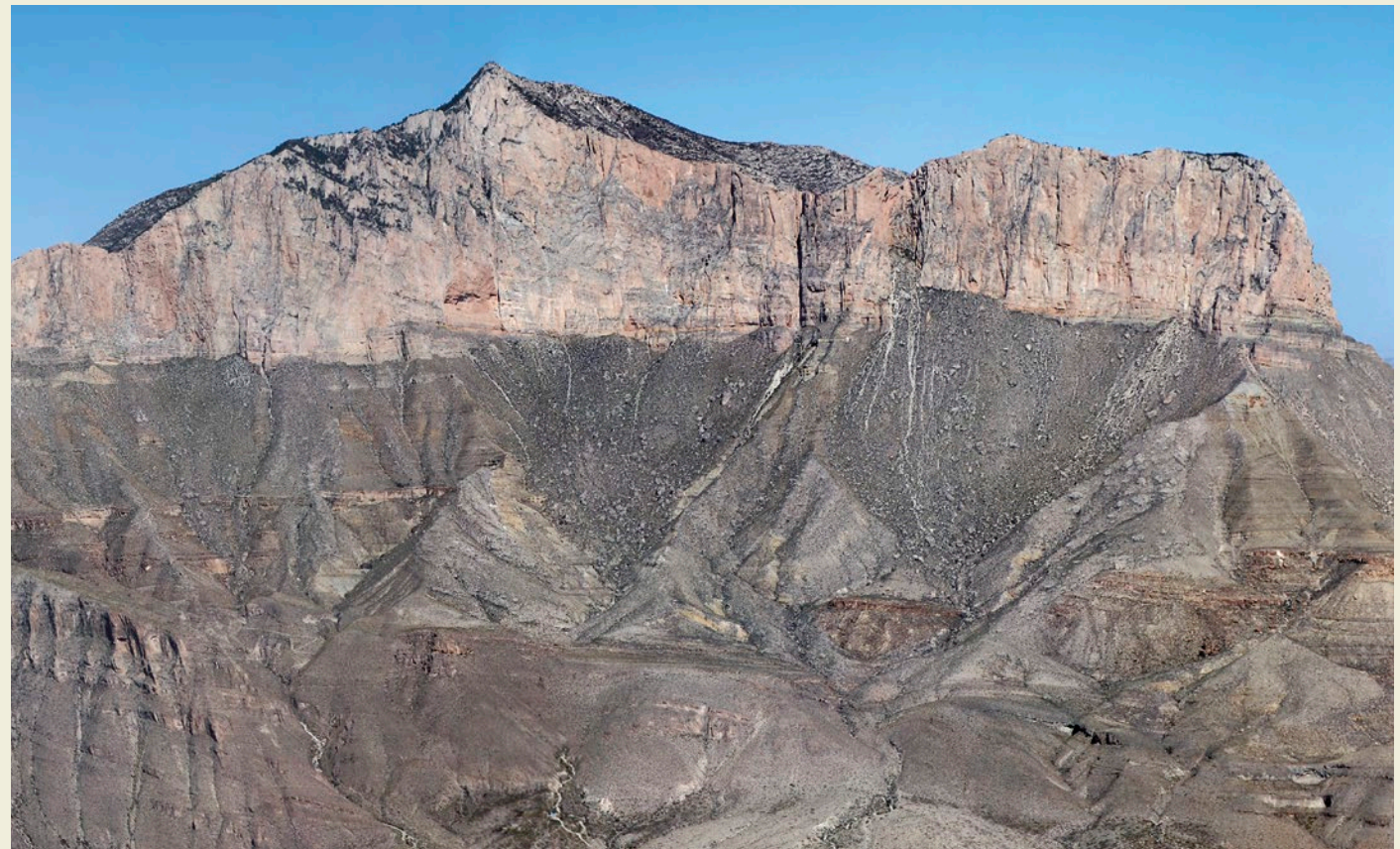
Scientific research and tradition

extends laterally for 3 km. The succession contains laterally extensive condensed horizons in shales with bands of ammonoids that range from the H1b to H1c ammonoid biozones (Chokierian to Kinderscoutian regional substages). Thin sandstones known locally as 'Moher Flagstones' contain an abundance of the trace fossil *Psammichnites*, that are used for facing, paving and roofing.

The Cliffs of Moher and the Burren were first documented by geologist Frederick J. Foot in 1863. In the mid-twentieth century the area was central to development of biostratigraphy based on ammonoids (Hodson and Lewan, 1962). Since then the area has informed basin evolutionary and oil-reservoir models, some applied globally.

Map and stratigraphy of the Burren and Cliffs of Moher section.

PERMIAN REEF COMPLEX OF THE GUADALUPE MOUNTAINS UNITED STATES OF AMERICA



The Western Escarpment of the El Capitan (on the right) and Guadalupe Peak (highest in the image), part of the Guadalupe Mountains where a unique stratigraphic profile of the Permian Reef is shown.

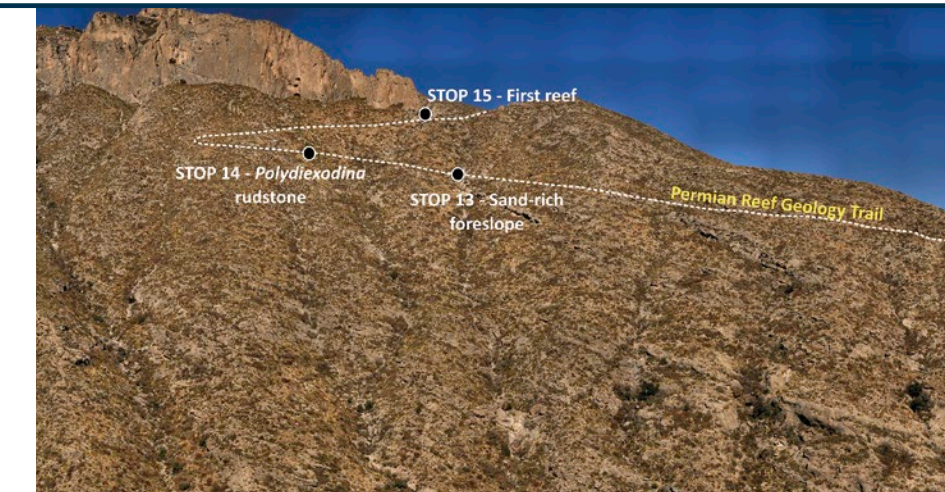
ONE OF EARTH'S BEST EXPOSED AND MOST ACCESSIBLE ANCIENT REEF COMPLEXES.

The well-documented stratigraphic relationships of the Capitan Reef (including Bebout and Kerans, 1993, a thoroughly illustrated trail guide) make PRGT a must-see locality for geoscientists. Alongside a state-of-the-art stratigraphic framework, world renowned deep-water deposits (Beaubouef *et al.*, 1999), and nearby Carlsbad Caverns, Guadalupe Mountains

National Park is one of the most visited by geoscientists. The Western Escarpment, with its 2 km vertical exposure of shelf-to-basin successions, is one of the world's primary references for sequence stratigraphy (Kerans *et al.*, 2021). The park also contains three GSSPs, Middle Permian reference datums for the international Geologic Time Scale (Glenister *et al.*, 1992).

GEOLOGICAL PERIOD	Permian (Cisuralian to Guadalupian)
LOCATION	West Texas (or Desert Southwest), United States of America 31°53'39"N 104°49'18"W
MAIN GEOLOGICAL INTEREST	Stratigraphy and sedimentology Paleontology

SITE 119



The Capitan Reef profile and reef trail at McKittrick Canyon, Guadalupe Mountain National Park, Texas. A detailed trail guide exists to guide observations.

Geological Description

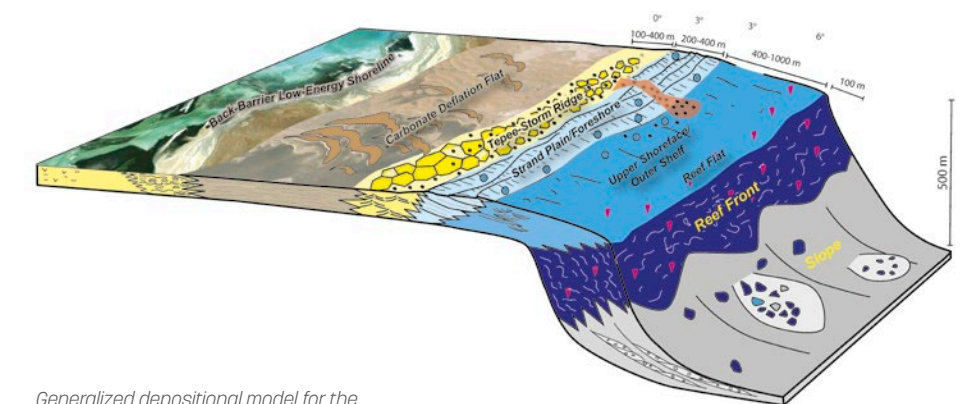
Exposures of Permian strata within Guadalupe Mountains National Park represent one of Earth's best exposed and most accessible ancient reef complexes. Using the Permian Reef Geology Trail (PRGT), thousands of visitors a year hike the ancient sea floor profile extending from a 700 m deep basin floor to the top of the shallow water shelf, crossing an extensive transect of the well-documented Capitan Reef. The exquisite depositional facies observed along the PRGT are a fundamental teaching tool for geoscientists, where the evolution of sedimentary facies can be linked directly to the dramatic bathymetric profile. Geologists since the classic work of Philip King (1948) and Norman Newell *et al.* (1953) have illustrated this world class exposure, and hundreds of students and researchers have undertaken the pilgrimage in their footsteps. In addition to the PRGT, the Western Escarpment of the Guadalupe Mountains, which is as tall as the Grand Canyon is deep, provides a unique stratigraphic profile where the entire vista of shallow water shelf strata can be observed to transition through the reef to the basin floor. No single exposure in the stratigraphic

record of North America so well exposes this shelf to basin transition and all its associated complexities.

Scientific research and tradition

The Guadalupe Mountains have been intensively studied since the early 1900's as the Permian Basin became a focus for energy exploration. King (1948) stands today as one of the most exemplary geologic characterizations of a national park. Reef paleoecology, sequence stratigraphy, and global GSSPs are other key areas of research.

Depositional Dip
(subtract 2° from avg. dips assuming tepee complex flat)



Generalized depositional model for the Capitan Reef and associated shelf and slope-basin deposits.

LATEMAR TRIASSIC CARBONATE PLATFORM ITALY



The well layered platform interior facies of the Latemar platform (Cimon del Latemar, 2846 m a.s.l.).

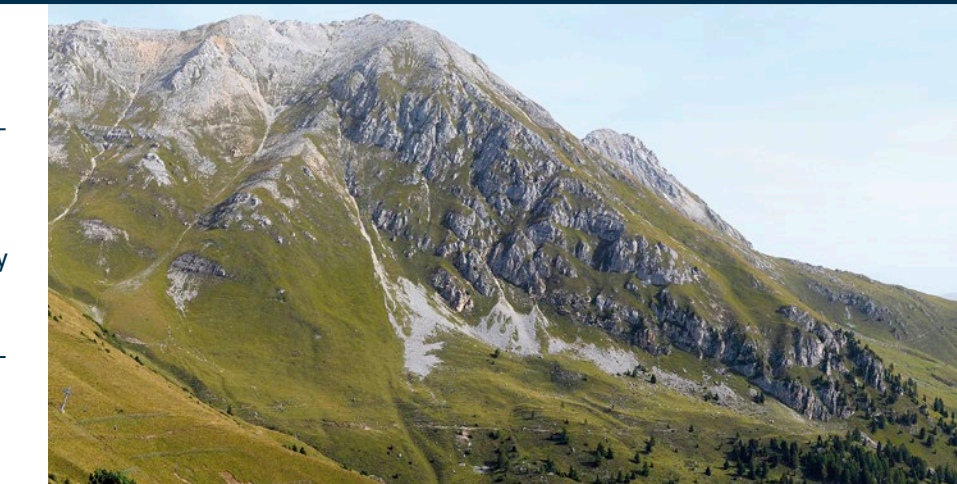
A FULLY PRESERVED ISOLATED CARBONATE PLATFORM, PROBABLY WITH THE BEST EXPOSED FACIES TRANSITIONS AND DEPOSITIONAL GEOMETRIES IN THE WORLD.

The Latemar is in the World Natural Heritage Site of the Dolomites, which are a World reference for depositional geometries and stratigraphy of high-relief carbonate platforms (Gianolla *et al.*, 2008). The Latemar well represents this geological value by being an isolated carbonate platform, somehow a fossil atoll, that exposes some of the best facies transitions and depositional geometries globally, and

the one with longer and wider tradition of geological studies. Due to its perfect exposure and completeness of depositional features, it became a standard for the study of the evolution of Phanerozoic carbonate platforms (Gaetani *et al.*, 1981), cyclostratigraphy; dolomitization processes and the geometry of microbial carbonate platforms (Preto *et al.*, 2021).

GEOLOGICAL PERIOD	Middle Triassic
LOCATION	The Dolomites of Northern Italy, between the provinces of Trento and Bolzano/Bozen, Italy 46°22'51"N 011°34'30"E
MAIN GEOLOGICAL INTEREST	Stratigraphy and sedimentology

SITE 120



The flat top of the Latemar between Torre di Pisa and Cima Feudo and its regular southern slope inclined at ca. 30°. It corresponds to the shape of the platform in the Late Anisian (ca. 242 Ma).

Geological Description

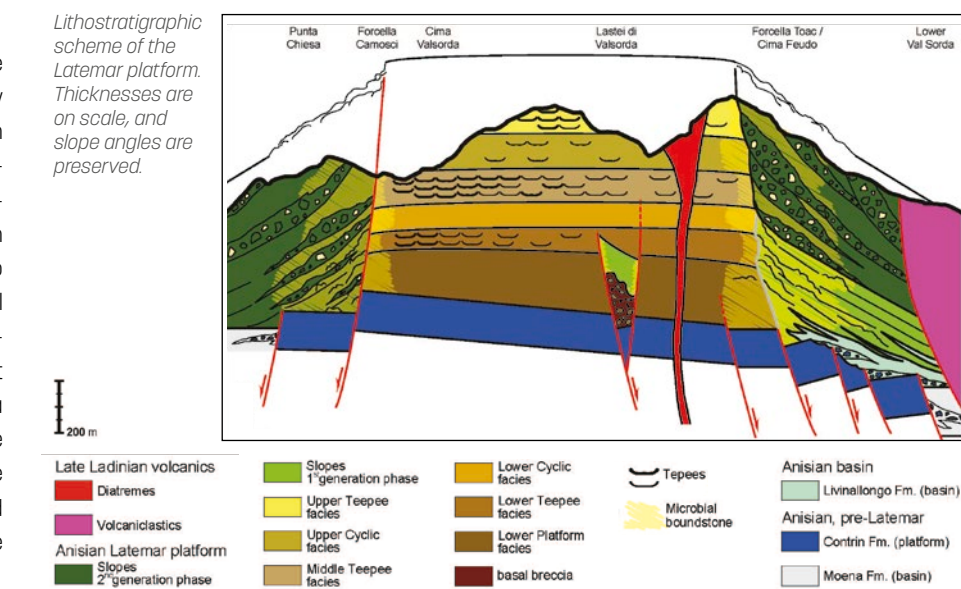
The Latemar is a small mountain group ca. 6-8 km in diameter and with an elevation of its highest peak of. It is a fossil carbonate platform made of late Anisian (middle Triassic) limestone, which in the central part is well layered, each layer corresponding to a peritidal cycle and recording a high-frequency oscillation of relative sea-level (Goldhamer *et al.*, 1987).

The layered nucleus contains green algae and molluscs; it is surrounded by a narrow belt of massive microbial boundstones with few calcareous sponges and corals. Seaward, steep slopes with a primary inclination of ca. 30° are preserved, and contain coarse breccia deposits with blocks up to few m large and made mostly of microbial boundstone. At their base, slopes are interfingering with nodular limestones with chert nodules and a pelagic biota, deposited in a basin many hundreds of meters deep. These facies transitions and geometries can be viewed from a ring of roads that run around the massif, which is also crossed by a dense network of hiking trails.

The calcareous massif was later affected by partial dolomitization. It exhibits a sharp and articulated dolomitization front, which has been the object of several studies (Jacquemin *et al.*, 2014).

Scientific research and tradition

The Dolomites have been a hotspot for geological thinking since the 19th century thanks to studies on carbonate sedimentology. Within the Dolomites, the Latemar became a reference because many geological features are fully exposed. As of December 2023, more than 70 papers on the Latemar geology are indexed in Scopus.



END-TRIASSIC FLOOD BASALTS AT THE OLD WIFE CANADA



UNESCO Global Geopark

Seacliffs at the Old Wife, with dark flood basalts overlying red sedimentary strata of the Triassic rift valley

**ONE OF THE WORLD'S
GREATEST TESTIMONIALS TO
THE BREAKUP OF PANGEA,
IMPLICATED IN THE END-
TRIASSIC MASS EXTINCTION
EVENT.**

This IUGS Geological Heritage site bears witness to forces and events generally unseen: the plate tectonic forces of a dynamic Earth and its consequences to life on our planet. The breakup of the supercontinent Pangea and a cause of one of

the greatest mass extinction events in the history of Life on Earth are both recorded here. The dramatic cliffscape in which these are exposed are consequences of the erosive power of the world's greatest tides in the Bay of Fundy.

GEOLOGICAL PERIOD	Upper Triassic
LOCATION	Cliffs of Fundy UNESCO Global Geopark, Nova Scotia, Canada 45°23'15"N 064°02'54"W
MAIN GEOLOGICAL INTEREST	Stratigraphy and sedimentology Tectonics

SITE 121



Runners pass by the Old Wife geosite at low tide.

Geological Description

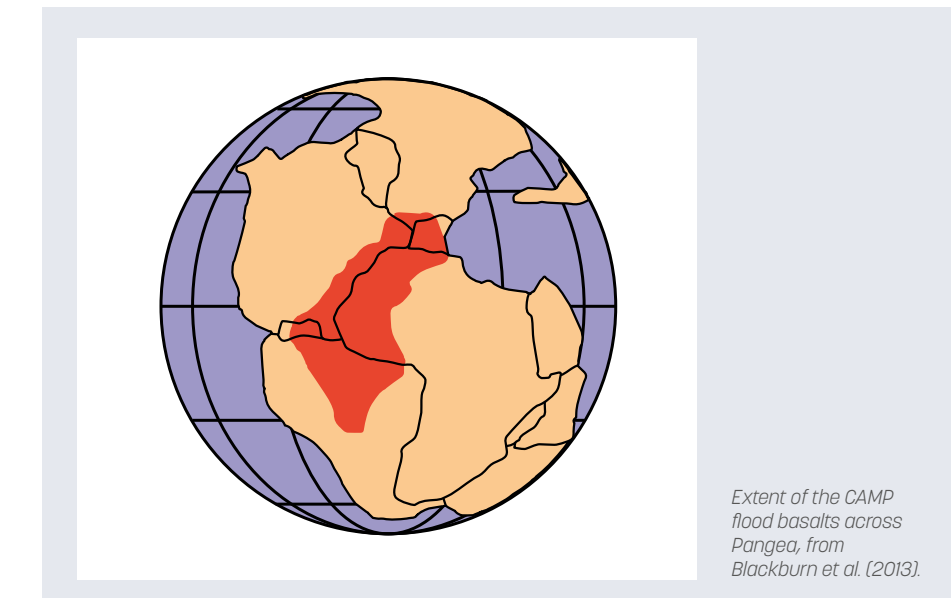
The flood basalts of the Central Atlantic Magmatic Province, the most areally extensive in Earth history, attended the breakup of the supercontinent Pangea at the close of the Triassic Period. The resulting, profound global change is implicated in the end-Triassic mass extinction event that provided dinosaurs free reign to become the dominant animals on terrestrial Earth for the remainder of the Mesozoic Era, approximately 135 million years.

The basalts cooled from lava flows that erupted as North America separated from northwestern Africa, eventually giving birth to the Atlantic Ocean in the Jurassic Period. Zeolite-rich vesicular basalts occur at the western end of the section, whereas columnar structures are evident at the Old Wife headland itself. The distinctive orange-red sedimentary strata below the flood basalts were deposited within a semiarid failed rift valley in which are found fossils of the precursors to dinosaurs and their contemporary fauna. The dominant mud-rich sediments are punctuated by thin pale grey lacustrine beds that have been ascribed to climatic cy-

Scientific research and tradition

clicity of the Milankovitch band. At Red Head in the far eastern part of the cliff section, cross-bedded aeolian sandstones form part of the rift valley-fill in this classic section.

The coastal cliff section at the Old Wife has been studied by geologists for more than a century as a classic example of rift valley evolution from basin infilling through eruption of flood basalts. More recently, it has served as a geochronological point in deciphering the end-Triassic extinction event.



Extent of the CAMP flood basalts across Pangea, from Blackburn et al. (2013)

THE JURASSIC NAVAJO SANDSTONE AT COYOTE BUTTES AND THE WAVE UNITED STATES OF AMERICA



Wind funnels and circulates to form The Wave in aeolian Jurassic Navajo Sandstone. Cyclic cross bedding informs paleoclimate conditions, accentuated by diagenetic iron coloration. Image: M. Chan.

**AN ICONIC OUTCROP OF
AEOLIAN STRATIGRAPHY, THIS
COLORFULLY SCULPTED NAVAJO
SANDSTONE LANDSCAPE
RECORDS THE LARGEST ERG IN
GEOLOGIC HISTORY.**

The Jurassic Navajo Sandstone preserves cyclic packages of thick aeolian cross bedding. These cross beds collectively record past wind directions and climatic conditions for the largest erg in geologic history, including preserved evidence of life and the dynamic processes of the vast, ancient desert (Loope and Rowe, 2003). Vibrant iron coloration reflects the

diagenetic fluids that interacted within the porous sandstone. The Wave and Coyote Buttes capture the convergence of coloration and the exquisite etching and enhancement of cross bedding through modern erosion. This stunning combination is a world renowned destination for geologists, photographers, and outdoor enthusiasts.

SITE 122

GEOLOGICAL PERIOD	Lower Jurassic
LOCATION	Vermilion Cliffs National Monument, Utah and Arizona, United States of America 36°59'45"N 112°00'23"W
MAIN GEOLOGICAL INTEREST	Stratigraphy and sedimentology Geomorphology and active geological processes



Vivid coloration follows aeolian laminae and strata leading towards The Wave at the Coyote Buttes. Image: V. Thompson.

Geological Description

The Lower Jurassic Navajo Sandstone preserves the largest erg in Earth's history. Of all Navajo Sandstone outcrops, the Coyote Buttes is renowned for stunning coloration and outcrop features including The Wave — where vivid colors accent aeolian cross strata to resemble a cresting ocean wave.

Red, orange, pink, purple, yellow, brown and white colors document a complex history of chemical interactions between iron enriched fluids and ground water — concentrating or removing iron oxide grain coatings and cement within the sandstone. Coloration patterns are influenced by sedimentary textures

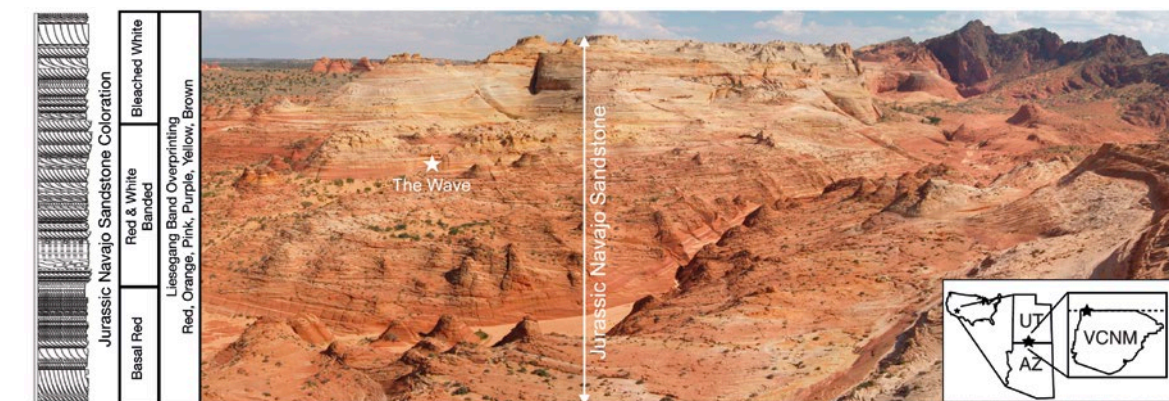
and tectonic structures at microscopic to outcrop to regional scales (Seiler and Chan, 2014). The Wave's sculpted form initiated with water incision along a prominent joint; winds actively scour and accentuate the aeolian bedding as the predominant contemporary erosional force (Loope *et al.*, 2008).

The larger Coyote Buttes region likewise displays unique and spectacular alcoves, bowls, faces and bluffs shaped by wind and dramatically colored by fluid flow. Large dune sets show cyclic cross bedding driven by paleoclimate. Dinosaur tracks document a rich paleontologic history. Extensive soft sediment deformation suggests seismic shaking during

the Jurassic (Chan and Bruhn, 2014). Contemporary weathering crack patterns compose analogs to Mars (Chan *et al.*, 2008).

Scientific research and tradition

The Coyote Buttes' geologic history and corresponding research spans sand dune deposition, dinosaur trackways, burial, diagenetic coloration, and later exhumation with fine finishing touches of smooth, wind sculpted weathering. This geosite is unparalleled for exquisite preservation of aeolian laminae in dramatic colors.



The Coyote Buttes and The Wave (star) located along the Utah – Arizona border within the Vermilion Cliffs National Monument, United States. Image: W. Seiler.

THE OLIGOCENE-MIOCENE MOLASSIC AND ROCK PINACLES OF METEORA GREECE



UNESCO World Heritage Site

UNESCO Global Geopark

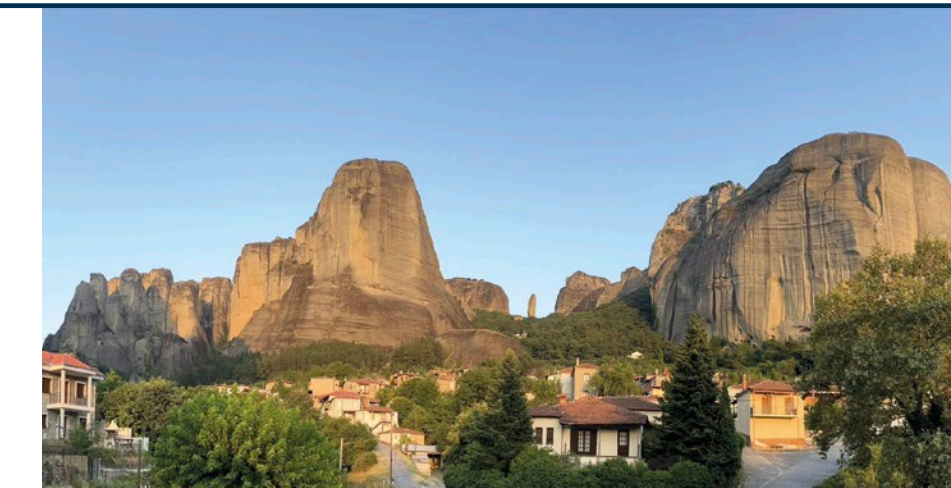
ONE OF THE MOST IMPRESSIVE MOLASSIC ACCUMULATIONS OF THE WORLD WITH AN ICONIC LANDSCAPE OF PINNACLES AND ROCK PILLARS FORMATIONS.

Meteora is one of the most iconic geological landscapes of the World. It is a complex of impressive rock pillar formations made by a huge accumulation of molassic sediments. The complex of Meteora is a perfect conjunction of tectonic, sedimentologic and geomorphologic processes which are very important for understanding the geology of the Hellenic orogen

Byzantine monasteries were built on the top of many of these rocks pillars, creating a unique sacred landscape declared as a mixed UNESCO World Heritage Site in 1988, including criteria viii for its geological value. Meteora is one of the most important touristic destination of Greece with over 2 million visitors every year.

SITE 123

GEOLOGICAL PERIOD	Oligocene to Miocene
LOCATION	Thessaly Region, Greece 39°43'18"N 021°37'50"E
MAIN GEOLOGICAL INTEREST	Stratigraphy and sedimentology Geomorphology and active geological processes



Spectacular pinnacles located just above the small town of Meteora. (Photo: Asier Hilario).

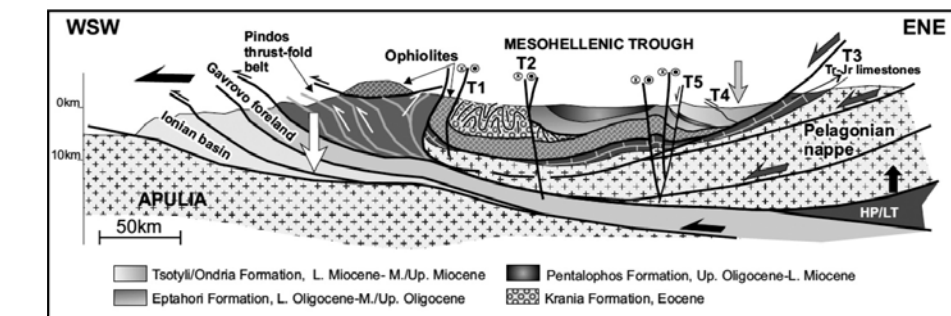
Geological Description

Meteora landform is a complex of impressive rock pillar formations composed of molassic sediments deposited in the Mesohellenic trough. The spectacular pinnacles are 200 meters high and up to 300 meters wide. The Meteora rocks belong to the "Pentalophos Formation," of Upper Oligocene - Lower Miocene age (Brunn, 1956). The maximum thickness of the formation is about 4,000 meters. It is mainly characterized by thick beds of sandstone and the intense presence of conglomerates of various sizes, which in Meteora reach large dimensions. The sediments are essentially of marine origin; however, there have also been interpreted as fluvial and terrestrial material. The stratigraphic succession of the Meteora conglomerates includes the Lower Meteora Conglomerates composed of fan-deltas and the Upper Meteora Conglomerates, composed of dominantly fluvial deposits. The conglomerates were deposited in a Gilbert-type deltaic system, where large channels occurred, entrenched vertically to the progression axis of the delta. The current formation of Meteora landforms is due to tectonic fracturing, which formed surfaces of discontinuities, erosion by flow-

ing water and to a smaller extent by aeolic erosion of the materials of the molassic series. However, the tectonic activity had a significant impact on their formation and distribution to form this unique morphology. Meteora, beyond their natural beauty, is a very important site for understanding the geology of the Hellenic orogen.

Scientific research and tradition

The most comprehensive sedimentary description of the formations comprising the Meteora rock spires is that of Brunn (1956). Since then several other national and international researchers studied the area from different geological disciplines. Meteora is a common destination for universities from all over Greece and surrounding countries.



Geological structure of Meteora Pyli area (Kilias, A. et al., 2015).

PLIOCENE CYCLOSTRATIGRAPHY OF SCALA DEI TURCHI ITALY



Panoramic view of Punta di Maiata. Deposition of the distinct lithological cycles of calcareous and marly limestones of the Trubi Formation was astronomically controlled. Layers richer in carbonate correspond to eccentricity minima.

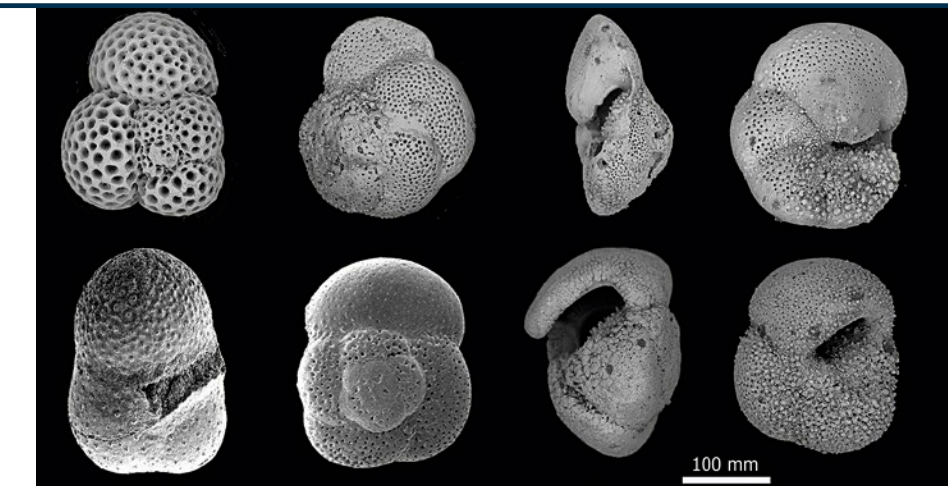
A BEAUTIFUL NATURAL CLIFF WHERE ZANCLEAN CALCAREOUS AND MARLY LIMESTONES REFLECT DEPOSITIONAL CONTROL BY MILANKOVITCH CYCLES

The Punta di Maiata (Scala dei Turchi) and Eraclea Minoa sections represent the reference sequences of the entire Pliocene and contain the Messinian-Zanclean boundary at the Arenazzolo-Trubi contact. The boundary represents the return to normal marine condition after the Messinian Salinity Crisis. The beautiful exposure

and the clear signal of the Milankovitch cycles make these sections a clear scientific example recognized worldwide. Punta di Maiata was previously chosen for the Messinian-Zanclean GSSP, but due to the weak paleomagnetic signal was then replaced by the Eraclea Minoa section that outcrops only 25 kilometers away.

SITE 124

GEOLOGICAL PERIOD	Miocene to Pliocene
LOCATION	Sicily - Realmonte, Italy 37°17'23"N 013°28'21"E
MAIN GEOLOGICAL INTEREST	Stratigraphy and sedimentology Paleontology



Key planktonic foraminiferal species from the Scala dei Turchi section, providing a Zanclean-Piacenzian age for the Trubi Formation.

Geological Description

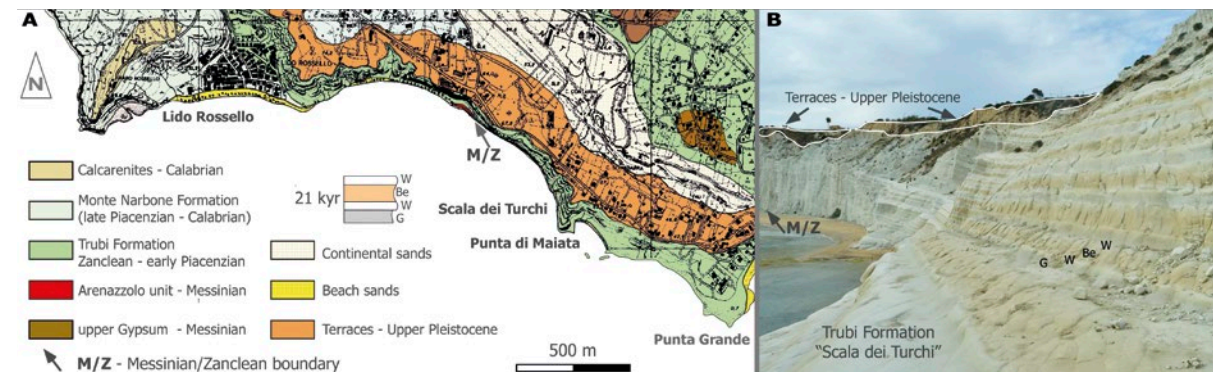
The Punta di Majata sequence is a beautiful sedimentary succession from Messinian to Pleistocene constituted by 93 m of calcareous marls and marly limestones, known as Trubi Formation and represent the return to normal marine conditions after the Messinian Salinity Crisis. The outcrop is known as "Scala dei Turchi" and includes the Messinian-Zanclean boundary. The section is constituted by 96 lithological cycles made by a quadriplet (grey-white-beige-white) that reflects astronomical controlled. The colour variations are due to precessional cycles that induced climatic and oceanographic

variations in the Mediterranean Sea. Here was proposed the astronomical tuning for the whole Pliocene sequence. Grey layers are richer in warmer planktonic foraminifers, lower oxygen isotope values and higher content of illite and chlorite. The clays minerals formed in warmer and humid conditions during insolation maxima. On the contrary, beige layers are richer in temperate species and in palygorskite that is a clay mineral typical of arid conditions, transported as dust from north African during insolation minima. The thickness of some beige layers is due to the obliquity of earth's axis. The richer carbonate layers, clearly visible in the profile of

the cliff, formed by an increase of calcareous planktonic microfossils deposited during eccentricity minima (100-400 kyr).

Scientific research and tradition

The succession was studied in the 1970's when it was proposed as the stratotype for the Zanclean Stage (Cita and Gartner, 1973). In 1991 it became the reference section for the Pliocene Astronomical Time Scale (Hilgen, 1991; Lourens *et al.*, 1996). Numerous teams published data on foraminifera, paleomagnetism, mineralogy, stable isotopes and alkenones.



A) Geological map of Realmonte-Scala dei Turchi; B) particular view of the quadriplet precessionally controlled at Scala dei Turchi; to the left of the Messinian-Zanclean boundary.

ETOSHA PAN

NAMIBIA



Panorama of the Etosha Pan.

ONE OF THE LARGEST PALAEOLAKE SALT PANS IN THE WORLD, WHICH SUPPORTED A DIVERSE NEOGENE TO PLEISTOCENE FOSSIL FAUNA.

The extensive Kalahari Supergroup is a key component of the geology of Central and Southern Africa. Consisting of unconsolidated to calcrete-cemented fluvial, pedogenic and aeolian sediments, it is poorly understood and difficult to date. Fossils discovered by Hipondoka (2005) and studied by Miller *et al.* (2010) and Pickford *et al.* (2016), together with the

geomorphological evolution of Etosha Pan recorded by Buch and Rose (1996) and Buch *et al.* (1992), have highlighted for the first time the late-stage evolution of the upper Kalahari through alternating periods of seasonal rainfall and hyper-aridity that match palaeoclimate records from East Africa (DeMenocal, 2004).



GEOLOGICAL PERIOD	Miocene to Pleistocene
LOCATION	Oshikoto and Oshana Regions, Namibia 18°46'00"S 016°22'00"E
MAIN GEOLOGICAL INTEREST	Stratigraphy and sedimentology Geomorphology and active geological processes Paleontology

Excavated 4-5 million year old fossil skeleton of the most complete southern mammoth, *Mammuthus subplanifrons*.

Geological Description

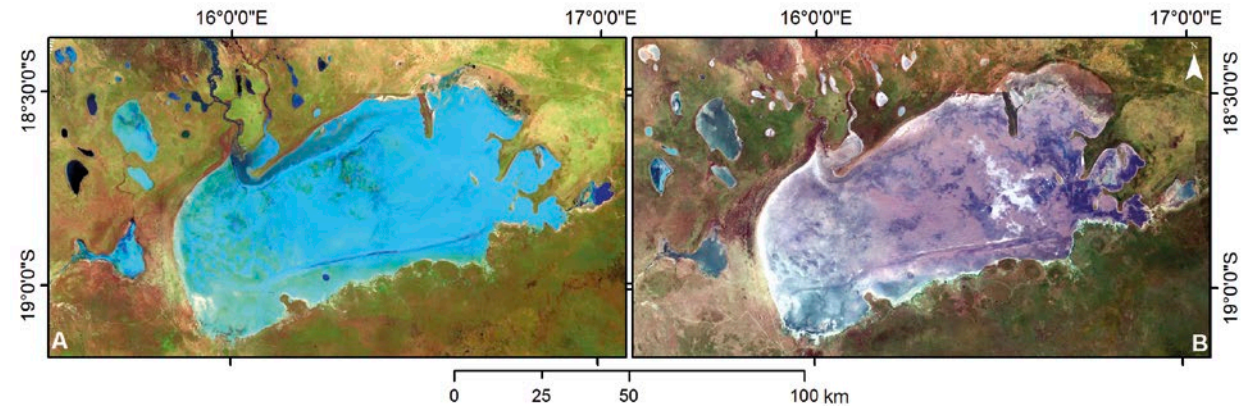
The Etosha Pan was a Neogene, saline palaeolake at the endpoint of Angolan-sourced Cubango Megafan (Hipondoka, 2005; Buch and Rose, 1996; Miller *et al.*, 2010) and the Cuvelai-Ekuma River System. Alternate flooding and desiccation occurred under semi-arid climatic conditions. Green, analcime-bearing clays of the Etosha Pan Clay Member formed the palaeolake bed. Fossils in interfingering sandstones include 4 – 6 million-year-old plants, invertebrates, birds, bovids, mammoth, white rhinoceros, crocodiles, hippopotamae, carnivores, turtles and fish. The fresh-water aquatic and riparian fossils were washed down the Ekuma River.

The saline conditions supported flamingo populations. Arid conditions set in at about 4 Ma. Both river systems ceased to flow but palygorskite-bearing calcrete started to spread northwards over the lake bed clays. This calcrete was deposited by hard water sourced from highly karsted Neoproterozoic mountains south of the pan. Arid conditions prevailed for about 3 million years after which the cycle of flooding and desiccation resumed. Salt fragmented the calcrete. Deflation by easterly winds inverted the palaeolake stratigraphy in lunette dunes that accumulated along the western margin of the pan by first excavating the palygorskite-bearing

calcrete then the analcime-bearing clays. Groundwater seeps support vibrant wildlife that is Namibia's main tourist attraction.

Scientific research and tradition

The Etosha Pan has been studied since the 1920s until present. Two schools of thought persisted for some time, one of which was that the pan had a standing lake. Much research has been done on its geomorphology (Hipondoka, 2005), geology (Miller, *et al.*, 2010) and palaeontology (Pickford *et al.*, 2016).



PLIOCENE TO HOLOCENE RECORDS FROM RACIŠKA PECINA CAVE SLOVENIA



Anthropogenic activity during the 20th century, that is, military use of Raciška Pecina Cave, led to the exposure of calcite layers in the stalagmite dome section. Additionally, the natural cave floor was leveled during this time. (Photo: Jurij Hajna).

A MULTI-PROXY RECORD OF LANDSCAPE AND PALEOENVIRONMENTAL CHANGES DURING THE LAST 3.4 MILLION YEARS, INCLUDING PLIOCENE-PLEISTOCENE AND MATUYAMA-BRUNHES GEOMAGNETIC FIELD REVERSALS.

The Raciška Pecina section contains multiple chronostratigraphic and paleoclimatic proxies that allow global correlations. In particular, the Matuyama/Brunhes boundary is accurately documented within 6 mm interval. Anchored in an age model derived from oxygen isotope stratigraphy, this brief but incisive event is characterized by discernible changes in oxygen and carbon isotope ratios, trace

element concentrations and calcite fabric. The remains of the fauna provide valuable insights into past ecosystems and the biodiversity dynamics. The discovery of the first known cave gastropod fossil underlines the paleontological importance of the site. The radiocarbon dating of soot layers, indicating the presence of humans, further enhances the scientific value of the site.

SITE 126

GEOLOGICAL PERIOD	Pliocene to Pleistocene
LOCATION	Classical Karst, Slovenia 45°30'12"N 014°09'00"E
MAIN GEOLOGICAL INTEREST	Stratigraphy and sedimentology

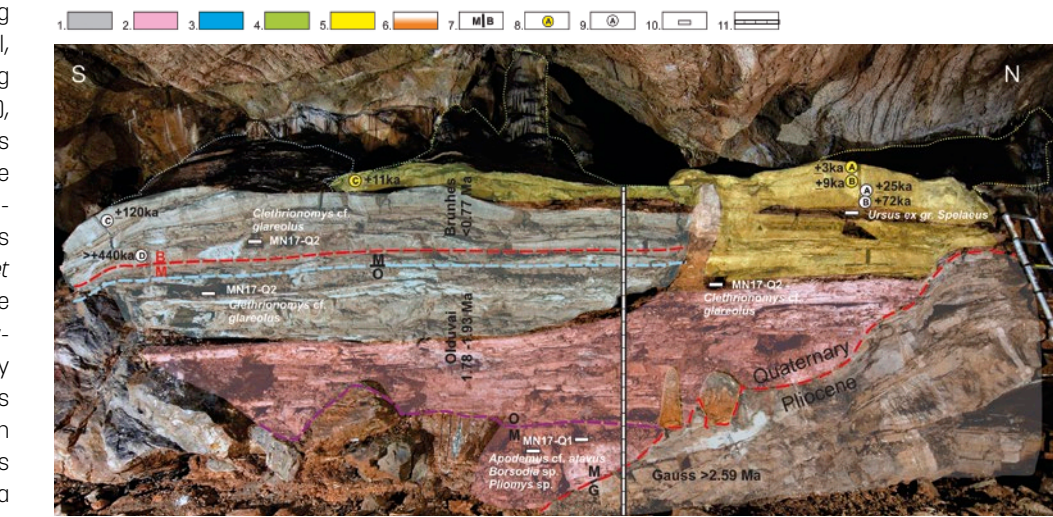


The sedimentary sequence of Raciška Pecina Cave consists of calcite flowstone layers interrupted by long hiatuses filled with clay and silt that include Pleistocene fossils. (Photo: Jurij Hajna).

Geological Description

The Raciška Pecina limestone cave situated in the External Dinarides has a sedimentary sequence spanning from the Late Pliocene to the present day. The deposition of speleothem layers, intermittently interrupted by infiltrations of clay and silt from the surface, contributes to a comprehensive chronostratigraphic record. The chronology, based on magnetostratigraphy, isotope-oxygen stratigraphy and various dating methods, including paleontological, U-series and radiocarbon dating (Zupan Hajna *et al.*, 2020, 2021), highlights important milestones such as the Pliocene to Pleistocene transition and the precise identification of the Matuyama/Brunhes transition at 777.7±6 ka (Pawlak *et al.*, 2024). The fluctuations in stable isotopes within the stratigraphic layers, which range from approximately 3.4 Ma to 80 ka, serve as indicators of environmental change (Sierpien *et al.*, 2021). The stratigraphic layers also harbor a diverse fossil fauna that provides invaluable insights into past ecosystems. Representative fauna from the Early and Late Pleis-

tocene (Horáček *et al.*, 2007; Zupan Hajna *et al.*, 2021), including *Ursus ex gr. spelaeus* (±72 ka) and the first known fossil cave gastropod *Zospeum* sp. (±2 Ma) populate the stratigraphic layers and offer insights into past ecosystems. In addition, radiocarbon dating of soot material in three layers suggests the presence of humans in the cave.



The section provides insight into various aspects including the growth relations of speleothem domes (1-5), stalagmites (6), paleomagnetic boundaries (7), dating results (8 - radiocarbon, 9 - U/Th), paleontology (10), and a stable isotopes log (11). Notably, the M/B boundary is highlighted in red, standing out as particularly significant. Modified from Zupan Hajna *et al.* (2021).

HOLOCENE CORAL REEF TERRACES OF KIKAIJIMA ISLAND JAPAN



Uplifted coral reefs along the coastline of Kikajima Island (photo by Kaito Fukuda).

HISTORY OF CORAL REEFS OVER A PERIOD OF 100,000 YEARS RECORDED CHANGES IN CLIMATE, SEA LEVEL, AND ECOSYSTEM.

Researchers have attempted to describe and date the terraces of Kikajima Island, providing a detailed record of sea-level changes during the last glacial cycle and periodic (6.3, 4.1, 3.1, and 1.4 ka) seismic uplift events (e.g., Sugihara *et al.*, 2003; Sasaki *et al.*, 2004; Inagaki and Omura, 2006).

The remarkable uplift rates have exposed well-preserved, fresh coral skeletons, which enable detailed climatic reconstructions during the Holocene (e.g., Garas *et al.*, 2022).

SITE 127

GEOLOGICAL PERIOD	Pleistocene to Holocene
LOCATION	Forearc region of Ryukyu, Kagoshima Prefecture, Japan 28°17'31"N 129°57'51"E
MAIN GEOLOGICAL INTEREST	Stratigraphy and sedimentology Tectonics



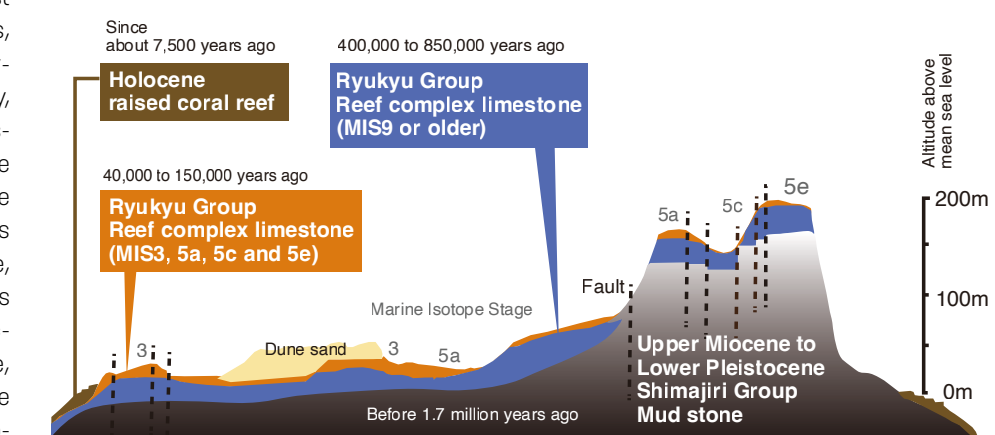
Late Pleistocene and Holocene coral reef terraces produced by sea level change and uplifting of the island.

Geological Description

The unique coral reef terraces of Kikajima Island were formed by rapid sea-level changes during the late Pleistocene glacial cycle, with seafloor uplift at an extremely high rate. For the past 100,000 years, the Kikajima Island has been ascending at a rate of 2.1–2.3 m/ky (Inagaki and Omura, 2006). These terraces are built upon the foundation of Ryukyu Group and have experienced continuous development and repeated uplift of coral reefs. These coral reef terraces correspond with the interglacial highstands of sea-level. The contrast between the terrace surfaces and cliffs, formed from the coral reefs during this cycle, creates a beautiful stepped topography, serving as a remarkable record of late Pleistocene sea-level changes, including marine isotope stage 3 (Sasaki *et al.*, 2004). The consistent uplift rate on Kikajima Island has been maintained since the late Pleistocene, and the series of four terraces and cliffs provide a record of past seismic activity occurring on a millennial scale. Furthermore, well-preserved coral fossils from Holocene reefs have been used as continuous paleo-

climatic indicators for the North western Pacific (Garas *et al.*, 2022).

Geologic section and topographic profile of the southern part of Kikajima island. Vertical lines are faults that displace terraces. Modified from Omura and Ota (1992).



Scientific research and tradition

The geology and topography of Kikajima Island has been studied since the 1930s. Dating methods for coral fossils revealed that the terraces on the island correspond to eustatic sea-level changes (e.g., Omura and Ota, 1992; Sasaki *et al.*, 2004). This island plays a crucial role in studying human-induced global environmental changes, including changes in coral community composition and paleoclimatic reconstructions (e.g. Abram *et al.*, 2001).

SHARK BAY

AUSTRALIA



UNESCO World Heritage Site

Stromatolite heads forming a coalesced reef-like body in southern Hamelin Pool (location shown in Figure).

SHARK BAY WORLD HERITAGE SITE - AN AREA OF OUTSTANDING GEOLOGICAL, GEOMORPHOLOGICAL, AND BIODIVERSITY VALUES.

Of global geoheritage significance, Shark Bay is one of only a few World Heritage areas listed for all 4 outstanding natural values. The region is a globally important classroom for aspects of megascale coastal geomorphology, arid zone marine sedimentation, the interplay of sedimentation and coastal geomorphology with Quaternary tectonics, and smaller fea-

tures such as stratigraphy, stromatolites, and crystal beds (Brocx and Semeniuk, 2007, 2010). The Shark Bay stromatolites are unique and globally important, providing valuable analogues of the early history of life on Earth. Geodiversity underpins the unique vegetation associations, and the region supports abundant marine flora and fauna.

SITE 128

GEOLOGICAL PERIOD	Pleistocene to Holocene
LOCATION	Gascogne Region, Western Australia, Australia 25°55'28"S 113°48'17"E
MAIN GEOLOGICAL INTEREST	Stratigraphy and sedimentology Geomorphology and active geological processes

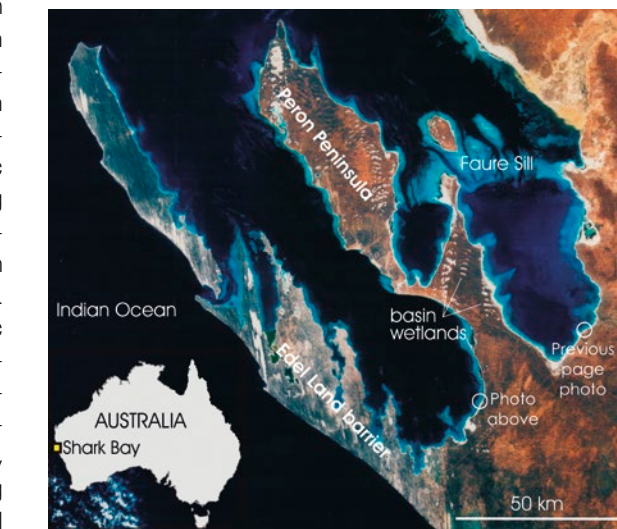


Southerly-wind-generated shore-parallel sand bars and spits with seagrass wrack in swales, eastern shore Hopeless Reach (location shown in Figure).

Geological Description

Shark Bay comprises large semi-enclosed elongate coastline-hugging twin embayments on the low-lying coast of the Indian Ocean on the most western point of Australia. Set in a climate with high evaporation, low rainfall, and strong southerly winds, Shark Bay is complex geomorphologically, sedimentologically, hydrochemically, and diagenetically. The embayments are framed by two Pleistocene linear barriers – a western limestone barrier (the Edel Land barrier), and an eastern red aeolian quartz sand peninsula (Peron Peninsula, a former barrier; see satellite image; Logan, 1970, 1974) that is studded with gypsum-filled wetland basins (birridas). Generally, these embayments have geomorphic units of a deep water basin, shoreline-fringing subtidal shallow-water platforms and/or seagrass banks, beaches, tidal flats, and beach ridges (Logan *et al.*, 1970; Berry *et al.*, 1990). Hydrochemically, Shark Bay borders oceanic water and, through evaporation, low circulation, and cross-embayment barriers, its salinity progressively grades southwards to metahaline and hypersaline. Where metahaline, embayments are fringed by shore-hugging seagrass banks, beaches, and shore-parallel

spits (Photo, above). In the far southeast and separated by a cross-embayment barrier (the Faure Sill), Shark Bay becomes hypersaline - here are developed smaller embayments, ooid shoals and beach ridges, coquina sheets and beach ridges, tidal algal mats and stromatolites (stromatolite heads; Photo, previous page), tidal/supratidal gypsum crusts, subtidal to supratidal cemented carbonate crusts and pavements, and breccia sheets.



Satellite photograph of Shark Bay showing the twin elongate northwest-oriented embayments, deep water basins (dark blue), shore-hugging shallow water sandy platforms (light blue), invaginated eastern shoreline and cliffted straight western shore of the western peninsula, wetland-rich nature of the eastern peninsula, and the submarine sill bisecting the eastern embayment.

Scientific research and tradition

Shark Bay has been investigated for its coastal features formed over thousands of years through a combination of sedimentation, erosion, and evaporation. These include marine stratigraphy, seagrass banks, coquina shores, tidal flat deposits, beaches, cliffs, dunes, and other features such as stromatolites, calcrite, limestone aeolian formations, and fossil shell banks.

UYUNI SALT FLAT

BOLIVIA



Hexagonal cracks from evaporation on Uyuni salt flat; Tunupa Volcano at the bottom.

THE WORLD'S LARGEST AND HIGHEST EXTENSIVE EVAPORITIC DEPOSIT WITH THE GREATEST RESERVES OF LITHIUM BRINES.

Holocene Uyuni Salt Flat contains the largest evaporite deposits in the world and records the climatic evolution of the Pleistocene lake during the Quaternary of the Andean Altiplano. That it is accessible and scenic at any season of the year has made this salt flat a world class tourist

attraction. The endorheic basin of the Altiplano, dry and desert where evaporation is greatest, has a depth of 460 meters (Carvajal, 2018). The world's largest salt flat, where the earth and sky are one and the same, holds a world class deposit of evaporitic Lithium and Magnesium brines.

SITE 129

GEOLOGICAL PERIOD	Pleistocene to Holocene
LOCATION	Potosí, southwest of Bolivia, Bolivia 20°11'02"S 067°36'16"W
MAIN GEOLOGICAL INTEREST	Stratigraphy and sedimentology Geomorphology and active geological processes



Waterlogged for precipitation and runoff showing the waves and clouds in rainy season at Uyuni salt flat.

Geological Description

Located in the highlands of the Andes, the Uyuni Salt Flat is a result of the evaporation of Tauca paleolake. The Altiplano is an extensive endorheic mountain basin of the Andes located in the volcanic arc and the Eastern Mountain Range of the Andes. It is characterized by an arid climate. During the Pleistocene, glacial and interglacial episodes gave rise to different lake systems. During the thawing of Choqueyapu II, Lake Tauca formed 12,500 to 10,000 years ago (Servant and Fontes, 1978).

Uyuni Salt Flat is the largest salt crust in the world that comes from the drying of the Tau-

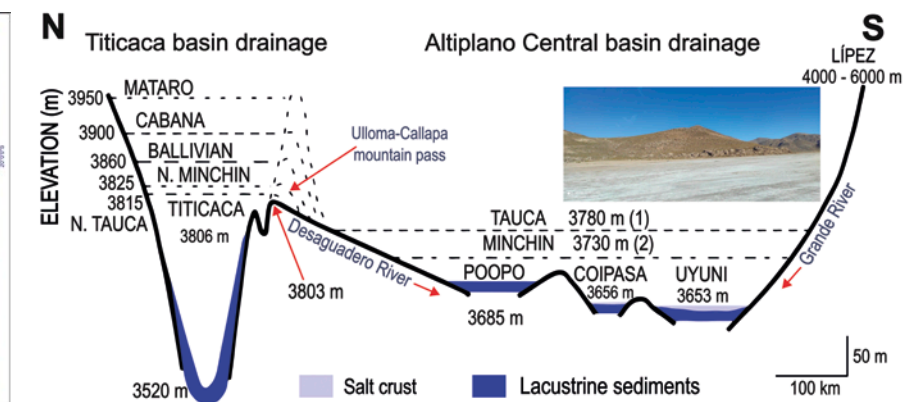
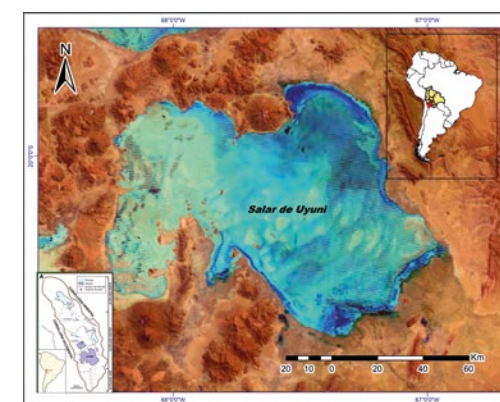
ca paleolake, a sacred lake that covered the southern Altiplano more than 10,000 years ago. It consists of an alternating sequence of the highly porous saline layers, composed mainly of halite, and clay-rich lacustrine sediments (Sieland, 2014), which are the source of the globally important lithium reserves (Quzada and Carvajal, 2022). The halite deposits are associated with diapirs, previous salt crusts and the dilute waters of the Altiplano (Risacher and Fritz, 1995).

The Pleistocene to Holocene evolution of the lake resulted in Uyuni Salt Flat, which is the largest and highest in the world and a world class example of lithium brines production.

Scientific research and tradition

Being a reference of evaporite deposits and lithium brines, the Uyuni Salt Flat has been studied by international missions such as ORSTOM to understand the origin and geological, hydrogeological and geochemical characteristics, mainly through drilling. The United States Geological Survey considers the Uyuni Salt Flat to hold one of the largest lithium deposits in the world.

Paleolakes in the Altiplano endorheic Basin evolution (Quzada and Carvajal, 2022) and a satellite image of Salar de Uyuni surrounded by volcanic terrain.



THE DEAD SEA

ISRAEL AND JORDAN



Geomorphological and geochemical processes along the Dead Sea. Previous shorelines showing a 'Staircase' morphology, halite deposits, and a sinkhole. Photographer: Liran Ben Moshe.

THE DEAD SEA IS AN EXCELLENT SITE FOR OBSERVING GEOMORPHOLOGICAL, SEDIMENTOLOGICAL, LACUSTRINE, AND GEOCHEMICAL PROCESSES AND STUDYING TECTONICS AND PALEOCLIMATE.

The Dead Sea is a terminal hypersaline lake, along a plate boundary, containing an unparalleled record for deciphering tectonic and climatic history. Changes in the lake environment and composition are prime examples of rapid geomorphological development and brine evolution under extreme conditions. Lake bed sediments provide an excellent record of paleocli-

mate shifts, historical and paleo seismology, and more. The lake's chemistry developed through extreme evaporation and interaction with local rocks and is a unique example of brine development in an arid area. Continuous rearrangement of the shoreline, channels, and sinkholes around the lake opens a window to geomorphological processes.

GEOLOGICAL PERIOD	Holocene
LOCATION	Levant, Israel and Jordan 31°33'32"N 035°28'24"E
MAIN GEOLOGICAL INTEREST	Stratigraphy and sedimentology Geomorphology and active geological processes

SITE 130



A northeast view from the Ein-Gedi beach at the Dead Sea with a 'sediment plume'. Photographer: Yair Paz.

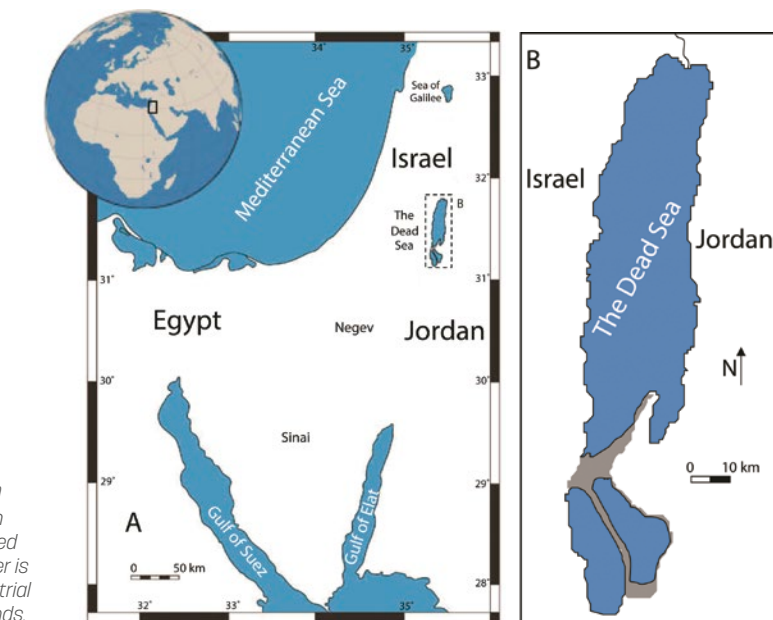
Geological Description

The Dead Sea is a unique hypersaline lake. Situated in a pull-apart basin along an active plate boundary, at 437 meters below sea level and continuously decreasing, it is the lowest place on Earth. The lake is an exemplar of geomorphological and limnological development serving as a natural laboratory for understanding sedimentological, geochemical, tectonic, seismological, and climatic history in an important region for human cultural development (Ben-Avraham *et al.*, 1997; Enzel *et al.*, 2006). The Dead Sea brine originates from an ingressional of the Mediterranean flooding the basin. Climate change induced shifts in the water volume and composition, leading to three successive 'amplifier lakes', the current Dead Sea succeeding Lakes Amora (740-70 ka) and Lisan (70-14 ka). Sediments deposited from these lakes provide an excellent paleoclimatic record (Stein and Goldstein, 2020). A negative water balance during dry periods drives the evolution of the lake and its surroundings. Receding shorelines continuously rearrange the beach, channels, and regional hydrology, causing extensive sinkhole activity. Increasing brine density and saturation following evaporation

also cause changes in lake stratification and mineral deposition. For several millennia, the lake's beautiful settings and unique properties captivated travelers' minds. The lake's distinctive geologic history and characteristics are the basis for ongoing research.

Scientific research and tradition

An 1847 expedition led by William Lynch determined the Dead Sea lies 400 meters below sea level (Lynch, 1849). Ever since, hundreds of publications covering all aspects of Earth science originated from researching the lake, which remains a valuable source of knowledge, leading to dozens of publications a year.



The Dead Sea.
(A) Geographic location, and (B) North and South basins (separated 1980's). The latter is utilized as industrial evaporation ponds.

MARS ANALOG OF LAKE SALDA

TURKEY



Western shorelines of Lake Salda with older and modern hydromagnesite beaches covering the entire shorelines (Photo by Ali İhsan Gökçen).

A DEEP ALKALINE LAKE DEPOSITS HYDROMAGNESITE MICROBIALITES THAT MAY HAVE CLUES FOR POSSIBLE ANCIENT LIFE ON MARS.

NASA recognized Lake Salda as unique and the only compositional and process analog for the Jezero paleolake on Mars. As with Jezero crater, Lake Salda is surrounded by altered and Mg-rich ultramafic terrains, and it contains hydrated Mg-carbonate bearing deposits. Thus, it offers an exceptional setting to investigate the microbially mediated precipitation of hydrat-

ed magnesium carbonates in an ultramafic-rich terrain due to the morphological and microbial diversity of microbialites. The study of hydromagnesite microbialites has significant implications for the detection and understanding of similar formations on Mars, providing clues about the potential existence of past life on the Red Planet (Garczynski *et al.*, 2019, 2020).

GEOLOGICAL PERIOD	Quaternary
LOCATION	SW Anatolia, Turkey 37°33'09"N 029°40'53"E
MAIN GEOLOGICAL INTEREST	Stratigraphy and sedimentology Paleontology

SITE 131



Close-up view of extensive subfossil hydromagnesite microbialites with cauliflower morphology, up to 5 meters high and 20 meters wide (Photo by Nurgül Balci).

Geological Description

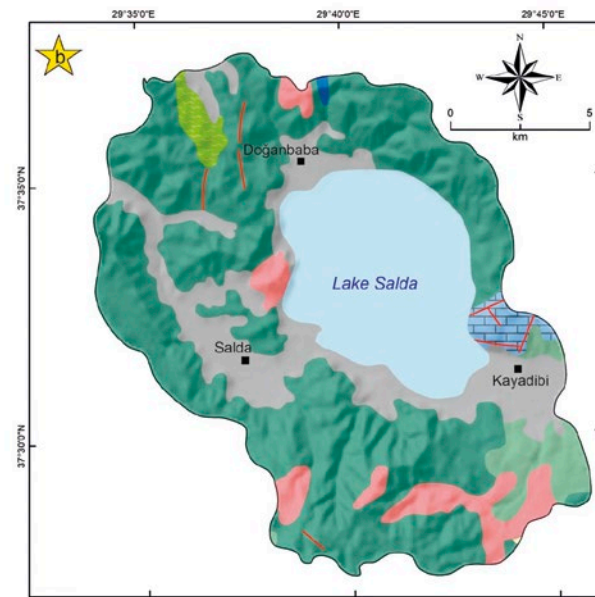
Lake Salda is a closed alkaline water body ($\text{pH} > 8.4$) at 1140 m a.s.l. It has a surface area of ca. 45 km² and an average depth of 80 m and maximum of 200 m. The lake is surrounded primarily by primitive ultramafic allochthonous rocks Mesozoic in age, and the autochthonous formations are only Quaternary alluvial fans. The stratigraphy of the region reflects the Alpine Orogeny; however, the lake appeared after the Pliocene, according to the lacustrine records. Lake Salda has a rare water chemistry with exceptionally high Mg/Ca ratios from 3 to 7000 (Kazancı *et al.*, 2004; Kaiser *et al.*, 2016; Balci *et al.*, 2020). It is one of the only environments on Earth where extensive microbialites of hydromagnesite $[\text{Mg}_5(\text{CO}_3)_4(\text{OH})_2 \cdot 4(\text{H}_2\text{O})]$ are currently forming as mounds that are locally called "white island". Lake Salda hosts modern, subfossil and fossil microbialites along its perimeter, providing a time capsule for decoding signs of past life. Modern microbialites with different morphotypes (e.g., stromatolite, thrombolite) are currently growing in the shallow (< 1 m) and deeper waters (up to 20 m) of the lake and are one

of a kind with their rare chemical compositions on Earth and possibly on Mars.

Scientific research and tradition

Lake Salda's carbonate stromatolites have been attributed to cyanobacterial and algal

activity (Russell *et al.*, 1999). Later, Balci *et al.* (2022) documented multiple microbialite types in an associated microbial community in the lake. Since recognition of the lake as the best terrestrial analog for the Jezero paleolake on Mars, it has been the center of the international scientific community.



Location map (a) and rocks in the drainage area of Lake Salda (b) following the geological map at scale of 1/500 000 published in 2002 by Turkish Geological Survey (MTA).

3

PALEONTOLOGY

SITE 132 - SITE 145



Fossils are crucial in piecing together the timeline of life on Earth, documenting the emergence, diversification, and extinction of different species over millions of years. This record allows palaeontologists to trace the evolutionary pathways of organisms, illustrating how life has adapted to changing environments and recovered from mass extinction events. By examining these patterns, scientists can better understand the mechanisms of evolution and the resilience of life.

Furthermore, the fossil record plays a crucial role in determining the relative age of sedimentary rocks using biostratigraphy. The resulting chronological frameworks are of utmost importance in reconstructing the geological history of our planet and placing significant evolutionary milestones into context.

The fossil record also provides essential data for reconstructing past climates and environments, shedding light on atmospheric oxygen levels, climate change cycles, and the changing landscapes between land and sea. This information is critical for comprehending the Earth's climatic evolution and forecasting upcoming environmental shifts.

Since Henri Marie Ducrotay de Blainville used the French term *Palaeontologie* in 1822, the discipline continues to highlight the diversity of past life through notable fossil sites around the world. In this context, the Second 100 IUGS Geological Heritage Sites presents a selection of 14 Sites that possess significant scientific value and are essential for understanding the evolution of life on Earth. These fossil sites provide an intriguing journey through time, starting with the diverse metazoan fossil records of the terminal Ediacaran Period of the Nama Group (ca. 540 Ma) in Namibia. Following that is the Late Devonian fossil-fish Lagerstätte of Miguasha (375 Ma) in Canada, which showcases the lobe-finned fish that serve as the evolutionary link to terrestrial life and the remarkable Triassic dinosaurs and mammalian reptiles from Ischigualasto (230 Ma) in Argentina. Next in line is the coal-forming tropical rainforest of the Wuda Fossil Site (295 Ma) from the Permian Period in China. The Jurassic Period is represented by dinosaur footprints from the Sierra de Aire and Candeeiros in Portugal, the Dashanpu fossil site in China, and the Carneige Quarry Dinosaur Bone Site in the United States. The remarkable discoveries of the Early Cretaceous wetland of Las Hoyas (128 Ma) in Spain, the Cariri Stone Lagerstätte (100 Ma) in Brazil, and the Upper Cretaceous Dinosaur Nesting Grounds of the Willow Creek Anticline (75 Ma) in the United States vividly illustrate the diverse paleoenvironments of the Cretaceous Period. The fossil record found in 'Whale Valley' focuses on a plethora of Eocene fossils of Cetacea and Sirenia from Wadi Al-Hita (35 Ma) in Egypt. The La Venta middle Miocene neotropical biome (12.5 Ma) in Colombia reveals a Lagerstätte that contains fossils of a vibrant neotropical rainforest. The fossil record related to the evolution and adaptation of humans includes the modern human fossils discovered in the Kibish Formation (200 ka) in Ethiopia, as well as the Human Footprints of Acahualinca (2 ka) from Nicaragua.

Artur Abreu Sa

Universidade de Trás-os-Montes e Alto Douro (UTAD). Vila Real. Portugal.

Executive committee. GGN – Global Geoparks Network.

IUGS Geological Heritage Sites referee.

Isabelle Rouget

Muséum National d'Histoire Naturelle. Paris. France.

IPA - International Paleontological Association.

IUGS Geological Heritage Sites referee.



EDIACARAN FAUNA OF THE NAMA GROUP NAMIBIA



View from Swartpunt mountain.

ONE OF THE MOST CONTINUOUS STRATIGRAPHIC AND PALEONTOLOGICAL RECORDS WITH CRUCIAL INFORMATION TO UNDERSTAND THE EVOLUTION OF COMPLEX LIFE DURING THE EDIACARAN-CAMBRIAN TIME INTERVAL.

The Ediacaran-Cambrian transition (~550-538 million years ago) marks one of the most important geobiological revolutions in Earth history with the appearance of biological and ecological innovations that continue to dominate marine ecosystems into the present day. The Nama Group records this interval in unparalleled extent, including exquisitely preserved fossils

that are helping us reconstruct the origin of modern-looking marine ecosystems. Among many other aspects, Nama Group fossils record the advent of calcified skeletons, the first appearance of complex bioturbation, and the rise of benthic suspension feeding – all behaviors that arguably form part of the ‘fuse’ for the subsequent Cambrian explosion.

SITE 132

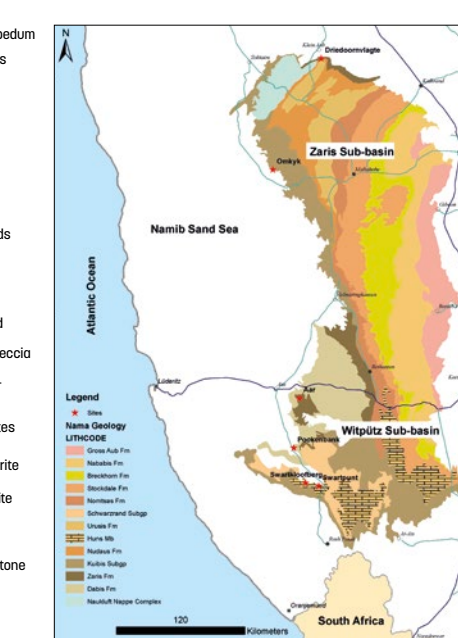
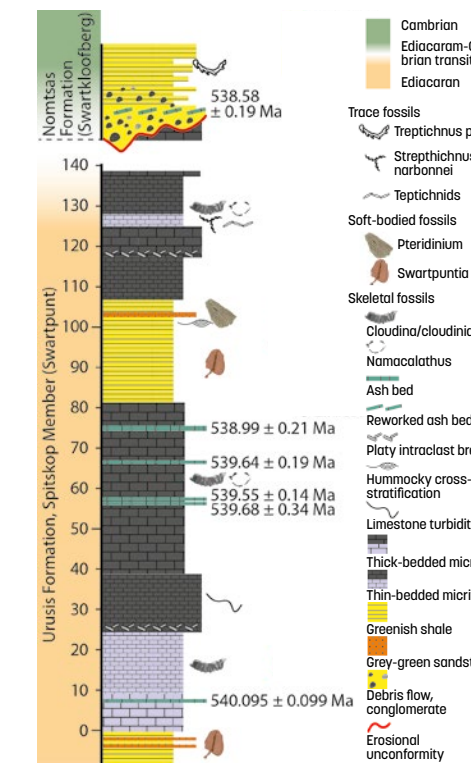
GEOLOGICAL PERIOD	Ediacaran to Cambrian
LOCATION	Karas and Hardap Regions, Namibia 26°43'56"S 016°29'59"E
MAIN GEOLOGICAL INTEREST	Paleontology Stratigraphy and sedimentology



Pteridinium simplex fossils in the Seilacher block.

Geological Description

The Ediacaran to Cambrian-aged Nama Group is a >3000 meter thick succession of interbedded shallow marine carbonates and siliciclastics, deposited on an extensive



peneplain on the southern foreland of the Damara Orogen as part of the Neoproterozoic pan-African orogeny (Germs, 1983). In the present day, the Nama Basin extends over 1000 km from Gobabis in the north to the banks of the Orange River in the south, and is subdivided into 3 subbasins – the Witvlei, Zaris, and Witputs. The succession preserves numerous, iconic fossil deposits that have been

studied since the 1930's. Quartzites belonging to the Dabis Formation on Farms Aar, Plateau and Pockenbank contain enigmatic soft-bodied fossils that continue to influence debate surrounding the early evolution of animals. In the north, Farms Omkyk and Driedoornvlakte host extensive reef tracts that include the oldest calcifying metazoans (Grotzinger *et al.*, 2000; Penny *et al.*, 2014). Higher in the stratigraphic column, the Urusis Formation on Farm Swartpunt preserves among the youngest Ediacaran fossils in the world, alongside complex trace fossils that augur the beginning of the Cambrian substrate revolution (Narbonne *et al.*, 1997). Radiometric dating of ash beds in the succession provides geochronological context for these fossils, helping to refine the age of the Ediacaran-Cambrian boundary (Linnemann *et al.*, 2019).

Scientific research and tradition

Fossils in the Nama Group were discovered by geologists in the early 20th century, following reports made by German soldiers stationed in the Aus region. This has led to intensive geological research that has placed the Nama Group at the forefront of debates surrounding the Precambrian evolution of animals and dynamics of the Ediacaran-Cambrian transition.

THE LATE DEVONIAN FOSSIL-FISH LAGERSTÄTTE OF MIGUASHA CANADA



UNESCO World Heritage Site

THE WORLD'S MOST OUTSTANDING SITE FOR LATE DEVONIAN FOSSIL FISH, INCLUDING THE LOBE-FINNED FISHES THAT ARE THE EVOLUTIONARY LINK TO VERTEBRATE LIFE ON LAND.

Late Devonian strata at Miguasha National Park. These rocks contain beautifully preserved fossil fish and other animals and plants. (Photo: Mathieu Dupuis, Miguasha National Park).

The site holds worldwide significance owing to its remarkable yield of exceptionally well-preserved fossils over the past 180 years, including an impressive number of vertebrate fossils (more than 18,000 specimens housed in various museums around the world). These fossils represent most of the major evolutionary groups of vertebrates that inhabited the Devonian

period, known as the "Age of Fishes." Not only are these fossils crucial for understanding vertebrate evolution, but they also shed light on the paleoecology and paleoenvironment during the transition from water to land. It is for these reasons that the site was granted UNESCO World Heritage status in 1999.

SITE 133

GEOLOGICAL PERIOD	Upper Devonian
LOCATION	Quebec, Canada 48°06'18"N 066°21'11"W
MAIN GEOLOGICAL INTEREST	Paleontology History of geosciences



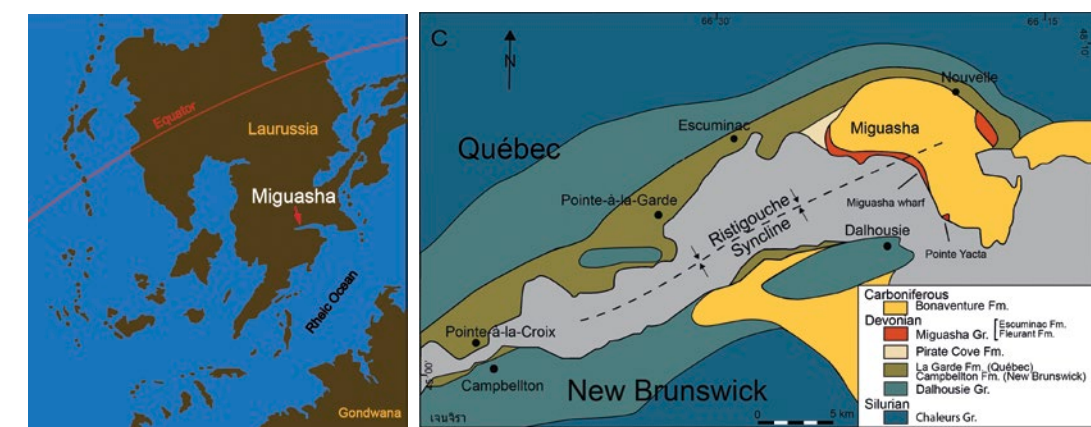
Exceptional preservation of the Devonian lobe-finned fish *Eusthenopteron foordi* from Miguasha. (Photo: Mathieu Dupuis, Miguasha National Park).

Geological Description

Miguasha National Park, spanning 87.3 hectares, is situated on Chaleurs Bay in eastern Québec. It preserves the fossiliferous cliff of the Late Devonian (Frasnian) Escuminac Formation, where organisms were buried 375 million years ago in an equatorial paleoestuary on the southeast coast of the paleocontinent Laurussia, connected to the Rheic ocean (Cloutier *et al.*, 2011). The site boasts an abundance and diversity of beautifully preserved fossil fish, including specimens of *Elpistostege watsoni*, a transitional species between fishes and four-limbed vertebrates (Cloutier *et al.*, 2020). This species exhibited fingers embedded in its pectoral fins, as well as gills, lungs, and internal nostrils, enabling it to breathe air. Alongside the fish, terrestrial arthropods and plants, such as scorpions, millipedes, and remains of tree-like ferns, were washed into the estuarine sediments (Cloutier, 2013). Many specimens are complete and fully articu-

lated, some preserved in three dimensions (Cloutier, 2013), others exceptionally-preserved larvae and juveniles (Chevrinaias *et al.*, 2017), and some exhibit fossilized soft tissues (Klug *et al.*, 2021; Cloutier, 2013). It is these characteristics that enable paleontologists to understand minute details of deep-time biodiversity, making it no surprise that Miguasha has been visited by many paleontologists from around the world.

Localisation of Miguasha in (A) eastern Canada and (B) in Laurussia during the Upper Devonian. (C) Geological map of the Escuminac Formation (modified from Cloutier (2013)).



PERMIAN VEGETATION OF THE WUDA FOSSIL SITE CHINA



A number of trunks and tree crowns preserved in place.

A COAL-FORMING TROPICAL RAINFOREST PRESERVED IN EXCEPTIONAL DETAIL BY VOLCANIC ASH.

The Wuda Fossil Site yields the largest number of reconstructed fossil plants and the largest precisely (by quadrat sampling method) reconstructed actual landscape of a coal-forming vegetation globally, offering a unique window to understand past floral community ecology. More than fifty taxa illustrate the high diversity and evolutionary status of the

coal-forming forest. Some species are described as whole-plants (e.g., Wang *et al.*, 2021), delivering scientific breakthroughs in plant systematics and in restoring live trees. The Wuda Fossil Site is exceptional for best demonstrating those plants that formed coal and what a coal-forming forest looked like.

SITE 134

GEOLOGICAL PERIOD	Permian (Cisuralian)
LOCATION	Wuda Coalfield, Wuhai City, Inner Mongolia, China 39°32'03"N 106°37'36"E
MAIN GEOLOGICAL INTEREST	Paleontology Stratigraphy and sedimentology



Whole-plant fossil and its reconstruction of the progymnosperm *Paratingia wuhai*.

Geological Description

The Wuda fossils represent an exceptional record of an ancient forest that has been termed the Permian "vegetational Pompeii" (Wang *et al.*, 2012). The forest was peat-forming and buried in place by ash-fall, now appearing as a tuff bed between two coal seams in the Wuda Coalfield, Inner Mongolia. The tuff is dated to 298.34 ± 0.09 Ma from the earliest Permian and lies approximately on the Carboniferous-Permian boundary (Schmitz *et al.*, 2021). Plant remains are preserved as unusually complete plants showing gross form, but also are often partly permineralized preserving internal structure. Vegetation includes more than 50 species from seven groups, namely lycopsids, sphenopsids, filicalean ferns, progymnosperms, seed ferns, early conifers and cycads. Many lines of evidence record insect-plant interactions (e.g., feeding) and plant-plant interactions (e.g., climbing, Zhou *et al.*, 2019), preserving intricate details of an ancient tropical rain forest community and interplay between different organisms.

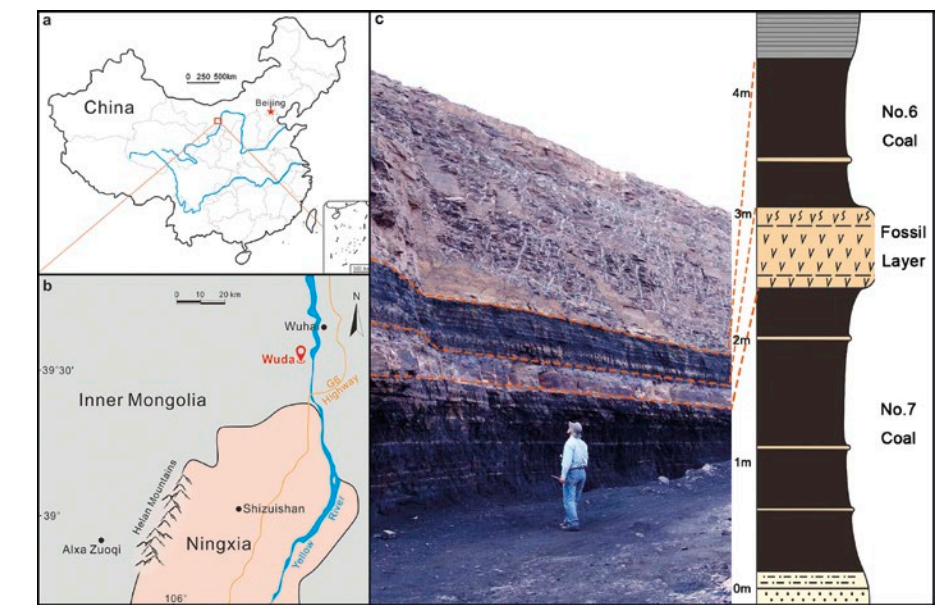
This unique "Permian Coal Forest offers a glimpse of late Paleozoic ecology" (Bashforth and DiMichele, 2012) and has been

headlined as "Primeval Land Rises from the Ashes: A 'vegetational Pompeii' buried in a coal deposit that is shedding light on ecosystem structure and climate during the Permian period" in SCIENCE by Hvistendahl (2012).

Location information and section of the Wuda Fossil Site.

Scientific research and tradition

Wuda Fossil Site was discovered in 1998 and recognized as a forest buried by ash in 2003. Subsequently an international research team of about 30 experts from England, the United States, the Czech Republic, Germany and China have published over 60 papers on its taxonomy, ecology and geology. Active research continues.



TRIASSIC DINOSAURS AND MAMMALIAN REPTILES FROM ISCHIGUALASTO ARGENTINA



UNESCO World Heritage Site

Appearance presented by the Ischigualasto Formation, gray in color. In the background, outcrops of the Los Colorados Formation constituting the so-called Barrancas Coloradas.

CONTINUOUS FOSSIL RECORD THAT RECORDS THE ORIGIN OF DINOSAURS AND EVOLUTION FOR FIRST MAMMALS.

The Ischigualasto-Villa Unión basin (Stipanicic and Bonaparte, 1972) is the only place in the world with a complete succession of Triassic continental strata. Its outcrops in Ischigualasto have attracted the interest of geologists and paleontologists around the world because its fossils record the origin of the dinosaurs and the evolution of the first mammals. Its natural beauty makes it an important attraction for tourists. The area has been protected by the Province of San Juan since 1971. It was declared an Archaeological, Paleontological and Ecological Site in 1995 and a World Heritage Site in 2000 (Dingwall, 2000).

SITE 135

GEOLOGICAL PERIOD	Triassic
LOCATION	Province of San Juan, Argentina 30°09'48"S 067°50'32"W
MAIN GEOLOGICAL INTEREST	Paleontology Stratigraphy and sedimentology



Herrerasaurus ischigualastensis, one of the most primitive dinosaurs known (Marcos Carrizo).

Geological Description

The continuous succession of Triassic strata exposed in the park was deposited in an open basin 251 million years ago. The continuous sedimentation allowed for a comprehensive record in that environment of the evolution of primitive turtles and the replacement of therapsids by archosaurs during the Early Triassic (Benton, 1993). Moreover, fossils of the oldest and most primitive dinosaurs known to date (Sereno and Novas, 1992) occur in the Upper Triassic along with therapsids, cynodonts and dicynodont types. The latter constitute the category of mammalian reptiles, from which mammals later evolved. The formation of the Andes Mountains uplifted this ancient basin to 1,300 meters above sea level, exposing the rocks to erosion that carved out a particular landscape known as "Valle de la Luna" (Valley of the Moon). The brick red, greenish and ochre sandstones are exposed in cliffs up to 200 meters high where the different strata and their internal structures highlighted by wind abrasion can be distinguished. Gigantic columns, thin obelisks, unusual rock shapes, ravines and gorges complete this spectacular landscape.

Scientific research and tradition

Victorino Herrera discovered the fossil deposit in 1927. In 1940, Dr. Joaquin Frenguelli discovered that the largest paleontological sample from the Triassic lay there. The pale-

ontologist William Sill was the architect of its declaration as a World Heritage Site by UNESCO in the year 2000.

PERIOD (THICKNESS)	TECTONIC ENVIRONMENT	SEDIMENTARY ENVIRONMENT	PALEONTOLOGY
Upper Triassic (1400 m)	Post rift	Meandering rivers	Aetosaurus, rausuchids, ornithischians of typical Triassic. Protosuchians typical of Jurassic
	Rift	Braided rivers	Anfibians laberintodonts, arcosaurus cordilomorphs, arcosaurus, ornithodirs, prearcosaurs proterochampsidos, rincosaurs y therapsids cynodonts and dicynodonts. Vertebrates like Myrilepis elongatus and invertebrates like Estheria and Palacometula. Fingerprints of Rigalites Ischigualitanus and tridáctilas indeterminates.
Middle Triassic (1500m)	Post rift	Deltas and rivers	Cynodonts (direct ancestors of modern mammals) and Dicynodonts. Archosaurs (ancestors of dinosaurs)
Lower Triassic (800m)	Rift	Tuffic flows	Few incomplete fossils, assigned to dicynodonts.
		Braided rivers	

MIDDLE JURASSIC DINOSAUR FOOTPRINTS FROM THE SERRAS DE AIRE AND CANDEEIROS PORTUGAL



Panoramic view of the Galinha quarry with the main sauropod trackways.

THE LONGEST AND BEST PRESERVED TRAILS OF DINOSAUR FOOTPRINTS IN THE MIDDLE JURASSIC

These quarries constitute a world-class Serial Site for understanding some of the oldest paleoenvironmental and paleoethological interactions involving sauropods and theropods. The ichnites of the Galinha quarry, with oval pes prints and speech-bubble-shaped manus prints (Castanera *et al.*, 2016), have provided an important contribution to the knowledge of sauro-

pods at an early stage of their development. It was even possible to describe *Polyonyx gomesi* as a new sauropod ichnotaxon (Santos *et al.*, 2009). Vale de Meios quarry, is one of the most important sites with Middle Jurassic theropod tracks. The occurrence of *Megalosauripus* tracks represents the oldest occurrence of this ichnotaxon (Razzolini *et al.*, 2016).

SITE 136

GEOLOGICAL PERIOD	Middle Jurassic
LOCATION	Serras de Aire e Candeeiros Natural Park, Portugal 39°34'11"N 008°35'21"W
MAIN GEOLOGICAL INTEREST	Paleontology Stratigraphy and sedimentology



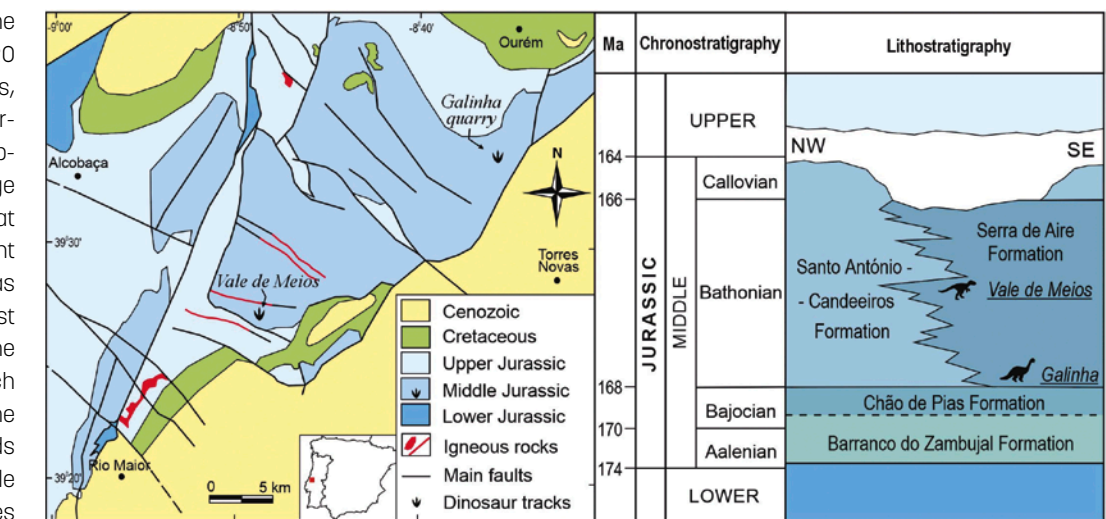
Theropod footprint of the Vale de Meios quarry.

Geological Description

The Dinosaur Footprints Natural Monument of Ourém/Torres Novas, known as Galinha quarry, and the Vale de Meios quarry, are located in the Serras de Aire e Candeeiros Nature Park (Central Portugal). They are two geosites, duly geoconserved, of recognized international scientific value, due to the exceptional age, size, and quality of preservation of ichnites. Both quarries are located in limestones of the Serra de Aire Formation (Bathonian, Middle Jurassic) (Azeredo, 2007). The Galinha quarry preserves 20 trails with sauropod footprints, in an excellent state of conservation, and it is possible to observe finger marks and a ridge formed by the sediment that was removed under the weight of the animal. This deposit has some of the oldest and longest sauropod tracks known in the world (up to 147 m long), which provide a dynamic image of the locomotion of these sauropods (Santos *et al.*, 2009). The Vale de Meios quarry preserves

more than 700 theropod tracks. They are organized in at least 80 unidirectional trackways, arranged in a bimodal orientation pattern (W/NW and E/SE). Paleoenvironmental studies in this quarry indicate an inter-tidal flat located at the margin of a coastal barrier (Razzolini *et al.*, 2016).

Geological map of the Maciço Calcário Estremenho (MCE) and stratigraphic column of the Jurassic lithologies, with reference to dinosaur footprints outcrops.



Scientific research and tradition

Discovered and studied since the 1990s, multiple scientific studies have been carried out on these dinosaur track sites (Santos, 2016), involving several international researchers. Similarly, since their discovery attracted educational and tourist visits, from nationals and foreigners, they are currently duly protected and equipped for that purpose.

DASHANPU MIDDLE JURASSIC DINOSAUR FOSSILS SITE CHINA



UNESCO Global Geopark

Concentrated dinosaur fossils in the site.

A HIGHLY CONCENTRATED MIDDLE JURASSIC DINOSAURS SITE THAT DEMONSTRATES HIGH VERTEBRATE DIVERSITY.

This site has a highly diverse vertebrate fauna and the greatest concentration Middle Jurassic dinosaurs known. The site is the type locality of the Shunosaurus Fauna. Its fossils represent basal taxa of several different lineages, such as, the eusauropod *Shunosaurus lii*, the macrocnarian *Dashanpusaurus dongi*, the stegosaur *Huayangosaurus taibaii*, and the neornithischian *Agilisaurus louderbacki*.

Some specimens exhibit unique bone structures, such as the bony tail clubs of sauropods and the parascapular spines of stegosaurs, which provide evidence of dinosaur behaviors. The fossils from this site fill a gap in the knowledge of dinosaurs evolution and provides exceptional good samples for studying many paleobiological aspects of dinosaurs and their relations with other vertebrates.

SITE 137

GEOLOGICAL PERIOD	Middle Jurassic
LOCATION	Zigong City, Sichuan Province, China 29°23'49"N 104°49'27"E
MAIN GEOLOGICAL INTEREST	Paleontology Stratigraphy and sedimentology



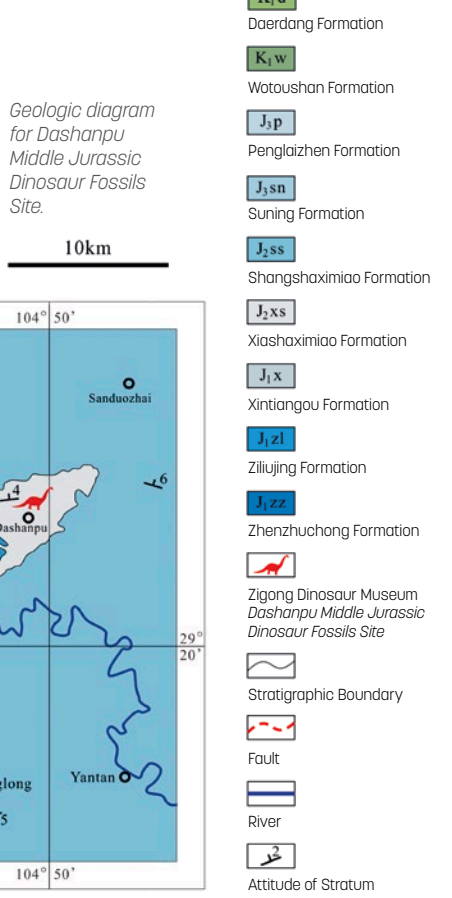
Part of the Dashanpu Middle Jurassic Dinosaur Fossils Site.

Geological Description

The site is located at the northeastern end of the Ziliujing Anticline of Sichuan Basin, which is a well-known red-bed basin in the Upper Yangtze Platform of South China. Late Triassic to Early Cretaceous terrestrial strata are exposed within the basin. The Lower Shaximiao Formation of the Middle Jurassic, which has dinosaur fossils, is about 180 meters thick and is composed of lacustrine and fluvial clastic deposits, mainly purplish red mudstones with several intercalations of yellowish grey or greyish green middle to fine-grained feldspathic quartz sandstone or feldspar lithic sandstone. The dinosaur fossils are concentrated in a layer 3-5 meters thick of greyish green fine-grained feldspar lithic sandstone in the lower part of the formation. Up to now, more than 200 individuals of dinosaurs and other vertebrates have been uncovered. Among them, 29 species of 26 genera have been identified. They include sauropods, theropods, basal neornithischians, stegosaurs, and fish, amphibians, turtles, crocodiles, plesiosaurs, pterosaurs and therapsids. This is a highly diversified vertebrate community of the Middle Jurassic.

Scientific research and tradition

The site, with an area of about 70,000 square meters, was first uncovered in 1972. An on-site museum was built thereafter. Extensive studies have been carried out by scientists at home and abroad. Six monographs, 2 special issues and more than 100 published papers document the fossils and interpret their paleobiology.



UPPER JURASSIC CARNEGIE QUARRY

DINOSAUR BONE SITE

UNITED STATES OF AMERICA



Articulated skull and cervical vertebrae of *Camarasaurus* as seen on the quarry face.

SHOWCASING AN IN-SITU WALL OF OVER 1500 BONES REPRESENTING NINE LATE JURASSIC DINOSAUR SPECIES.

The Quarry stands as a prime example of a geoconservation site, housing authentic dinosaur bones preserved in rock and protected by a steel, concrete, and glass structure. Discovered in 1909 by Carnegie Museum crews, the site quickly became a geotourist attraction. The on-site exhibition showcases dinosaur bones in their original setting, mirroring their deposition some 150 million years ago in an ancient riverbed. Complementary exhibits explore the Late Jurassic paleoenvironment of the region, spotlighting fossils excavated from both the Quarry and its environs.

bition showcases dinosaur bones in their original setting, mirroring their deposition some 150 million years ago in an ancient riverbed. Complementary exhibits explore the Late Jurassic paleoenvironment of the region, spotlighting fossils excavated from both the Quarry and its environs.

SITE 138

GEOLOGICAL PERIOD	Upper Jurassic
LOCATION	Northeastern Utah, United States of America 40°26'26"N 109°18'04"W
MAIN GEOLOGICAL INTEREST	Paleontology Stratigraphy and sedimentology



In-situ dinosaur bones embedded in sandstone as seen in the Quarry Exhibit Hall.

Geological Description

The Carnegie Quarry Exhibit Hall, situated in Dinosaur National Monument, spans 585 square meters of steeply inclined fluvial sandstone. Within, 1500 in-situ dinosaur bones from nine dinosaur species and freshwater bivalves offer insights into the biodiversity and an ecosystem in the Upper Jurassic Morrison Formation. A recent Pb/U date of 150.77 Ma places the bone deposit near the top of the Kimmeridgian.

Sedimentological and taphonomic analyses attribute the three bone layers to drought periods, when decaying carcasses accumulated in a braided river system. Various bone configurations, from complete skeletons to

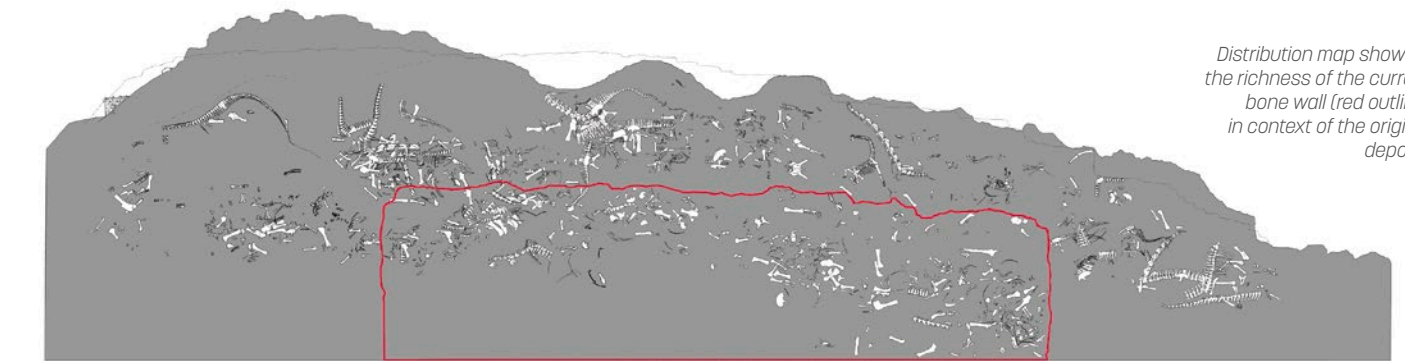
scattered parts, reveal fluvial transport. Significantly, many bones display evidence of upstream scour, indicating a novel finding that bones within dynamic depositional settings facilitated their own burial.

The deposit showcases diverse Late Jurassic dinosaur species, including sauropods, theropods, stegosaurs, and ornithopods and has long been used as representing Late Jurassic dinosaurs to the public. Furthermore, the Quarry produced the *Apatosaurus louisae* type specimen, unveiling the first evidence of a whip-like tail in sauropods. Size variation in *Camarasaurus* provides insights into growth changes. Dinosaurs from the

quarry are displayed in various North American museums, some as the sole skeletons of their species, highlight the Quarry's paleontological significance.

Scientific research and tradition

Discovered in 1909, the dinosaur fossils from the quarry have played an important role in defining Late Jurassic dinosaur taxonomy and paleoecology in North America. More recent studies have focused on the depositional and taphonomic settings [Bilbey *et al.*, 1974; Lawton, 1977; Carpenter, 2013, 2020, 2023] and site history [Carpenter, 2018].



Distribution map showing the richness of the current bone wall (red outline) in context of the original deposit.

EARLY CRETACEOUS WETLAND OF LAS HOYAS SPAIN



The gobicodon early mammal *Spinolestes xenarthrosus* with body hair, external ear skin, and lungs in ribcage. Housed at Museo Paleontológico de Cuenca (MUPA).

A WETLAND WITH MICROBIAL MATS FAVORING THE EXCEPTIONAL FOSSILIZATION OF ANIMALS AND PLANTS INCLUDING THEIR SOFT TISSUES.

Las Hoyas provides unique insight into the ecological structure of an Early Cretaceous wetland inhabited by microorganisms, vascular and non-vascular plants, and invertebrates and vertebrates. Its fossils exhibit the first evidences, with exquisite macro and micro details, of crucial evolutionary novelties that flourished at that time, such as seeds and flowers in

the angiosperm *Montsechia*, modern flying apparatus in the iconic enantiornithine birds (e.g., *Iberomesornis*; Sanz *et al.*, 1996), and the evolution of hair complexity and the presence of lungs in the eutrichodont mammal *Spinolestes* (Martin *et al.*, 2015). The fossils are exhibited in the Museo Paleontológico de Cuenca.

SITE 139

GEOLOGICAL PERIOD	Lower Cretaceous
LOCATION	Cuenca, Castilla-La Mancha region, central Spain, Spain 40°05'25"N 001°53'45"W
MAIN GEOLOGICAL INTEREST	Paleontology Stratigraphy and sedimentology



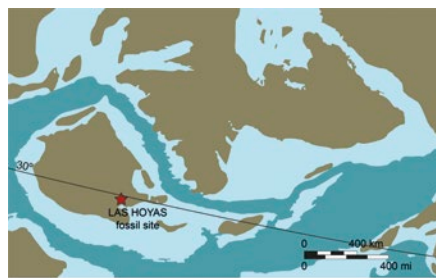
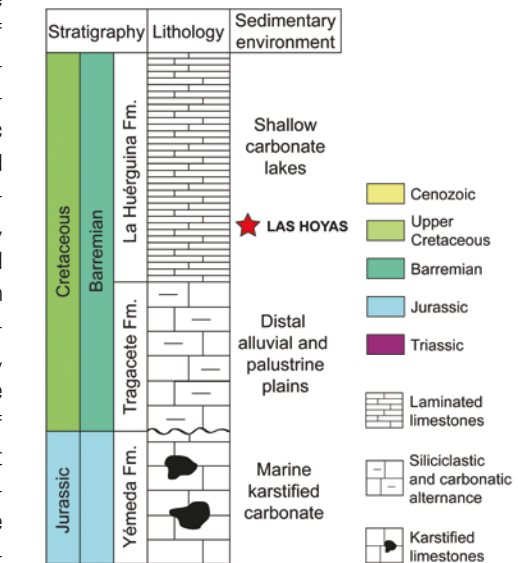
Las Hoyas onsite systematic sampling of the finely laminated limestones. Photo: Javier Lobón Rovira.

Geological Description

Las Hoyas is a remarkable fossil site known for its complete Barremian wetland Biota, which includes approximately 250 species of soft-bodied organisms, plants, and animals (Marugán-Lobón *et al.*, 2023). The site was in a microbasin within the Cuenca sub-basin of the Iberian Domain. The La Huérguina Formation, which yields the fossils, was dated by charophyte and ostracod associations, and was deposited in lacustrine and palustrine environments. The formation is composed of finely laminated limestones that were deposited in depressions formed by tectonic activity over pedogenic and karstified Jurassic marine limestones (Fregenal-Martínez and Meléndez, 2016). The locality was a shallow lake situated in an extensive, perennial, carbonate inland wetland in a subtropical climate. The lake was drained by water rich in carbonates, which was fed by karstic aquifers. The system was seasonally regulated, with water-level oscillations, favoring the growth of microbial mats. The microfacies of mats indicate drier periods with abundant fossil remains, while wetter periods are characterized by microfacies composed of fine carbonate particles and debris with a limit-

ed number of fossils. A systematic excavation layer by layer is essential for obtaining detailed information on fossil assemblages and for the recognition of ichnological evidence and microbially induced sedimentary structures.

Paleogeographic, geological and sedimentary setting of Las Hoyas in the Iberian Plate, remarking its location (red star) within the Barremian deposits.



Scientific research and tradition

Multidisciplinary research at Las Hoyas initially focused on characterizing the diversity and evolution of the biota. Subsequently, researchers aimed to explain the exceptional preservation through actuataphonomy, particularly emphasizing the role of microbial mats (Iniesto *et al.*, 2015). Ongoing efforts explore paleowetland ecological complexity using network and foodweb analyses.

CRETACEOUS LAGERSTÄTTEN OF CARIRI STONE

BRAZIL



UNESCO Global Geopark

HIGH DIVERSITY AND ABUNDANCE OF LARGE REPTILES, DINOSAURS AND PTEROSAURS, FISH, INSECTS, CRUSTACEANS, AND PLANTS IN HYPERSALINE LACUSTRINE DEPOSITS.

Cordulagomphus fenestratus (MPSC I 485). Fossilized dragonfly (Odonata) preserved in the Crato Formation, bearing witness to these insects' ancient flight 110 million years ago.

The Cretaceous Lagerstätten of the Cariri Stone is esteemed for its remarkable fossil deposits standing as a landmark in paleontological significance globally. The fossils of dinosaurs and pterosaurs, with their deep-rooted cultural significance, especially resonate with the public. Angiosperms, marking a significant evolutionary shift in the planet's vegetation by

progressively overtaking gymnosperms, are commonly found in these deposits, together with a variety of pollinating insects, potentially signaling a coevolutionary relationship between these groups. This area's rich biodiversity attracts a significant number of scholars and sightseers and plays a crucial role in enhancing the local economy.

GEOLOGICAL PERIOD	Cretaceous
LOCATION	Cariri, Brazil 07°07'12"S 039°41'32"W
MAIN GEOLOGICAL INTEREST	Paleontology Stratigraphy and sedimentology

SITE 140



Dastilbe crandalli Jordan 1910 (LPU PF 37), an abundant Actinopterygii fish, preserved in the laminated limestones of the Crato Formation. Image credits: José Lúcio.

Geological Description

The Cretaceous Lagerstätten of Cariri Stone is situated within the territory of the Araripe Geopark, in the Araripe Sedimentary Basin, Northeast Brazil. Its name is derived from the "Pedra Cariri," the principal sedimentary rock of the Crato Formation, part of the Santana Group. It consists of limestone layers in fine beige and gray colors that belong to the post-rift mega-sequence dated to the Aptian-Albian Age (Assine *et al.*, 2014). It is divided into six units (C1 to C6) of laminated limestone intercalated with marls, calcareous siltstones, and shales (Neumann *et al.*, 2003). The C6 layer is the most commercially exploited, resulting in the majority of fossils originating from this unit.

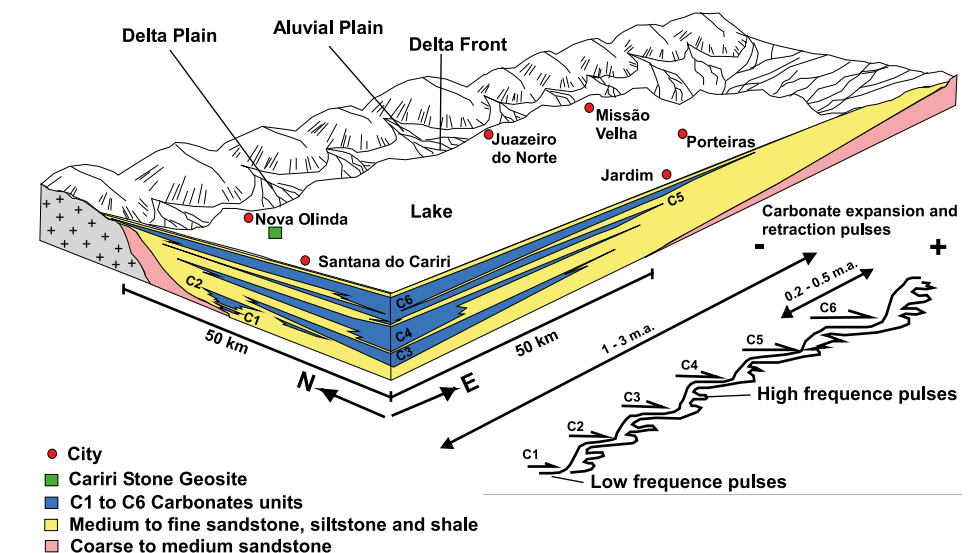
The Crato Formation represents the primary lacustrine phase of the continental succession in the Araripe Basin, often influenced by hypersaline conditions. It is characterized by a high diversity and abundance of fossils in pristine preservation, stemming from a wide range of taphonomic processes. Large reptiles such as dinosaurs and pterosaurs, fish, insects, crustaceans, and plants are among the principal groups preserved in

strata, rendering the Crato Formation a crucial component in comprehending the history of life on Earth.

Location of the Geosite Cretaceous Lagerstätten of Cariri Stone in the ancient Cretaceous lake.

Scientific research and tradition

Research on the Crato Formation began with the discovery of *Dastilbe* fish fossils in 1947. Limestone mining exposed these fossils, and as illegal trade intensified, institutions were established from the 1970s onwards to study, register, and designate protected areas. Since the 1980s, this deposit has been recognized as extraordinary.



THE CRETACEOUS DINOSAUR NESTING GROUNDS OF THE WILLOW CREEK ANTICLINE UNITED STATES OF AMERICA



Maiasaura hatching from its egg. Reconstructed cast by J. Horner; on exhibit at Museum of the Rockies.

THE AREA THAT REVEALED THE FIRST EVIDENCE OF COLONIAL NESTING AND PARENTAL CARE IN DINOSAURS.

One of the most significant dinosaur localities, these exposures of the Two Medicine Formation produced the first dinosaur eggs and babies discovered in the western hemisphere. The fossils of the duck-billed dinosaur *Maiasaura* indicate these animals nested in groups and cared for their young, discoveries which helped shift the public and scientific perception

of dinosaurs and their behavioral complexity. Histologic analyses of bones revealed insights into dinosaur growth and ecology, elevating histology as standard paleontologic practice. Based on its abundant fossils from the WCA, *Maiasaura* is now considered a model organism for dinosaur paleobiology studies (Woodward *et al.*, 2015).

SITE 141

GEOLOGICAL PERIOD	Upper Cretaceous
LOCATION	Teton County, Montana, United States of America 47°49'08"N 112°11'18"W
MAIN GEOLOGICAL INTEREST	Paleontology



Outcrops of the Willow Creek Anticline in Teton County, Montana.

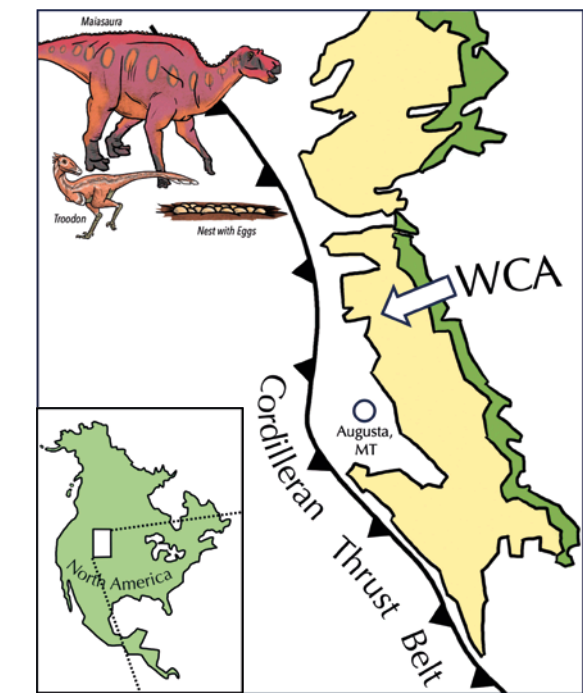
Geological Description

Exposures of the Upper Cretaceous Two Medicine Formation within the Willow Creek Anticline (WCA) consist of interbedded mudstones and sandstones representing an ancient floodplain. In 1978, Marion Brandvold found baby duck-billed dinosaur bones here. Investigation of the area by paleontologists John R. "Jack" Horner and Robert "Bob" Makela led to the discovery of the first dinosaur nests with associated eggs and babies in the western hemisphere (Horner and Makela, 1979). The close proximity of nests indicated these dinosaurs nested in groups. Examination of the fossils suggested this dinosaur cared for its young after they hatched and inspired its name: *Maiasaura* (the "good mother reptile"). Thousands of larger bones of *Maiasaura* were preserved nearby in an extensive bone bed and have been the subject of robust taphonomic and histologic studies. Nearby sites, including "Egg Mountain", preserve egg clutches of the theropod dinosaur *Troodon* and the first *in ovo* dinosaur embryos (Horner and Weishampel, 1988). The WCA preserves not only fossil bones, but also trace fossils from a variety of Cretaceous animals. Nesting

structures, footprints, coprolites, gastric pellets, insect pupae, burrows, and more have been discovered here, providing an unparalleled window into this ancient ecosystem (e.g. Varricchio *et al.*, 1997; Chin, 2007).

Scientific research and tradition

Several dinosaur, mammal, and lizard species are named based on fossils from the WCA. Today, many of these localities are part of Museum of the Rockies' Beatrice R. Taylor Paleontology Research Area, a site of ongoing research.



Generalized geologic map of the Willow Creek Anticline (WCA) area, after Weaver *et al.* (2021). Produced by Brian Helms.

WHALE VALLEY, CETACEA AND SIRENIA EOCENE FOSSILS OF WADI AL-HITAN EGYPT



UNESCO World Heritage Site

A complete *Basilosaurus* whale skeleton surrounded by hills. (Photo by Miguel Ángel Sainero).

HUNDREDS OF COMPLETE SKELETONS OF THE EARLIEST WHALES ALONG WITH FOSSILS OF MANGROVE ROOTS.

In 2015 UNESCO and 2018 IUCN recognized Egypt's initial natural world heritage site as a World Heritage Site, emphasizing its worldwide significance in understanding our planet's biological history. The presence of whale skeletons, shark teeth, sirenians, and reptiles in this region provides a captivating glimpse into their evolutionary past, spanning 40 million

years. Therefore, scientists highly regard this collection of whale fossils found in moon-like landscapes as a valuable scientific treasure. It provides unparalleled insights into the transition of whales from land-dwelling creatures to marine beings, as well as their migration patterns, evolution, and the environmental conditions that existed millions of years ago.

GEOLOGICAL PERIOD	Paleogene (Eocene)
LOCATION	Fayum province, Egypt 29°15'54"N 030°01'20"E
MAIN GEOLOGICAL INTEREST	Paleontology Stratigraphy and sedimentology

SITE 142

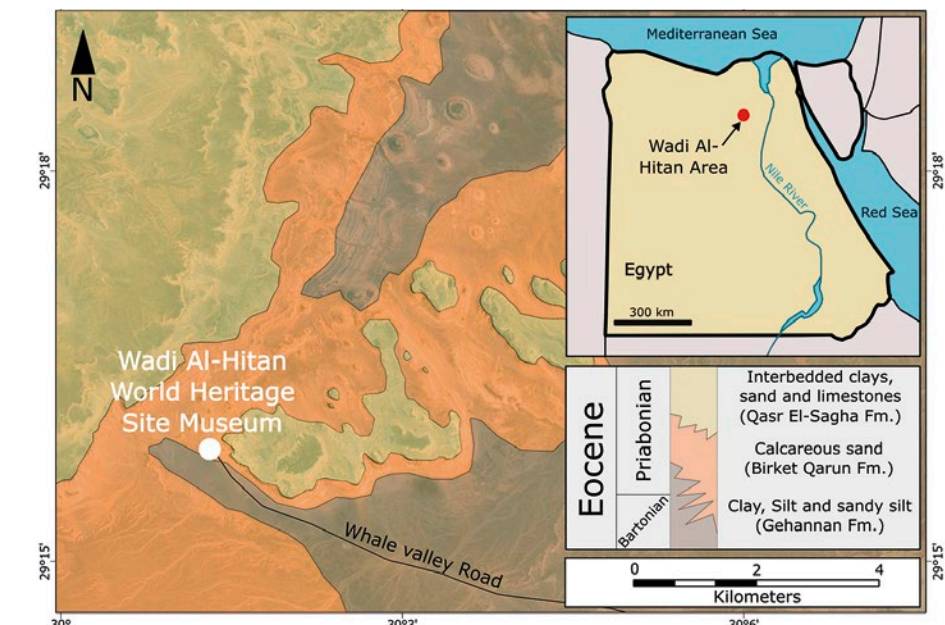
Detail of the *Basilosaurus* skeleton shown in the previous page image. (Photo by Miguel Ángel Sainero).

Geological Description

Wadi Al-Hitan "Valley of the Whales" serves as an extraordinary paleontological site situated in the Fayum Governorate of Egypt. It is an exceptional record of the ancient history of our planet when marine life flourished along the coast and the mysterious migration of whales took place. Researchers in Wadi Al-Hitan have discovered numerous fossils of archaeoceti, an extinct sub-order of whales that includes some of the earliest species of whales. Specimens are impressive, and the largest skeleton discovered has a length of 21 meters. These fossils offer vital evidence for unraveling one of the most significant enigmas in the evolution of whales: their transition from terrestrial creatures to marine mammals. Remarkably, the fossils preserve primitive features in their skull and tooth structure. Certain skeletons within the study of archaeoceti exhibit hind legs, feet, and toes, which is an unforeseen discovery. These fossils not only shed light on the evolution of whales but also provide insights into the surrounding environmental conditions millions of years ago. The present landscape, resembling the moon's surface and scattered with fossil remains, encourag-

es us to delve into the captivating narrative of Earth's gradual evolution. This exceptional area was officially recognized as a UNESCO World Heritage Site because of an exceptional scientific treasure due to the unparalleled abundance and quality of whale fossils.

Simplified geological sketch of Wadi Al-Hitan. (Based on King et al., 2014). Source: Maxar with ArcGIS Pro, Esri.



Scientific research and tradition

Beadnell (1905) discovered *Basilosaurus*, the first fossil whale. After a revival of research, the site was designated as a Special Protected Area within the Wadi El-Rayyan Protected Area in 1997. In 2005, the site was added to the World Heritage list under Natural Criterion viii for the hundreds of fossils of archaeoceti.

THE LA VENTA MIDDLE MIocene NEOTROPICAL BIOME COLOMBIA



The 'La Tatacoa Desert': the iconic badland landscape of the La Venta Konzentrat-Lagerstätte. Some levels of this variegated middle Miocene rock succession are remarkably fossiliferous.

A KONZENTRAT-LAGERSTÄTTE THAT HOSTS ONE OF THE MOST DIVERSE AND EXUBERANT BIOMES FROM AN EXTINCT NEOTROPICAL RAINFOREST.

The paleontological record of the La Venta Konzentrat-Lagerstätte provides valuable insights into the response of the biome to the middle Miocene Climatic Transition. Its remarkable fossil preservation is evidence of the rich biodiversity of endemic faunal groups prior to the Great American Biotic Interchange, and its geological history exemplifies the intricate paleobiogeographic

and tectonostratigraphic evolution of northern South America. Additionally, its characteristic mammalian assemblage is the basis for the Laventan Stage and the corresponding geochronologic unit, the Laventan Age (13.5 to 11.8 Ma), which is also utilized as a Land Mammal Age for South America (Kay *et al.*, 1997; Montes *et al.*, 2021; Carrillo, 2023).

SITE 143

GEOLOGICAL PERIOD	Miocene
LOCATION	La Venta, Villavieja, Huila, Colombia 03°15'32"N 075°10'03"W
MAIN GEOLOGICAL INTEREST	Paleontology Stratigraphy and sedimentology



Cranial, dental and appendicular remains of *Purussaurus neivensis* (Mook, 1941) and *Gryposuchus colombianus* (Langston, 1965), representative species of the site's hyperdiverse crocodyliform assemblage. MGN-SGC (Bogotá).

Geological Description

The La Venta Konzentrat-Lagerstätte documents the astonishing biodiversity of one of the most fascinating neotropical biomes, through its abundant fossil concentrations. Its variegated fine- to medium-grained rock succession, part of the Honda Group, accumulated in dynamic fluvial and alluvial environments between ~15.9 Ma and ~10.5 Ma (Kay *et al.*, 1997; Spradley *et al.*, 2019; Carrillo, 2023).

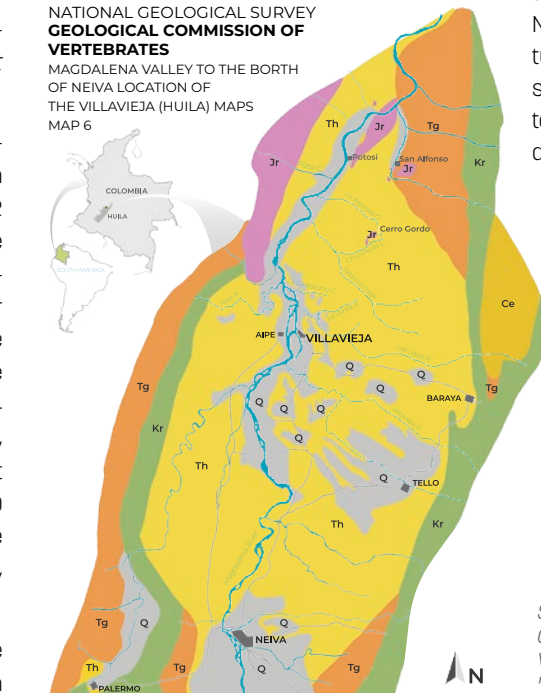
In addition to plant remains and ichnofossils, over 190 different fossil taxa have been identified, including 50 new genera and 102 new species. The fossil fish assemblage documents the establishment of the rich extant fauna of the Orinoco and Amazon River basins, and the reptilian fossil remains give evidence of specialized adaptations. The Laventan mammalian fauna consists of 34 new fossil species of rodents, primates, bats, and sirenians, 26 new species of extinct native ungulates and xenarthrans, and 20 new taxa of oldest representatives of some extant metatherians (Kay *et al.*, 1997; Defler, 2019; Carrillo, 2023).

Its emblematic "badlands" scenery and the development of excellent outcrops over an

extensive area, results from the interplay between lithology, long-term weathering, and the dry conditions induced by the orographic rain shadow of Los Andes (Dill *et al.*, 2020; Montes *et al.*, 2021).

NATIONAL GEOLOGICAL SURVEY GEOLOGICAL COMMISSION OF VERTEBRATES

MAGDALENA VALLEY TO THE BORTH OF NEIVA LOCATION OF THE VILLAVIEJA (HUILA) MAPS
MAP 6



LEGEND

- Jr Payandé Formation with porphyritic rocks (Jurassic-Triassic)
- Kr Cretaceous (Guadalupe Formation, mainly)
- Tg Lower Tertiary (Gualanday Series)
- Th Upper Tertiary (Honda Formation)
- Ce Cenozoic (upper Tertiary and Quaternary)
- Q Quaternary

Schematic geological map adapted from Royo y Gómez & Varón (1945) during the "Commission of Vertebrates", featuring the fossil-rich strata of the "Honda Formation" (Th).

THE MODERN HUMAN FOSSILS OF THE KIBISH FORMATION ETHIOPIA



UNESCO World Heritage Site

A view of the Kibish Formation exposures at the southern banks of the Omo River (Photograph credit, Celine Vidal).

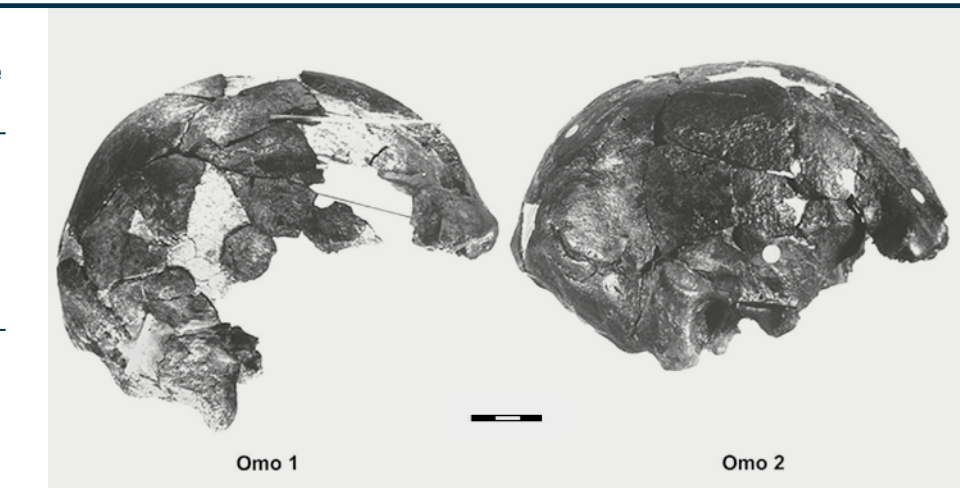
HOME OF ONE OF THE OLDEST FOSSILS OF HOMO SAPIENS FOSSILS WITHIN A 105-METER-THICK MIDDLE PLEISTOCENE TO HOLOCENE LACUSTRINE AND DELTAIC SUCCESSION.

The Kibish Formation is a unique sedimentary terrain where Omo I (dated to ~233 ka) and Omo II fossils have been discovered. These are some of the oldest known modern human fossils in the world. The Kibish Formation is a well-studied and well-dated formation exposed at the

shores of the Omo River. It is located within the Lower Omo Valley, a World Heritage site, inscribed by UNESCO in 1980. The Kibish Formation presents an otherworldly landscape with dissected and eroded layers of all members of the Kibish Formation exposed on either side of the Omo River.

SITE 144

GEOLOGICAL PERIOD	Pleistocene to Holocene
LOCATION	Southern, Ethiopia 05°18'46"N 035°56'22"E
MAIN GEOLOGICAL INTEREST	Paleontology Stratigraphy and sedimentology



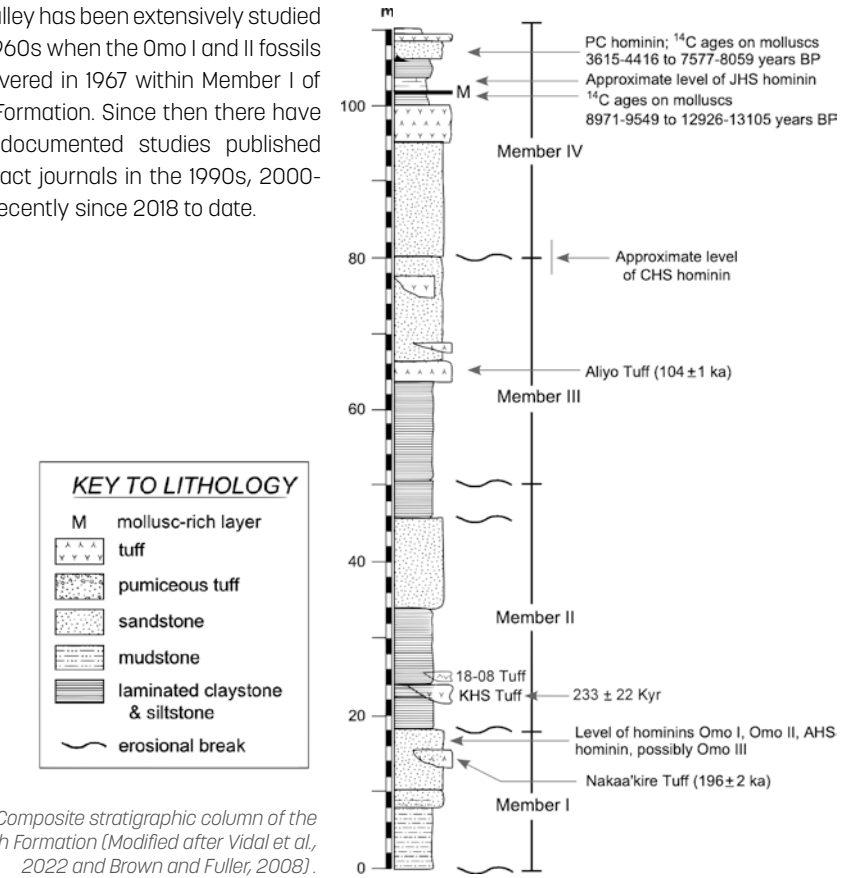
Omo 1 and Omo 2 fossil crania from the Kibish Formation (Photograph credit: Michael Day).

Geological Description

The Kibish Formation at the Lower Omo valley, with an aggregate thickness of 105m consists of lacustrine and deltaic deposits divided into four members (Brown and Fuller, 2008). It is a Middle Pleistocene to Holocene Formation, where two fossils of early *Homo sapiens* (Omo I and Omo II) were discovered in the lower sections of Member I. The Omo fossils were recently dated to 233 ± 22 kyr based on geochemical analyses that link the Kamoya's Hominid Site (KHS) Tuff, which conclusively overlies Member I that contains Omo I, with a dated major explosive eruption of Shala volcano in the Main Ethiopian Rift (Vidal et al., 2022). Member I (~20m thick) is composed of sandstones, siltstones, and claystones, with minor tuffs, while member II (~32m thick) consists of a tuff at the base, overlain by uniformly bedded and laminated silty clays, thin sand stringers and fine sandstone. Member III (~30m thick) comprises sandstones with conglomerate lenses and one prominent 3-4m thick tuff at its base, the Aliyo tuff dated to ~104 ka. Member IV (~28m thick) forms laterally extensive deposits of sandstones and laminated silty clays forming the Kibish plain (Brown and Fuller, 2008).

Scientific research and tradition

The Omo valley has been extensively studied since the 1960s when the Omo I and II fossils were discovered in 1967 within Member I of the Kibish Formation. Since then there have been well-documented studies published in high impact journals in the 1990s, 2000-2018, and recently since 2018 to date.



Composite stratigraphic column of the Kibish Formation (Modified after Vidal et al., 2022 and Brown and Fuller, 2008).

THE HUMAN FOOTPRINTS OF ACAHUALINCA NICARAGUA



Close view of footprints showing them extending away. The details of the mud squashed up by each foot is perfectly preserved.

A LONG FOOTPRINT SEQUENCE OF AT LEAST 16 PEOPLE WALKING IN AN ANCIENT GEOLOGICAL ENVIRONMENT BY LAKE MANAGUA.

The Acahualinca Footprints are a unique record of the Holocene stratigraphic, volcanic, tectonic and geomorphological history of the Central American isthmus. They are overlain by six lithostratigraphic units, representing at least 14 volcanic eruptions. The footprints are globally important as one of the few accessible

sites with exceptionally well exposed human footprints. They have a unique value, being a long sequence of footsteps of at least 16 people taking a walk in an ancient geological environment. The site excavation and preservation allows observation of both footprints, paleogeomorphology and stratigraphy in one glance.

SITE 145

GEOLOGICAL PERIOD	Holocene
LOCATION	Managua, Nicaragua 12°09'44"N 086°18'48"W
MAIN GEOLOGICAL INTEREST	Paleontology Volcanology



View from above showing footprints crossing a small paleostream (the infants were carried across). The well preserved stratigraphy is seen on either side.

Geological Description

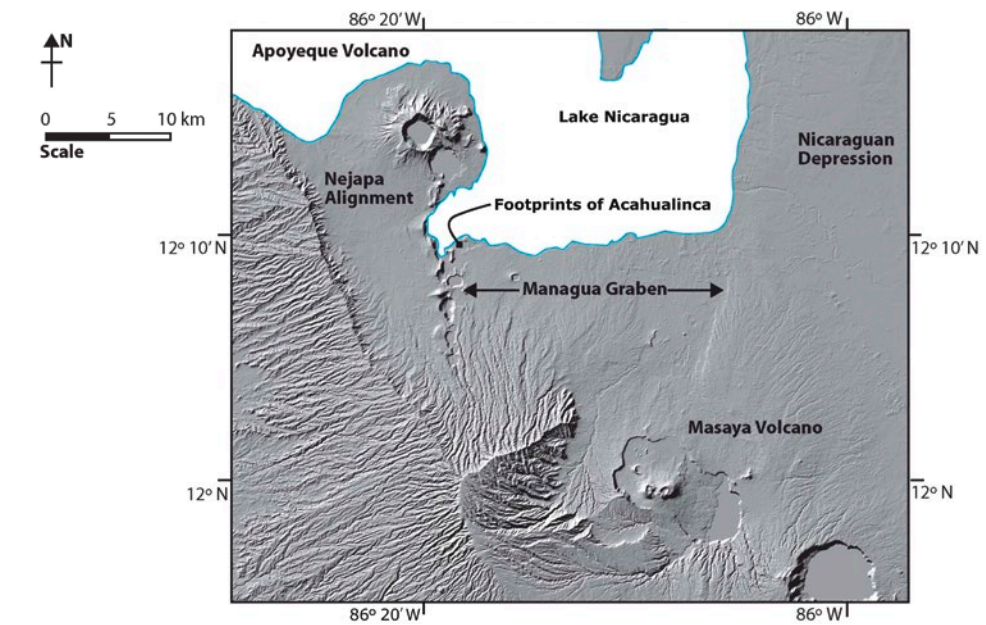
The Footprints of Acahualinca incorporate a double record: 1) they provide anthropomorphic traces and cultural characteristics of early human occupation of Central America. Debated to be between 2,000 and 8,000 years old (Brown, 1947; Bryan, 1973; Schmincke *et al.*, 2009; Sachiko, 2017), the more recent work indicates that the older dates are more likely. 2) they record active geodynamics associated with intense explosive volcanism, including huge Masaya Volcano basaltic ignimbrites, and activity in the Managua Graben, a pull-apart structure in the Nicaraguan Depression.

The footprints were discovered in 1874 (Flint, 1884; Chávez, 1920). In 1953 the Footprints of Acahualinca Museum was founded. The site is protected under Nicaraguan law. Footprints of about 16 adults and children can be seen. There are over 1,000 fossil footprints of humans and animals, as well as evidence of flora, all preserved under a 4 meter thick sequence of tuff. This stratigraphy is a type sequence for the region, including globally important basaltic ignimbrite surge deposits from the Masaya volcano and the nearby Nejapa Volcanic alignment. The Acahualinca

Scientific research and tradition

Footprints record a unique geological-cultural lakeside landscape outstanding in their evidence of humans associated with important water sources in an active volcanic and tectonic environment.

The Footprints of Acahualinca have been an object of strong debate since their discovery in 1874. The debates still range over the exact date of the prints, the environment, and what the people were doing (escaping from an eruption, or just taking an easy walk).



Shaded relief map with the main geological features, including Masaya, Nejapa Alignment, Chiltepe Volcanoes, the Managua Graben and the Nicaraguan Depression.

4

IGNEOUS AND METAMORPHIC PETROLOGY

SITE 146 - SITE 153



Pegmatite Bergell, Switzerland

Igneous petrology involves the study of rocks that form by crystallization from magma. If the magma crystallises below the surface of the Earth it cools slowly, forming coarse-grained igneous rocks known as plutonic rocks. Conversely, if the magma reaches the surface of the Earth then it cools more quickly and finer-grained volcanic rocks result. The former type of igneous rock is featured in this chapter, and volcanic rocks are the focus of chapter 5.

Metamorphic petrology relates to the study of rocks that have been metamorphosed, meaning 'changed in form', due to changes in the rock's environment. These changes are most commonly in terms of varying temperature or pressure and are typically linked to intense deformational processes deep in the Earth during plate tectonic processes, e.g. when lithospheric plates collide to form mountains. Following erosion, vast belts of metamorphic rocks are exhumed to the Earth's surface, which represent the vestiges of ancient plate movements.

The two fields of igneous and metamorphic petrology are closely connected as local metamorphism also occurs in the 'country rocks' surrounding cooling plutonic rocks. Furthermore, if metamorphism occurs at sufficiently high temperatures, they start to partially melt and transition into igneous rocks. Earth is a dynamic planet, and igneous and metamorphic rocks attest to the tremendous forces at work in creating and transforming Earth's lithosphere throughout geologic time. Therefore, igneous and metamorphic petrology are central to understanding the origin and evolution of the Earth. Igneous and metamorphic rocks are also important hosts of metallic ore deposits and sources of building stones.

Owen Weller – Gibbs

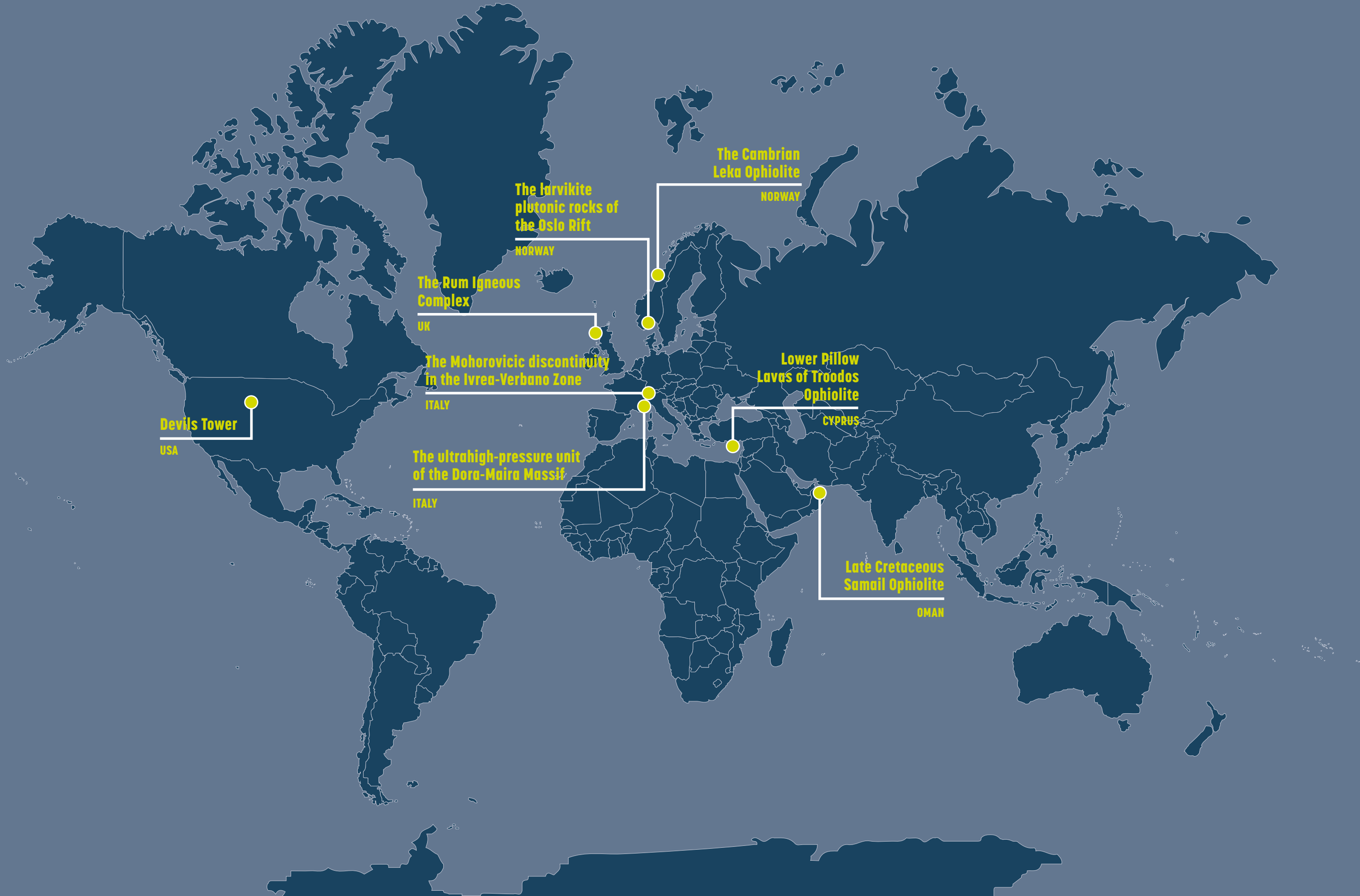
Department of Earth Sciences, University of Cambridge, Cambridge, United Kingdom
Chair, MSG - Metamorphic Studies Group.
IUGS Geological Heritage Sites referee.

Michele Lustrino

Dipartimento di Scienze della Terra, Sapienza University of Rome, Italy.
Chair, TGIR, - IUGS Task Group on Igneous Rocks.
IUGS Geological Heritage Sites referee.

Sebastian Tappe

UiT The Arctic University of Norway, Tromsø, Norway
Chair, TGIR, - IUGS Task Group on Igneous Rocks.
IUGS Geological Heritage Sites referee.



THE LARVIKITE PLUTONIC ROCKS OF THE OSLO RIFT NORWAY



UNESCO Global Geopark

The larvikite landscape along the coast of Larvik. The rocks showing wonderful glacial features and a pegmatite to the left.

**ONE OF THE FEW PLACES TO
STUDY THE BLUE MONZONITIC
PLUTONIC ROCKS FORMED
BENEATH A CONTINENTAL RIFT
ENVIRONMENT.**

"Larvikite" represents a group of monzonitic plutonic rocks formed beneath a continental rift environment. The Oslo rift is one of the few places where such deep continental rift magmatism can be studied. The larvikite complex is also important as the host of a number of scientific discoveries, such as being type area for a number of minerals and the discovery of

the element Thorium. Still new minerals are documented, as alflarensite (2008) and peterandresenite (2012), named after local collectors. Larvikite was one of the first rocks to be approved as "heritage stone". Features of larvikite intrusions are perfectly exposed and can be studied along the coastline between Ula and Nevlunghavn village.

SITE 146

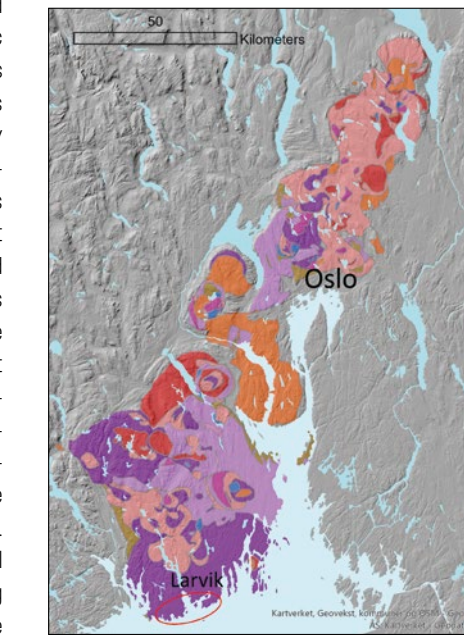
GEOLOGICAL PERIOD	Permian (Cisuralian)
LOCATION	Larvik municipality, Vestfold County, Norway 58°34'48"N 010°00'36"E
MAIN GEOLOGICAL INTEREST	Igneous and Metamorphic petrology



Close up of a polished, dark blue variety of larvikite, also known as "Pub stone".

Geological Description

The Carboniferous-Permian Oslo Rift represents an early internal rifting on the Pan-gaea continent that never evolved into an oceanic spreading ridge. The ancient rift valley suffered intensive volcanic activity, leaving vast deposits of alkaline lavas and pyroclastic rocks. Among the lavas, the most prominent type is latite, traditionally named "rhomb porphyry". Larvikite is the plutonic equivalent to these porphyries. As a series of monzonitic rocks, the larvikites stands out by being primarily composed of ternary feldspars, displaying cryptoperthitic intergrowths. Interference between light waves and the intergrowth lamellae creates bright blue iridescence, which is highly appreciated in the natural stone market. Thus, larvikite is among the most attractive dimension-stone resources in the world, and it is likely to find it in a façade or kitchen top near you. The larvikite complex is a series of ring-shaped plutons becoming younger and more undersaturated from east to west. Thus, they range from quartz-bearing to nepheline-bearing. They display magmatic layering and crystal orientation patterns reflecting the overall ring structure. Larvikites also host a wide range



Legend

- Volcanic breccia
- Rhyolite
- Trachyte
- Latite (rhomb porphyry)
- Basalt
- Alkali feldspar syenite
- Alkali feldspar granite
- Granite
- Larvikite
- Site area

Map of the Carboniferous - Permian Oslo Igneous Province.

THE RUM IGNEOUS COMPLEX

UNITED KINGDOM



Rhythmically layered feldspathic peridotite close to Long Loch in the Central Intrusion (Brian O'Driscoll).

SUPERB ARRAY OF SHALLOWLY EMPLACED ULTRAMAFIC TO FELSIC IGNEOUS ROCKS THAT DIFFERENTIATED IN AN OPEN SYSTEM AND CONCENTRATED PRECIOUS METALS.

The Rum Layered Complex is a world class example of open system magma differentiation, featured heavily in classic subject texts (Wager and Brown, 1968). The ELI typifies this and has been returned to for decades to test concepts of magma differentiation by crystal fractionation. Other parts of the intrusion (WLI) contain some of the type examples of in situ crystalli-

sation in plutonic settings - specifically harrisite (considered an equivalent of spinifex texture) formed by relatively deep undercooling of picritic magma. Extreme precious metal (platinum group elements) enrichment in chromitite seams of the ELI have also been used to evaluate models of ore deposit formation.

GEOLOGICAL PERIOD	Eocene
LOCATION	NW Scotland, United Kingdom 57°00'00"N 006°21'00"W
MAIN GEOLOGICAL INTEREST	Igneous and Metamorphic petrology History of geosciences

SITE 147



Northwestern slopes of Hallival, the resistant pale rock steps are the upper troctolite parts of each macro-rhythmic unit in the Eastern Layered Intrusion (Brian O'Driscoll).

Geological Description

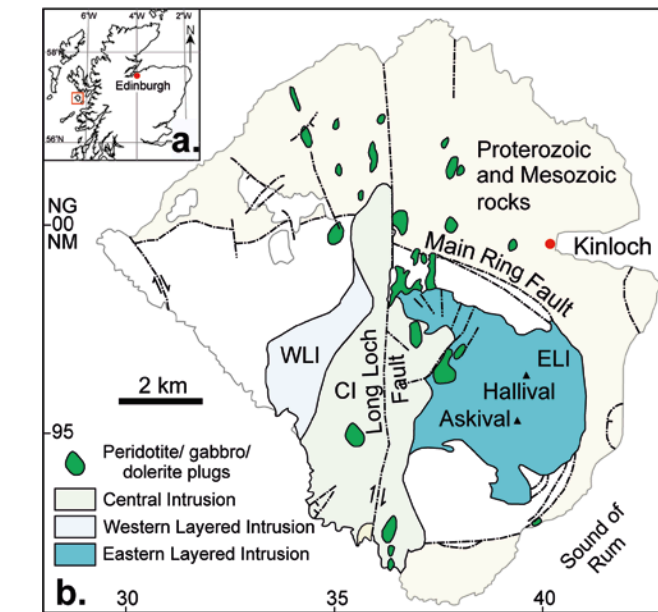
The Rum Igneous Complex was intruded ~60 million years ago, during rifting and formation of the North Atlantic ocean. The Rum Igneous Complex was intruded into a rifting basin containing Archaean Lewisian gneisses to Mesozoic strata and contemporaneous lavas flows that are all exposed, enabling examination of their relationship with the igneous complex. Sedimentary breccias are possibly associated with proto-caldera forming processes and mafic/ultramafic satellite plugs possibly represent solidified fire fountain roots.

The Rum Igneous Complex is constructed from layered massifs divided into three geographic sectors the: (1) Eastern Layered Intrusion (ELI), built up of 16 macro-rhythmic units that differentiated in batches, composing the majestic Hallival and Askival mountains. Platinum-group element rich Cr-spinel horizons can be found within the ELI; (2) Western Layered Intrusion (WLI), representing the lowest structural level of intrusion, with evidence of picritic magmas and in situ crystallisation to form the spectacular harrisite (up to 2 m long olivine crystals) and (3) Central Layered Intrusion (CLI), which is the feeder

zone (Long Loch Fault) of the layered intrusion, into which unconsolidated cumulate slumped and deformed during final stages of solidification. Within the complex are a spectacular array of deformation features, rock types and complex textures.

Scientific research and tradition

Early work was done by Harker in the early 1900s. Eminent geologists Bailey, Richey and Geikie all visited after the war. Malcolm Brown wrote classic 1956 paper and Rum featured heavily in the classic Wager and Brown 1968 text. Proliferation of work followed sale of island in 1950s - before this, it had been the 'forbidden isle'.



Location map of the Rum Layered Intrusion, NW Scotland and simplified geological map of the Rum Layered Intrusion, modified after Emeleus (1994).

DEVILS TOWER, MATEO TEPE

UNITED STATES OF AMERICA



Overview of Mateo Tepe showing prominent 'pillar-like' relief above the surrounding plain; the vertical lineation of the columnar jointing is also apparent (image from Alamy).

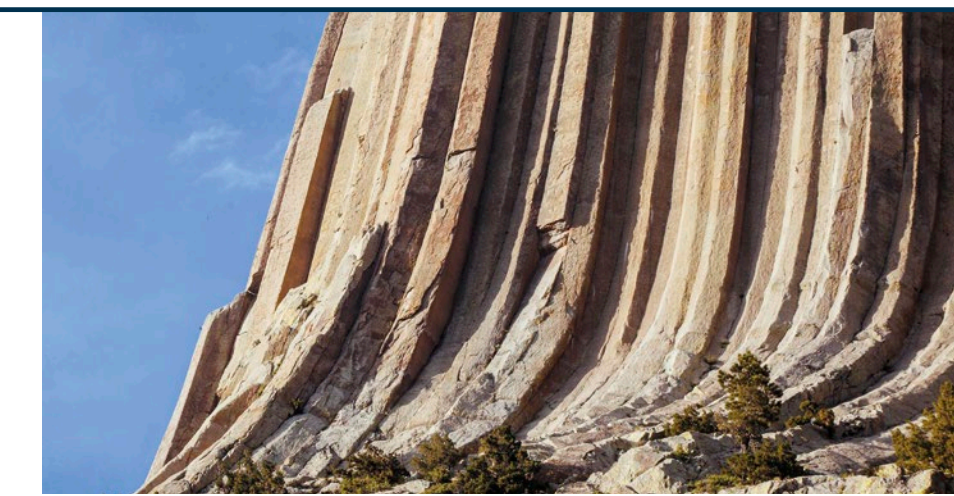
AN ICONIC AND PROMINENT IGNEOUS ROCK FEATURE WITH THE WORLD'S LARGEST EXAMPLE OF COLUMNAR JOINTING.

Mateo Tepe (Devil's Tower) is an iconic geological feature and an example of what is called a self-voiced protuberance. As an iconic and prominent igneous rock feature, it is the World's largest example of columnar jointing. Dramatically rising from a flat landscape, it is the most geologically and culturally important component of the topography for hundreds of

kilometers. While there are a number of geological and culturally derived reconstructions of its formation, meaning, and appropriate management (Brady, 1999; Hanson and Moore, 1999; Jenkins, 2013), the tall polygonal columns are generally viewed as being paths to another dimension made by a spiritual bear.

SITE 148

GEOLOGICAL PERIOD	Paleogene
LOCATION	Wyoming, United States of America 44°35'25"N 104°42'53"W
MAIN GEOLOGICAL INTEREST	Igneous and Metamorphic petrology Geomorphology and active geological processes



Close-up of columnar jointing with outwards curvature towards the base of the columns (image from Alamy).

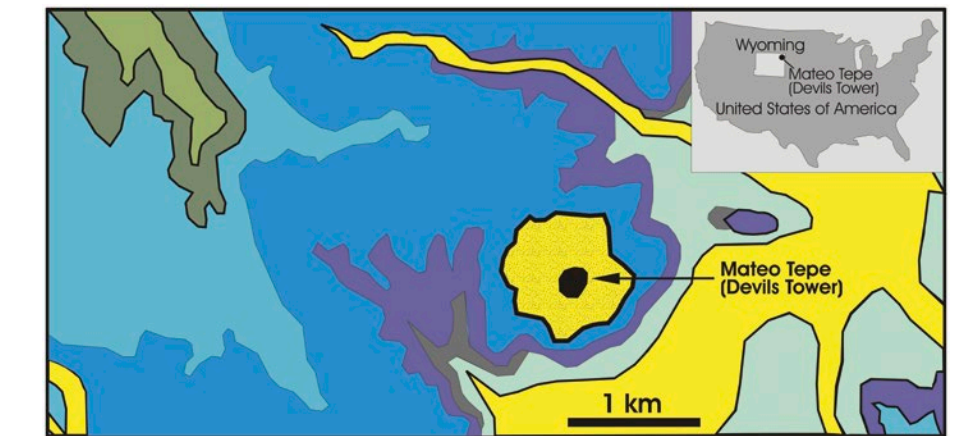
Geological Description

Mateo Tepe (or Devil's Tower, and also known as Bear Lodge) is a high-relief igneous rock mega-columnar formation (Figure 1) rising some 386 m above the valley of the nearby Belle Fourche River. It is comprised of porphyritic phonolite, and is the World's largest example of polygonal columnar jointing (Robinson, 1956). On its lower slopes the Tower is flanked by an apron of talus deposits. There are a number of theories as to its geologic origin including volcanic plug, stock origin, laccolith origin, or maar-diatreme origin (Dutton and Schwartz, 1936); at present, our preferred model is that it is an exhumed volcanic neck that intruded the sedimentary rock sequence about 40.5 Ma ago (Bassett, 1961). However recently, Závada *et al.* (2015) plausibly suggest an origin as a lava coulée emplaced into a maar-diatreme volcano. Geomorphically, it formed as a resistant rock body as the enclosing and overlying softer Mesozoic sedimentary rock formations of sandstone, shale, and gypsum were eroded away. Mateo Tepe is a sacred place to over 20 Native American tribes and was inscribed as America's first national monument in 1906 by President Theodore Roosevelt.

Scientific research and tradition

Aside from geological investigations cited above, Mateo Tepe also has been researched in relation to its archaeological content and its relationship to adjoining regions. The Tower is considered sacred by Northern Plains

Indians and many oral histories and sacred narratives connect indigenous peoples with the site, including the Arapaho, Crow, Cheyenne, Shoshone, and Lakota.



Devil's Tower Regional Geology, and Location

THE MOHOROVICIC DISCONTINUITY IN THE IVREA-VERBANO ZONE ITALY



A CLASSICAL MOHO OUTCROP IN EUROPE SHOWING THE CONTACT BETWEEN CONTINENTAL MANTLE AND LOWER CONTINENTAL CRUST.

The mantle-crust transition is exposed in a few sections in the world, and most of these involve oceanic crust. The Premosello outcrop displays the boundary between mantle and lower continental crust, which normally lies at a depth of 30-35 kilometers or more below collisional chains. For more than 40 years this

area has served scientists as an unprecedented crustal reference section in which geophysical observations and physical processes may be interpreted in the context of geology that is observable on the ground. Since 2013 the site is included in the UNESCO Sesia – Val Grande Geopark.

GEOLOGICAL PERIOD	Permian
LOCATION	Premosello, Piemonte Region, Italy 46°00'20"N 008°19'16"E
MAIN GEOLOGICAL INTEREST	Igneous and Metamorphic petrology Tectonics

SITE 149



Detail of the boundary between serpentized peridotite (below) and mafic granulite (above), representing respectively upper mantle and lower continental crust.

Geological Description

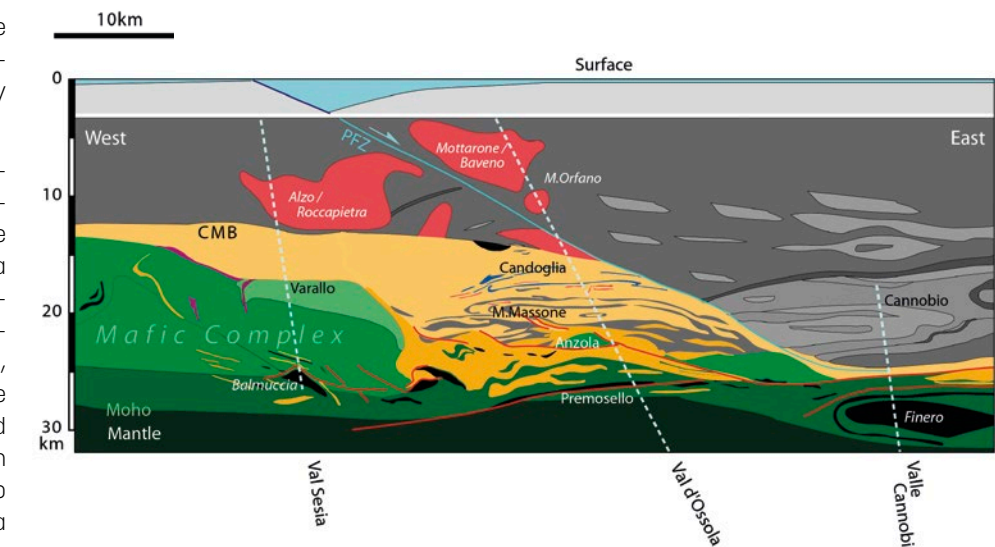
The outcrop shows the contact between lithospheric mantle rocks and the lower continental crust. The mantle is represented by a serpentized peridotite, in the lower part of the outcrop; the lower crust is represented by a mafic granulite, part of the Mafic Complex of the Ivrea-Verbano Zone, in the upper part. Serpentization results from hydration of olivine to serpentine minerals. Mafic granulite consists of prevailing pyroxene and plagioclase and may be described as well as a gabbro.

The contact surface represents the Mohorovicic discontinuity, marking the transition from upper mantle to lower crust. The Ivrea-Verbano Zone mainly consists of a metamorphosed volcano-sedimentary sequence, referred to as the Kinzigite Formation, and gabbroic to dioritic intrusive rocks, referred to as the Mafic Complex. Mantle peridotite lenses, tectonically interfingered with the metasedimentary rocks, occur in the northwestern part of the Ivrea-Verbano Zone, near the Canavese Line (Balmuccia in the Sesia valley and Finero in the Cannobina valley). At Premosello the Mohorovicic discontinuity appears to have been

brought to surface through exhumation processes occurred during the subsequent Alpine orogeny.

Scientific research and tradition

The Ivrea-Verbano Zone is easily accessible (less than 100 km from Milano and 100 km from Turin) and has been intensively studied. The number of scientific papers referencing the Ivrea-Verbano Zone alone has increased exponentially since 1970 and now exceeds 2500.



Restored cross-section during Middle Jurassic time (ca. 170 Ma), before Alpine tilting. Brack et al. (2010), after Rutter et al. (1999) and Schaltegger and Brack (2007).

THE CAMBRIAN LEKA OPHIOLITE

NORWAY



UNESCO Global Geopark

ONE OF THE BEST EXPOSED AND ACCESSION CALEDONIAN OPHIOLITE COMPLEX SHOWING THE REMNANTS OF THE IAPETUS OCEAN.

The Leka Ophiolite is outstanding among the world's ophiolite complexes. The exposures of upper mantle and lower crustal lithologies are spectacular and among the best observed anywhere. Here, mantle peridotites and the transition to ultramafic cumulates are 100% exposed along glacially eroded and polished surfaces. This facilitates studies of the magmatic processes below, along and above the

petrological MoHo. The Leka ophiolite also displays all aspects of a classical ophiolite section, including layered and massive gabbro, sheeted dyke complex, pillow lavas and deep sea sediments. In addition to being well studied, the continuous, unweathered sections make it possible for the visitors to grasp the complexity of the oceanic crust.

Layered peridotites from the lower section of Leka ophiolite complex. The colours reflect varying proportions of olivine, clinopyroxene and orthopyroxene. Photo: Arnfinn Holand.

GEOLOGICAL PERIOD	Cambrian (Miaolingian) to Lower Ordovician
LOCATION	Leka municipality/ Trøndelag County, Norway 65°05'49"N 011°38'57"E
MAIN GEOLOGICAL INTEREST	Igneous and Metamorphic petrology Tectonics

Geological Description

In Northwest Europe, a number of Caledonian ophiolite complexes have been distinguished as remnants of the ancient Iapetus Ocean, formed in a supra-subduction setting (SSZ ophiolites), more closely related to island arcs than ocean ridges. Dating of these complexes has revealed that most of them formed within a 10-million-year period in the Late Cambrian and Early Ordovician (Dunning and Pedersen, 1988). Of all the Caledonian ophiolite complexes, the Leka ophiolite is outstanding. From the exceptionally exposed mantle peridotites one can cross the mantle-crust boundary on foot. When passing across this boundary, the rocks change their character from typical mantle peridotite to layered sequences displaying tens to hundred-meter-thick units of olivine-rich rocks (dunite) interlayered with pyroxene rich units. This layered peridotite sequence demonstrates that the influx of magma from the mantle to the lower crust is episodic – in a similar way as volcanic eruptions occur as discrete events. The layered series also provide insights into the nature of crustal magma reservoirs and the crystallization of magma within the lower crust (Furnes *et al.*, 1992; Carter *et al.*, 2021). Further up-section,

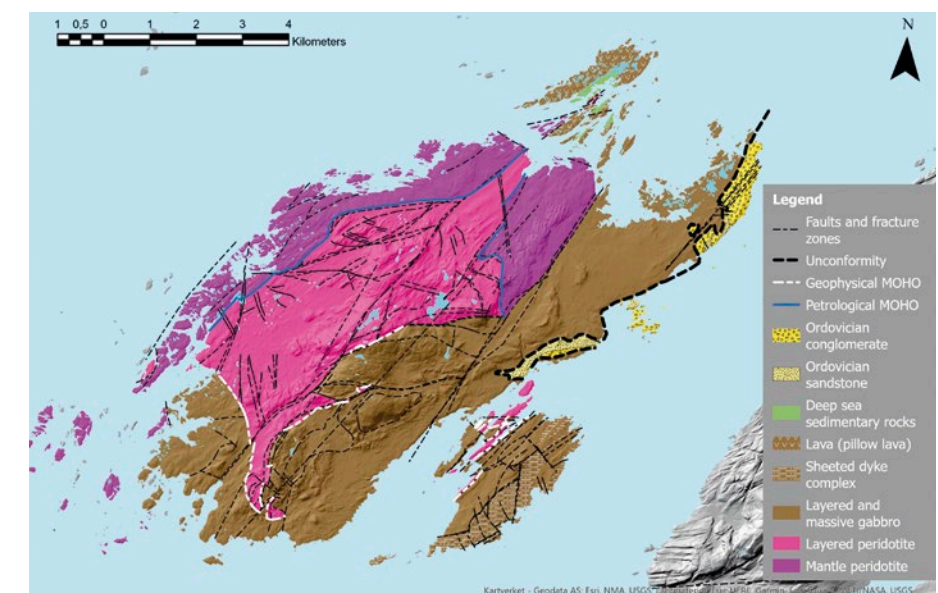
SITE 150



Well preserved pillow lava from the upper part of the ophiolite. Photo: Kristin Floa.

Scientific research and tradition

Together with the Karmøy Ophiolite, Leka was the first ophiolites described in the Scandinavian Caledonides (Prestvik and Roaldset, 1978; Furnes *et al.*, 1988). Since then, research teams have over the years added new knowledge about formation age, plate tectonic setting and obduction history (i.e. Dunkel *et al.*, 2017). Twenty-three scientific papers have been published on the ophiolite.



LATE CRETACEOUS SAMAIL OPHIOLITE OMAN



Mantle section of the Samail Ophiolite with white granitic dikes (Wadi Fizh). Brown to purple Quaternary wadi sediments in the foreground. View to the NNW.

**THE LARGEST, BEST PRESERVED
AND EXPOSED OCEANIC
LITHOSPHERE ON LAND. A
WORLD REFERENCE FOR
OBDUCTION AND IGNEOUS
PROCESSES RELATED STUDIES.**

The Samail Ophiolite is a unique natural laboratory of high global geoscientific relevance for process-related research on the oceanic lithosphere, magmatism, ocean-floor metamorphism and ophiolite obduction. Oceanic lithosphere covers most the Earth, but is usually hidden under oceans and difficult to access, but in Oman/U.A.E., oceanic lithosphere covers >10,000 square km on land allowing for

convenient access of various lithospheric key positions and lateral and vertical comparisons. The ophiolite commonly displays primary magmatic features. Other special aspects are that obduction ensued when the oceanic lithosphere was young, hot and buoyant and while spreading occurred as well as continental subduction and exhumation.

SITE 151

GEOLOGICAL PERIOD	Cretaceous
LOCATION	Oman Mountains, Oman 23°10'00"N 058°00'00"E
MAIN GEOLOGICAL INTEREST	Igneous and Metamorphic petrology Tectonics



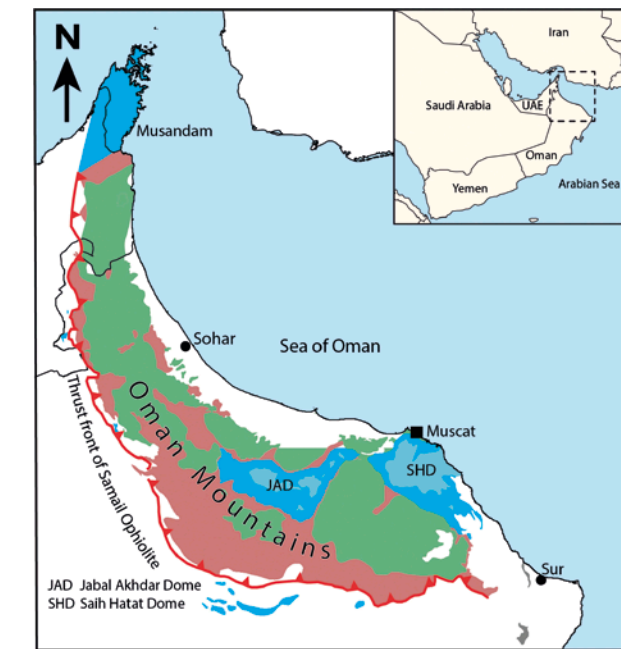
Pillow lava at Wadi Jizzi. Note the hammer for scale.

Geological Description

The Samail Ophiolite is the world's largest, best preserved and exposed thrust sheet of oceanic lithosphere on land (>10,000 square km; Nicolas *et al.*, 2000). It has a thickness of <16 km and consists of oceanic mantle (mainly harzburgite, some dunite, and wehrlite) and oceanic crust (gabbro, sheeted dikes, pillow lava). The rocks formed in a spreading center above an intra-oceanic subduction zone at ~95 Ma in the Neo-Tethys Ocean (e.g., Tilton *et al.*, 1981). Coeval with its formation, these rocks were thrust upon deep-sea sediments and were eventually obducted above thinned continental lithosphere of a >450-km-wide oceanic basin (Hawasina Basin, Glennie *et al.*, 1974). Coeval formation and thrusting explains the limited presence of deep-sea sediments blanketing the Samail Ophiolite as there was hardly any time for deposition. The ophiolite had been thrust over the Arabian platform for another ~150 km, when obduction ceased at ~75 Ma. In contrast to other ophiolites at the northern margin of Gondwana (Iran, Turkey), the Samail Ophiolite was not affected by continent-continent collision. In Oman, many outstanding outcrops exist, including world-

class examples for the Moho, gabbro, sheeted dikes, pillow lava and listwaenite, which is fully carbonated peridotite (important for carbon sequestration).

Geological map of the Oman Mountains.



Scientific research and tradition

Since the first descriptions of the Samail Ophiolite in the late 1960's and early 1970's (Reinhardt, 1969; Allemand and Peters, 1972), a wealth of publications have been published, focusing on the mineralogy/petrology, geochemistry, magmatism, dating, origin and tectonic setting, as well as on the continental subduction/exhumation (e.g., Hansman *et al.*, 2021).

LOWER PILLOW LAVAS OF TROODOS OPHIOLITE CYPRUS



UNESCO Global Geopark

The Akaki (Maroullena) River canyon consists of volcanic and intrusive rocks that were formed in the depths of the ancient Neotethys ocean in Upper Cretaceous.

THE TRANSPORTATION CONDUITS THROUGH WHICH THE MAGMA REACHED THE ANCIENT NEOTETHYS OCEAN-FLOOR FORMING THE PILLOW LAVAS 92 MILLION YEARS AGO.

This site illustrates in a remarkable way the transportation conduits through which the magma reached the ancient Neotethys ocean-floor approximately 92 million years ago and subsequently erupted resulting in the creation of hyaloclastites and pillow lavas. The dykes contain abundant elongate nearly horizontal overlapping vesicles, that are ex-

cellent evidence of the lateral magma flow direction within the transportation conduits. Some dykes exhibit a pitch-black glassy zone testifying to the strong chilling effect of water-saturated hyaloclastite during intrusion. At this site one can study all these geological processes that nowadays occur at the depths of recent oceans at divergent margins.

SITE 152

GEOLOGICAL PERIOD	Upper Cretaceous
LOCATION	Kalo Chorio Oreinis, Nicosia, Cyprus 35°00'42"N 033°09'13"E
MAIN GEOLOGICAL INTEREST	Igneous and Metamorphic petrology Volcanology



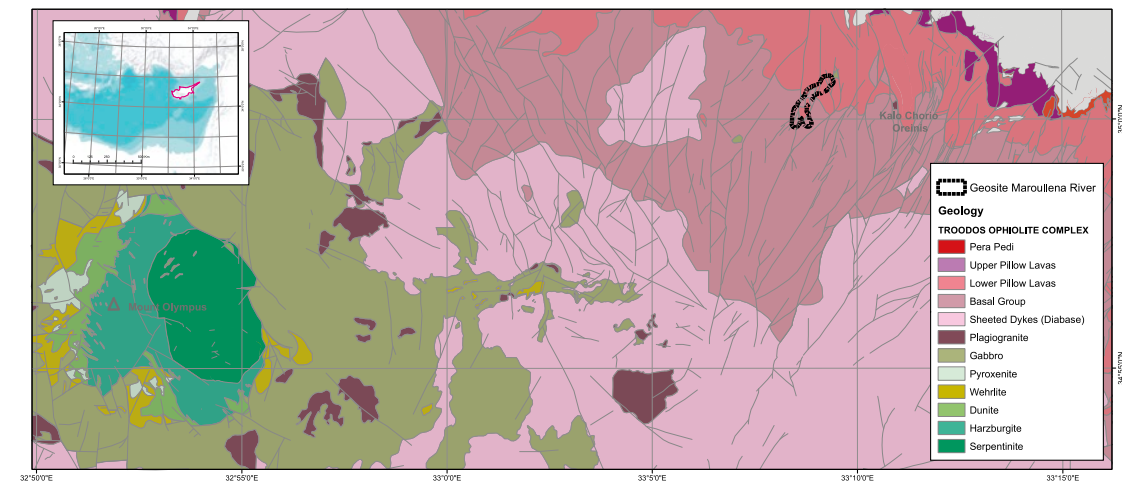
A lower unit of hyaloclastites and an upper unit of pillow lavas are cut by swarms of near-vertical dykes along the Akaki (Maroullena) River.

Geological Description

One spectacular exposure of the Troodos Ophiolite volcanic sequence is identified at a canyon of the Akaki river, which is a classic location for the study of these rock types. A lower unit of hyaloclastites and an upper unit of pillow lavas are cut by swarms of near-vertical dykes. The hyaloclastite is a breccia of black volcanic glass that formed from underwater volcanic eruptions. The pillow lavas were formed by the extrusion of high-viscosity lava on the Neotethys ocean seafloor near the axial eruption center. The dykes are of basaltic composition and constitute the transport conduits through which the magma flows towards the surface of the ocean-floor.

The observed chilled margins are an indication of several events that predate one another. The

Geological map of the Akaki (Maroullena) River broader area.



Scientific research and tradition

elongated vesicles that were examined at the site, indicate that the magma flow direction was nearly horizontal, contrary to the notion that magma only flows upwards and intrudes vertically. Another unique process that has been recorded at this site is that the vesicles, as well as the cracks that were created by the rapid cooling of lava, had been later in-filled with chalcedony as a result of the circulation of low temperature gel-like hydrothermal fluids rich in silica.

Scientific research focuses on the geochemical composition of the magma, the palaeomagnetic evolution of the Troodos Ophiolite in conjunction with the tectonic reconstruction of the Neotethys ocean and evidence on the creation of the dykes/pillow lavas/hyaloclastites and the direction of magma flow.

THE ULTRAHIGH-PRESSURE UNIT OF THE DORA-MAIRA MASSIF ITALY



The ultrahigh-pressure metamorphic Brossasco-Isasca Unit (middle and foreground) overlain by lower-grade units of the southern Dora-Maira Massif (background). View towards SW and Brossasco, Varaita valley.

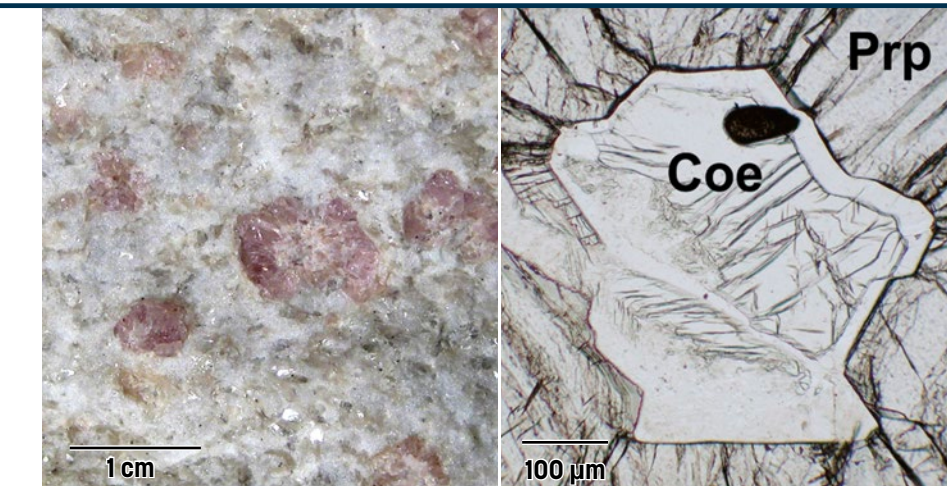
THE FIRST PLACE WHERE ULTRAHIGH-PRESSURE (UHP) METAMORPHIC ROCKS WERE DESCRIBED ON EARTH AND RECOGNISED AS FORMING A COHERENT UNIT.

The discovery of coesite in the DMM, in metamorphic rocks (Chopin, 1984) later shown to form a coherent UHP unit (Chopin *et al.*, 1991; Compagnoni *et al.*, 2012), documented for the first time that continental crust can be subducted to mantle depths, revolutionizing the role imparted to continental crust in geodynamics and

the relevant exhumation rates. The term UHP metamorphism was coined; about 40 years later, some 25 further UHP terranes are known on Earth, some of which even contain metamorphic diamond. This first UHP terrane remains unique for the composition of pure pyrope garnet and as sole ellenbergerite locality.

SITE 153

GEOLOGICAL PERIOD	Eocene
LOCATION	Cuneo, Piedmont, Western Alps, Italy 44°36'25"N 007°20'40"E
MAIN GEOLOGICAL INTEREST	Igneous and Metamorphic petrology Mineralogy



Fine-grained pyrope-kyanite-mica-quartz 'whiteschist' with coesite inclusions in pink pyrope crystals (left). Thin-section photomicrograph (right): coesite (Coe) included in pyrope (Prp) and partly transformed into (low-relief) quartz.

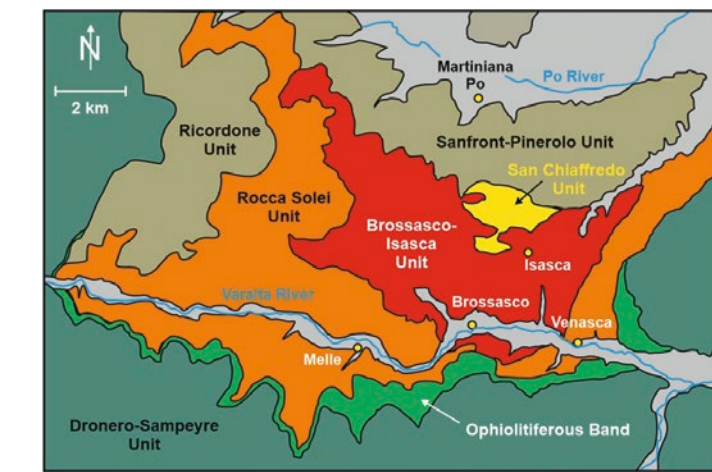
Geological Description

The Dora-Maira Massif (DMM) is one of the internal crystalline massifs of the Western Alps; it was part of the margin of the European continent before its collision with the Adria microcontinent during the Oligocene, after the opening of an intervening ocean during the Mesozoic and its subduction during the Paleocene. Below eclogite-facies remnants of this oceanic crust - the Monviso meta-ophiolite, the DMM exposes a pile of slivers of upper continental crust that reached different metamorphic grades during the Eocene. In the southern part of the massif, one of these slivers, the Brossasco-Isasca Unit, is less than one-kilometer thick and consists of Permian granite and its country-rocks (metapelite and minor marble). The whole unit underwent an Alpine UHP metamorphism epitomized by the occurrence of coesite, a high-pressure polymorph of quartz, in various rock-types and by the presence of near-end member pyrope garnet (Py99) in 'whiteschist', a highly magnesian coesite-pyrope-kyanite-white mica +/- talc metasomatic rock occurring as lenses within metagranite. The stability of the kyanite-jadeite assemblage and the

presence of the silicate ellenbergerite as inclusions in pyrope megacrysts (up to 25 cm, Schertl *et al.*, 1991) are additional features attesting peak metamorphic pressures exceeding 3 GPa (i.e. = 100 km depth) at temperatures near 700-750°C.

Scientific research and tradition

As "type locality" for UHP metamorphic rocks and terranes, the Dora-Maira Massif has been continuously attracting new studies: mineralogical (six new phases), petrological (benchmarking of new barometers), geochemical (Mg-metasomatism) or geochronological (continental subduction rate, peak metamorphism, very rapid exhumation), e.g. Gebauer *et al.* (1997); Rubatto and Hermann (2001).



Geological sketch map of the UHP-metamorphic Brossasco-Isasca Unit in the southern Dora-Maira Massif (Western Alps) and its geographical location in Italy (right).

5

VOLCANOLOGY

SITE 154 - SITE 163



Goubbet el Kharab, Djibouti

Photo: Bernhard Edmaier

Volcanism plays a crucial role in shaping geoecosystems by facilitating the exchange of energy and matter between the Earth's interior and its surface. This process creates diverse landscapes ranging from majestic mountains to stunning lakes, fertile plains, and valleys. Volcanism significantly impacts the atmosphere through the release of gases and particles during eruptions, highlighting the complex interactions between geological processes and the Earth's climate system over variable timescales. Volcanic activity influences the hydrosphere by changing watersheds and basins, forming new water bodies, and affecting the chemical composition of existing ones. Furthermore, nutrient-rich volcanic soils are particularly beneficial for carbon storage and provide an ideal substrate for the colonization of pioneer species, fostering ecological succession and contributing to the natural cycle of ecosystem regeneration and development. Volcanism drives both geodiversity and biodiversity and holds significant cultural importance. It is recognized worldwide for its powerful nature, both life-giving and hazardous.

Therefore, volcanic environments hold immense cultural, scientific, and educational value, reflecting their profound geoheritage significance as endorsed by the International Association of Volcanology and of the Earth's Interior (IAVCEI). Volcanic sites also attract tourists, educators, and researchers, promoting geotourism and fostering an appreciation for natural history as part of geoeducation and geoconservation. The distinctive manifestation of volcanism that can modify or create volcanic landscapes and diverse biodiversity within volcanic environments not only deepen our comprehension of geological and ecological mechanisms governing the evolution of the Earth system but also sustain the transmission of culture and knowledge across generations. Furthermore, they offer additional support for local economies through sustainable tourism and educational programs playing key role in geosystem services.

The representative sites selected for the Second 100 IUGS Geological Heritage Sites offer valuable information about globally unique volcanic landscapes. The geosites in this chapter provide critical insights into Earth's volcanic history. Your journey will take you from the vast continental flood basalts of the Deccan Traps in India in good contrast with the submarine lava flows of Lower Pillow Lavas, Akaki (Maroullena) River in Cyprus to the small yet pristine scoria cones of the Paricutín volcano in Mexico, preserved in various artistic and historical archives. You'll also encounter the colourful nature of the ancient and modern volcanic environment of New Zealand from mega pillow lavas of basaltic volcanism at Murawai, the centre of Māori cosmovision at Ruapehu or the extreme environments at Rotorua's geothermal fields as the closest analogy of the geoenvironment in the time life born on Earth. We can also embrace the unique processes demonstrating the global impact of volcanism in volcanic islands capable of unexpected high intensity explosive events, such as those at Hunga volcano in Tonga. Iconic majestic volcanoes such as the Ngorongoro Crater in Africa provide graphic examples of long running edifice growth, and Heisei Shinzan Lava Dome in Japan is a good example how small silicic lava can create a "blister" on Earth's surface. The explosive interaction of magma and water can be admired in an enormous maar crater in the middle of the arid Arabian Peninsula at Al Wahbah. This selection also contains one of Earth's most peculiar lava flows exposed at El Laco (Chile) that is composed almost entirely of magnetite making it literally an iron flow.

Embark on an unparalleled journey to these remarkable geosites, where the Earth's story unfolds before your eyes, offering unparalleled insights into past and present volcanic forces shaping geodiversity and ecosystems.

Natalia Pardo

Universidad de los Andes. Bogota. Colombia.
IAVCEI. International Association of Volcanology
and Chemistry of the Earth's Interior.
IUGS Geological Heritage Sites referee.

Karoly Nemeth

National Program of Earthquakes and
Volcanoes, Saudi Geological Survey.
Institute of Earth Physics and Space Science,
Sopron, Hungary.
IAVCEI. International Association of Volcanology
and Chemistry of the Earth's Interior.
IUGS International Commission on Geoheritage.
IUGS Geological Heritage Sites referee.



DECCAN TRAPS INDIA



Deccan Traps panorama looking east from Kate's Point, Mahabaleshwar. The peaks rise ~1400 meters above sea level and ~600 meters above the Krishna river valley.

THE BEST-STUDIED SECTION AND TOURIST HOTSPOT IN THE DECCAN TRAPS, ONE OF THE WORLD'S GREAT CONTINENTAL FLOOD BASALT PROVINCES.

The Deccan Traps is of great importance in volcanology, igneous petrology, geochemistry, geochronology, planetary geology, geophysics, geodynamics, palaeontology, and flood basalt-hosted groundwater and petroleum reservoirs and carbon dioxide sequestration. It is also important for Palaeogene-age ferricrete duricrusts formed by basalt weathering (Ollier and Sheth, 2008), hundreds of

rock-cut caves (including UNESCO World Heritage sites) depicting human history and culture (Sheth, 2023), heritage stones (Kaur *et al.*, 2019), spectacular secondary minerals (Ottens, 2003), and Lonar, Earth's only known hypervelocity impact crater in basalt (Bodas and Sen, 2014). Mahabaleshwar, the best-studied Deccan section, is already prominent on the tourism map of India.

SITE 154

GEOLOGICAL PERIOD	Upper Cretaceous to Paleocene
LOCATION	Southern Asia, India 17°55'16"N 073°40'30"E
MAIN GEOLOGICAL INTEREST	Volcanology Igneous and Metamorphic petrology



Deccan Traps panorama and ~1200 meter-thick flood basalt sequence (~800 m visible), looking west from Arthur's Seat (1347 meter elevation), Mahabaleshwar, Western Ghats. Photo: Shyam Mude.

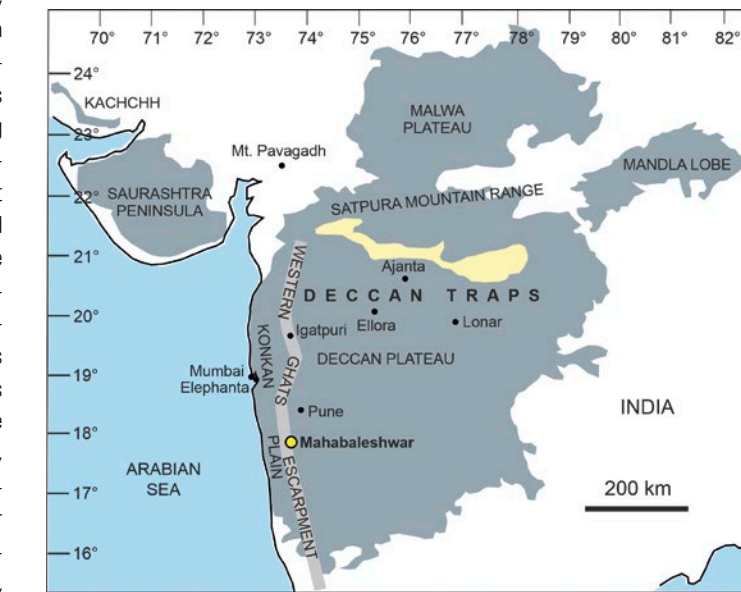
Geological Description

The Late Cretaceous to Palaeocene (~65 Ma) Deccan Traps continental flood basalt province contains hundreds of tholeiitic basalt lava flows. Each flow represents a dyke-fed fissure eruption similar to, but vastly larger than, modern Hawaiian and Icelandic eruptions. With individual 1000 km³ eruptions releasing 10 gigatons of carbon dioxide and sulphur dioxide each to the atmosphere, Deccan volcanism played a critical role in the Cretaceous/Palaeocene (K/Pg) boundary mass extinction. The province still covers 500,000 km² in west-central India, excluding substantial parts downfaulted into the Arabian Sea during India-Seychelles rifting at 62.5 Ma, or eroded away. The still-preserved basalt thickness (including subsurface thickness) in the Western Ghats escarpment, beside the rifted margin, is ~2 kilometers. Mahabaleshwar town (1436 meters above mean sea level) in the Western Ghats sits atop an ~1200 meter-thick sequence of about 50 lava flows, capped by a thick, regional ferricrete duricrust formed by Palaeogene weathering. The Mahabaleshwar section is the most intensely studied stratigraphic section in the province for petrology,

geochemical stratigraphy, geochronology and palaeomagnetism. Mahabaleshwar, with its pleasant climate, great scenic beauty and easy access, also attracts hundreds of thousands of tourists every year, and thus has very high geoheritage and geotourism value (Sheth, 2014).

Scientific research and tradition

Deccan Traps research dates back at least two centuries (~1830's), with most of the early works by geologists of the Geological Survey of India, many of them British. Modern Deccan research is vigorous and truly international, with many active groups particularly from India, France, Italy, Japan, Russia, UK, and USA.



Sketch-map of the Deccan Traps (green), showing older rocks (white), younger rocks (yellow), geographic regions, and some important localities including Mahabaleshwar. Simplified from Sheth (2023).

MURIWAI MEGAPILLOW LAVA FLOWS

NEW ZEALAND



Part of the larger megapiillow lava flow at Muriwai showing huge fans and rosettes of cooling columns formed as several internal feeder tubes solidified.

WORLD'S LARGEST, MOST COMPLEX AND SPECTACULAR MEGAPILLOW LAVA FLOW WITH INTERNAL FEEDING TUBES WITH GIANT FANS OF COOLING COLUMNS.

Easily accessible Muriwai pillow lavas have an international reputation as the best example anywhere of a large and complex megapiillow lava flow with spectacular huge fans of cooling columns formed in the internal lava feeder tubes. Megapiillow lava flows occur elsewhere (e.g. Sardinia, Spain, Tasmania), but none match the cross-sectional exposure of the

larger Muriwai megapiillow flow in terms of exposure, size and complexity. Exposures of dikes feeding attached pillows are extremely rare in the international literature. The three dimensional exposure of the smaller pillow lava flow with branching lobes and surface corrugations is similar to the spectacular Oman example.

SITE 155

GEOLOGICAL PERIOD	Miocene
LOCATION	Auckland, New Zealand 36°50'06"S 174°25'39"E
MAIN GEOLOGICAL INTEREST	Volcanology Stratigraphy and sedimentology

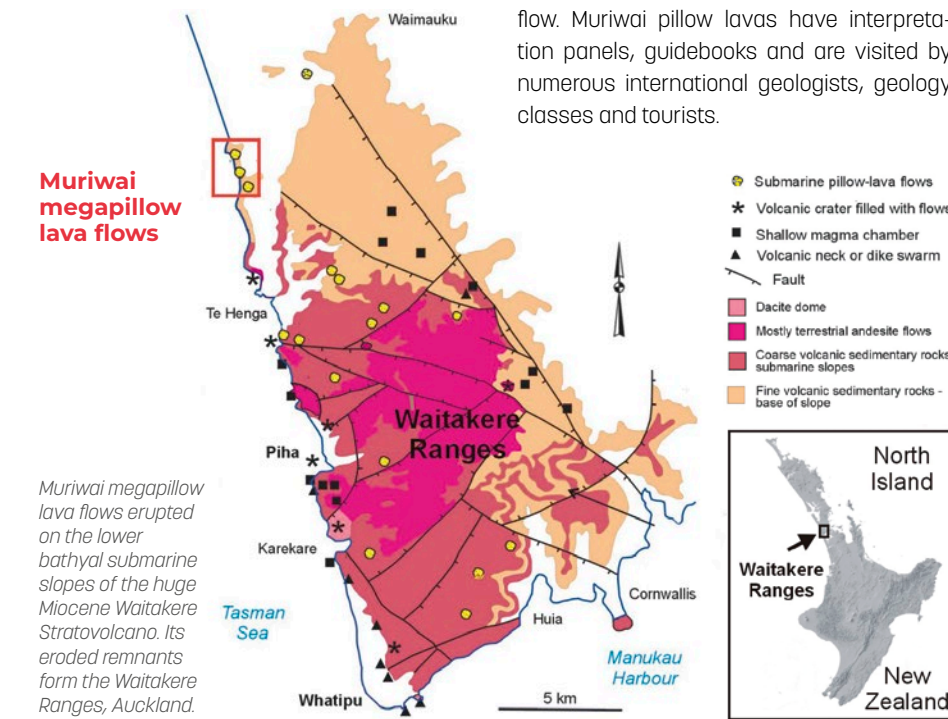


A 17-million-year-old dike of andesite at Muriwai intruding stratified sedimentary rocks and feeding a 3-meter-diameter pillow roll along its upper edge.

Geological Description

Two basaltic andesite pillow lava flows and two dikes that feed large (3-5 meter diameter) pillow rolls along their upper edges are beautifully exposed in the 50-70-meter-high sea cliffs at Muriwai. These flows are preserved within volcaniclastic sediments that were deposited on the sea floor and in submarine canyons at lower bathyal depths (1000-2000 meters) during the early Miocene (Hayward, 1976, 2022). The larger megapiillow lava flow (30 meters thick, 600 meters across) has complex internal structure with three large (up to 30 meter diameter) feeder tubes separated and surrounded by units of pillow and megapiillow lava lobes. These feeder tubes of molten lava fed the front of the advancing flow. Lava, that leaked from cracks in the feeder tube skins, created a carapace of pillow lava lobes mixed with 1-3 meter-thick columnar-jointed flow sheets, that flowed out more quickly (Bear and Cas, 2007; Allen *et al.*, 2007). The cooled and solidified tubes consist of huge fans and rosettes of polygonal columns, recording their complex cooling histories. Nearby, two separate dikes intrude the stratified sediments with large (3-5 meters) pillow rolls along their

upper edges where lava was extruded into soft sediment just below the seafloor.



Scientific research and tradition

Earliest studies by Bartrum (1930) inferred the fans formed inside spherical megapillows like nearby large pillows with feeders. Hayward (1979) reinterpreted them as internal feeding tubes inside a large pillow lava flow. Muriwai pillow lavas have interpretation panels, guidebooks and are visited by numerous international geologists, geology classes and tourists.

THE PLEISTOCENE AL WAHBAH DRY MAAR CRATER SAUDI ARABIA



View of Al Wahbah maar cut deeply into the Neoproterozoic basement and pre-existing Pleistocene scoria cones and lava flows.

THE WORLD LARGEST, YOUNG DRY MAAR VOLCANO, CROSS CUTTING OLDER SCORIA CONES.

Al Wahbah is a maar crater that is in an area currently located in hyper arid climate. Al Wahbah formed in the Pleistocene (~1.147 +/- 0.004 Ma) due to explosive interaction of magma and ground water. The sheer size and the thick pyroclastic sequence of the maar suggest the presence of abundant ground water during the

Pleistocene reflecting the global changes the Arabian Peninsula experienced in the recent geological past. The perfectly exposed tuff rings and the half sectioned older scoria cone(s) provide a unique geological setting to allow the visitor to see the deposits associated with monogenetic volcanism.

SITE 156

GEOLOGICAL PERIOD	Pleistocene
LOCATION	Middle East, Arabian Peninsula, Saudi Arabia 22°54'02"N 041°08'22"E
MAIN GEOLOGICAL INTEREST	Volcanology Geomorphology and active geological processes



Salt precipitations along the margin of the ephemeral lake formed in May 2023 within the maar crater.

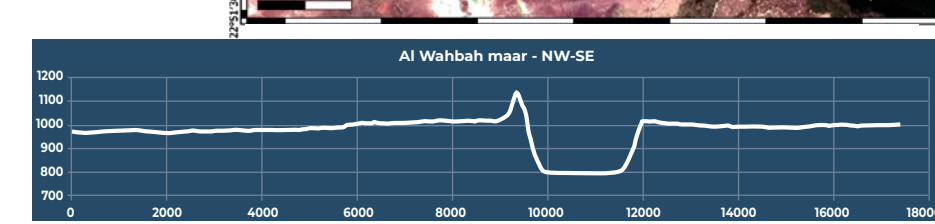
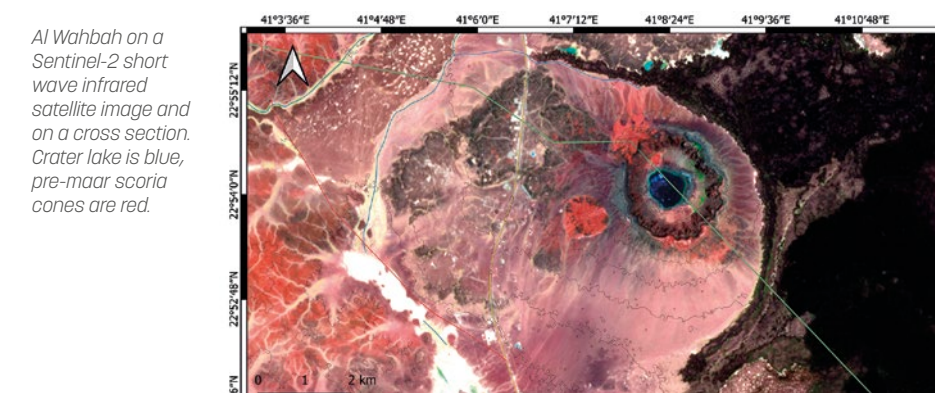
Geological Description

Al Wahbah is one of the largest and deepest Quaternary maar craters on Earth that is also accessible through sealed roads and dedicated visitor facilities. It has perfect exposures of the pre-maar and the maar-forming volcanic successions in its crater wall. It is today a ~2.3 kilometer wide, ~250 meter deep NW-SE-elongated crater surrounded

by a scalloped near-perpendicular crater wall that cuts into the Neoproterozoic diorite basement and two Quaternary basanite lava flows. Al Wahbah formed by the explosive interaction of magma and water about 1.15 Ma that deposited pyroclasts from pyroclastic density currents, ballistic curtains and pyroclastic falls. The uniqueness of the exposed

crater wall sequence is that deposits resulting from the phreatomagmatic explosions engulfed two pre-maar scoria cones and underlying multiple lava flow units. Al Wahbah uniquely demonstrates that subsequent highly explosive eruptions can take place on a field that showed very different eruption styles thousands of years prior the violent explosive blasts that cut a hole-in-the ground within earlier volcanic landforms. The original tephra ring of the maar acted as an obstacle against younger lava flows nearby vents that were diverted along the margin of the tephra ring creating unique pahoehoe lava surface textures marking the original position of the tuff ring.

Al Wahbah on a Sentinel-2 short wave infrared satellite image and on a cross section. Crater lake is blue, pre-maar scoria cones are red.



Scientific research and tradition

Scientific research has been conducted only in recent years when the Maar has been subject to studies of its geochronology, geomorphology, geochemistry, lithosphere structure and petrogenetic modelling based on mantle derived nodules from the pyroclastic successions. Geoheritage work has also been conducted with identification of its main geoheritage values.

EL LACO IRON LAVAS

CHILE



Circular segment with a diameter of 0.75 kilometer corresponding to an emission dyke of magnetite lava from Laco Norte, which reaches 0.8 kilometers in length and a variable width between 20 and 80 meters. It has a concave curved shape towards the north and is surrounded by hydrothermally altered andesites. View towards the east (by José Antonio Naranjo).

**UNIQUE MAGNETITE LAVAS
DUE TO THEIR PRESERVATION
QUALITY, SURFACE
STRUCTURES AND OTHER
FEATURES OF IRON ERUPTIONS.**

In small proportions as microcrystals called "accessories", magnetite is a common mineral in silicate lavas. However, the concentration, proportion and volume of eruptive products, lavas and pyroclasts, of magnetite in a volcano is a really rare phenomenon on Earth. On the other hand, the quality of preservation and environ-

mental and structural volcanic conditions of the forms and products of magmatic iron within the El Laco Volcanic Complex represent a case of extraordinary quality and provides new understandings for geology in general and iron geology in particular.

SITE 157

GEOLOGICAL PERIOD	Pleistocene
LOCATION	Antofagasta Region, Chile 23°49'37"S 067°29'29"W
MAIN GEOLOGICAL INTEREST	Volcanology



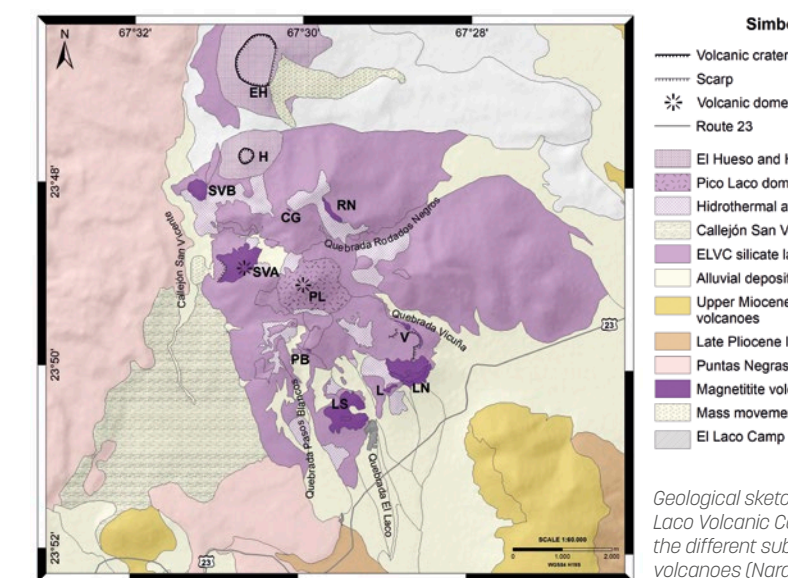
Stalaphytes of ca. 18 centimeters length and 2.5-3 centimeters width of frozen magnetite in cavities developed in the northern free wall of the Laco Norte magnetite dyke (by José Antonio Naranjo).

Geological Description

The geology of El Laco Volcanic Complex (ELVC) includes the exogenous andesitic dome Pico Laco (5,310 meters a.s.l.), and nine subsidiary magnetite eruptive centers at altitudes between 4,600 and 5,100 meters a.s.l. Although the accessibility conditions are through a paved route, due to the altitude at which it is located, you can easily get altitude sickness.

The ELVC in the Central Andes (23°48'S, 67°30'W; 5,300 meters a.s.l.) is formed by andesitic domes, up to 10-meter-thick andesite lava flows and sphene porphyritic bodies. K-Ar dating gives ages from 0.3 to 5.3 Ma. ELVC presents an extensive zone of hydrothermal alteration with differential erosion and subsequent alluvial deposits. Similar to carbonatites (Ol Doinyo Lengai,

Tanzania), El Laco contains unique iron oxide eruptive products including lavas emitted from fissures (0.3 to 0.7 kilometer long and 10 to 30 meters wide), pyroclastic fall material as bombs, lapilli and ash, and pyroclastic density currents. Among the latter, remarkable surge deposits are common. All these eruptive products contain clinkery, aa, and smooth surface textures, like pahoehoe stalactites. The rough appearance of the former is due to the growth of small octahedral magnetite crystals and dictaxitic-type porosity, which contrasts with the bright surfaces and smooth-walled vesicular porosity of the latter. These products resulted from the eruption of an iron-rich lava flow with a high volatile content, together with a strong degassing process that contributed to the rapid consolidation, the great variation in viscosity and the formation of the observed textures.



Geological sketch map of the El Laco Volcanic Complex showing the different subsidiary magnetite volcanoes (Naranjo et al., 2010).

Scientific research and tradition

Since the early 1960's, it has been considered the most spectacular case of iron lava volcanism in the world.

NGORONGORO CRATER

TANZANIA



UNESCO World Heritage Site
UNESCO Global Geopark

THE WORLD'S LARGEST UNFLOODED AND UNBROKEN CALDERA.

Ngorongoro Crater is the largest unflooded and unbroken caldera in the world in contrast with many other larger calderas which are either have broken rims or are flooded to form lakes. The crater is an important geological heritage site for scientific studies of volcanology and seismic activities as well its relationship with

pyroclastic depositions at Laetoli-Olduvai Gorge paleoanthropological sites of human evolution. Nevertheless, the Crater is a most spectacular feature - a self-contained sanctuary for a premier collection of diverse wild animals and plants species that live within its borders. It is true "Garden of Eden".

SITE 158

GEOLOGICAL PERIOD	Pleistocene to Holocene
LOCATION	Ngorongoro, Arusha, Tanzania 03°10'28"S 035°33'55"E
MAIN GEOLOGICAL INTEREST	Volcanology



Clouds covering one of the elevations that completely surround the crater (Photo: Mariola Crobelska in Unsplash).

Geological Description

Ngorongoro Crater is among of the nine complex coalescing basaltic shield volcanoes forming Ngorongoro Volcanic Highlands (NVH), which lies at the center of Northern Tanzania Divergence Rift Zone of the Gregory Rift Valley. The volcanoes formed during the period of voluminous volcanism, 4 Ma, associated with the first phase of faulting of the "Eyasi Rift" at 20 Ma. The collapse and formation of calderas at some of the NVH vents were caused by the second phase faulting "Natron-Manyara Rift", 2 Ma, to the east of NVH. A part of Ngorongoro crater, Olmoti "the cooking pot" and Empakai are the two craters to the north of Ngorongoro crater; remaining volcanoes form dome shaped features with small craters on top.

The Ngorongoro Crater is the largest deeply eroded volcanic feature of the NVH. It is 22 kilometers in diameter, stands at an elevation of 3,000 meters, and has walls that on average are 610 meters high. Prior to collapse, the volcano may have attained an elevation that exceeded 5,000 meters, thus rivaling Kilimanjaro. The crater is composed largely of lava, ranging from basalt to rhyolite, and it includes ignimbrites and agglomerates. On

Scientific research and tradition

the crater floor are several small cones, hill-rocks, knolls, and a alkaline lake which occupies the lowest area. The crater have an internally-drained basin fed by two external streams. Several freshwater springs support wetlands.

The NVH, for decades, attracts geologists and paleontologists to study seismic and volcanism activities of the northern Tanzania region associated with the East African Rift System, as well as the deposition relationship of volcanic material and sedimentary sequences of the two worlds' important paleoanthropological sites of Olduvai Gorge and Laetoli.



Geological setting of the Ngorongoro Crater (NC), Ngorongoro Volcanic Highlands, and the branches of Gregory Rift (modified from Scoon, 2018). Source: Landsat/Copernicus. Google Earth.

RUAPEHU VOLCANO

NEW ZEALAND



UNESCO World Heritage Site

TE MATUA O TE MANA. AN ICONIC SUBDUCTION RELATED STRATOVOLCANO.

Ruapehu is an iconic stratovolcano that dominates the landscape of New Zealand. This volcanic plateau has internationally unique endemic species, intrinsically linked to the geological and geothermal processes occurring in the region, which has a dual UNESCO World Heritage Status for its biodiversity, recreation (ski fields), and cultural importance. The lithologies and geomorphic features are revered by

the indigenous, Maori, peoples. This active volcanic and geomorphically diverse landscape has provided the foundational data and models to drive new scientific understandings related to subduction volcanism, ring-plain construction, laharic processes as well as illuminating indigenous peoples' connections to volcanic regions.

GEOLOGICAL PERIOD	Holocene
LOCATION	Tongariro National Park, New Zealand 39°17'00"S 175°34'00"E
MAIN GEOLOGICAL INTEREST	Volcanology Stratigraphy and sedimentology

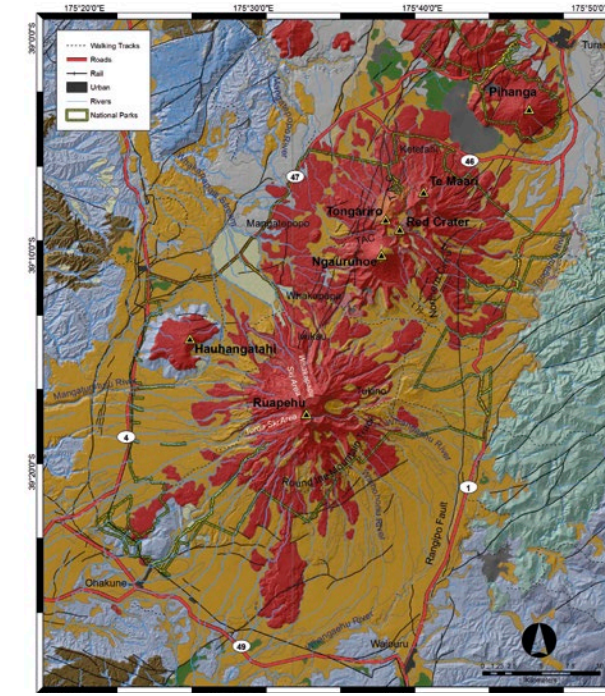
SITE 159



Geological and geomorphic features, Ruapehu Volcano. Andesitic lava, columnar features representing lava flow and ice interaction within the Wahianoa Formation (115-160 ka). (Photo: Procter, 2022).

Geological Description

Ruapehu Volcano is an iconic volcano, which is synonymous with subduction related volcanism. This stratovolcano is the protuberant tip of the Taupo Volcanic Zone, and has produced large volumes of basaltic-andesites and andesites over the last ~200 ka. Volumetrically this geomorphically diverse volcanic structure has a massif of ~150 km³ with an extensive ring plain of 150 km³ (Leonard *et al.*, 2020). The massif's lithologies of plagioclase-two-pyroxene andesites are typically sourced from 5-10 kilometer depth, and contain a record of crystal growth, representative of the complex pathways and sources of convergent subduction related to volcanism, elevating Ruapehu as an archetypal model of andesitic volcanism (Gamble *et al.*, 1999; Price *et al.*, 2012). The presence of the Crater Lake (Te Wai-a-Moe) at the summit, the current active vent, has focused inquiry into understanding small volume (VEI 1-2) eruptive processes (Voloschina *et al.*, 2020). The ring-plain is composed of well exposed tephra and laharic deposits that provide insights into multi-hazard, constructional processes in a tectonically active environment. The impacts of lahars (1953: 151



Simplified geological and topographic map of the Tongariro Volcanic Centre including Ruapehu Volcano. Map compiled by Procter (2013), Massey University.

Scientific research and tradition

deaths) have also driven the development of hazard models and provided a leading experimental site for the application of simulation tools to aid hazard management (Cronin, 1999; Procter, 2010).

Studies at Ruapehu from numerous disciplines have driven transdisciplinary scholarship. New science and knowledge created in the geological disciplines have focused on using this natural laboratory to understanding volcanic phenomena and hazards. Ruapehu is a foundational model to understand the genesis and creation, as well as the emplacement, of andesites.

Faults	melange
Geology	mud
Rock Type	mudstone
andesite	peat
basalt	pumice
breccia	pyroclastic breccia
claystone	rhyolite
conglomerate	sand
debris	debris
gravel	sandstone
greywacke	gravel
ignimbrite	schist
limestone	scoria
	silt
	siltstone

PARÍCUTIN VOLCANO

MEXICO



View of the Parícutin cinder cone and surrounding ash deposits

THE FIRST VOLCANO WHOSE ERUPTION AND ENTIRE ACTIVITY WAS OBSERVED AND DOCUMENTED IN REAL TIME (1943-1945).

Parícutin volcano is the first volcano whose eruption was observed in detail by modern scientists since its birth in a cornfield in the state of Michoacán in central Mexico. It is the youngest edifice of the Michoacán-Guanajuato volcanic field, which is one of the most extensive mono-

genetic fields in the world, formed by more than 1,100 Quaternary volcanic centers (Hasenaka and Carmichael, 1985). The historical record of the volcano is exceptional because its entire activity was documented in real time by an international group (Foshag and Gonzalez Reyna, 1956).

SITE 160

GEOLOGICAL PERIOD	Holocene
LOCATION	Uruapan, state of Michoacán, Mexico 19°29'35"N 102°15'05"W
MAIN GEOLOGICAL INTEREST	Volcanology Igneous and Metamorphic petrology

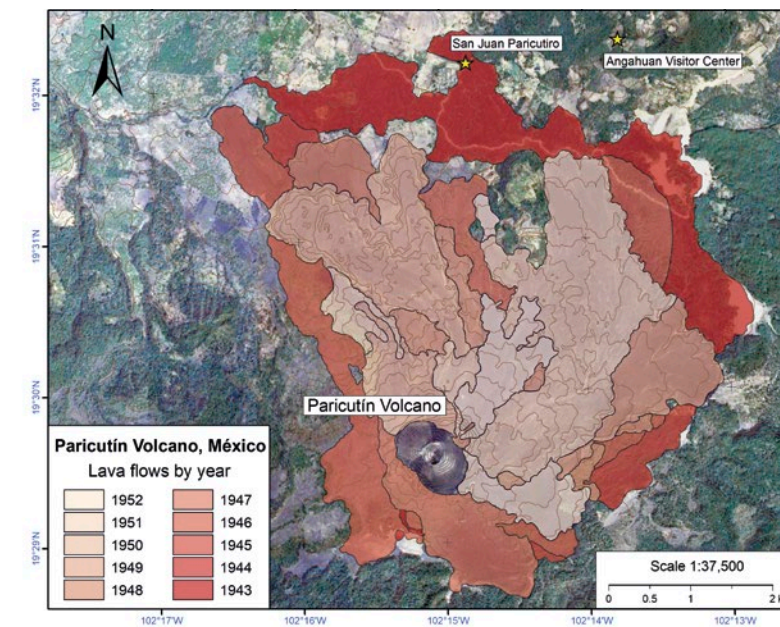


Local indigenous residents observe Parícutin volcano, in march 1944. Photo by Amo Brehme (U.S. National Archives, published in Foshag and González Reyna, 1956).

Geological Description

Parícutin is an 80 years old small-volume volcano that consists of a pristine 424-meter-high scoria cone and a 25 square kilometer lava flow field that formed during a 9-year eruption (1943-1952). The evolution of the volcano has been divided into four

stages (Luhr and Simkin, 1993). The first two stages (1943-1945) are related to the main growth episodes when the cone almost reached its present-day height, and the lavas attained their maximum distance from the vent (4 kilometers). These stages con-



Geologic map of the Parícutin volcano showing the lava flows erupted every year from 1943 to 1952 (modified from Luhr and Simkin, 1993).

sisted of violent Strombolian activity with high gas and ash columns and the birth of a subsidiary vent that fed abundant lava. Parícutin emitted at least 23 distinct lava flows and a widespread ash blanket. The calc-alkaline composition of its rocks is related to the active subduction of the oceanic Cocos plate beneath the North American continent along the Middle America Trench. The volcanic products vary from olivine-bearing andesitic basalt to orthopyroxene-bearing andesite (McBirney *et al.*, 1987; Cebriá *et al.*, 2011). Nonetheless, a recent geochemical study indicates that compositional variability can be explained by mantle source heterogeneity and fractional crystallization (Larrea *et al.*, 2019).

Scientific research and tradition

Parícutin is an emblematic volcano due to its history, beauty and excellent state of preservation. It is in a region with a rich indigenous culture. The lava flows buried the indigenous village of San Juan Parangaricutiro, but the church tower still stands in the middle of a lava flow.

HEISEI SHINZAN LAVA DOME

JAPAN



UNESCO Global Geopark

Northeast view of Heisei Shinzan, formed in the 1990–1995 eruption, with the endogenous part at top. Taken from above the Taruki Forest Park.

SCIENTIFICALLY BEST-DOCUMENTED DOME GROWTH DURING THE HENSEI ERUPTION (1990-1995) AT UNZEN VOLCANO.

The Heisei Era eruption that occurred at Mount Unzen, one of the Decade Volcanoes of the International Decade for Natural Disaster Reduction (IDNDR), has been thoroughly studied, and it has become one of the best-documented lava dome eruptions. This eruption was unlike the explosive eruption of Pinatubo, which

erupted at about the same time; however, the compositions of their magmas were similar. This contradiction led to a challenging project by the International Continental Scientific Drilling Program (ICDP) to excavate the path followed by the magma immediately after the eruption of Mount Unzen (Sakuma *et al.*, 2007).

SITE 161

GEOLOGICAL PERIOD	Holocene
LOCATION	Shimabara Peninsula, Nagasaki Prefecture, Japan 32°45'41"N 130°17'55"E
MAIN GEOLOGICAL INTEREST	Volcanology Geomorphology and active geological processes



The dome surface structure of Heisei Shinzan, showing the endogenous mound behind the exogenous part (foreground) that grew earlier.

Geological Description

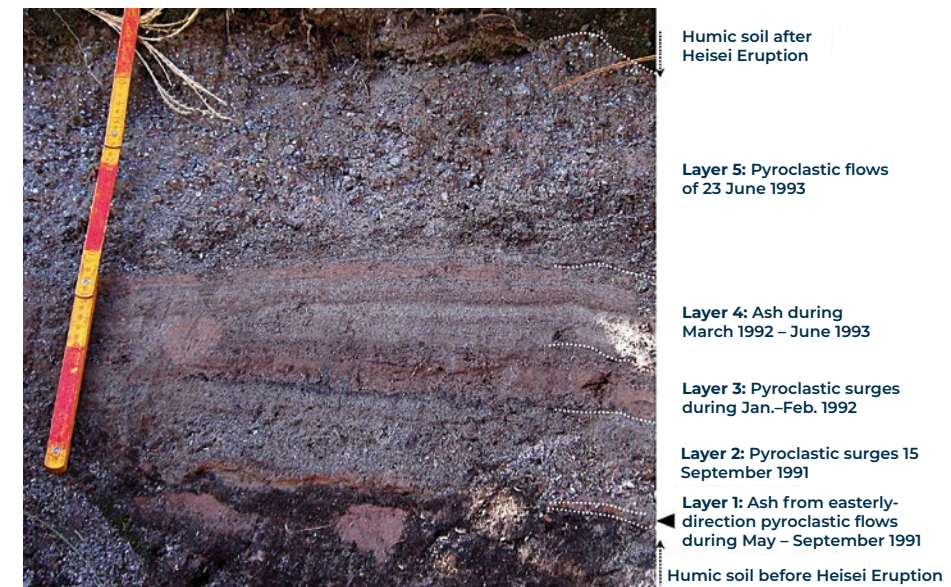
Heisei Shinzan is a dacite lava dome that formed during the Heisei Era eruption (1990–1995) of Mount Unzen. The dome first grew exogenously and then endogenously, indicating a decreasing effusion rate (Nakada *et al.*, 1995; 1999; Umakoshi *et al.*, 2011). Its formation was accompanied by thousands

of pyroclastic density currents due to partial collapses of the lava dome (Nakada and Fujii, 1993). Pyroclastic flows ran down the slope in the growth direction of the dome and resulted in the dome's advance over thick talus and a wide deposition of pyroclastic materials. Furthermore, lahars were repeatedly gener-

ated during the subsequent rainy seasons. On the outcrops, volcanic ash layers serve as timestamps that reveal the chronology of the eruption. Forty-three people (including media personnel, local residents, and volcanologists Katia and Maurice Krafft and Harry Glicken) were killed by pyroclastic surges on June 3, 1991. The surge in the largest pyroclastic-flow event during this eruption burnt down an elementary school. These events, along with the June 1991 eruption of Mount Pinatubo in the Philippines, triggered a reconsideration of volcanic disaster preparedness. Heisei Shinzan was designated as a national natural monument and now access is granted only for scientific research and monitoring.

Scientific research and tradition

Geophysical, geochemical, and geological observations were conducted during the eruption, and the observational data and timestamped ejecta have been studied. The drilling project revealed the mechanism of eruption, and its cores are still used for research (Yilmaz *et al.*, 2021). Volcanic observations have been conducted since the eruption, including the monitoring of dome stability.



Section of pyroclastic deposits at Taruki Forest Park, northeast of the dome, telling the story of the eruption. The scale bar is 50 centimeters.

THE ACTIVE HUNGA VOLCANO TONGA



Hunga Volcano's subaerial landscape during a smaller surtseyan eruption in the lead up to the January 2022 phreatoplinian event (Photo credit: Taaniela Kula).

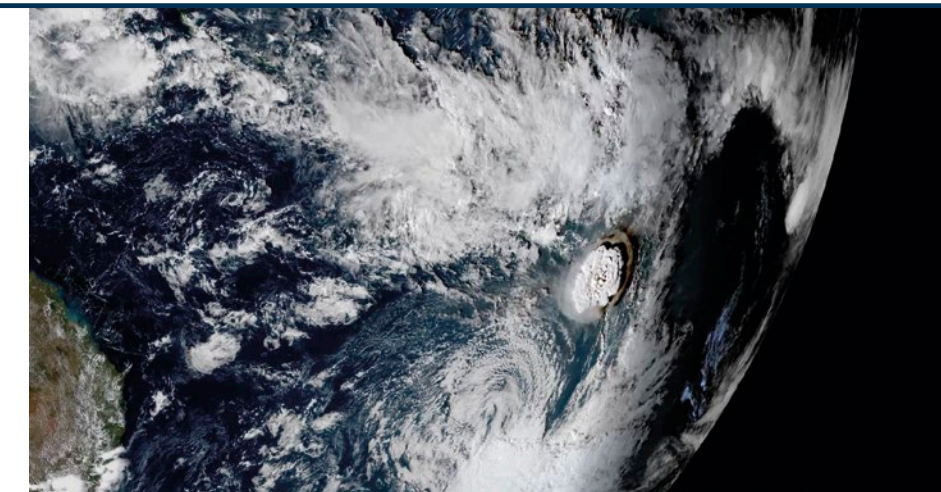
THIS VOLCANO SHOCKED OUR WORLD WITH ONE OF THE MOST EXTRAORDINARY GEOLOGICAL EVENTS EVER OBSERVED.

We must conserve Hunga in the collective memory of humankind to ensure that its extraordinary geoheritage is not forgotten beneath the ocean. The record-breaking 15/01/2022 phreatoplinian eruption encompassed the deepest caldera collapse ever observed (~1kilometer-deep), ~9km³ of material ejected to the highest altitude ever recorded (~58kilometers), the first observation of an eruption reaching the

mesosphere, deadly ~45meter-high megatsunami, sonic booms which traversed Earth four times, and destructive pyroclastic density currents. It caused devastating impacts and death in communities as distant as Peru. Unprecedented observations before, during and after the eruption make Hunga an unparalleled reference for understanding volcanic hazards and promoting resilience.

SITE 162

GEOLOGICAL PERIOD	Pleistocene to Holocene
LOCATION	Tofua Volcanic Arc, Tonga 20°32'50"S 175°23'25"W
MAIN GEOLOGICAL INTEREST	Volcanology Geomorphology and active geological processes



As seen from space: a satellite image of the January 2022 eruption. The first eruption observed to reach beyond the stratosphere and into the mesosphere. (Imagery credit: CSU/CIRA & JMA/JAXA).

Geological Description

Hunga Volcano is a remarkable site located in the SW Pacific Ocean. This predominantly submarine volcano rises approximately 1,800 meters above the surrounding seafloor. At its summit, there is a central caldera 5 kilometers in diameter and ~1 kilometer deep. Two islands, Hunga-Tonga and Hunga-Ha'apai, emerge from the northern and western caldera rim.

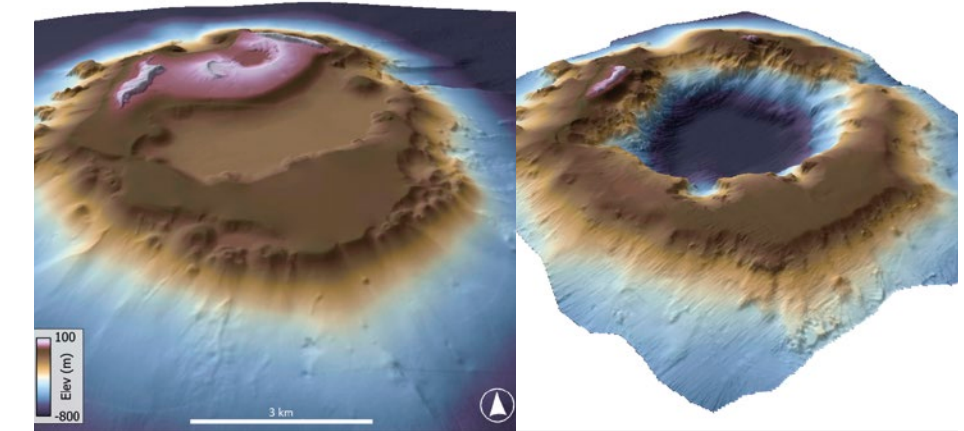
Situated within the Tofua Volcanic Arc -Earth's fastest-converging and most seismically active subduction boundary- the volcano formed during the Late-Pleistocene period (0.5 Ma) in response to subduction of the Pacific Plate beneath the Indo-Australian Plate. This geological setting is characterized by ongoing tectonic activity and active volcanic processes. The site has witnessed historical eruptions in 1912, 1988, 2009 (Bohnenstiehl, 2013) and 2014-15 (Cronin *et al.*, 2017), with earlier eruptions dated at 210AD and 1125AD.

Hunga Volcano's phreatoplinian eruption in January 2022 is one of the most extraordinary geological events ever observed with modern technology, making the site a global scientific reference.

Scientific research and tradition

Scientists closely study Hunga Volcano to gain insights into its formation, eruptive behavior, and hazards. By understanding the complex geological processes shaping this site, we can enhance our knowledge of similar volcanic systems on earth and other planets (Garvin *et al.*, 2018), and improve mitigation strategies for volcanic hazards.

Distinguished researchers have investigated Hunga Volcano's eruptive activity & hazards (Bohnenstiehl *et al.*, 2013; Cronin *et al.*, 2017), notably volcanic tsunami (Lane, 2022; Purkis *et al.*, 2023). The site offers significant insights into volcanic systems, including the evolution of new volcanic islands (Garvin *et al.*, 2018), contributing to science and geo-heritage (Nemeth, 2022) traditions.



Comparative pre-eruption (2016) and post-eruption (2022) bathymetric-topographic models of Hunga Volcano, showing the dramatic caldera collapse of the 15/01/2022 eruption (Garvin and Slayback, 2023).

ROTORUA'S GEOTHERMAL FIELDS, AHI-TUPUA NEW ZEALAND



Waiotapu's Champagne Pool (left), with orange sinter rim, and Artist's Palette sinter terrace (right) are among the most colourful geothermal features globally. Photo: Alastair Jamieson.

OUTSTANDING COLOURFUL SINTERS, GEYSERS, BOILING MUD POOLS AND SILICEOUS LILY-PAD STROMATOLITES.

The several thousand discharge features in three Rotorua geothermal fields (Ahi-Tupua) are globally significant. Whakarewarewa has strong cultural values and has been used by the indigenous Maori for many centuries. It is best known for the five geysers and sinter stalactites at Te Puia sinter mound. Pohutu is the largest geyser in the Southern Hemisphere,

erupting hourly and reaching heights of 30 meters. Waiotapu is known for its colourful Champagne Pool and Artist's Palette sinter terrace, its numerous collapse craters, sulfur-lined fumeroles, and its boiling mud pools and mud volcanoes. Waimangu is the world's youngest geothermal field and has lily-pad stromatolites.

SITE 163

GEOLOGICAL PERIOD	Holocene
LOCATION	Bay of Plenty, New Zealand 38°09'49"S 176°15'15"E
MAIN GEOLOGICAL INTEREST	Volcanology Geomorphology and active geological processes



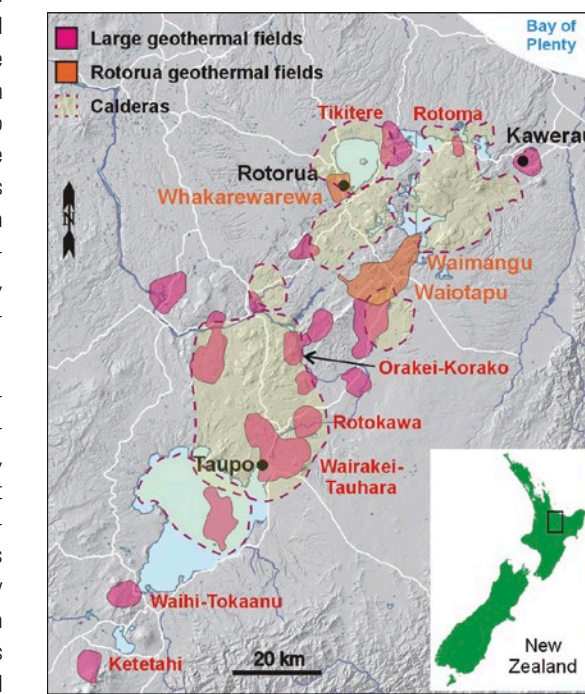
Pohutu Geyser is the largest geyser in the Southern Hemisphere. It erupts hourly and is Rotorua city's most significant tourist attraction. Photo: Bruce Hayward.

Geological Description

New Zealand's Taupo Volcanic Zone (southern end of Tonga-Kermadec Volcanic Arc) is home to eight caldera complexes, with two active. By-products of this volcanism are numerous high-temperature geothermal systems along caldera margins. New Zealand pioneered the development of geothermal energy, which has impacted many surface geothermal features. Legally protected from this development are three fields close to Rotorua, containing the best examples of the wide diversity of surface discharge features (Hayward, 2022). These three fields are run by their indigenous tribal owners as environmentally-sensitive tourist attractions, being the most popular sight-seeing destination in New Zealand for overseas visitors.

Best known of these three fields is Whakarewarewa with its outstanding geysers and boiling pools of clear, alkaline chloride or murky, acid sulfate waters. Waiotapu Field is best known for its brightly-coloured sinter deposits and colourful mixed fluids and fumeroles in numerous collapse craters. It also has New Zealand's largest geothermal mud pool with numerous mud volcanoes. Waimangu Field is the world's youngest geothermal field, created

by the 1886 Tarawera eruption that destroyed the eighth wonder of the world - the Pink and White terraces (Hunt *et al.*, 1994). Growing at Waimangu on the edge of Frying-Pan lake are siliceous lily-pad stromatolites.



The Rotorua geothermal fields of Whakarewarewa, Waiotapu and Waimangu have the most significant discharge features of many similar fields in the Taupo Volcanic Zone.

Scientific research and tradition

These geothermal fields have been natural laboratories for diverse research, including investigation of deep exploitable areas, utilisation, preservation and restoration of surface features (Chambefort and Bignall, 2016; Scott *et al.*, 2016), extensive study of thermophilic microbes (Power *et al.*, 2023) especially as modern analogues for early life formation on Earth.

6

TECTONICS

SITE 164 - SITE 174



Fidenrathorn, Switzerland

Tectonics (from ancient Greek, *τεκτονική*, "pertaining to building") concerns the evolution of the lithosphere, its dynamics and associated deformation. Plate Tectonics predicts that the Earth's outermost rigid shell, the lithosphere, is divided into a mosaic of plates that move on and sink into the weaker ductile asthenosphere. This network of plates is interconnected by three types of plate boundaries: (i) constructive boundary, where new lithosphere is created at mid-oceanic ridges, (ii) destructive boundary, where lithosphere is recycled in the asthenospheric mantle along subduction zones, and (iii) conservative boundary, where plates slip past each other along transform structure, without creating or destroying lithosphere. Thus, Plate Tectonics demonstrates how our Earth is a Dynamic Planet, continuously shaping and modifying its "skin".

To describe Plate Tectonics, representing the central unifying theory for geologists, we cannot find better words than those of Trümpy R. (2001) "*like Venus, the theory of Plate Tectonics is very beautiful and born out of the sea*". Indeed, compared to other important unifying theories such as the Evolution in Biology or the Relativity in Physics, Plate Tectonics is quite young, having been discovered after World War II thanks to advances in exploring oceanic basins. Basically, all processes including mountain building, volcanoes and earthquakes, sedimentary basins, genesis and distribution of georesources, landscape evolution, water or carbon cycles, and speciation and evolution of life are related to Plate Tectonics.

Despite being a well-established theory, Plate Tectonics is not a dogmatic paradigm and is still evolving. For example, the exact location of some plate boundaries or the mechanisms of rapid rock exhumation remain unresolved. The interaction between Tectonics and Climate, its co-evolution with life, its origin on Earth, and the possible tectonic styles on other planets and their habitability are among the most fascinating active research frontiers in Tectonics. Plate Tectonics is closely connected to humans, from their evolution to daily life. A better understanding of Plate Tectonics is fundamental for humanity to face future challenges such as energy transition, global change and natural hazard mitigation.

The Second 100 IUGS Geological Heritage sites feature eleven key localities across three continents that showcase the role of Tectonics in shaping our planet, from the birth of oceans, such as the Mid-Atlantic ridge on Reykjanes, Iceland, to the construction of mountains, such as the 1,800 my history in the Colca Canyon in Peru, the Monte Perdido massif tectonic structure, and the exhumed mid-crust in the Patos shear zone in Brazil.

Some sites show active deformation, such as surface faulting at Mt. Vettore in Italy. Others display remarkable thrusting-process features, such as the Esla Unit thrust system in Spain, the brittle structures of the Somerset Coast in the UK, and the Glarus thrust in Switzerland, or spectacular exposures of salt domes in the Zagros belt in Iran, Earth's youngest collisional zone, and the world's largest superposed buckle folds in Aliaga, Spain. Additionally, the Nazca Ridge's impact on the continuous uplift of marine terraces is showcased at San Juan de Marcona, Peru.

Laura Giambiagi

CONICET. Consejo Nacional de Investigaciones Científicas y Técnicas. CCT- Mendoza. Argentina.

TECTASK. IUGS Commission on Tectonics and Structural Geology. IUGS Geological Heritage Sites referee.

Salvatore Laccarino

Dipartimento di Scienze della Terra. Università di Torino. Italy

TECTASK. IUGS Commission on Tectonics and Structural Geology. IUGS Geological Heritage Sites referee.



THE MID-ATLANTIC RIDGE ON REYKJANES ICELAND



UNESCO Global Geopark

Gunnuhver hot spring, with the Fagradalsfjall volcanic eruption (2021) in the background (Photo Lovísa Ásbjörnsdóttir).

ACTIVE RIFT ZONE ONSHORE WITH FAULTING, FISSURE ERUPTIONS, HYALOCLASTITE RIDGES AND A GEOTHERMAL AREA.

The Reykjanes Ridge is part of the Mid-Atlantic Ridge which extends onshore on Reykjanes, the southwestern most part of the Reykjanes Peninsula. The most prominent structural features show complex pattern of deformation in a highly oblique rifting in the presence of a transform segment (Khodayar *et al.*, 2018). The main tectonic fractures are fissures, normal

faults, and strike-slip faults. The geothermal field is in a highly fractured bedrock, with hot springs, mud pools and fumaroles. Three volcanic and rifting episodes have occurred on Reykjanes Peninsula in the past 4000 years (Sæmundsson *et al.*, 2020). A new episode is believed to have started in 2019.

SITE 164

GEOLOGICAL PERIOD	Pleistocene to Holocene
LOCATION	Reykjanes Peninsula, Iceland 63°48'47"N 022°42'56"W
MAIN GEOLOGICAL INTEREST	Tectonics Volcanology



Reykjanes with postglacial lava fields, volcanic fissures, faults, and the geothermal field. (Photo Sigurður K. Guðjohnsen).

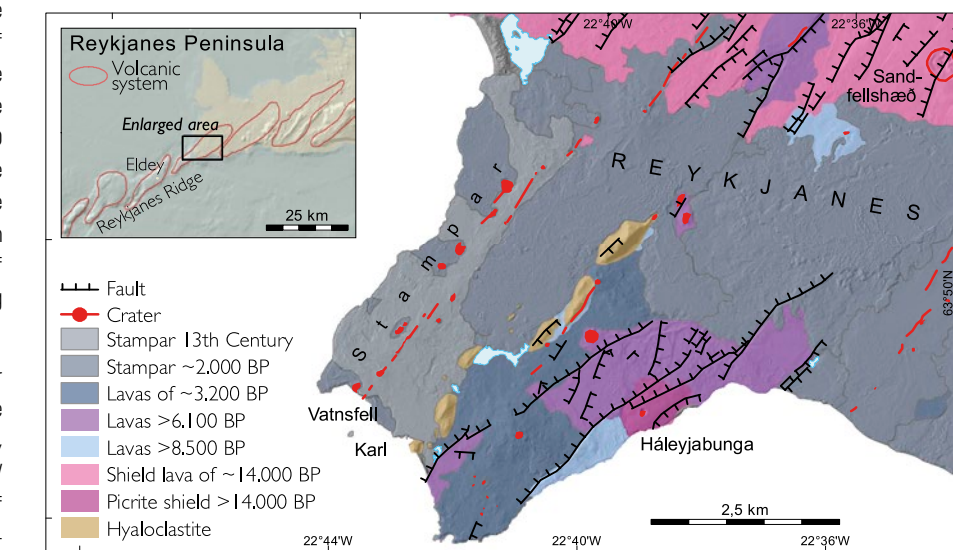
Geological Description

Reykjanes volcanic system with its well-defined fissure swarms is an actively rifting volcanic area, around 45 kilometers in length, 30 of which are on land; the rest is submarine and connects with the Reykjanes Ridge. The center of the volcanic system is within a 5 kilometer-wide rift zone, consisting of normal and transform faults running NE-SW creating a rough graben-like structure. The bedrock of the site consists of subglacially erupted basalt ridges (tindar) of Pleistocene age, a >14,000-year-old picrite shield lava of Háleyjabunga, and a 14,000-year-old olivine tholeiite shield lava of Sandfellshæð in the north. Postglacial lavas younger than 8,500 years cover much of the southern part of the area. The youngest lava erupted from the Stampar cone row in 1210-1211 CE. It began with an offshore eruption creating the tuff cones of Vatnsfell and Karl before extending northwards inland.

Faults with over 20 meters of throw occur throughout the older lavas and tindar. The rate of subsidence is around 6.5 mm/year, the rate of extension is around 8-9 mm/year (Sæmundsson *et al.*, 2020). The core of volcanic system has a productive geother-

mal system of 1.5 km², with a reservoir temperature up to 320°C at 3 kilometers depth (Khodayar *et al.*, 2018).

Geological map of Reykjanes showing the main faults, craters and lavas (Sæmundsson *et al.*, 2020).



Scientific research and tradition

Research has been ongoing since the late 20th century to understand the geothermal systems as well as studying plate boundary, fractures and volcanics (Sæmundsson *et al.*, 2020). Recent research includes the International Deep Drilling Project, which reached 4500 meter depth (Friðleifsson *et al.*, 2020), structural analysis (Khodayar *et al.*, 2018), and monitoring of earthquakes and the volcanic system.

THE EVOLUTION OF THE ANDES IN COLCA CANYON PERU



UNESCO Global Geopark

Northeastern view Colca Canyon. Right: Quaternary volcanic rocks on the surface, intersected by normal fault; to the backdrop: Plio-Quaternary volcanic arc glacial mountains.

**1800 MILLIONS YEARS OF
EARTH'S HISTORY INCLUDING
SIX GEOLOGICAL PERIODS OF
ACTIVE CONTINENTAL MARGINS
LOCATED IN ONE OF THE
DEEPEST CANYONS ON EARTH.**

The Colca River canyon exposes a unique section of lithosphere in the Central Andes with rocks of different origin, age, lithology and tectonic structures, in 120-kilometer-long continuous walls 1-3 kilometer high. Located in the Western Cordillera of southern Peru, it is one of the deepest valleys in the Andes. The incision is strictly

related to active tectonic processes related to the subduction zone of the Nazca Plate below the South American Plate. The Andes, and especially its middle sector channeled by the Colca River, are considered a model of active continental margin (Paulo, 2008).

SITE 165

GEOLOGICAL PERIOD	Paleoproterozoic (Statherian) to Holocene
LOCATION	Arequipa, Peru 15°36'41"S 071°54'21"W
MAIN GEOLOGICAL INTEREST	Tectonics Geomorphology and active geological processes



Colca Canyon section, near to Choco town, upstream view. The river is eroded Cenozoic volcanic rocks hanging and reveals ancient Proterozoic Andean bedrock.

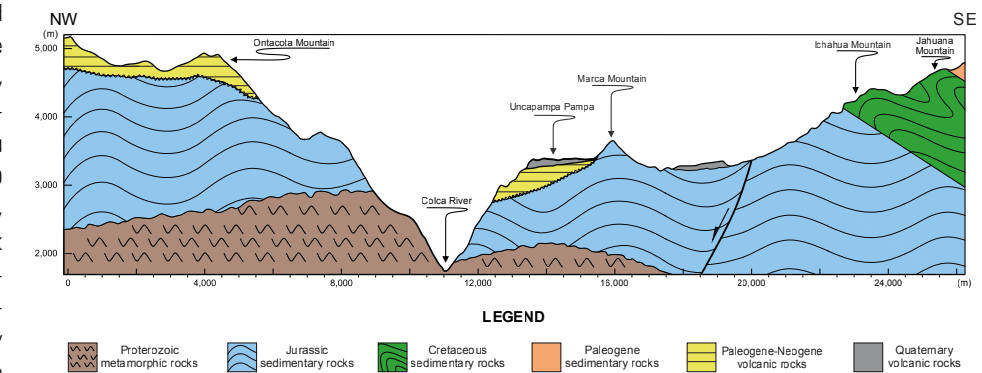
Geological Description

The Colca Canyon, an important tourist destination in Peru, records six geological periods between the Proterozoic (Statherian) and Phanerozoic Eons (Quaternary). At its base lies a Paleo-Proterozoic metamorphic basement intruded by Cretaceous-Paleogene plutons (Caldas, 1993; Romero, 2001) and unconformably overlaid by folded and faulted Jurassic and Cretaceous rocks containing marine fossils (logs and footprints). The Western Andean Volcanic Arc contributes a vast Cenozoic volcanic cover. Resting on an Eocene-Miocene basement, eroded Plio-Pleistocene stratovolcanoes and active Pleistocene-Holocene stratovolcanoes (e.g., Sabancaya volcano) are prominent, alongside monogenetic cones and fissural lava fields. The rocky mountainous front (1000 to 5200 meters asl) is covered by moraines, glacial meltwater, alluvium, lakes, and rock avalanches deposits. The Colca's neotectonic, volcanic and seismicity activity is related to active faults within the Quaternary Volcanic Arc, where the Colca fault system has the most representative structures (Benavente *et al.*, 2017; Delacourt *et al.*, 2007; Rivera *et al.*, 2016). The Colca Canyon incision

is a result of the Andean uplift, deglaciation, and erosion in 120 kilometers of escarpments between 1 to 3 kilometers. The primitive canyon must have started about 10 million years ago; its current landscape would correspond to the last million years (Thouret *et al.*, 2007).

Scientific research and tradition

The Colca's depth compared with other canyons around the world (New York Geographical Society, 1831; Reparáz, 1955; Guines Record Magazine, 1984), its stratigraphic record (Caldas, 1993), Polish expeditions (Paulo, 2008) and structural-tectonics and thermochronological studies (Thouret *et al.*, 2007; Schildgen *et al.*, 2007, 2009, 2018) reveal an extensive geologic record of the central Andes.



The Colca Canyon exposes a geological section that spans from the Central Andes basement to the Quaternary period. The lithostratigraphic units present notable angular and erosive discordances, product of the Andean uplift and erosion that affected part of this sequence.

SALT DOMES AND GLACIERS OF THE ZAGROS FOLD AND THRUST BELT

IRAN



UNESCO Global Geopark

Ediacaran-Early Cambrian Hormuz salt extruded in the eroded core of a whale-back anticline of the Zagros mountain of southern Iran. The folded strata belong to Cretaceous to Pliocene sequence.

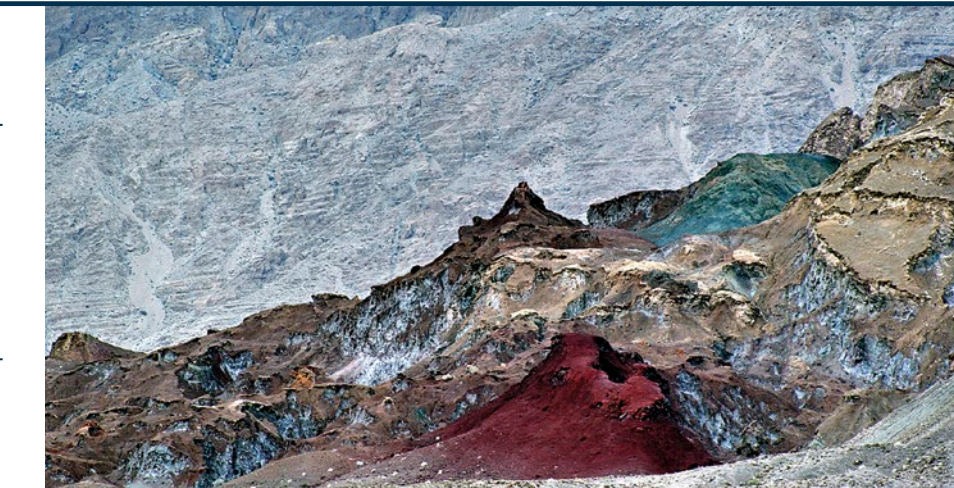
**THE MOST SPECTACULAR
MANIFESTATION OF SALT
TECTONICS IN ONE OF THE
YOUNGEST COLLISIONAL ZONES
IN THE WORLD.**

The Zagros fold and thrust belt hosts the most unique outcrops of the Neoproterozoic-Cambrian salts which have travelled up to 11 kilometers through their sedimentary overburden and have produced versatile beautiful salt domes and salt glaciers. No other continental (non-marine) salt domes, distributed in such a scale,

may be found on the planet. The salt diapirism is accompanied by exclusive folded structures of young Zagros collisional belt. The fold and thrust belt hosts huge reserves of oil and gas and bears more than 200 salt domes mostly concentrated in the south of the belt.

SITE 166

GEOLOGICAL PERIOD	Neoproterozoic (Ediacaran) to Cambrian
LOCATION	The outcrops are distributed in the Zagros Mountains in southern Iran and the Persian Gulf, Iran 27°18'11"N 055°07'20"E
MAIN GEOLOGICAL INTEREST	Tectonics Geomorphology and active geological processes



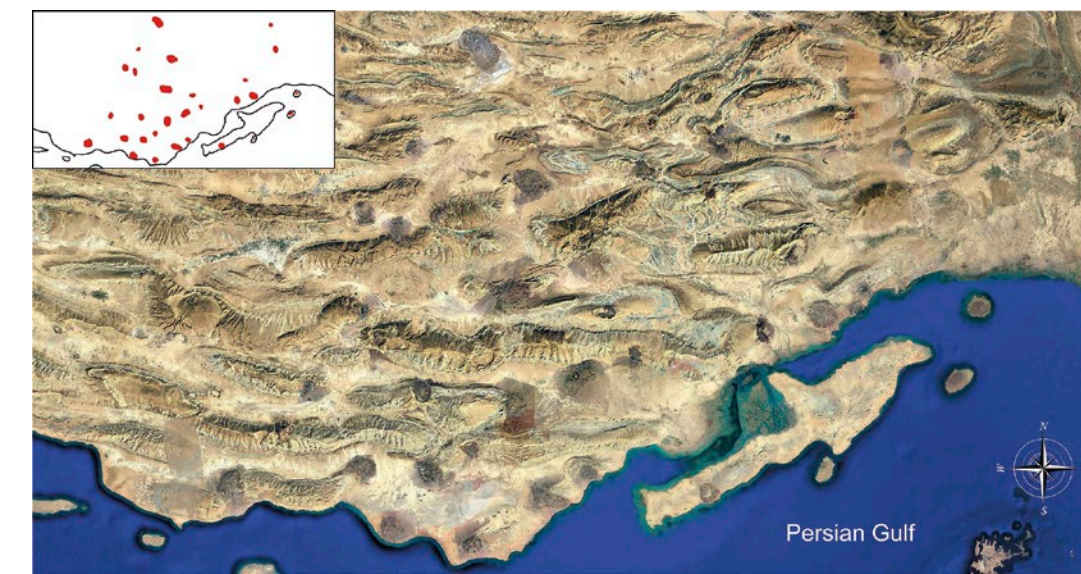
Variegated landscape in the Tange-Zagh salt dome (Hormozgan Province) is formed through the exposure of salt, iron ore, and rock inclusions.

Geological Description

The Zagros fold and thrust belt and the Persian Gulf foreland basin in southern Iran hosts a great number of emerged and buried salt domes, which root in the Hormuz series of Neoproterozoic-Cambrian age. The salt is associated with a mixture of gypsum, dolomite, and volcanic rocks [Faramarzi *et al.*, 2015]. This salt has risen through a thick

overburden of sedimentary units [Talbot and Jarvis, 1984]. The Hormuz series has played an important role in style of deformation and folding of the Zagros orogen following the collision between the Arabian and Iranian plates. The source of the evaporites is likely an oceanic system comparable to the present-day Red Sea [Omran, unpublished data].

The salt rises through vertical conduits to form salt domes and spreads on the ground as salt glaciers (namakiers). The first pulse of the diapiric movements was in the Mesozoic; however, major salt kinematics has occurred in more recent times in Cenozoic [Talbot, 1979; Ghassemi and Roustaei, 2021]. Many hidden salt diapirs are detected in the seismic reflection profiles of Zagros and Persian Gulf. The Hormuz evaporites occur over a vast area of Iran, Middle East and Pakistan [Smith, 2015].



Satellite image of dozens of salt diapirs distributed in the southern part of Zagros Mountain Ranges.

Scientific research and tradition

The very first paper in the first issue of the Journal of Structural Geology was published by Talbot (1979) on the Kuh-e-Namak (Dashti) in Iran, and since then the salt diapirs of the Zagros are used as the best natural labs for study of salt tectonics.

THE PATOS SHEAR ZONE

BRAZIL



Migmatitic rocks from the high-temperature part of the Patos shear zone near Patos where melt formed during late Proterozoic shearing.

IMPRESSIVE EXAMPLE OF AN EXHUMED MID-CRUSTAL STRIKE-SLIP INTRACONTINENTAL SHEAR ZONE.

Strain localization into crustal-scale shear zones is an important process during crustal deformation, and the Patos Shear Zone in the Borborema Province is an outstanding example of the role of shearing during the Neoproterozoic Brasiliano–Pan-African orogeny. This tens of kilometers wide and hundreds of kilometers long shear zone offers locations that expose the funda-

mental crustal processes related to strike-slip dominated movement of continental blocks: the role of partial melting, kinematic indicators, strike-slip duplexing, strain, mylonitic structures from the grain scale to tens of kilometers. This is also a superb area for studying reactivation of shear zone fabrics during the Cretaceous.

GEOLOGICAL PERIOD

Neoproterozoic (Cryogenian to Ediacaran)

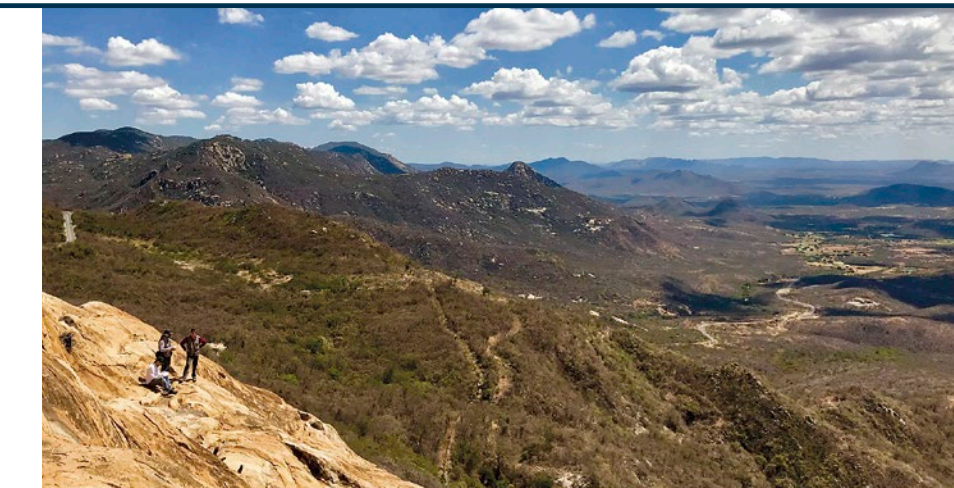
LOCATION

Borborema Province, States of Paraíba and Ceará, Brazil
07°02'19"S
037°16'35"W

MAIN GEOLOGICAL INTEREST

Tectonics

SITE 167



Looking east along the southern margin of the Patos SZ, where deformed Ediacaran granitic plutons form hills in the semi-arid landscape of NE Brazil.

Geological Description

In NE Brazil, rocks of Archean to Ediacaran age are dragged in and out of an impressive network of continental shear zones. The largest one is the Patos Shear Zone, where the older igneous, metamorphic and metasedimentary rocks are transformed into sheared rocks with mylonitic and gneissic fabrics. This transcurrent shear zone transects NE Brazil from the Atlantic coast and 700 km westwards until being covered by the Paleozoic-Mesozoic Parnaíba basin (Fossen *et al.*, 2022). Pre-Atlantic Ocean reconstructions indicate that the shear zone continues on the African side as part of a network of intracontinental shear zones.

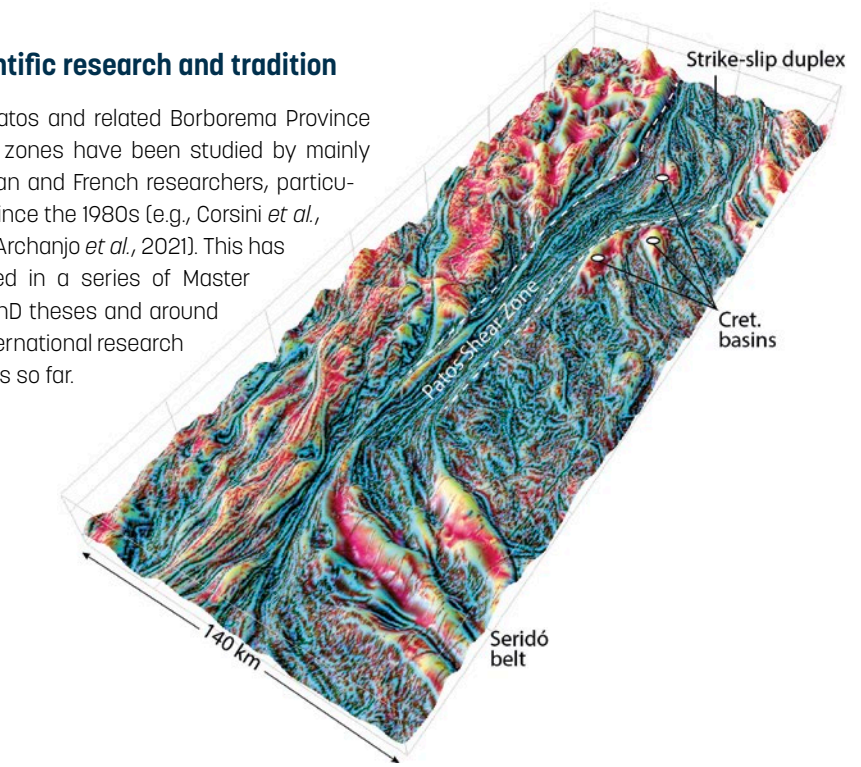
More than three hundred kilometers of dextral offset on this shear zone reflect the forces involved during completion of the late Neoproterozoic Gondwana supercontinent. Today we can study the processes that occurred at mid-crustal levels in well-exposed migmatitic rocks and lower temperature (ultra) mylonites (e.g., Cavalcante *et al.*, 2016, 2022). The shear zone exposes an impressive large-scale strike-slip duplex. There are spectacular examples of brittle reactivation during Cretaceous pre-Atlantic rifting, where

shear zone fabrics acted as guides for fault nucleation during the rifting. Publicly available seismic data combined with field examples gives good control on this reactivation behavior.

Scientific research and tradition

The Patos and related Borborema Province shear zones have been studied by mainly Brazilian and French researchers, particularly since the 1980s (e.g., Corsini *et al.*, 1996; Archanjo *et al.*, 2021). This has resulted in a series of Master and PhD theses and around 30 international research articles so far.

Magnetic anomaly model of the Patos SZ. Colors indicate lithologies with different magnetic properties. Cretaceous rift basins with margins controlled by basement structure are shown.



ESLA UNIT THRUST SYSTEM

SPAIN



In the foreground ridge, Cambrian dolostones of the Esla Nappe (right) rest over Devonian limestones (left) along an overturned thrust. In the distance, folded unconformable succession.

IMPRESSIVE EXAMPLE OF AN EXHUMED MID-CRUSTAL STRIKE-SLIP INTRACONTINENTAL SHEAR ZONE.

The Esla Unit has attracted the attention of numerous international research groups since the 1930s owing to its variety of thin-skinned deformation-related structures, its outstanding examples of post-emplacement deformation of thrust sheets, its fault rock assemblages in basal nappe shear zones, the complete Palaeozoic record of its sedimentary succession and, in addition,

its excellent outcropping conditions. The unit has proven to be a key area in the understanding of the geological evolution of the Cantabrian Zone and the Ibero-Armorican Arc. The area has contributed to the educational training of numerous generations of geologists from several European geoscience institutions.

SITE 168

GEOLOGICAL PERIOD	Upper Devonian to Carboniferous (Pennsylvanian)
LOCATION	Cantabrian Mountains, León Province, Spain 42°52'26"N 005°09'50"W
MAIN GEOLOGICAL INTEREST	Tectonics Stratigraphy and sedimentology



Primajas Duplex, formed by horsts with Cambrian carbonates of the Láncara Formation and shales of the Oville Formation. Succession is overturned, younging towards the valley.

Geological Description

The Esla Unit is located in the SE Cantabrian Zone, the external foreland fold and thrust belt of the Variscan Orogen (NW Iberian Massif). It is formed by a sedimentary succession that displays an almost complete record of the Palaeozoic Era, starting in lower Cambrian strata and ending in Pennsylvanian synorogenic deposits (Comte, 1959). The unit, structured into three nappes and three duplexes of kilometric scale that accommodate a total displacement of 92 kilometers, was emplaced during the Moscovian towards the NE in present-day coordinates (Alonso, 1987). The unit contains outstanding examples of thrust-related fault rocks (Arboleya, 1989; de Paz-Ál-

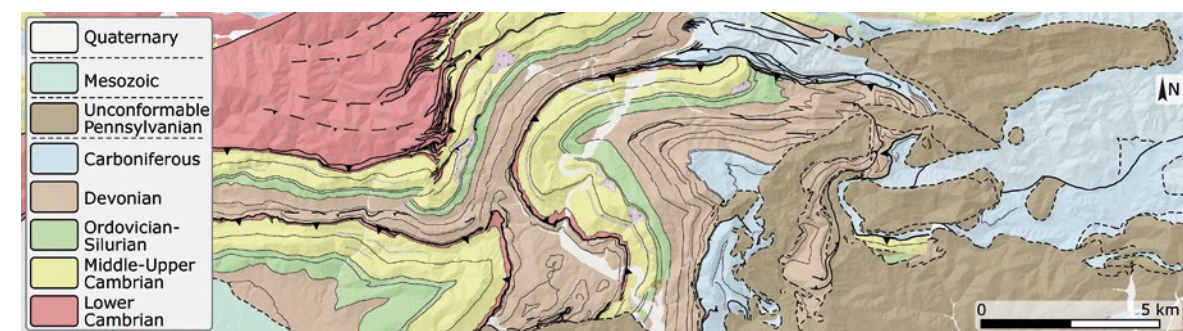
varez *et al.*, 2021) and structures, including fault-bend folds, frontal and lateral culmination walls formed in response to the geometry of deeper thrust surfaces, and duplexes (Alonso, 1987).

Post-nappe emplacement deformation in the Esla Unit resulted in the rotation of its western area around a horizontal axis, generating a cartographic pattern that shows zenithal and cross-sectional views of the unit that allow a three-dimensional observation of the structures. Late deformation also resulted in fold interference patterns and a variety of geometrical relations between reactivated folds

and unconformity surfaces truncating them which depend on the folding mechanism active during reactivation (Alonso, 1989).

Scientific research and tradition

The Esla Unit is at the forefront of studies regarding the stratigraphy and deformation of the Cantabrian Zone. With modern studies starting in the 1930s (e.g. Comte, 1959), it still constitutes an active research area and an outstanding laboratory visited by numerous European geology departments for field courses.



Geological map of the Esla Unit (modified from Merino-Tomé *et al.*, 2014). Variable fold orientations result from nappe frontal and lateral structures and post-emplacement deformation.

GLARUS THRUST

SWITZERLAND



UNESCO World Heritage Site

Famous view of Tschingelhörner with Martin's Hole. The Glarus thrust is visible as a line along the cliff where the rock changes color.

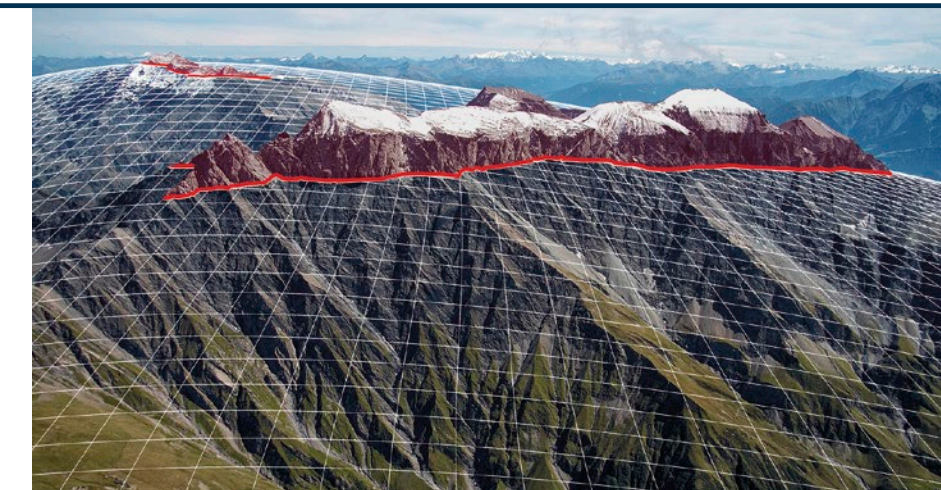
AN EXCEPTIONAL AND DRAMATIC DISPLAY OF MOUNTAIN BUILDING THROUGH CONTINENTAL COLLISION WITH PHENOMENAL OUTCROPS IN AN ALPINE MOUNTAIN LANDSCAPE.

Thrust faults represent unique features in collisional orogens, where through the collision of continental plates the crust is thickened and uplifted to form mountain ranges. The stacking of nappes along thrusts is one of the main mechanisms responsible for thickening of the upper crust, uplift, erosion and thereby forming of a mountain relief. In this way the Glarus

thrust is a witness of processes that take place at great depths within the Earth's crust in all major mountain ranges (Pfiffner *et al.*, 2006; Pfiffner and Schmid, 2008). The scenic exposure and the numerous outcrops of the thrust surface inspired generations of geologists to study its secrets (Westermann, 2009).

SITE 169

GEOLOGICAL PERIOD	Permian to Quaternary
LOCATION	Cantons of Glarus, St. Gallen and Grisons, Switzerland 46°55'22"N 009°15'05"E
MAIN GEOLOGICAL INTEREST	Tectonics History of geosciences



The domelike Glarus thrust, here visualized as a grid structure crosscutting the mountain ranges for dozens of kilometers.

Geological Description

The Glarus thrust is a unique structure which can be followed over several kilometers and numerous outcrops in eastern Switzerland. It is visible as a baffling, seemingly perfect geometric surface, cutting through the mountain landscape and cropping out as a sharp line along cliffs.

The Glarus thrust formed during Oligocene to Miocene times and put older rocks onto younger rocks in the entire region. The minimal displacement along this large-scale shear zone is estimated to be more than 50 kilometers.

The large Glarus thrust surface once formed as a ramp reaching some 10–15 kilometers

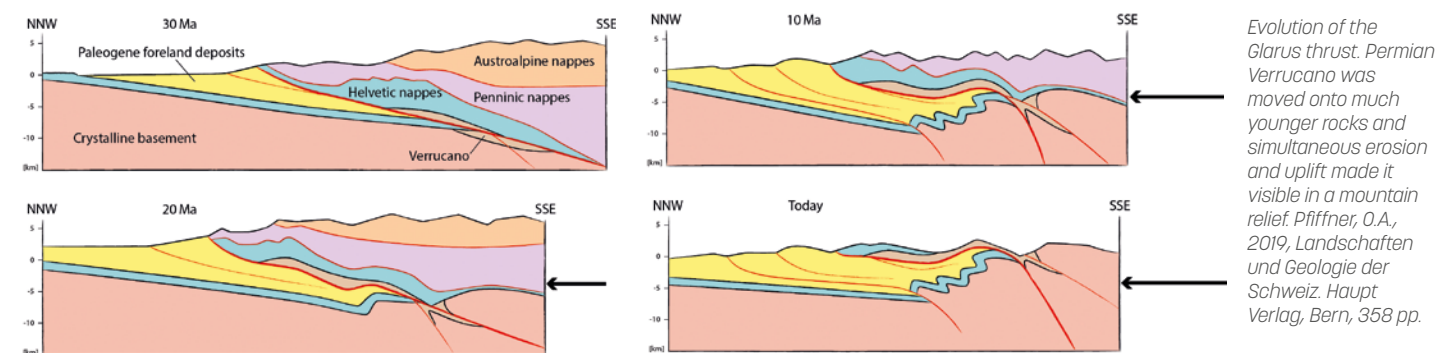
deep in the upper crust. It was exposed following rapid uplift rates of more than 1 mm/year and ensuing fast erosion rates such that rivers cut deep valleys, some of which were further deepened and widened by glaciers. As a result, a unique clear three-dimensional visibility of the Glarus thrust in a mountain landscape emerged.

Erosion further resulted in several klippen of Permian Verrucano rocks sitting on top of much younger rocks. In some instances, the age difference between hanging wall and footwall rocks across the Glarus thrust is more than 200 million years, observed over

a distance of only a few centimeters (Herwegen *et al.*, 2008; Schmid, 1975).

Scientific research and tradition

The observation that older rocks lie above younger rocks puzzled the early workers in the 19th century. Different explanations for this observation led to heated debates and inspired scientists until the present. Discussions incited the question how mountain ranges form and -besides tectonics- opened research on metamorphism, geochemistry and geomorphology (Westermann, 2009).



MONTE PERDIDO MASSIF TECTONIC STRUCTURE SPAIN



UNESCO World Heritage Site

UNESCO Global Geopark

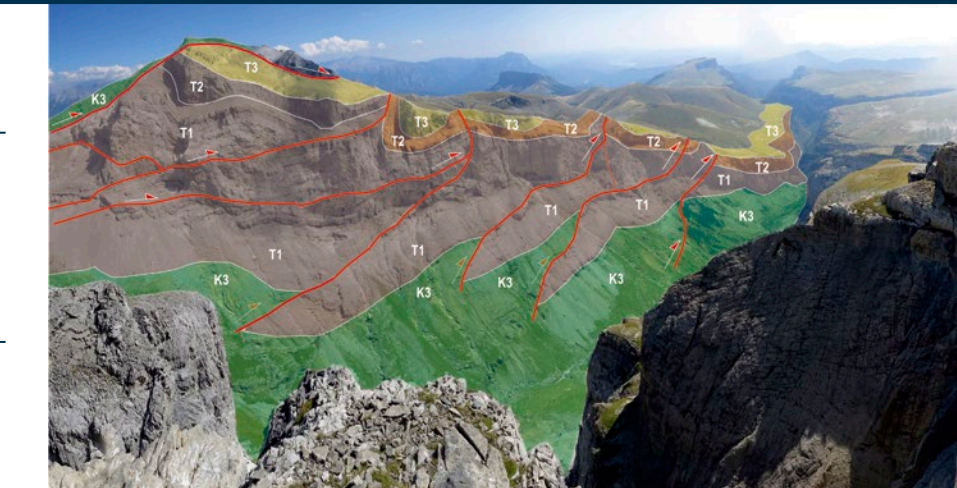
A KEY SITE FOR UNDERSTANDING THE RELATIONS BETWEEN SEDIMENTATION AND DEFORMATION IN MOUNTAIN BUILDING PROCESSES.

It is a world reference for analysing the relationships between the orogenic growth of a mountain range and the sedimentation and deformation in a synorogenic basin. The outcrop conditions are exceptional, showing the spectacular stacking of tectonic structures left exposed by glacial erosion. The stratigraphic record spans 35

million years in a single succession more than 1500 metres thick partly contemporary with the uplift of the mountain range. The representativeness of the regional and global stratigraphic changes of these series make this succession a world reference. It is a UNESCO World Heritage Site, a Biosphere Reserve and a Global Geopark.

SITE 170

GEOLOGICAL PERIOD	Eocene to Oligocene
LOCATION	Pyrenees, Spain 42°40'15"N 000°04'02"E
MAIN GEOLOGICAL INTEREST	Tectonics Stratigraphy and sedimentology



Stack of thrusts in the upper part of the Añisclo canyon. Units shown in the figure below.

Geological Description

In the Monte Perdido massif, the Gavarnie thrust together with the Monte Perdido system are the main structure responsible for the Pyrenees as a mountain belt, but also it is the generator or part of the subsidence that made possible the existence of the South Pyrenean synorogenic basin (Seguret, 1972). The spectacular fold and thrust stack of Monte Perdido system is partly responsible for producing the highest limestone massif in Western Europe. It includes rocks from Paleozoic to Paleogene as part of the Gavarnie thrust footwall; Devonian rocks compose the hangingwall (Rousell, 1904; Van der Velde, 1967).

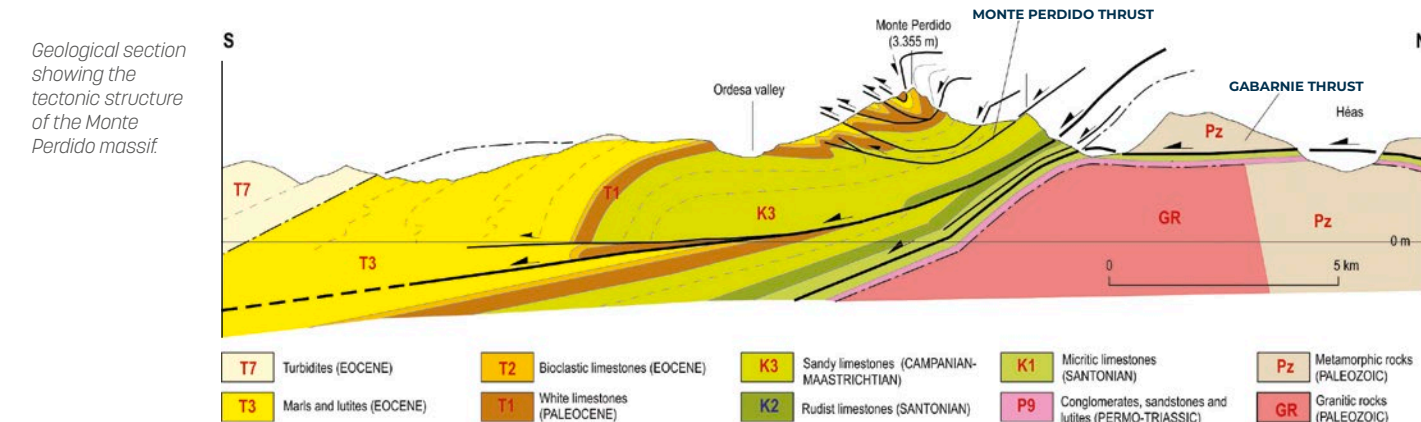
The Monte Perdido system formed during the Lutetian to Bartonian (Eocene) (Pujalte *et al.*, 2016). It is composed of several sheets affecting rocks from upper Cretaceous to Eocene. The entire system was folded during the displacement of the Gavarnie thrust, from Bartonian to Rupelian (Oligocene) (Labaume *et al.*, 2016). Due to this major structural feature, the Monte Perdido system is tilted to the south and is the southern flank of a great anticlinal of regional scale (Muñoz *et al.*, 2013).

The transfer of deformation to the south associated with the Gavarnie thrust is related

to the generation of important folds and syntectonic sediments located in the South Pyrenean synorogenic basin.

Scientific research and tradition

Research started early, as Charles Lyell was here in 1830 and in 1903. The first thrust in the Pyrenees was here identified. After that, the main geologists who have dealt with the sedimentary record and tectonics of the Pyrenean mountain belt have worked in the area and research continues today.



BRITTLE STRUCTURES OF THE SOMERSET COAST UNITED KINGDOM



Photograph taken from a drone looking eastwards from Kilve, showing normal faults and folds exposed on the beach and cliffs.

SPECTACULAR AND MOST STUDIED EXPOSURES OF BRITTLE STRUCTURES RELATED TO BASIN DEVELOPMENT AND INVERSION.

The Somerset coast is a wonderful natural laboratory for studying the geometries, kinematics and mechanics of a range of related brittle structures. These include normal fault zones that allow detailed investigations of fault growth and linkage at various stages of faulting, damage zones

around a range of fault types, the relationships between faults, folds and joints, and the patterns of joints exposed on bedding planes. The area has been used increasingly as a World-class location for both research and teaching on brittle tectonics.

SITE 171

GEOLOGICAL PERIOD	Upper Triassic to Lower Jurassic
LOCATION	Somerset, United Kingdom 51°11'33"N 003°13'37"W
MAIN GEOLOGICAL INTEREST	Tectonics Stratigraphy and sedimentology

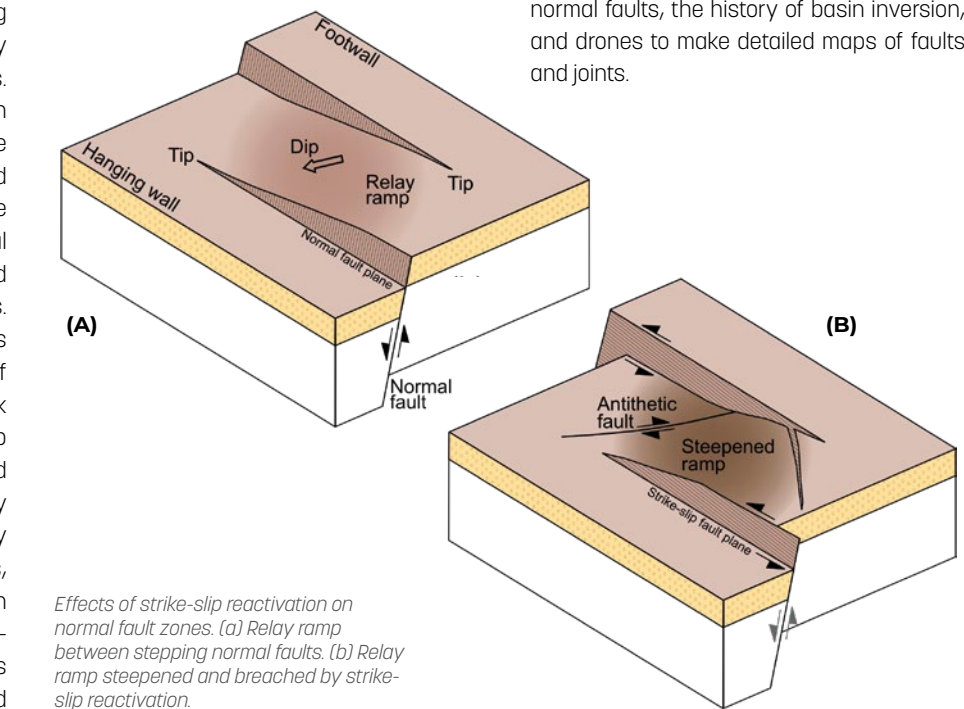


Normal fault and associated structures in the cliff at Kilve.

Geological Description

The Somerset coast displays fantastic exposures of faults, folds, veins and joints (Hancock, 1985) in Permo-Triassic marls and sandstones and in Liassic shales and limestones (Whittaker and Green, 1983). The ~E-W striking normal faults formed during Mesozoic extension (Dart *et al.*, 1995). They have throws of up to several hundred metres. The faults exhibit various stages of growth and linkage, which in many cases can be observed on both the wave-cut platform and in the adjacent cliffs. Folds accommodate displacement variations along the normal faults, veins occur in damage zones, and gouge and veining occurs along the faults. Sandstone dykes and deformation bands occur in Permo-Triassic sandstones west of Watchet. Some normal faults east of Lilstock show evidence of reactivation as strike-slip faults, including steepened and breached relay ramps. Cenozoic contraction, probably related to the Alpine Orogeny, inverted many of the normal faults and created thrusts, strike-slip faults, veins, pressure solution cleavage and folds. The strike-slip faults typically cross-cut the inverted normal faults and the folds and typically show veins and

pressure solution in damage zones (McGrath and Davison, 1995). The youngest structures are joints (Passchier *et al.*, 2021), which abut or cross the strike-slip faults.



Effects of strike-slip reactivation on normal fault zones. (a) Relay ramp between stepping normal faults. (b) Relay ramp steepened and breached by strike-slip reactivation.

Scientific research and tradition

Hancock (1985) recognised the importance of the area ~ 40 years ago. Somerset has been used increasingly to make fundamental observations and models about brittle tectonics, from the geometry and growth of normal faults, the history of basin inversion, and drones to make detailed maps of faults and joints.

SURFACE FAULTING OF A SEISMIC SEQUENCE IN MT. VETTORE ITALY



Mt Vettore, coseismic surface faulting associated with the earthquakes of 24th August and 30th October 2016, crossing the mountain from north to south.

THE MOST RECENT, DOCUMENTED AND PRESERVED SURFACE FAULTING RELATED TO THE 2016 EARTHQUAKES IN CENTRAL APPENNINES.

Initiating in August 2016, a series of moderate to large earthquakes struck the central Apennines producing severe damage and 299 casualties in several small towns. Detailing all coseismic surface effects is crucial to identify and define primary surface faulting and its structural arrangement. This contributes to imaging the shallow

low-crust brittle deformation complexities and may provide useful information for describing the seismic source. Moreover, understanding the relations between the seismic source at depth and its evidence at the surface provides the basis for using the active faults at the surface to determine those faults that can rupture next.

SITE 172

GEOLOGICAL PERIOD	Holocene
LOCATION	Umbria-Marche, Italy 42°49'06"N 013°15'10"E
MAIN GEOLOGICAL INTEREST	Tectonics Geomorphology and active geological processes



A white stripe of rock exposed on the surface by the 2016 October 30th earthquake is still clearly visible and represents the fault displacement.

Geological Description

Mt. Vettore is the peak of the Sibillini Mountains in central Italy. Its western slope is the morphological expression of a NNW-SSE striking SW dipping primary extensional tectonic element (the Mt. Vettore – Mt. Bove fault line, total length of 30 kilometeers), cutting through carbonates of the Umbria-Sabina Meso-Cenozoic succession for a total stratigraphic offset of about 1000 meters. The southern end of the fault was coseismically reactivated by the 2016 Central Italy seismic sequence. Here the slope is marked by at least two major Holocene bedrock fault scarps. The lower scarp runs at the base of the Vettore mountain front and bounds the Castelluccio basin. The upper scarp (visible from afar and locally known as "Cordone del Vettore") runs very closely to the watershed. An approximately 2 meter high strip of whitish rock at the base of the Cordone del Vettore is the evidence of the dislocation along the fault plane due to the two main events (24th August, Mw 6.0 and 30th October 2016, Mw 6.5).

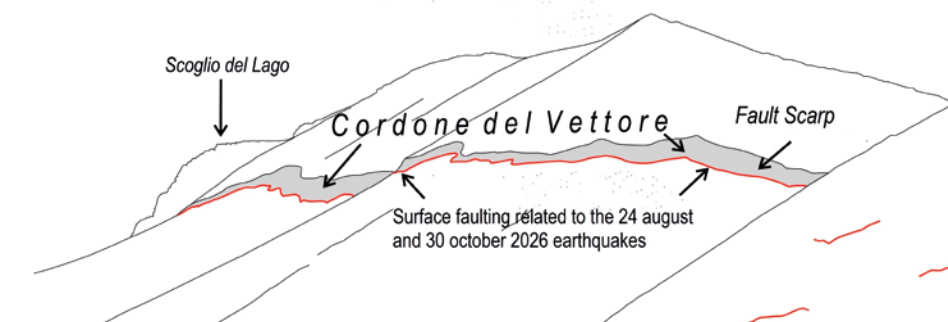
Due to its impressive structure and relatively recent formation, it represents a unique case within the National Geosite Inventory.

Scientific research and tradition

The assessed primary surface faulting along the Mt. Vettore Fault is relevant to earthquake geology and paleoseismology, and therefore to seismic hazard assessment

based on geological investigation. The ongoing studies will hopefully shed light on this matter of great relevance for reliable seismic hazard assessment.

The Cordone del Vettore fault scarp as seen from Sella del Vettoretto.



ALPINE SUPERPOSED BUCKLE FOLDS IN ALIAGA SPAIN



UNESCO Global Geopark

La Olla anticline, second-generation vertical-axis fold affecting Lower Cretaceous marine formations. In front: Aliaga medieval castle. Horizon: Late Neogene planation surface.

PROBABLY THE LARGEST AND MOST ORIGINAL EXAMPLE OF SUPERPOSED BUCKLE FOLDING REPORTED IN THE WORLD.

The superposed folds of Aliaga (Iberian Chain, Spain) represent a global reference for this type of tectonic structures. Most of them correspond to geometries reproduced in laboratory analogue models, but no other comparable large-scale real examples have been described. Among them, a number of vertical, 'snake-like' folds con-

stitute a singular type of fold interference, as well as a case of erosion-driven tectonic structure. It shows how earth-surface processes can exert a control on fold geometry. The most representative structure, La Olla anticline, is the icon of the Geological Park of Aliaga, embryo of the Maestrazgo Unesco Global Geopark.

GEOLOGICAL PERIOD	Eocene to Miocene
LOCATION	Teruel province, Aragón region, Spain 40°40'05"N 000°41'55"W
MAIN GEOLOGICAL INTEREST	Tectonics Geomorphology and active geological processes

SITE 173



Multiple refolded vertical beds in the surroundings of Aliaga. Sharp, convulsing limestone crests represent a magnificent example of structural landforms and geological landscape.

Geological Description

The Aliaga area exhibits a complete inventory of large-scale examples of superposed buckle folds deforming the Mesozoic-Cenozoic cover. They resulted from successive, diversely oriented contractional episodes developed during the Alpine Orogeny, which caused inversion of a series of extensional Mesozoic basins and built the intraplate Iberian Chain (NE Spain).

ENE-WSW trending buckle folds (Early Miocene in age) are superposed to a large NNW-SSE anticline (Eocene-Oligocene). North of Aliaga, the earlier hinge zone in the competent unit controlling buckling (Urgon facies, Lower Cretaceous marine limestones) constituted a mechanical obstacle to refolding. This induced development of conical second-generation folds that buckle the hinges and axial surfaces of the former ones in a complex manner. On the contrary, to the south, erosional removal of the hinge zone allowed the vertical eastern limb to behave almost independent, being refolded into cylindric, nearly vertical folds, as La Olla anticline. Lower Miocene conglomerates adjacent to the earlier NNW-SSE trending anticline contain pebbles of Jurassic origin,

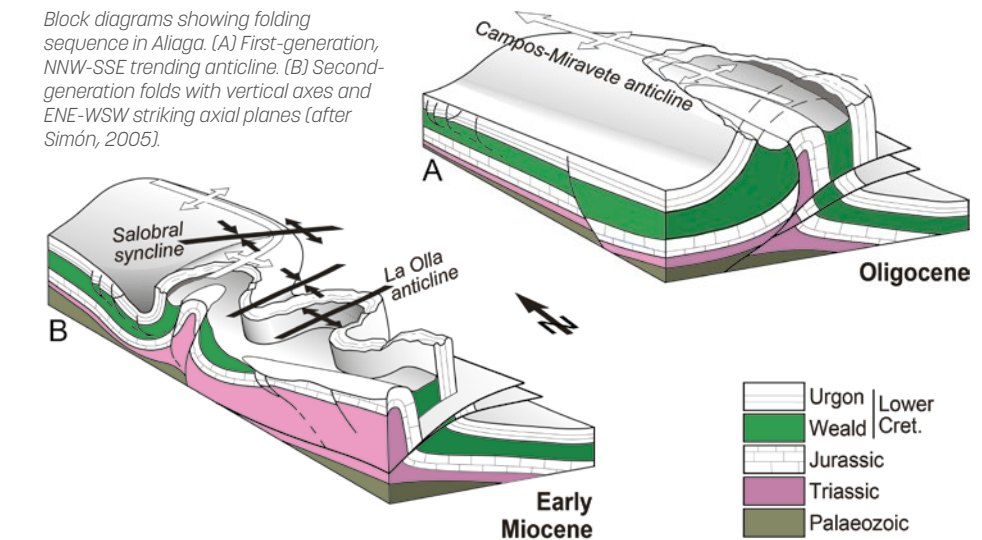
whose source area was the fold core. This evidences that the latter had been effectively exhumed before refolding.

Scientific research and tradition

These folds were first described by Simón (1980) and later analysed in detail by Simón (2004, 2005). They are the object of numer-

ous scientific and educational publications and activities: e.g., Geological Park of Aliaga guidebook (Simón *et al.*, 1998); Practical Geology Course of the Teruel Summer University. La Olla anticline provides the cover image for the popular textbook by R. J. Lisle "Geological structures and maps: A practical guide" (Butterworth-Heinemann, 2020), as it provided for its first edition (Pergamon Press, 1988).

Block diagrams showing folding sequence in Aliaga. (A) First-generation, NNW-SSE trending anticline. (B) Second-generation folds with vertical axes and ENE-WSW striking axial planes (after Simón, 2005).



MARINE TERRACES OF SAN JUAN DE MARCONA

PERU



Shows eight marine terraces of Cerro El Huevo. These marine terraces provide important information on the tectonic uplift processes during the Quaternary in the area.

EXCEPTIONAL SITE SHOWCASING THE INFLUENCE OF THE NAZCA-RIDGE ON THE CONTINUOUS UPLIFT OF THE WESTERN EDGE OF THE CENTRAL ANDES.

Marine terraces of San Juan de Marcona are exceptional because they have a higher regional uplift rate than other areas on the west coast of South America. The average uplift rate for the west coast of South America is about 0.16 m kyr^{-1} (Freisleben *et al.*, 2021). However, the San Juan

de Marcona area has an uplift rate varying between 0.44 and 0.87 m kyr^{-1} , increasing over the last 800,000 years (Saillard *et al.*, 2011). Thus, this area holds an exceptional record of the tectonic history of the South American forearc associated with the subduction of the Nazca Ridge.

SITE 174

GEOLOGICAL PERIOD	Miocene to Pleistocene
LOCATION	Ica, Nazca, Peru 15°21'21"S 075°09'04"W
MAIN GEOLOGICAL INTEREST	Tectonics Geomorphology and active geological processes



Overview of the sequence of marine terraces at Cerro Tres Hermanas.

Geological Description

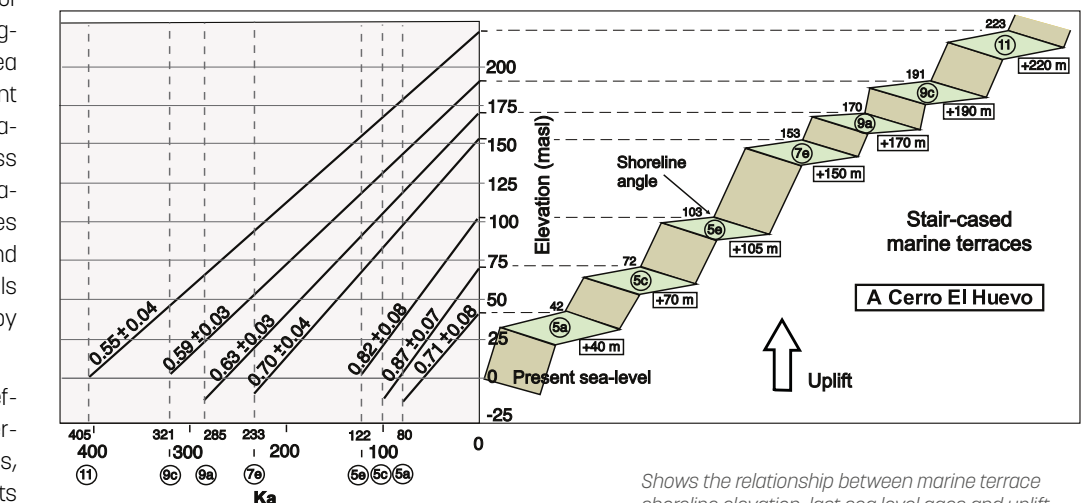
Bay of San Juan de Marcona is renowned for its extraordinary twin sequences of well-preserved marine terraces that exhibit 20 staircased levels. These terraces are spectacular witnesses of the complex interaction between past sea-level variations and tectonic uplift of the coast. Each level corresponds to a paleo-sea-level position, now emerged and preserved in the landscape. San Juan de Marcona is located on the southern coast of Peru above the subducted segment of the Nazca Ridge. The area is characterized by significant coastal tectonic activity and major normal faults cutting across the coastal region. The two famous sectors where the terraces develop are Cerro El Huevo and Cerro Tres Hermanas, forming hills and peninsulas, but separated by ~8 kilometers and the bay.

In recent decades, scientific efforts have been made to determine the ages of these terraces, leading to more reliable results using cosmogenic nuclides such

as ^{10}Be . For example, the terrace now at an elevation of 220 meters formed 400 ka ago. The ages and present-day elevations of the marine terraces are indicative of variable and cumulative uplift through time during the interseismic period. Coastal tectonics in the Central Andes reflect the interaction of crustal tectonics of the upper plate with the seismic cycle of the subduction interface.

Scientific research and tradition

Marine terraces of San Juan de Marcona are a natural laboratory for understanding tectonics at active margins. From geomorphological or climatic interpretations (Broggi, 1946) to the use of geochronology uplift rates were determined for the last 125 kyr (Hsu, 1988; Ortílieb and Macharé, 1990) and 800 kyr (Saillard *et al.*, 2011).



Shows the relationship between marine terrace shoreline elevation, last sea level ages and uplift rates in the San Juan de Marcona-Peru area.

MINERALOGY



Since the dawn of humanity, rocks and their constituent minerals have been for mankind a source of utility materials for tools and building as well as a source of wonder and curiosity through uncommon colours or the intriguing beauty of exquisite crystals. This made mineralogy one of the oldest disciplines of science, rooted in the expertise of the early smelters and alchemists long before the concept of crystallography arose.

The International Mineralogical Association (IMA) has officially recognized more than 6000 species of minerals, and mineralogists discover annually more than 100 new species. Beyond this diversity, minerals are also the fundamental units in geological processes controlling the dynamic evolution of the Earth. Recent advances in bio-mineralogy illustrate the role played by minerals in the emergence and evolution of life. Mineralogy is developing in several other directions including atomic-scale understanding using new tools such as advanced spectroscopies and ab initio numerical simulations, the stability of minerals under extreme conditions within the Earth and planets, and AI-supported machine learning of the big data on minerals to describe their diversity. Minerals are not only linked intimately to the development of our society, but also to threats to the global environment, biodiversity, and our health. At the same time, sample-return programs targeting other solar-system bodies open a new era of space exploration. These samples will lead to the discovering on new extraterrestrial minerals, which may uncover new phenomena and shed more light on the origin of the solar system and beyond.

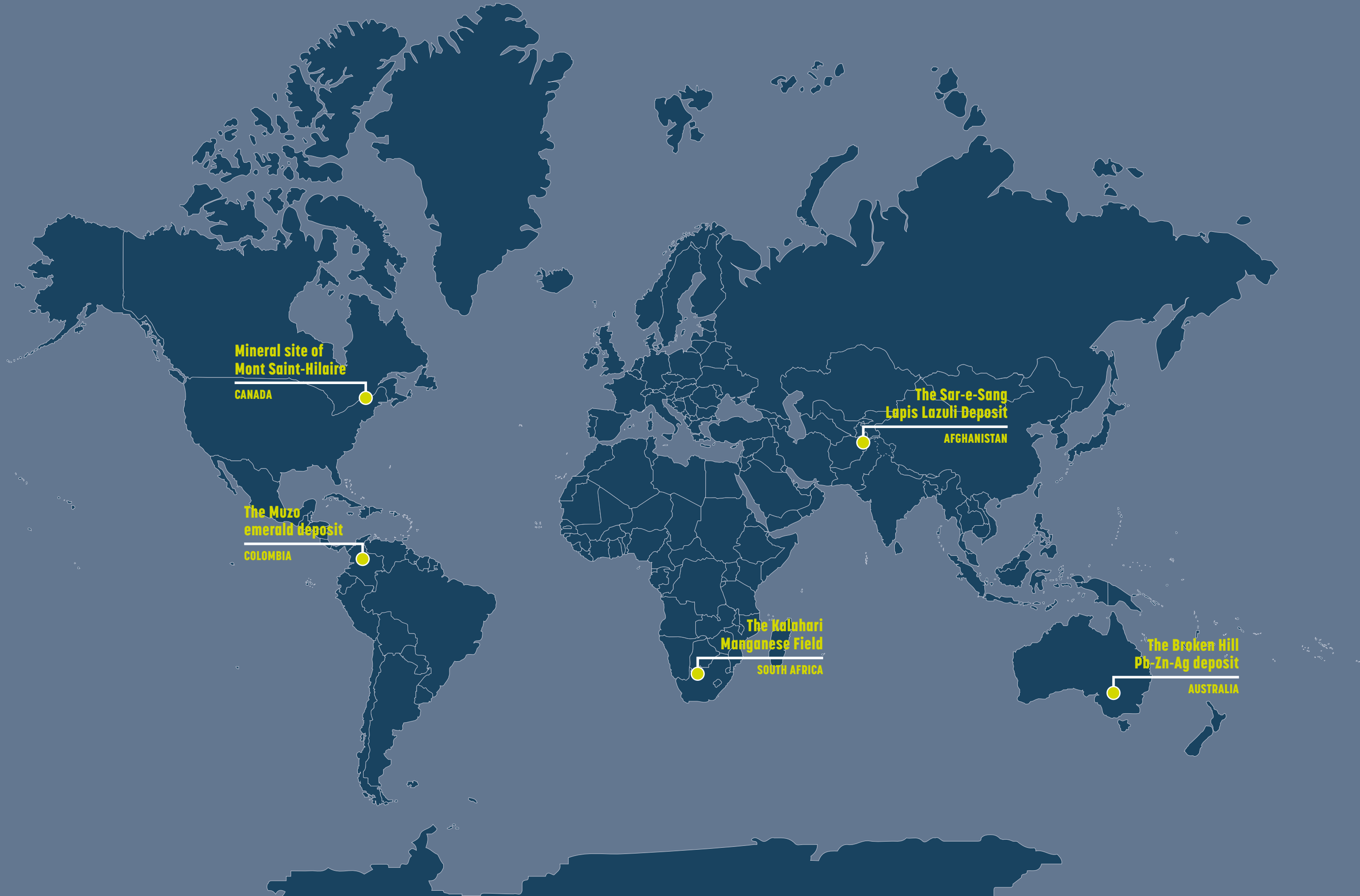
In this second 100 selection, five outstanding mineral deposits have been declared as IUGS Geological Heritage Sites; they perfectly illustrate the mineralogical duality of utility and curiosity-sparking beauty. These are (1) the Sar-e-Sang Lapis Lazuli Deposit in Afghanistan well known as the classical locality for Lapis Lazuli, which occupies a scientific key position between geoscience and archaeology, (2) the Kalahari Manganese Field in South Africa, which is the world largest land-based resource of manganese hosting rare, unique and world-renowned minerals, (3) the Broken Hill Pb-Zn-Ag deposit in Australia, well known as a 'mineralogical rainforest', having yielded 340 mineral species, 26 of which are types, (4) the mineral site of Mont Saint-Hilaire in Canada, which is the preeminent single-site mineral locality in the world with 445 mineral species and is well known for both the diversity of its minerals and the superb quality of its crystals, and (5) the Muzo emerald deposit in Colombia, famous since Precolumbian times, which yielded the finest gem emeralds on Earth and a case study for its hydrothermal-sedimentary genesis.

Eiji Ohtani

Tohoku University, Sendai, Japan.
President, International Mineralogical Association (IMA).
IUGS Geological Heritage Sites referee.

Christian Chopin

Ecole normale supérieure – CNRS, Paris, France.
Member of the IMA Advisory Committee.
IUGS Geological Heritage Sites referee.



THE SAR-E-SANG LAPIS LAZULI DEPOSIT

AFGHANISTAN



Afghanite crystals (12.5 x 7.5 centimeters; photo by H. Meyer).

ONE OF THE MOST CLASSICAL LOCALITIES OF LAPIS LAZULI ON EARTH THAT OCCUPIES A SCIENTIFIC KEY POSITION BETWEEN GEOSCIENCE AND ARCHAEOLOGY.

Lapis Lazuli and its related localities at Sar-e-Sang are of unique mineralogical interest, since this material represents the most spectacular occurrence on Earth. In addition, Lapis Lazuli plays a crucial role in Archaeology. It is known to be mined even in the Neolithic Period where it already became transported over long distances.

Lapis Lazuli was discovered as pieces of jewelry in graves dated between 7,000 and 5,000 B.C., the most stunning artefact, however, is the golden funerary mask of Tutankhamun that contains inlays of Lapis Lazuli from Sar-e-Sang and that was excavated by Howard Carter in 1925.

SITE 175

GEOLOGICAL PERIOD	Archean
LOCATION	Badakhshan, Afghanistan 36°12'36"N 070°47'36"E
MAIN GEOLOGICAL INTEREST	Mineralogy Igneous and Metamorphic petrology



Lazurite (left, crystal size 7 x 4.5 centimeters; photo by J. Wittig) and Lapis Lazuli (right, 23.5 x 13 centimeters; photo by H. Meyer).

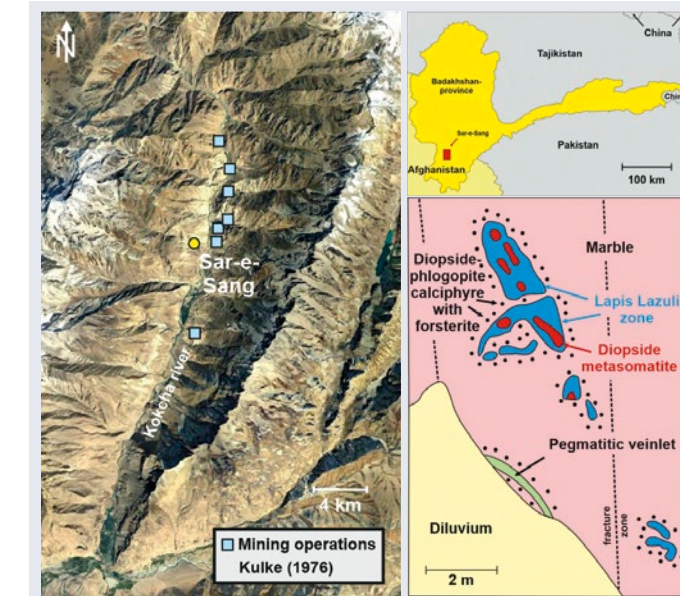
Geological Description

In the Hindu Kush Mountains, in the far northeast of Afghanistan, a mining district is located that has occupied mankind for more than about 10,000 years. This district comprises spectacular outcrops of lazurite, a mineral of the sodalite group that is the most important component of Lapis Lazuli. Commonly also pyrite and calcite are present. Lapis Lazuli forms up to 6 meter thick lens-like bodies and layers in calcite- and dolomite-marbles, associated with diopside skarn and forsterite-bearing calciphyre, which is essentially a Ca- and Mg-silicates-bearing marble skarn. The formation of Lapis Lazuli is interpreted to result from metasomatic reactions between granitoids and marble. A major contribution of evaporitic rocks is indicated by sequences of anhydrite and whiteschist (Schreyer and Abraham, 1976). A geological sketch map of a typical occurrence of Lapis Lazuli in such a setting is shown below (modified after Yurgenson and Sukharev, 2010). The major mines are located close to Sar-e-Sang at the east side of the Kokcha river. Stratigraphically the deposits belong to the Sakhi formation of the Archean Sanglich Group. The Sar-e-Sang area is well known for speci-

ular specimens of lazurite, haüyne, sodalite, phlogopite, richterite, marialite, diopside, dravite and even afghanite, some of which occur in gem quality.

Scientific research and tradition

The Lapis Lazuli mines of Sar-e-Sang belong to the oldest deposits on Earth. Although in our days novel provenance studies on related artefacts are widespread using for instance micro-PIXE, Raman- or FTIR-studies, the scientific processing goes even back to Pedanius Dioscorides and Pliny who lived in the 1st century.



Location of the Sar-e-Sang Lapis Lazuli deposits (Kulke, 1976) and geological sketch map of a typical occurrence (lower right, modified after Yurgenson and Sukharev, 2010).

THE KALAHARI MANGANESE FIELD

SOUTH AFRICA



Sunset in the Kalahari Manganese Field with the silhouette of the N'Chwaning manganese mine in the foreground.

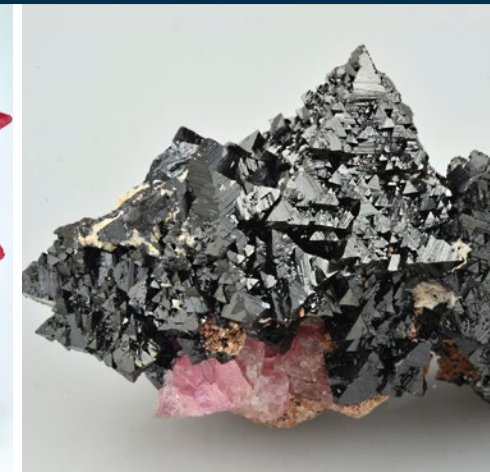
THE KALAHARI MANGANESE FIELD OF SOUTH AFRICA IS THE WORLD'S LARGEST LAND-BASED RESOURCE OF MANGANESE HOSTING RARE, UNIQUE AND WORLD-RENNED MINERALS.

The Kalahari Manganese Field is by far the largest land-based manganese deposit on Earth and the world's top producer of manganese metal tonnage. The Kalahari Manganese Field contains 182 valid minerals, including 28 type-locality species, several of which are unique to the deposit. In addition to its multifaceted mineralogy, this Palaeoproterozoic geological succession

is one of the best preserved that illustrates the deposition and depletion of iron and manganese from the ancient ocean waters, heralding the advent of free oxygen in the Earth's atmosphere. The complexity of the deposit, particularly the hydrothermally-altered ore, offers excellent opportunities for future mineralogical research.

SITE 176

GEOLOGICAL PERIOD	Paleoproterozoic
LOCATION	Northern Cape Province, South Africa, South Africa 27°12'07"S 022°58'13"E
MAIN GEOLOGICAL INTEREST	Mineralogy History of geosciences



Left: Rhodochrosite, 11.5 centimeters, became world famous after its discovery in the 1970s. Right: Crystals of hausmannite, 5.2 centimeters, one of the primary ore minerals.

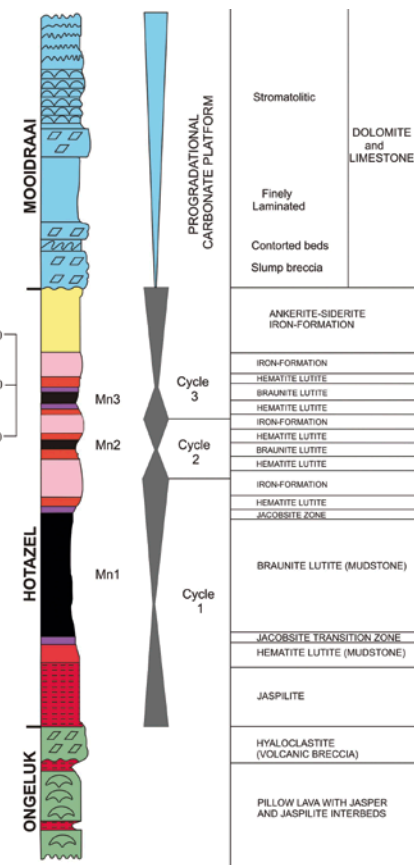
Geological Description

The Kalahari Manganese Field is located in the Northern Cape Province, South Africa. Mineralization consists primarily of manganese oxide minerals hosted in the Palaeoproterozoic ~2.2 billion-year old sedimentary Hotazel Formation of the Transvaal Supergroup, where three layers of manganese ore are intercalated with banded-iron formations and carbonates. Throughout its geological history, the Kalahari manganese field has undergone multiple episodes of uplift, deformation, folding, thrusting and hydrothermal and supergene alteration. (Tsikos *et al.*, 2003; Cairncross and Beukes, 2013). Two main ore types are present: 1) low-grade (~38 %Mn) primary sedimentary Mamatwan-type ore and 2) a billion years younger, high-grade (~45 %Mn) Wessels-type ore (Gutzmer and Beukes, 1995). The original, primary ore accounts for virtually all the manganese resources, yet the later Wessels-event produced the bulk of the world-famous rare and exotic minerals for which the Kalahari Manganese field is famous (Gutzmer and Beukes, 1996). The Wessels mine has produced half of the 28 type-species, including vonbezingite, effenbergerite, poldervaartite,

and wesselite all of which remain unique to the locality. The largest and finest aesthetic crystals of sturmanite, mozartite, ettringite and thaumasite known come from the Kalahari deposit, and the region's rhodochrosite crystals grace mineral collections around the world.

Scientific research and tradition

The area was first mapped in 1874 by G.W. Stow. De Villiers (1960) published the first memoir, and world-famous rhodochrosite was discovered in 1963. In 1983, sturmanite was described as one of the first type-species. Kleyenstüber (1984) documented the mineralogy. Most recent mineral discoveries in 2021 are hydroxymcglassonite and yuzuxiangite.



THE BROKEN HILL PB-ZN-AG DEPOSIT AUSTRALIA



Crystals of ferrorhodonite-rhodonite (red) to 1 centimeter with spessartine (brownish red) and fluorapatite (green) in galena. North Mine. Private collection. F. Coffa photograph.

**A 'MINERALOGICAL
RAINFOREST', HAVING YIELDED
340 MINERAL SPECIES, 26 OF
WHICH ARE TYPES.**

Since Charles Rasp pegged its gossanous outcrop in 1883, Broken Hill has yielded an array of both beautiful and rare minerals (Birch, 1999), reflecting the primary ore's diverse chemistry, metamorphic history and exposure to weathering. Broken Hill minerals have been assembled by museums and private collectors worldwide. Renewed opencut mining during 1980s

and 1990s produced over 100 previously unrecognised species (Birch and van der Heyden, 1997). Overall, some 340 distinct minerals have been recognised and 26 have Broken Hill as their type locality (e.g. Elliott, 2021). Even today, new species can be discovered in old collections (e.g. Shchepalkina *et al.*, 2017).

SITE 177

GEOLOGICAL PERIOD	Paleoproterozoic to Mesoproterozoic
LOCATION	Yancowinna County, New South Wales, Australia 31°57'00"S 141°28'00"E
MAIN GEOLOGICAL INTEREST	Mineralogy Igneous and Metamorphic petrology



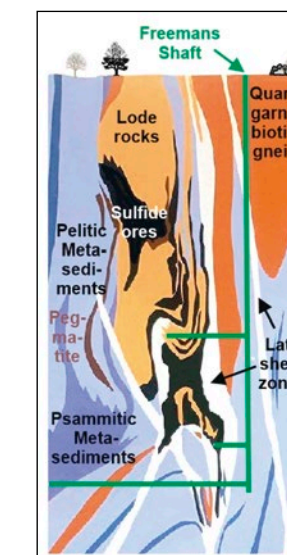
Manganese hedenbergite <3 centimeter (left; North Mine, private collection) and raspite (<4 millimeters) with black mottramite (Proprietary Mine; Museums Victoria collection). F. Coffa photographs.

Geological Description

The massive Broken Hill Pb-Zn-Ag deposit consists of nine separate stratabound sulfide lenses enclosed within strongly deformed and metamorphosed pelitic schists and gneisses. The ore lenses are now considered to have a syngenetic exhalative origin, representing periodic outpouring of hot metal-bearing fluids in a sea-floor setting in which pelitic and psammitic sediments were deposited. The entire sequence belongs to the Willyama Supergroup, dated at around 1700 million years (Stevens *et al.*, 2008). Peak metamorphism reached granulite facies conditions of 750-800 °C and 5-6 kilobar. It was during this episode that the sulfide lenses underwent partial melting and remobilisation, followed by recrystallisation into the characteristic assemblage of coarse-grained galena-sphalerite-manganese silicates (Frost *et al.*, 2005). There were later phases of intrusion and faulting, which had localised effects on the ore lenses. The structural geology of that part of the sequence where mining has taken place is extremely complex and has generated considerable discussion. Several generations of folding are present, at least one involving overturning of the ore lens se-

quence. Longitudinally, the shape of the orebody resembles a boomerang up to 8 kilometers long and 850 meters thick. Eventually the orebody was exposed as a ragged black gossanous ridge, giving rise to its name.

Simplified cross section near the southern end of the deposit, showing complex folding of the ore lenses and enclosing formations (900 meters vertically).



Scientific research and tradition

Broken Hill truly ranks as one of the world's great 'mineralogical rainforests'. Since its discovery, Broken Hill has provided professional mineralogists worldwide with an array of rare species to characterise. Recently, many have been discovered by private mineral collectors. Museums worldwide have assembled representative collections for both display and research.



MINERAL SITE OF MONT SAINT-HILAIRE CANADA



**WITH 445 MINERAL SPECIES,
IT IS THE PREEMINENT,
SINGLE-SITE MINERAL
LOCALITY IN THE WORLD.**

With 445 known species, Mont Saint-Hilaire has become renowned throughout the world for both the diversity of its minerals and the superb quality of its crystals. Mineral specimens from here are to be found in most major collections worldwide, both public and private. Currently, of the 445 known species, 73 were originally

described from this locality. Of those 73, 35 have not been found elsewhere. Mont Saint-Hilaire has had a profound effect on the study of alkaline rocks through hundreds of scientific papers describing the mineralogy of the locality and those elucidating its origins (Horváth *et al.*, 2019).

SITE 178

GEOLOGICAL PERIOD	Cretaceous
LOCATION	Québec, Canada 45°33'02"N 073°09'20"W
MAIN GEOLOGICAL INTEREST	Mineralogy Igneous and Metamorphic petrology



Mont Saint-Hilaire with the former Poudrette Quarry in 2002. This is the main source of mineral discoveries. Photograph courtesy R. Poudrette, Inc.

Geological Description

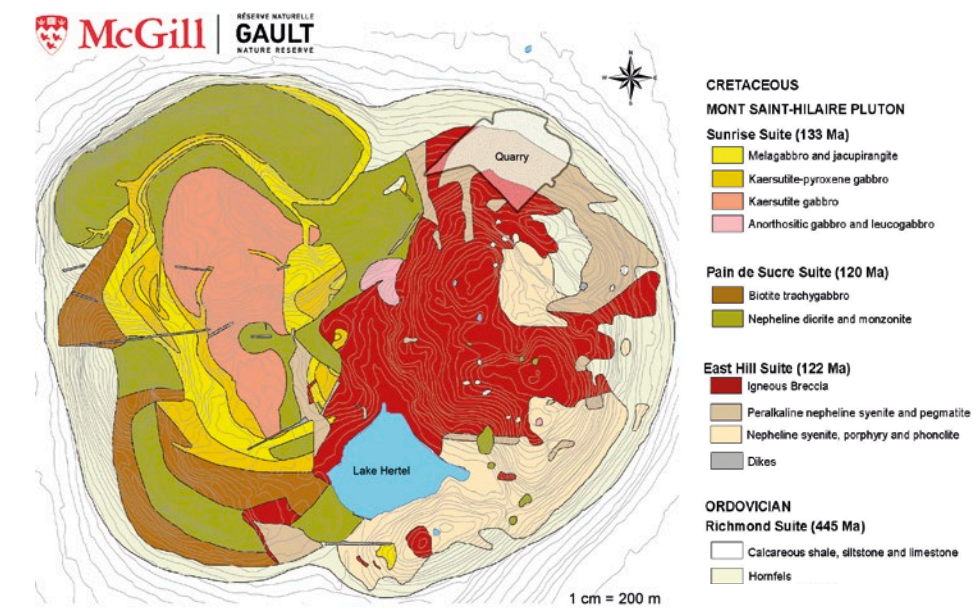
Mont Saint-Hilaire is a monadnock, 415 meters high and approximately 3 kilometers in diameter, lying 40 kilometers east of Montréal, Québec. It is one of 11 members of the Montréal Hills Petrographic Province, a series of related alkaline igneous complexes forming an east-southeast-trending belt, approximately 260 kilometers long (Feininger and Goodacre, 1995). They range in composition from carbonatite in the west to silica-saturated rocks in the east, and Mont Saint-Hilaire has the strongest expression of alkalinity. Their origins are postulated by some to be related to a mantle hot spot, which introduced a large volume of magma into a crustal fracture system (Foland *et al.*, 1986). Mont Saint-Hilaire intruded sedimentary Ordovician limestones and shales of the St. Lawrence Lowlands approximately at 125 Ma (Currie *et al.*, 1986). Quarrying operations have exposed many interesting features of the intrusion some of which are still preserved in the walls of the quarry, such as large hornfels and marble xenoliths and associated pegmatites and igneous breccias. The superb crystals and rare species for which Mont Saint-Hilaire is famous are found

in the millimetre to metre size cavities in the various rock types, particularly in the alkaline pegmatites.

Geological map of Mont Saint-Hilaire. Adapted from Currie (1989) by David Maneli of the Gault Nature Preserve, McGill University.

Scientific research and tradition

Minor reports in the scientific literature of Mont Saint-Hilaire date back to 1859, but it was not until the intrusion was exposed by quarrying, beginning in 1961, that more extensive mineralogical investigations were begun. Mineralogical research has continued unabated and at a furious rate until the present day.



THE MUZO EMERALD DEPOSIT

COLOMBIA



Emerald and pyrite (7 x 10.5 centimeters; coll. N. & J.-P. Voilhes). Photo: L.-D. Bayle.

**UNIQUE FOR ITS
HYDROTHERMAL-SEDIMENTARY
GENESIS THIS SITE IS KNOWN
SINCE PRECOLOMBIAN TIMES
AND YIELDED THE FINEST GEM
EMERALDS ON EARTH.**

The historical Muzo mines are the traditional source of the world's finest and largest green-coloured gem emeralds, including the famed trapiche crystals and parisite-(Ce), found exclusively in the black shales of the lower Cretaceous series from the Eastern Cordillera basin. The deposit, still actively worked, is characterized by compressive structures formed during the Paleogene.

Breccias and veins are infilled by carbonates and pyrite with accessory minerals such as emerald. The proposed hydrothermal-sedimentary model involves at 300°C the generation of brines through dissolution of evaporites by hot basinal waters that leached Be but also Cr and V from the black shales.

SITE 179

GEOLOGICAL PERIOD	Paleogene
LOCATION	Muzo, Colombia 05°32'22"N 074°08'43"W
MAIN GEOLOGICAL INTEREST	Mineralogy History of geosciences

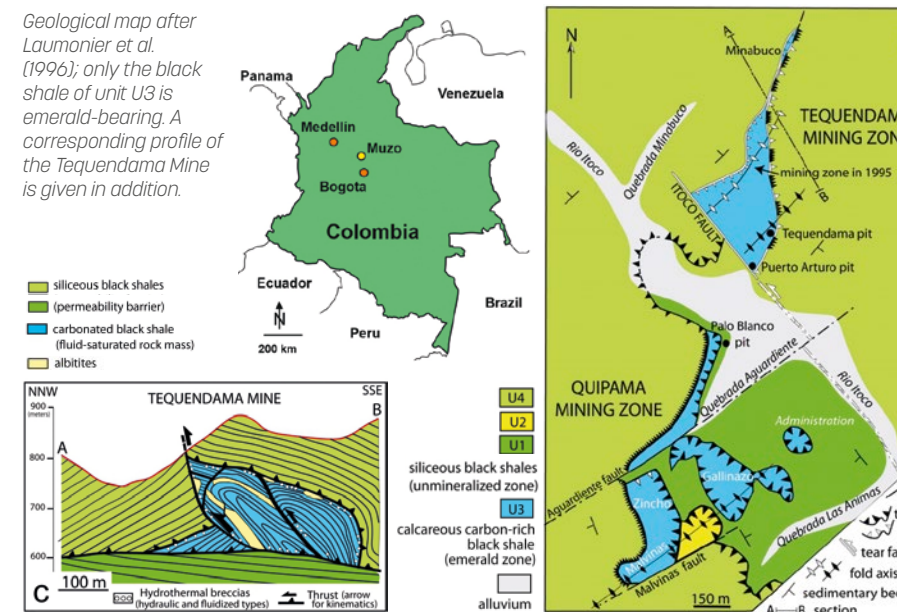


The Quipama mining zone, a highly productive zone in the 1990s, hosting several mining sites such as Cincho, Las Malvinas, Gallinazo, Aguardiente. Photo D. Schwarz.

Geological Description

The Muzo emerald deposits are located on the western flank of the Eastern Cordillera basin, 100 kilometers north of Bogotá. Emerald occurs in black shales intercalated with dolomitic limestones of Valanginian-Hauterivian age, the Rosablanca and Paja Formations. The deposits are linked by tear faults and as-

sociated thrusts formed during a Paleogene compressive phase; contemporaneously, circulation of hydrothermal fluids and emerald deposition occurred. All the tectonic contacts are marked by hydrothermal breccias, emerald-bearing banded carbonate veins and dykes, en-echelon sigmoidal tension gashes and drag folds indicating shearing in the roof of the breccia zones (Branquet *et al.*, 1999). The veins are filled by calcite, dolomite and pyrite with accessory quartz, barite, fluorite, bitumen, Cr-muscovite, emerald and parisite-(Ce). The Muzo deposits are famous also for trapiche gem emerald disseminated in black shales (Pignatelli *et al.*, 2015). Detailed geological and geochemical studies have led to a genetic model based on a hydrothermal-sedimentary origin. Key aspects of formation involve hot brines due to interaction of fluids with evaporites, resulting in intense albitionization, carbonatization, and pyritization of black shales, and coeval leaching of Be, Cr and V necessary for emerald formation. The thermochemical reduction of sulphates led to precipitation of pyrite, calcite, dolomite, bitumen and finally emerald.



Scientific research and tradition

Emerald mines of Muzo were exploited since Precolombian times and rediscovered in the 16th century by Spaniards (Giuliani *et al.*, 2022). Early scientific works refer to the discovery of parisite by Paris (1828-48) and the construction of the first geological maps (e.g., Pogue, 1916). Today a hydrothermal sedimentary model for the genesis of emerald is accepted (Ottaway *et al.*, 1994).

8

GEOMORPHOLOGY AND ACTIVE GEOLOGICAL PROCESSES

SITE 180 - SITE 196



Geomorphology is a branch of Earth sciences that deals with the most visible manifestations of processes that shape our planet – landforms and landscapes. Landforms are all around us, ranging from nearly featureless plains to high mountains. Although some can be produced almost instantaneously, during catastrophic events, others are the outcome of surface evolution lasting for millions of years. Therefore, landforms and landscapes, as rocks and fossils, are the testament of the history of the Earth and an inseparable component of global geoheritage. Moreover, they often record those periods in this history, for which the rock record is sparse. This is because many landscapes are predominantly erosional in nature and illustrate the power of destruction rather than creation.

Landforms and landscapes, as part of global biodiversity, have many values. Through deciphering processes that were shaping them in the past and looking at processes that mould them now, we get a better understanding of how and why the surface of the Earth changes. This knowledge is indispensable to correctly interpret past environments. The phrase “the present is the key to the past” – clearly one of the foundation stones of Earth sciences – is particularly applicable to geomorphology. But along with scientific values come educational and simply aesthetic values. The latter are by no means less important. Not only are they resources used by tourism industry, but they may also generate more serious interest in geosciences, as people are curious by their nature.

The second volume of IUGS Geological Heritage Sites includes 17 localities in the category of “Geomorphology and Active Geological Processes” from the Americas, Europe and Asia. Thematically, they mostly represent karst and geomorphological evidence of cold climates. Landform development by predominant rock dissolution is long known to produce astounding sceneries. Here they are illustrated by the famous tower and cone karst around Guilin in southern China – one of the globally most recognized karst terrains, partly submerged karst towers from Vietnam, and the unique mountainous landscape in Jamaica characterized by closed depressions surrounded by conical hills referred to as cockpit karst. All three developed in limestone, but perhaps even more intriguing is karst developed in quartzites of Gran Sabana in Venezuela. Quartzites were long regarded as least soluble rocks, and talking about karst in these regions was like a heresy. Progress in scientific understanding made it clear that rock dissolution is also very important for silicate rocks, and Gran Sabana is the cradle of this research. Underground karst, present in all above-mentioned localities, is specifically highlighted by the Mammoth Cave in USA – the longest known cave system in the world. Karst is also famous for its spectacular springs, and three of them from Bosnia and Herzegovina, France, and the United States are included. Research at these localities has revealed the astonishing complexity of karst hydrogeological systems.

Cold-climate landforms are different. The Mackenzie Delta in Canada is famous for the interactions between fluvial processes, marine processes, and permafrost. It is the global type locality for strange pingo hills. Ongoing dynamics of landscapes shaped by glaciers is excellently illustrated by two sister localities from Svalbard in Norway and by the Vatnajökull glacier in Iceland, the latter also showing interactions with volcanic processes. Other sites show impressive landform legacies of the ice ages. These are fjords of the South Island of New Zealand, the archetypal glacial trough of Yosemite Valley in the formerly glaciated part of Sierra Nevada, USA, and the upland of Dartmoor in Great Britain, which hosts textbook examples of periglacial landforms. The latter two have one more characteristic in common – granite as a landscape-supporting rock. Granites produce many spectacular landforms, such as domes and tors, and these are here perfectly illustrated. Finally, the selection includes landforms developed due to long-term landform evolution of old volcanic terrains, on the example from Hungary, one of the most famous salt flats in the world – the Great Salt Lake, USA, and last but not least, globally significant Getbol tidal flats from the Republic of Korea.

Piotr Migoń

University of Wroclaw, Poland.
IAG – International Association of
Geomorphologists.
IUGS Geological Heritage Sites referee.

David Kreamer

Department of Geosciences, UNLV – University
of Nevada Las Vegas, USA.
President, IAH – International Association of
Hydrogeologists.
IUGS Geological Heritage Sites referee.



GRANITE LANDFORMS OF DARTMOOR

UNITED KINGDOM



Haytor is among the most spectacular granite tors in Dartmoor. (By Nifanion - Own work, CC BY-SA 3.0, <https://commons.wikimedia.org/w/index.php?curid=28339418>).

EMBLEMATIC GRANITE LANDFORMS AND THE GLOBAL REFERENCE SITE FOR STUDIES OF GRANITE WEATHERING AND PLEISTOCENE COLD-CLIMATE LANDFORMS.

Dartmoor is a benchmark site for studies of the evolution of granite landforms and periglaciational uplands (Gunnell, 2020). The paper by Linton (1955), in which two-stage model of tor development was elaborated, became a major reference work in geomorphology. It inspired subsequent work on the origin of domes, inselbergs, and basins

in the tropics and high latitudes. Periglaciational landforms and deposits are particularly well-developed due to protracted evolution in cold environments (Eden and Green, 1971; Gerrard, 1988). Recent pioneering work using cosmogenic isotopes helped to constrain the ages of tors, opening new avenues of research (Gunnell *et al.*, 2013).

SITE 180

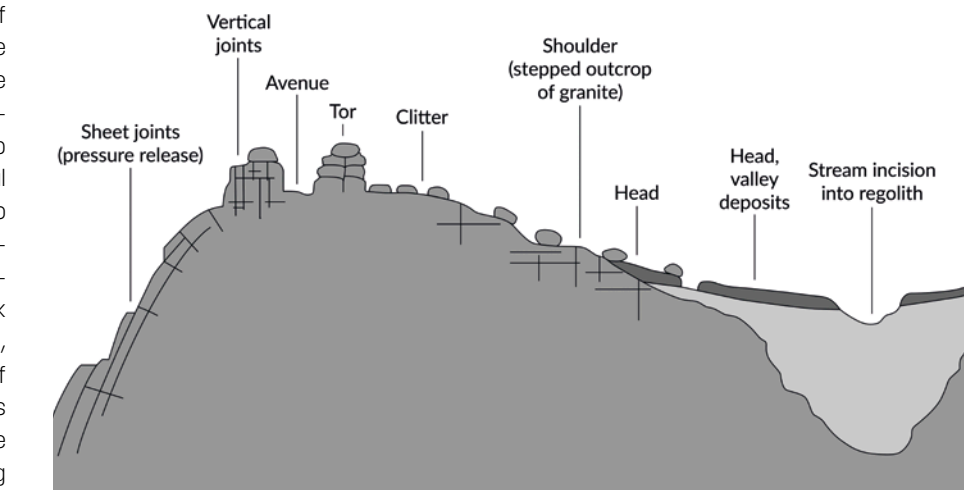
GEOLOGICAL PERIOD	Neogene to Pleistocene
LOCATION	Devon/England, United Kingdom 50°34'18"N 003°54'55"W
MAIN GEOLOGICAL INTEREST	Geomorphology and active geological processes Igneous and Metamorphic petrology



The rolling upland surface of Dartmoor with numerous granite tors and exposed boulders.

Geological Description

Dartmoor is a largely bare upland underlain predominantly by granite of Carboniferous age, intruded into metamorphic rocks. It is renowned for diverse rock landforms shaped by weathering and denudation (Linton, 1955; Gunnell and Jarman, 2020). The most evident and scenic are tors – castellated, tabular or dome-like outcrops of granite, some more than 20 m high, distinctively rising above smooth upland surfaces as recognizable landmarks. Diverse shapes of tors show how jointing patterns influence the evolution of landforms by controlling the progress of weathering. Many tors are products of two-stage process. A phase of deep selective weathering is followed by removal of regolith by gravity processes - a scenario later shown to be globally applicable. Dartmoor also hosts distinctive landforms inherited from the Pleistocene, including block fields and block streams, frost-riven cliffs, cryoplanation terraces, and a variety of hillslope deposits. The most elevated parts of Dartmoor may have had an ice cap in the Pleistocene. Products of granite weathering include famous kaolinite-rich mantles (China clay), which were subject to mining. There



Diversity of granite landforms and surface deposits in relation to jointing and topography, after Gunnell and Jarman (2020).

Scientific research and tradition

were also important tin deposits exploited since prehistoric times. The central part of Dartmoor selected as a geoheritage site represents extraordinary geodiversity, and many tors have attached cultural significance.

Various lines of geomorphological research were pursued in Dartmoor since the 19th century (Gunnell, 2020). They were focused on interrelated themes of granite weathering in changing climates, evolution of granite erosional relief, impact of cold-climate conditions on slope development, evidence of glaciation, and human-induced environmental change since antiquity.

INVERTED LANDSCAPE OF A PLIO-PLEISTOCENE PHREATOMAGMATIC MONOGENETIC VOLCANIC FIELD IN THE BAKONY-BALATON UPLAND HUNGARY



UNESCO Global Geopark

Basaltic mesas in the Tapolca Basin representing preserved proximal part of former maar-diatreme volcanoes. Lake Balaton is in the background. Photo by: Norbert Mészáros.

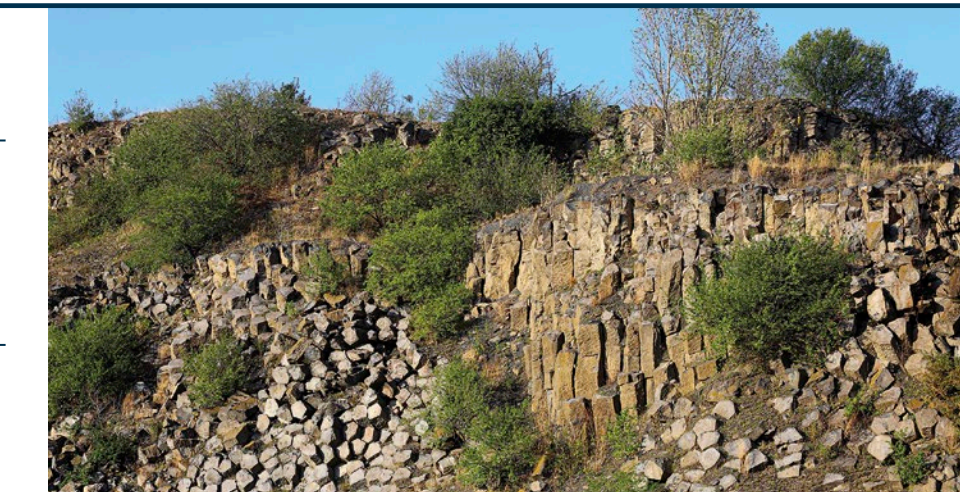
ONE OF THE BEST EXAMPLES ON EARTH OF COMPLETELY INVERTED RELIEF OF A HIGH VENT-DENSITY PHREATOMAGMATIC MONOGENETIC VOLCANIC FIELD.

Inverted landscapes are common features on Earth, but those composed of closely spaced phreatomagmatic volcanoes once filled with lava are rare. The Tapolca Basin has a visually attractive and geologically unique landscape produced by advanced geomorphic inversions on Earth (Wijbrans

et al., 2007; Kereszturi and Németh, 2012). Following volcanism, ideal climatic conditions for erosion to act and a unique geological setting that is dominated by the presence of hard basement rocks covered by erodible fluvio-lacustrine successions led to a dramatic inverted landscape.

SITE 181

GEOLOGICAL PERIOD	Pliocene to Pleistocene
LOCATION	Bakony–Balaton Region, Western Hungary, Hungary 46°50'38"N 017°27'07"E
MAIN GEOLOGICAL INTEREST	Geomorphology and active geological processes Volcanology



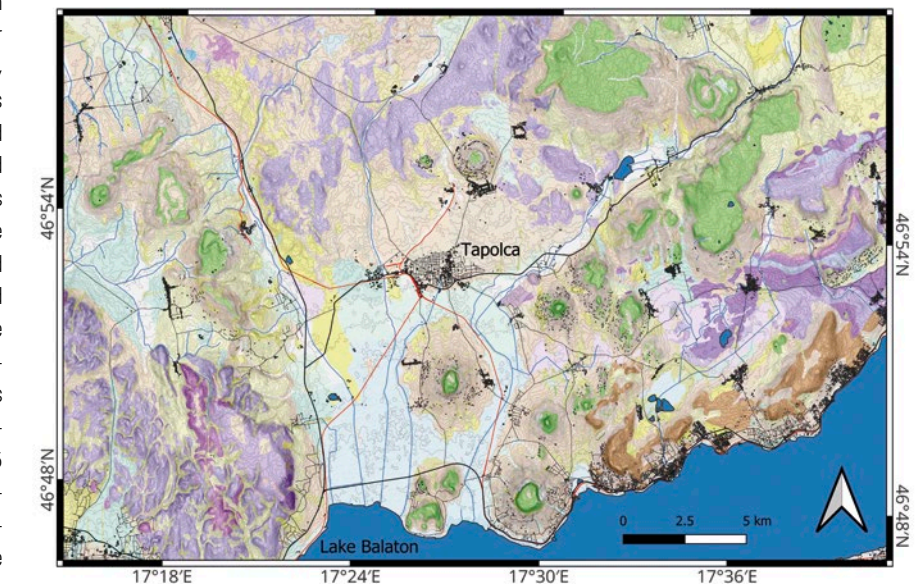
Columnar jointed basalt of the former lava lake within the Zalahaláp maar-diatreme craters demonstrates complex cooling history of lava. Photo by: Barnabás Korbél.

Geological Description

Tapolca Basin is the core of the Mio-Pleistocene Bakony–Balaton Uplands monogenetic volcanic field. In this area volcanic erosion remnants are closely spaced, and significant erosion produced a globally unique, aesthetically attractive inverted landscape (Németh and Martin, 1999). The preserved volcanic successions provide ample evidences that the volcanism was driven primarily by explosive magma and external water interaction to form volcanic landforms such as maar and tuff ring volcanoes (Martin and Németh, 2007; Kereszturi et al., 2011). These volcanoes have broad and deep craters that operated as sediment traps or more frequently hosted scoria cones, lava flows and in some cases lava lakes locked within the crater walls. The differential erosion relatively quickly removed the tephra rings around the wide craters and carved into the pre-volcanic fluvio-lacustrine sand, silt and mud layers leaving behind basalt lava and agglutinated scoria successions as hill tops. The volcanoes of the Tapolca Basin represent a volcanic flare-up between 4.5 and 3 millions of years ago. Erosion made typical volcanic buttes marking a geomorphological level similar to the paleosurface these

volcanoes erupted on. World-class examples of columnar jointed basalt, peperite and diatreme-filling pyroclastic rocks complete the geological wonders of this region.

1 to 100,000 scale geological map [<https://map.mbfesz.gov.hu/fdt100/>] of the vicinity of the Tapolca Basin on SRTM30 shaded relief map. Quaternary - grey/beige; Neogene volcanics - green; Pliocene fluvio-lacustrine deposits - yellow; Mesozoic - blue/purple; Paleozoic - brown.



Scientific research and tradition

Over 150 years of research made this region a type locality of landscape evolution studies and provided for internationally significant research (Martin and Németh, 2004). Basalt petrogenesis, monogenetic volcanism and volcanic geology aspects of maar-diatreme volcanism among the core subjects made this region an iconic locality of monogenetic volcanism research.

GREAT SALT LAKE

UNITED STATES OF AMERICA



Multiple horizontal Pleistocene Lake Bonneville shorelines at the north end of Antelope Island. Image: M. Chan.

THE LARGEST SALTWATER LAKE IN THE WESTERN HEMISPHERE CONTROLLED BY BASIN TECTONICS AND ISOSTASY AND RECORDING PLEISTOCENE CLIMATE CHANGE.

Well-dated shorelines provide a precise lake hydrograph unparalleled value linked to Pleistocene climate change (Oviatt and Schroder, 2016). These landscapes are an open space asset with historical significance in the exploration of the west (Chan *et al.*, 2024). Here, the methodology of multiple working hypotheses was worked

out and the concept of isostasy was first formulated (Gilbert, 1886, 1890). Even correlative shoreline elevations may vary due to the complex interplay of isostasy and basin tectonics. Great Salt Lake oolitic sand and microbialites at the north end of Antelope Island are fundamental examples of modern carbonate sedimentation.

GEOLOGICAL PERIOD	Pleistocene to Holocene
LOCATION	Antelope Island State Park, United States of America 41°03'00"N 112°15'51"W
MAIN GEOLOGICAL INTEREST	Geomorphology and active geological processes Stratigraphy and sedimentology

SITE 182



Distinctive microbialites (foreground) and polygonal features visible in oblique aerial view of Great Salt Lake at north end of Antelope Island. Image: B. Baxter.

Geological Description

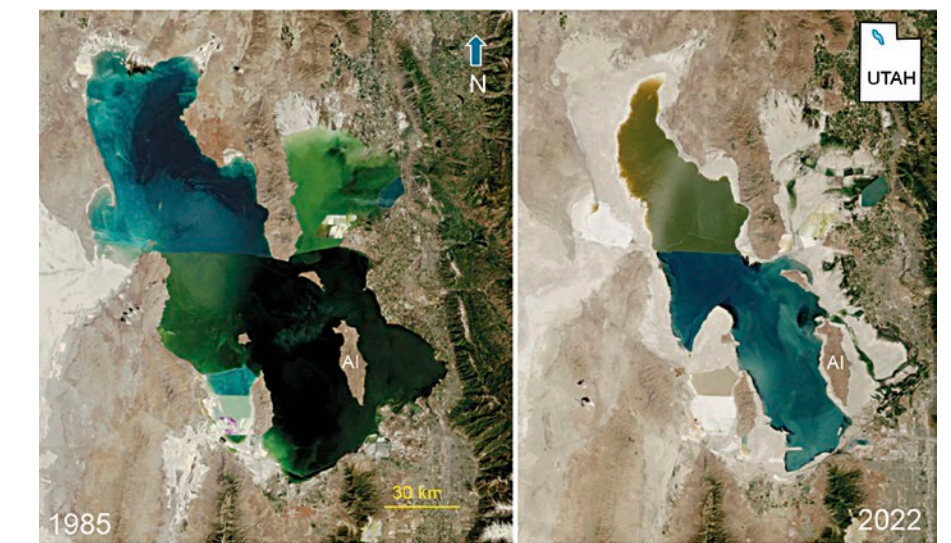
The Lake Bonneville shorelines are evidence of an extensive Pleistocene freshwater lake in the Basin and Range province in western Utah. The Bonneville shoreline expressions are vanishing due to urbanization. Antelope Island State Park hosts pristine records of these ancient shorelines. America's renowned geologist, G.K. Gilbert, deduced that valley floors were once covered by water, and isolated mountain ranges were islands. Gilbert used this area to propose the idea of isostasy (equilibrium adjustments of Earth's crust) because individual shorelines vary in elevation; highest elevations occur where the lake was deepest. This work was the case example for illustrating the methodology of multiple working hypotheses to overcome bias in human reasoning.

Drying of Lake Bonneville left the Great Salt Lake (Gwynn, 2022). This is the largest saline lake in the Western Hemisphere, and hosts an extreme ecosystem. Distinctive ooids, microbialites, and evaporite minerals (e.g., halite, mirabilite) of this modern lake have implications for astrobiology and understanding life in extreme environments. The dynamic responses to climate change are preserved

Scientific research and tradition

in the sedimentary records of the lake deposits. The surprising biodiversity and geo-diversity of the Great Salt Lake make this a remarkable jewel of the desert.

At Antelope Island, visitors can experience Great Salt Lake and see evidence of Pleistocene Lake Bonneville. Exemplary landforms have been classic localities for over a century in an amazing outdoor laboratory. Across the Bonneville basin, numerous geologic studies have and will continue to follow in G.K. Gilbert's footsteps.



Great Salt Lake high in 1985; low in 2022. AI = Antelope Island. Differences in salinity and microbes cause different water colors. Landsat images: NASA.

MACKENZIE DELTA

CANADA



The Mackenzie Delta is the most spectacular scenery in the Arctic. Dark green: delta, light green: uplands, beige: suspended sediments in channels, grey: lakes.

COMPLEX COASTAL LANDFORMS OF DIVERSE ORIGIN: GLACIAL, PERMAFROST, FLUVIAL, AND PSEUDOKARST IN THE NORTH-WEST CANADIAN ARCTIC.

The Mackenzie Delta (13,000 km²; the second largest Arctic delta) is the best example of a complex landscape combining forms of different origins from post-glacial rocky islands through permafrost-related landforms such as polygons and pingos to contemporary pseudokarst lakes, slumps and numerous migrating channels carrying huge bedloads and suspended sediment

(Carson *et al.*, 1998; Burn, 2010, 2017). Sedimentation rates over much of the outer delta are less than the rate of subsidence associated with sea-level rise. Permafrost is ubiquitous and the surrounding landscape testifies to the enormous forces that can be unleashed by seasonal freezing and thawing of the ground.

SITE 183

GEOLOGICAL PERIOD	Quaternary
LOCATION	Interior Plains, Northwest Territories, Canada 68°43'01"N 132°39'45"W
MAIN GEOLOGICAL INTEREST	Geomorphology and active geological processes



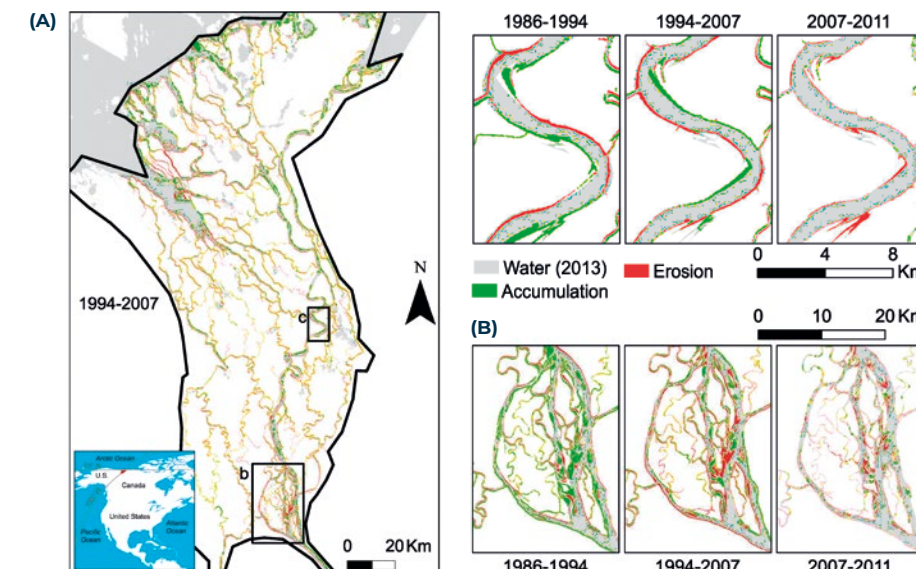
Pingo on Richards Island, Mackenzie Delta area, western Arctic Canada. Courtesy of Christopher Burn

Geological Description

The maximum extent of the Laurentide Ice Sheet in the Mackenzie Delta area was 30,000 years ago. The vast delta, with its branching channels, ponds and wetlands, covers more than 13,000 km² of alluvial coastal plain. The delta stretches nearly 210 kilometers from north to south and is 50 to 80

kilometers wide. Below Fort McPherson, the Mackenzie River divides into several major channels and hundreds of smaller tributaries, the largest of which flows north-north-east and empties into the Beaufort Sea west of Tuktoyaktuk. The Mackenzie Delta is a labyrinth of shifting channels and pseudokarst

lakes. Most of the land in the delta is permafrost. Bedrock is at great depth, and patches or taliks of unfrozen ground are controlled by shifting channels. Retrogressive thaw slumps, up to 200 meters wide, are common where ground ice is exposed by bank erosion. Rivers and lakes are ice-covered for more than half the year. The Mackenzie River carries a large load of sediment, transporting about 128 million tonnes to its delta each year. A characteristic feature of the delta are the numerous pingos (1400, the largest population in the world). They are conical, ice-cored, 50 meters high, and >100 meters in diameter at the base.



Complex accumulation-erosion patterns across the delta plain (a), in an anastomosing channel (b), and in the development of meander bends (c) (Vesakoski *et al.*, 2017).

Scientific research and tradition

The Mackenzie Delta is the best-studied of the polar regions. Especially the research and field experiments of J. R. Mackay (1998) have contributed to the understanding of permafrost phenomena. The Mackenzie Delta is the most spectacular geoecological landscape in the Arctic, which is nourished by the annual flooding of the Mackenzie River.

GETBOL TIDAL FLATS

SOUTH KOREA



UNESCO World Heritage Site

UNESCO Global Geopark

THE MOST COMPLEX TIDAL FLATS FORMED BY DYNAMIC PAST AND ONGOING SEDIMENTOLOGICAL PROCESSES DURING THE HOLOCENE.

A complex sedimentary system combined with the strong Asian monsoon climate provides a variety of tidal flat sedimentary environments characterized by an extremely high and complex geodiversity. At the same time, the system has maintained a sustained sedimentation equilibrium, resulting in one of the world's thickest Holo-

cene intertidal mud deposits as a result of sea-level rise since the Last Glacial Maximum. Together with the unique sedimentary features (chenier and sand stringer) produced by typhoon, the Korean Getbol displays the most complex and highly dynamic ongoing coastal processes and resultant coastal landforms in the world.

SITE 184

GEOLOGICAL PERIOD	Holocene
LOCATION	Western and southern coast of the Korean Peninsula, South Korea 34°49'44"N 126°06'16"E
MAIN GEOLOGICAL INTEREST	Geomorphology and active geological processes Stratigraphy and sedimentology



Multi-swash bars and spits connected to islands in Seocheon Getbol.

Geological Description

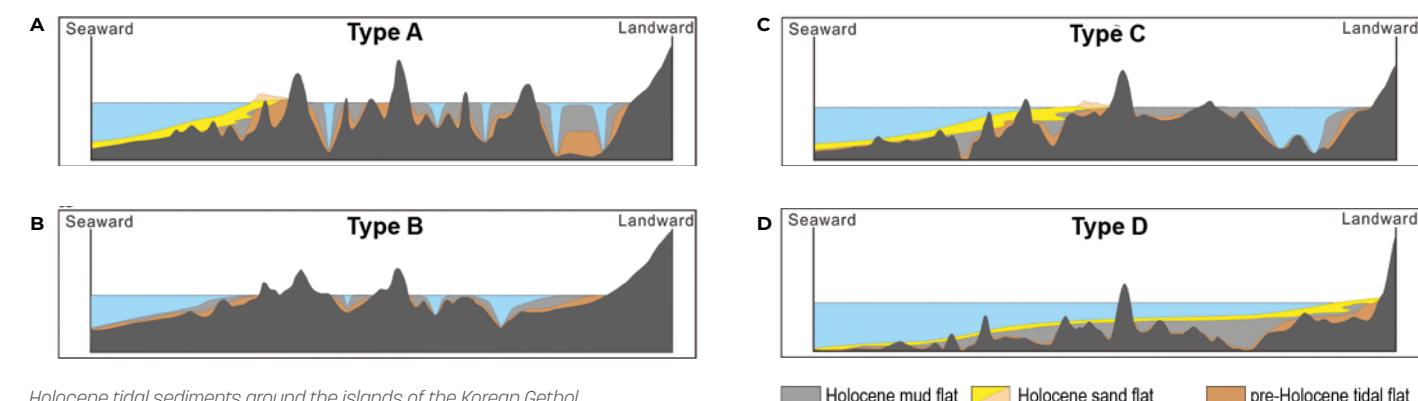
Due to the highly dynamic and complex combination of geological, oceanographic, and climatic conditions, the area is characterized by extremely dynamic past and ongoing sedimentary processes, thus representing one of the most intricate and diverse sedimentary systems in the world. Korean Getbol is a natural, stable and sustainable region and encompasses all geological, geomorphic, and ecological characteristics and ongoing tidal processes, which are a rarity in the world. Thousands of islands are scattered around a vast area adjacent to

the land. Rapid macrotidal currents flow between these islands through tidal channels that are narrow or wide, short or long, shallow or deep, changing their direction every six hours. This creates one of nature's most spectacular phenomena along the coast with diverse coastal landforms. Tidal sedimentation is also greatly influenced by the seasonal changes of the Asian Monsoon climate regime, resulting in high geodiversity exposed to constant changes in hydrology and sediment supply. As a result, the littoral environment includes tidal channels and gullies, tidal mudflats, mixed flats and sandflats,

together with all the related ecosystems to sustain highly dynamic yet stable mudflat sedimentation regimes.

Scientific research and tradition

Geological research has been supported by Korean Government since 2012. After the World Heritage inscription for criterion (x) in 2021, scientific monitoring and research are active for the maintenance of their attributes as well as for the additional criterion (VIII).



Holocene tidal sediments around the islands of the Korean Getbol.

FONTAINE DE VAUCLUSE

FRANCE



Upper outlet of the Fontaine de Vaucluse during high water period (64.5 m³/s). (Photo by E. Simon).

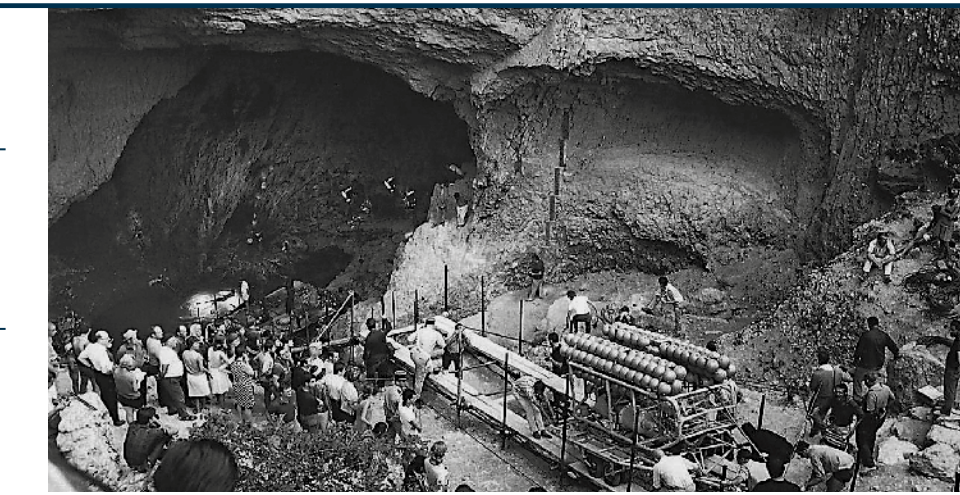
THE LOCUS TYPICUS ASCENDING SPRING WITH THE GLOBALLY LONGEST HISTORY OF RECORDED DISCHARGE.

The Fontaine de Vaucluse is a part of a large karst system developed during the Messinian Crisis of salinity at the end of Miocene (Audra *et al.*, 2004). It is a lake spring with deep siphonal karst conduits and is considered as locus typicus for all such springs worldwide (the term: "vau-

clusian type"). The spring discharge has been recorded since 1878, making this spring the best explored in the world in terms of drainage regime. Minimal discharge is 3.1 m³/s, average 17.3 m³/s which is the largest in France, while the maximum exceeds 80 m³/s.

SITE 185

GEOLOGICAL PERIOD	Miocene to Quaternary
LOCATION	Provence, France 43°55'04"N 005°07'57"E
MAIN GEOLOGICAL INTEREST	Geomorphology and active geological processes History of geosciences



The Telenauta ROV launching, 1967. (Photo by J.Y. Cousteau. Courtesy from Syndicat Mixte du Bassin des Sorgues).

Geological Description

The Fontaine de Vaucluse is one of the most famous and best explored karst springs in the world, located in Provence, about 30 kilometers east of the city of Avignon. The deep siphonal karst conduits, the huge discharges variation and the high minimal discharge values during low flows attracted researchers from all over the world. Blavoux *et al.* (1992) defined a catchment area of about 1,100 km² (today up to 1,160 km²). The Lower Cretaceous limestones of Urgonian facies (Barremian-Aptian age) are 1,500 meters thick and highly karstified. The thickness of the unsaturated zone can exceed 800 meters; four chasms on the plateau are more than 500

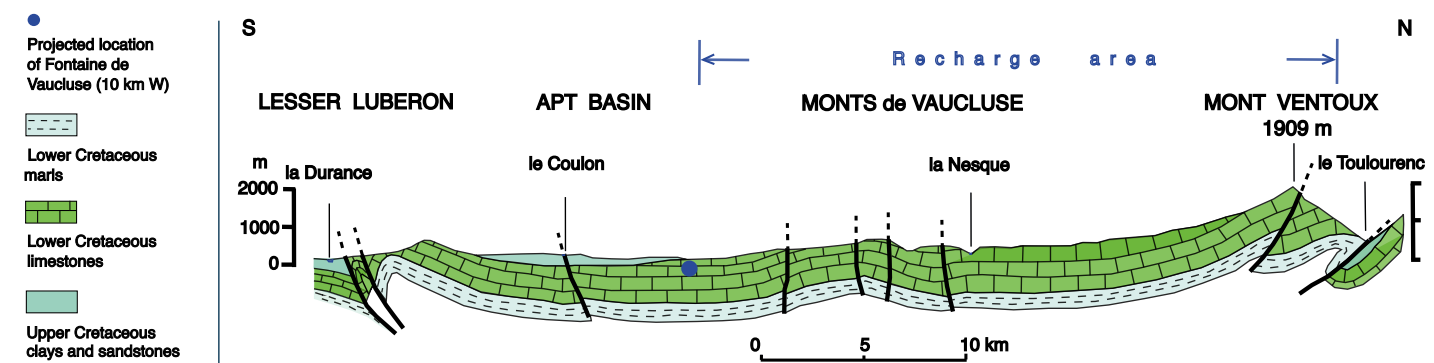
meters deep (Gaubert and Le Falher, 1990), and one shaft reaches the saturated zone 30 kilometers upstream the spring.

The spring comprises a siphonal pool with an upper outlet which flows only during high water periods and a downstream outlet where groundwater continuously discharges through thick debris zone with huge fallen blocks, giving rise to the Sorgue River, one of the Rhône's tributaries. Over one hydrological year, the mean water table level fluctuations at the outlet are of about 25 meters (Blavoux *et al.*, 1992; Cognard-Planqu *et al.*, 2006; Bonacci, 2007).

Scientific research and tradition

The Fontaine de Vaucluse has been surveyed by many speleo divers and underwater vehicles. The Vaucluse's museum "Le Monde Souterrain" provides information on history of speleodiving surveys starting with the one of Ottonei (1878), then of famous Commandant Cousteau (1944, 1955),... The deepest exploration at - 308 meters was made by the ROV Modexa (1985).

Sketch cross-section of the recharge area of Fontaine de Vaucluse. (After Puig, 1987, modified).



WAKULLA SPRING

UNITED STATES OF AMERICA



Aerial view overlooking Wakulla Spring pool and spring run (courtesy of Florida Geological Survey).

THE LARGEST INDIVIDUAL SPRING AND THE LONGEST SUBMERGED SPRING CAVE SYSTEM IN THE UNITED STATES.

Wakulla Spring is the strongest individual spring in the United States. As of January 2023, more than 72 kilometers of submerged channels have been explored by cave divers making it also the longest spring system in the country. Paleontological interest in the spring began in 1850, when the bones of an ancient mastodon

were found at its bottom. Since then, scientists have identified the remains of at least nine other extinct mammals that date to the last glacial period, deposited as far as 360 meters back into the main submerged passage. Humans had occupied the area for nearly 15,000 years.

SITE 186

GEOLOGICAL PERIOD	Neogene to Quaternary
LOCATION	Tallahassee, Florida, United States of America 30°14'06"N 084°18'10"W
MAIN GEOLOGICAL INTEREST	Geomorphology and active geological processes Paleontology



View of the Wakulla Spring from a cave diver's perspective (courtesy and copyright of David Rhea & GUE).

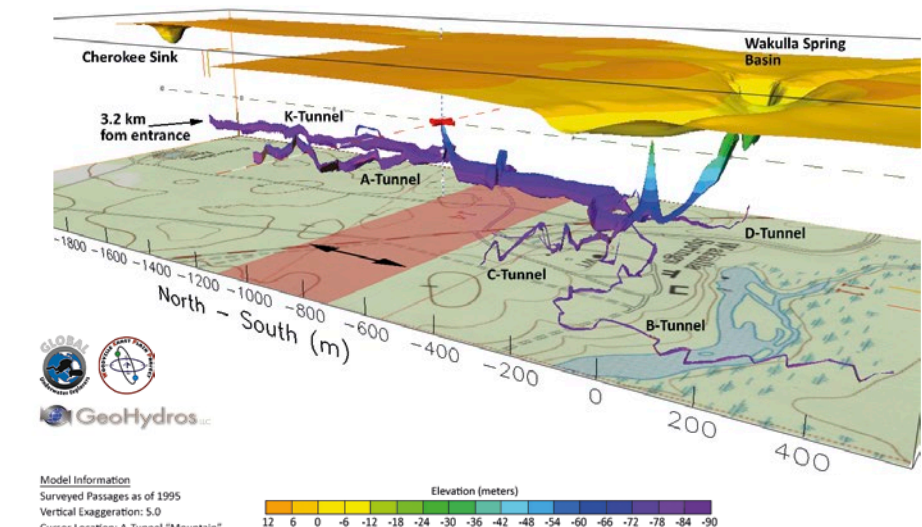
Geological Description

Wakulla Spring, the main source of Wakulla River, is in Edward Ball Wakulla Spring State Park, 22 kilometers south of Tallahassee, Florida. It is the largest individual spring in the United States and has an average discharge rate of 13.6 m³/s for the period of record between 1907 and 2019. Seasonal discharge ranges from 0.7 m³/s to 59 m³/s, which is the largest reported range of discharge for any spring in Florida (Rupert, 1988; Scott *et al.*, 2002; NFWFMD, 2021). The water flowing from Wakulla emerges from the vast Upper Floridan Aquifer which is here composed of Miocene St. Marks Formation and Oligocene Suwannee Limestone. The main recharge area of Wakulla Spring is in Woodville Karst Plain characterized by more than 1000 water-filled sinkholes and numerous sinking streams many of which were dye-traced to delineate the spring drainage area (Kincaid, 2006). Overlying the St. Marks Formation is a thin layer of sand and clay deposited during the Pleistocene. The fossil remains of mammoths, mastodons, giant sloths, camels, bison, and saber-tooth tigers have all been found both in Wakulla Spring and in the Wakulla River. Archaeological evidence sug-

gests that humans had occupied the area for nearly 15,000 years (Glowacki and Dunbar, 2019).

Wakulla Cave in 3D - 1995

Woodville Karst Plain, North Florida



The computer-generated scheme of submerged Wakulla Cave passages based on cave diving surveys (courtesy of Todd Kincaid).

Scientific research and tradition

Network of submerged spring conduits, ranging between 2 and 30 meters, have been explored by cave divers since 1950s, hydrologic investigations have been conducted since 1907, and paleontological investigations since 1850. Major Hollywood movies, including early Tarzan films, were filmed at the location.

VRELO BUNE SPRING BOSNIA AND HERZEGOVINA



Buna spring in Blagaj, Mostar (Bosnia & Herzegovina). Photo by Branislav Petrovic.

DEEP SIPHONAL SPRING WITH ENORMOUS MAXIMAL DISCHARGE.

The tectonic role is crucial for the creation of impressive karst landscapes. Due to its maximal discharge (Ford and Williams, 2007), Vrelo Bune is listed among the world's top five springs. Its minimal discharge is $3 \text{ m}^3/\text{s}$, the average is $23.7 \text{ m}^3/\text{s}$, while the maximum reaches $120 \text{ m}^3/\text{s}$. In January 1971, all of $380 \text{ m}^3/\text{s}$ have been

recorded at Buna River. The first divers to explore the spring's siphons in 1973 were G. Franczia-Kiss and C. Touloumdjian. A series of expeditions continued in 1984, 1999 and 2003. During high discharges, the visibility in the water is not good (2-4 meters). The water temperature is $10-11^\circ\text{C}$.

SITE 187

GEOLOGICAL PERIOD	Neogene to Quaternary
LOCATION	Neretva River valley in Blagaj, downstream of the city of Mostar, Bosnia and Herzegovina $43^\circ 15' 25''\text{N}$ $017^\circ 54' 15''\text{E}$
MAIN GEOLOGICAL INTEREST	Geomorphology and active geological processes



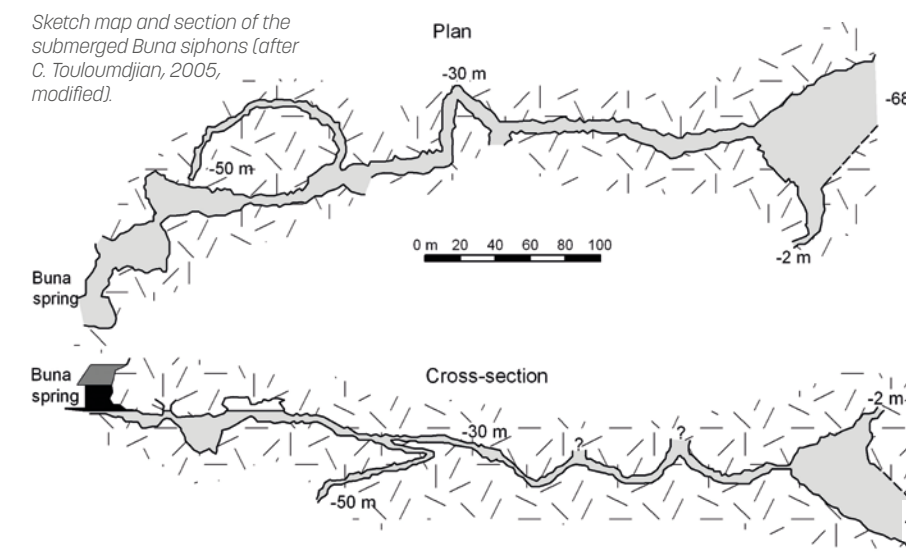
Vrelo Bune, panoramic view (courtesy of Ferid Skopljak).

Geological Description

The Vrelo Bune spring is located on the left border of the Neretva River valley in Bosnia and Herzegovina at the altitude of 36 meters. The spring outlet is situated at the point of tectonic contact between Cretaceous limestone and Eocene flysch. Water discharges from the cave underneath a high cliff make the ambience unique and quite spectacular (Stevanovic, 2009). The smaller cave open-

ings, situated along the fault at the cliff, were created at the earlier stages of karst evolution (Milanovic *et al.*, 2014). Buna is an ascending siphonal spring. The total length of the deep siphons that were explored by divers is 520 meters, and the vertical distance between the deepest explored point and the discharge point is 72 meters (Touloumdjian, 2005). The total estimated catchment area

of the Buna spring is approximately $1,100 \text{ km}^2$, including the Nevesinjsko Polje, the catchment of the Zalomka River, and the broad area of the Velež Mountain at the elevation above 900 meters (Milanovic, 2023). It is difficult to distinguish the watersheds of the neighbouring catchment of the Bunička spring (discharges from $0.72-207 \text{ m}^3/\text{s}$), and it is common to view these two catchments as a single karst system. Apparent groundwater velocity, as observed during the tracing tests, ranges between 0.03 and 0.04 m/s .



Scientific research and tradition

The Buna spring is a wonderful example of a fascinating spring and a developed karst system with tectonics that are actively shaping the landscape. It is visited by many tourists. Next to the spring is a tekke house from the Ottoman period. The spring is protected as a natural monument and with tekke represents a unique ambience with a significant cultural, social and economic significance.

MAMMOTH CAVE

UNITED STATES OF AMERICA



UNESCO World Heritage Site

The Mammoth Cave System contains the most extensive known system of cave passages in the world (Art Palmer).

THE MAMMOTH CAVE SYSTEM IS THE LONGEST KNOWN CAVE IN THE WORLD AND IS STILL BEING EXPLORED.

mapped regularly. Passages contain large rooms, vertical shafts, beautiful minerals, fossils, and other features that are superlative examples of their type. Cave passages record major events in landscape evolution of eastern North America back to the Pliocene (Granger *et al.*, 2001). This is

also a significant landscape with respect to biodiversity. Diverse surface and underground habitats are home to at least 1,925 species. Of these 43 are endemic, 49 are cave-limited, and 20 are threatened or endangered. This is the type locality for 33 cave-limited species.

SITE 188

GEOLOGICAL PERIOD	Miocene to Holocene
LOCATION	Southcentral Kentucky, United States of America 37°12'05"N 086°08'39"W
MAIN GEOLOGICAL INTEREST	Geomorphology and active geological processes



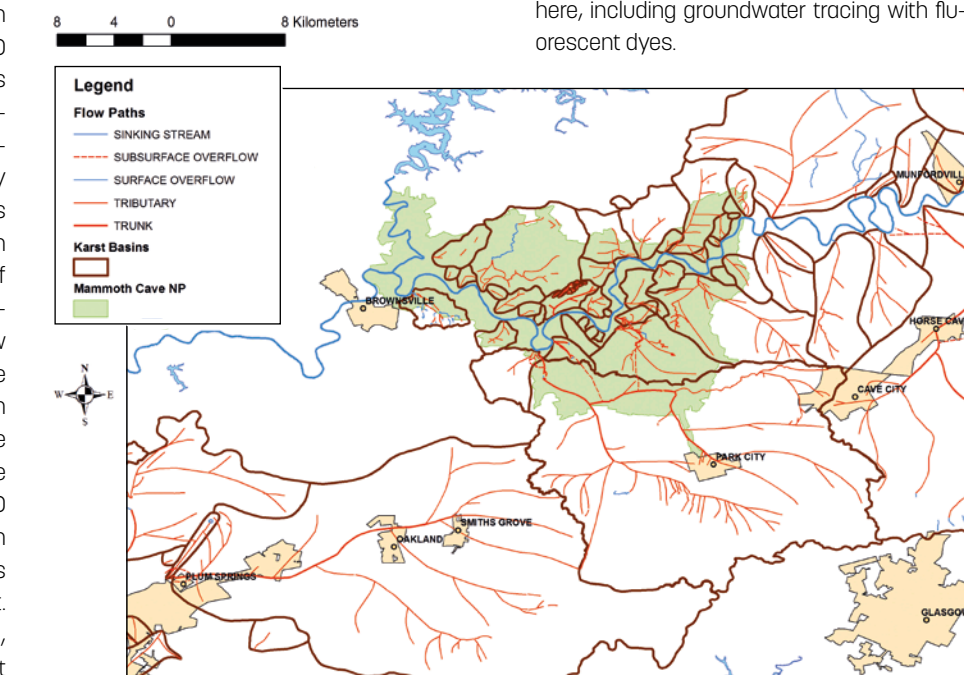
The cave contains superlative examples of subsurface karst features, including a collection of rare minerals (Chris Groves).

Geological Description

The Mammoth Cave System has a known length of more than 670 kilometers (Hobbs *et al.*, 2017; Bledsoe *et al.*, 2021). More than 300 kilometers of passages in nearby caves have also been explored and mapped, some of which may someday connect with Mammoth Cave. The caves are developed within a nearly horizontal sequence of about 120 meters of relatively pure carbonate rocks of Carboniferous age, overlain in many areas by clastic rocks that form resistant ridges. Mammoth Cave is a rare fossil locality that shows changes in ancient fish faunas through rock sequences. The Mammoth Cave aquifer drains an recharge area of several hundred square kilometers. Underground streams forming the cave flow northward from the extensive sinkhole plains of the Pennyroyal Plateau, beneath the Mammoth Cave Plateau, and emerge from springs on the Green River. Fisher Ridge Cave, with a known length of more than 200 kilometers, comes close to connecting with the eastern edge of Mammoth Cave, as does the 50+ km long Whigpistle Cave to the west. The cave systems are composed of several, interconnected levels that record the last

several million years of regional landscape development and, in particular, evolution of the Green and Ohio Rivers.

Drainage systems of the Mammoth Cave karst aquifer (National Park Service).



Scientific research and tradition

The area has a long history of cave and karst research, attracting scientists from around the world to study the cave and surroundings (Groves *et al.*, 2021). Techniques used to study karst hydrogeology, ecology, and other aspects of karst science were developed here, including groundwater tracing with fluorescent dyes.

THE WHITE LIMESTONE KARST OF COCKPIT COUNTRY JAMAICA



Fault and joint controlled linear alignments among cockpits, near to the Alps, along the north eastern boundary of the Cockpit Country (photograph: Mr. Jack Tyndale-Briscoe).

ONE OF THE MOST OUTSTANDING AREAS OF LIMESTONE COCKPIT KARST IN THE WORLD, LOCATED IN THE CARIBBEAN.

The type area for Cockpit Karst developed on uplifted limestone in a tropical region. The area represents one of the World's most important and spectacular geomorphological landscapes of 1300 km², 12% of the entire area of Jamaica. Geology and the microclimate generated high endemism and biodiversity.

The area is underlain by a network of underground streams and caves. The inhospitable environment served as refuge for freed Spanish enslaved Africans in 1655 and later served as refuge for runaway enslaved Africans, whose descendants still reside in the area.

SITE 189

GEOLOGICAL PERIOD	Miocene to Holocene
LOCATION	West Central, Jamaica 18°18'36"N 077°37'48"W
MAIN GEOLOGICAL INTEREST	Geomorphology and active geological processes Stratigraphy and sedimentology



Cockpit karst near Mulgrave, west of the Cockpit Country.

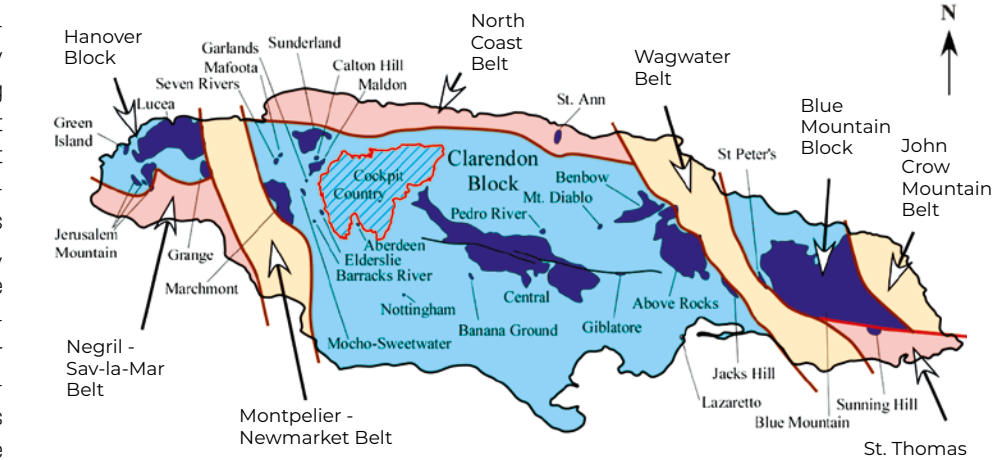
Geological Description

A thick sequence of platform limestones and dolostones was deposited in the late Eocene to early Miocene with combined thicknesses of 1,000 to 1,500 meters. A layer of early- to mid-Miocene ash from volcanos in Central America accumulated on the limestone plateau during its early emergence and underwent extensive leaching to form bauxitic soils. Uplift from the late Miocene to present has seen extensive karst formation characterized by the production of conical residual hills up to 100 meters high separated by star-shaped to linear depressions hosting bauxite deposits. Two mechanisms of karst formation are generally recognized. The first is due to solution following rainfall. The second is by collapse. The distinct land forms include conical residual hills (cockpit karst), steep-sided hills of limestone and dolostone (tower karst), isolated to star-shaped depressions (dolines or sinkholes), and larger more complex depressions with multiple dolines (uvalas). The resulting landscape lacks surface drainage. Despite the lack of surface drainage there is a tremendous network of underground streams that form part of an intricate caving system. The area is interna-

tionally recognized for its karst scenery and its tropical wet-limestone forests, which give rise to its high endemism and biodiversity.

Scientific research and tradition

Cockpit Country and its karst were described by Sawkins (1969) during the first government geological survey. Subsequently the limestones have been described by Mitchell (2013) and the karst by Sweeting (1958), Mitchell *et al.* (2003) and Miller (2004). Cockpit Country has been designated a protected area by the Government.



Boundaries of the Cockpit Country based solely on geological formations with the cockpit karst shown here as undifferentiated limestone on the geological map of Jamaica.

GUILIN KARST

CHINA



UNESCO World Heritage Site

Lijiang River with cone karst reflection, by LI Tengchao in 2008. The scene has been used as the symbol of China on the 20 Yuan CNY banknote.

A GLOBAL REFERENCE TO SHOW THE GEOLOGICAL AND GEOMORPHOLOGICAL EFFECTS OF CONTINENTAL KARST DEVELOPMENT.

Guilin Karst is considered a prime example of continental tower karst (fenglin) formation and perfect geomorphic expression of the end stage of karst evolution in South China Karst. Its geological setting in a basin with abundant allogenic water influences the development of distinct karst features,

making it an outstanding area for studying karst processes and their environmental impacts. The "Guilin model" of karst evolution, which describes the coexistence and interaction between fenglin and fengcong karst forms, is of international scientific significance (Zhu Xuewen, 1991).

SITE 190

GEOLOGICAL PERIOD	Neogene to Quaternary
LOCATION	Guilin, China 25°00'08"N 110°27'32"E
MAIN GEOLOGICAL INTEREST	Geomorphology and active geological processes



Putao Tower Karst, by ZHU Xuewen in 1988. It features tower-shaped peaks, the inside of the peaks is highly cavernous, often with foot caves.

Geological Description

The karst is in the central Nanling structural belt and a thick (3000 meters) Upper Devonian to Lower Carboniferous limestone succession within Guilin, China. Guilin Karst features beautiful continental tower karst and cone karst around the beautiful Li River and its tributaries and many caves (Yuan Daoxian, 1991).

Shaped by Paleozoic tectonic movements, the carbonate succession is deformed into distinct anticlines and synclines, which makes a unique basin ideal for karst development. The geomorphological setting, enriched by thick carbonate deposits and a warm, humid climate with plentiful rainfall, fosters extensive karst development. Differ-

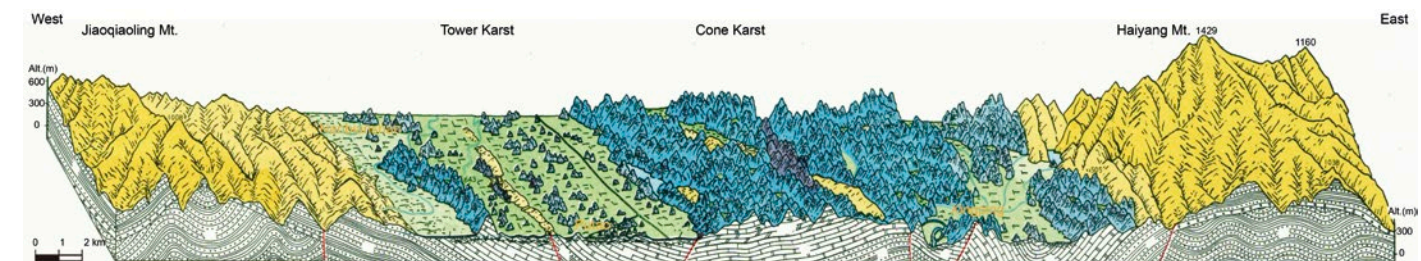
ential tectonic uplift since the Quaternary has led to a diverse range of topographies, facilitating the formation of two main karst landforms: tower karst and cone karst (Zhu Xuewen, 1988). Tower karst, or "surface flow karst," predominates in lower terrains where allochthonous water contributes to lateral erosion, while cone karst, or "vertical infiltration karst," occurs in elevated areas where deep water tables allow precipitation to cause vertical erosion.

This dynamic, exemplified by the 'Guilin model' of karst evolution, illustrates the ongoing development and transformation of karst features. Guilin's geological stability and comparatively slow tectonic uplift, unlike

more rapidly uplifting regions in the Yunnan-Guizhou Plateau, enhance its scientific relevance, making it an essential reference for global karst studies.

Scientific research and tradition

Research on Guilin Karst dates back to the 1600s by Xu Xiake, who explored 88 caves and created terms "fenglin" and "fengcong" (Tang Xireng, 1987). Contemporary studies focus on further understanding the karst dynamics, the establishment of, "fengcong" and "fenglin" simultaneous evolution model, as well as its aesthetic value influencing Chinese paintings and poems.



Geo-profile of Guilin Karst, edited by QIN Houren in 1983. Cone karst and tower karst evolved in a synergetic co-existence system resulted in these different formations.

HA LONG BAY-CAT BA ARCHIPELAGO VIETNAM



UNESCO World Heritage Site

THE MOST EXTENSIVE AND BEST KNOWN EXAMPLE OF MARINE-INVADED TOWER KARST IN THE WORLD.

Ha Long Bay-Cat Ba Archipelago is one of the world's most extensive areas of cone and tower karst that displays the full range of karst formation processes. The outstanding feature of this ideal model of mature tropical karst is that it had developed on-land before being repeatedly invaded and reworked by recent marine transgressions-regressions, and remains at present

a drowned seascape of karst landforms. Clusters of inter-connected cones and isolated towers become islands and islets, intra-mountain depressions become "closed lakes" and fault-controlled valleys become "channels". The site provides unique understanding of the complex geo-bio-climatic history and karst processes.

SITE 191

GEOLOGICAL PERIOD	Neogene to Quaternary
LOCATION	Quang Ninh Province and Hai Phong City, in the Gulf of Tonkin, Vietnam 20°54'00"N 107°06'00"E
MAIN GEOLOGICAL INTEREST	Geomorphology and active geological processes



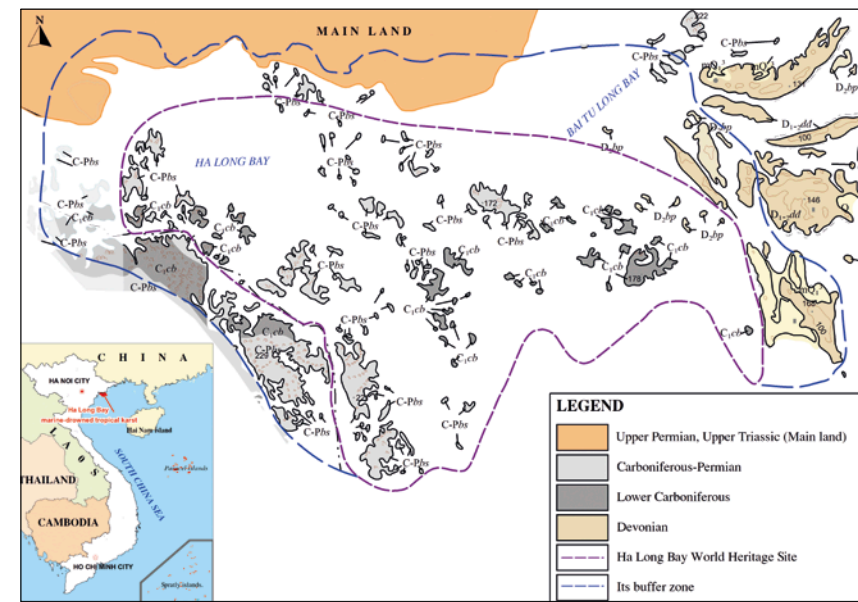
Sea notches and footcaves in the islands and islets of Ha Long Bay.

Geological Description

Ha Long Bay-Cat Ba Archipelago (Quang Ninh Province and Hai Phong City, in the Gulf of Tonkin, Northeast Vietnam) is located ca. 150 kilometers from Hanoi capital. Covering an area of ca. 2,000km² and including ca. 2,000 islands and islets, mostly made of Lower Carboniferous and Carboniferous-Per-

mian limestones and mostly uninhabited and unaffected by humans, Ha Long Bay-Cat Ba Archipelago is a spectacular seascape of limestone pillars, cones and towers of tremendous diversity of forms and shapes, of which Cat Ba Island (Hai Phong City), ca. 200km² in area, is the largest. Between the pillars, cones and towers are numerous ma-

rine closed lakes and fault-controlled channels. Many large-sized islands feature several levels of essentially dry, caves that had been formed on-land, while most islands and islets are carved in by several levels of sea notches and "foot-caves" that are actively formed by the current sea actions. The exceptional scenic beauty of the site is complemented by its great biodiversity. Three archaeological cultures, i.e. Soi Nhu (18,000-7,000 years AD), Cai Beo (7,000-5,000 AD) and Ha Long (5,000-3,500 AD), interrupted perhaps by repeated sea level fluctuations and climate changes, have been identified in this area.



Simplified geological map of the Ha Long Bay marine-drowned tropical karst, Vietnam.

Scientific research and tradition

Having been used since ancient time and subjected to first scientific studies since 1898 by the French, at present Ha Long Bay-Cat Ba Archipelago is still being systematically surveyed and studied. The central part, ca. 550km², of Ha Long Bay-Cat Ba Archipelago became a UNESCO World Natural Heritage three times thanks to its aesthetic (in 1994), geologic-geomorphologic (in 2000) and biodiversity (in 2023) values.

TEPUIS AND QUARTZITE KARST OF GRAN SABANA VENEZUELA



UNESCO World Heritage Site

Tepuis are surrounded by sheer cliffs hosting numerous waterfalls, including Angel Falls (979 meters), the highest waterfall on Earth.

THE WORLD'S FINEST QUARTZITE KARST IN AN SPECTACULAR TABLE MOUNTAINS LANDSCAPE WITH THE HIGHEST WATERFALL ON EARTH.

Landforms similar to those in limestone karst, but in apparently non-soluble rocks, were long considered as a natural curiosity of little wider significance. Research in Gran Sabana demonstrated the critical role of quartz dissolution in the formation of surface and subsurface landforms, including ruiniform relief, dolines, karren, deep shafts, caves and speleothems. The mech-

anism of arenization, that is corrosion along grain contacts leading to loosening of the rock mass and making grains available for transport, was elaborated in detail and serves as a model for sandstone and quartzite disintegration (Sauro, 2014). Gran Sabana is therefore a global reference site for silicate karst.

SITE 192

GEOLOGICAL PERIOD	Paleogene to Quaternary
LOCATION	Gran Sabana, Venezuela 05°51'29"N 062°31'07"W
MAIN GEOLOGICAL INTEREST	Geomorphology and active geological processes



Cave galleries with typical pillars formed by combined arenization and mechanical erosion in the Imawari-Yeuta cave system (Auyan tepui) (courtesy of Vittorio Crobu/La Venta).

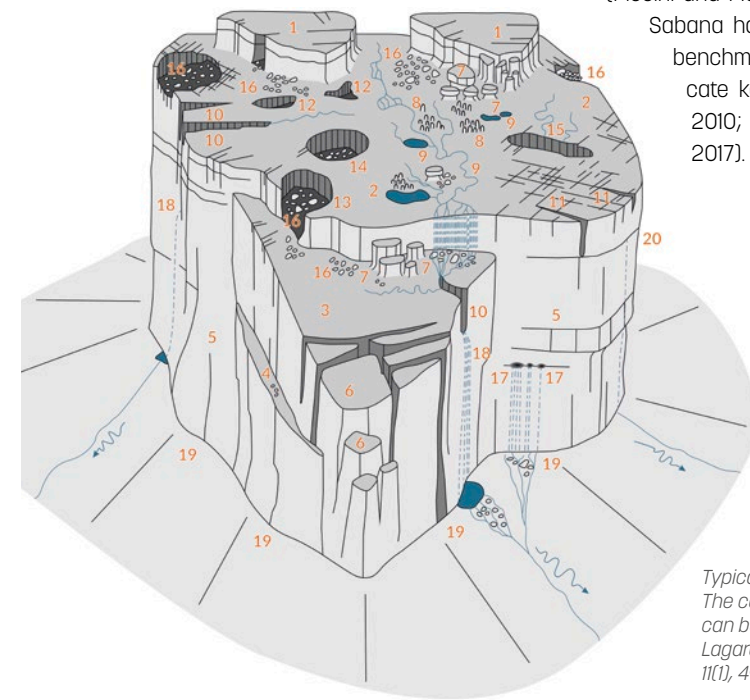
Geological Description

The Gran Sabana is part of the Guyana Shield, located in the humid tropics of South America, just north of the Equator. The basement of Precambrian magmatic and metamorphic rocks is overlain by a thick succession of clastic sedimentary rocks, mainly quartz sandstones and conglomerates also of Precambrian age. This succession is a few kilometres thick and includes the most resistant quartz sandstones of the Matauí Formation, exposed in spectacular rock cliffs hundreds of meters high. The most conspicuous landscape elements are tabular hills (tepuis, mesas), with flattish summit surfaces surrounded by sheer cliffs hosting numerous waterfalls, including the highest waterfall on Earth - Angel Falls (979 meters). The tepuis have various dimensions and some form multi-tiered extensive plateaus, tens of kilometres long. The top surfaces of the tepuis show extraordinary diversity of relief, best described as ruiniform. It includes rock walls, towers and pinnacles separated by narrow corridors and basins. Closed depressions, acting as sinkholes for surface streams, and deep shafts are common. Large, multi-level caves occur inside the

mesas. The region hosts some of the longest caves in quartz sandstones globally and several shafts exceed 300 meters deep.

Extensive karst in non-carbonate rocks was described in the 1970s (Urbani and Szczerba, 1974). Research intensified in the 1990s (Briceño and Schubert, 1990), followed by exploration of surface and underground karst

(Piccini and Mecchia, 2009). Gran Sabana has since become a benchmark locality for silicate karst globally (Wray, 2010; Wray and Sauro, 2017).



Typical landforms of tepuis. The complete description can be found in Galan and Lagarde (1988), Karstologia 11(1), 49-60.

FJORDS AND TOWERING SEA CLIFFS OF FIORDLAND NEW ZEALAND



UNESCO World Heritage Site

GLOBALLY SIGNIFICANT EXAMPLES OF SPECTACULAR FJORDS, DEEPLY CARVED BY GLACIERS THROUGH GNEISSIC ROCKS UPLIFTED HIGH ALONG A CONVERGENT PLATE BOUNDARY.

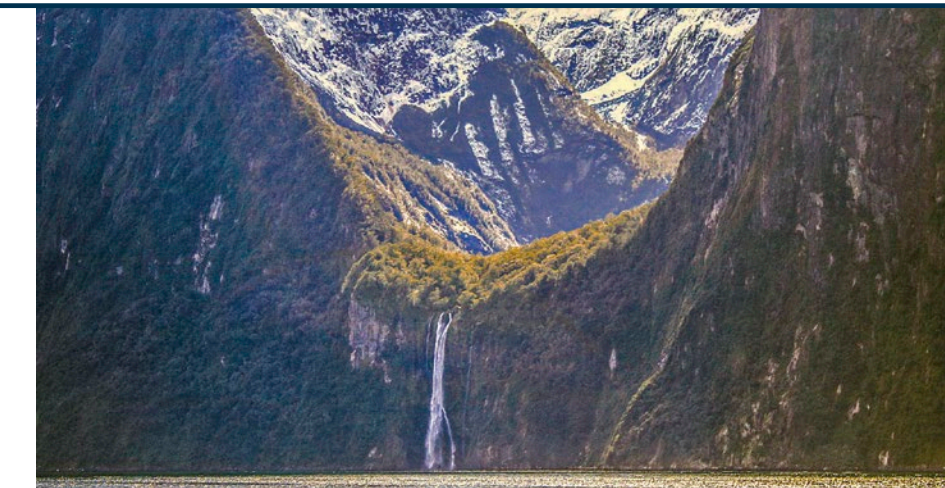
Annually one million tourists visit Milford Sound and marvel at Mitre Peak's (1683 meters) glacial horn. The fjord's cliffs tower 1500-2000 meters. Photo: Bernhard Spragg.

Fiordland has fourteen exemplary examples of fjords. Key features include: proximity to collisional plate boundary (subduction and strike slip) producing 1000-3000 meters of uplift in last 7 Ma; uplift balanced by subaerial erosion of uplifted mountains; massive annual precipitation (today up to 7 meters), producing glaciers up to 2 kilometers thick in glacials and unique marine

environment and biota beneath freshwater surface layer today; spectacular waterfalls from hanging valleys; over-deepening of upstream basins and silled-mouths made of bedrock and terminal moraine; fjord basin sediment archives of post-glacial history, climate and sea-level rise; world's highest sea cliffs (~2000 meters) (Hayward, 2022).

SITE 193

GEOLOGICAL PERIOD	Quaternary
LOCATION	Southland, New Zealand 44°38'10"S 167°53'38"E
MAIN GEOLOGICAL INTEREST	Geomorphology and active geological processes Igneous and Metamorphic petrology



Stirling Falls (150 meters high) cascade into glacier-carved Milford Sound, Fiordland, from this amazing U-shaped hanging valley that is dusted by winter snow. Photo: Maruf Zareb.

Geological Description

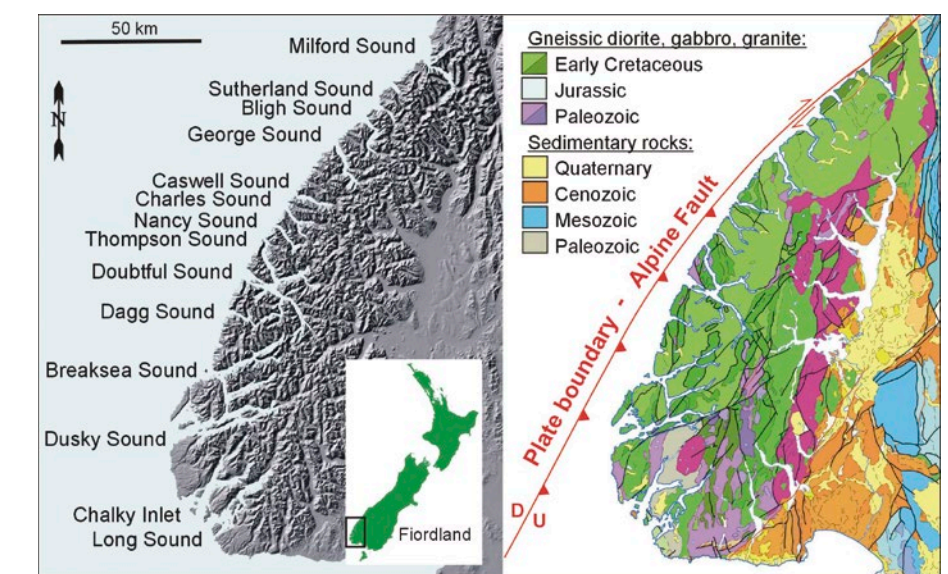
Fiordland is in Te Wahipounamu - South West New Zealand World Heritage Area characterised by uplifted snowy mountains and deeply incised glacial valleys. There are 14 marine-flooded fjords, each 10-40 kilometers long with internal basins (200-420 meters deep) and shallow sills (40-120 meters deep) at their seaward mouths. The fjords were river valleys widened and deepened by glacial erosion during Quaternary glacial periods. The glaciers cut deeply into hard crystalline plutonic and metamorphic rocks that were once buried to depths of 10-30 kilometers. A mid-Cenozoic erosion surface has been uplifted in the last 7 Ma along the east side of the Australia-Pacific plate boundary (combination of eastward subduction and oblique dextral displacement at the southern end of the Alpine Fault). Glacial erosion of the uplifted surface has resulted in numerous sharp peaks rising from 1000 meters in the south to 2700 meters in the north. The west-flowing glaciers have carved classical straight, U-shaped valleys with spectacular glacially-striated vertical rock faces and numerous hanging tributary valleys and high waterfalls. Extreme rainfall gives Fiordland the name "Land of Wa-

terfalls" and produces a thick freshwater layer on the surface of fjords. Post-glacial fjord sediments record switch from freshwater to marine environment (Dykstra, 2012).

Fiordland's glacially-carved fjords (left) have eroded deeply into uplifted gneissic plutonic rocks (right) pushed up along the collisional plate boundary (Turnbull et al., 2010).

Scientific research and tradition

Fiordland research includes studies on: complexity of Paleozoic and Mesozoic fault blocks and intrusions identified and mapped (Turnbull et al., 2010); plate boundary structure and seismic impacts (Klepeis et al., 2019); fjord sediment archives of climate, sea level (Dlabola et al., 2015); offshore Quaternary sediment processes (Strachan et al., 2016).



FJORDS AND GLACIERS IN HORNSUND AND VAN MIJENFJORDEN, SVALBARD NORWAY



Landscape of Hornsund, with rugged mountains and fast-receding tidewater Hansbreen glacier (Photo by Adam Nawrot).

A SHOWCASE OF GLACIERS AND LANDFORMS OF POLAR ENVIRONMENTS.

The two areas represent complete high-latitude geomorphological systems, with glacial, periglacial, coastal, glaciolacustrine, and marine subsystems. Systematic research has resulted in thorough understanding of these systems, which serve as a natural laboratory to monitor ongoing environmental changes. Many individual glacial and periglacial landforms are text-

book examples. It is foreseen that in a decadal perspective Hornsund will become a marine strait, isolating the southernmost part of Spitsbergen as an island. The Van Mijenfjorden area is a good reference for surging glaciers. Both areas are mostly pristine, with the legacy of past mining in Van Mijenfjorden largely reintegrated with the landscape.

SITE 194

GEOLOGICAL PERIOD	Quaternary
LOCATION	Spitsbergen, Svalbard Archipelago, Norway Hornsund 76°58'19"N 015°47'04"E Van Mijenfjorden: 77°50'30"N 016°42'26"E
MAIN GEOLOGICAL INTEREST	Geomorphology and active geological processes



The Paulabreen moraines crosses the Van Mijenfjorden at the former mining city of Svea. In the foreground the restored landscape. Photo: Ove Haugen 2023.

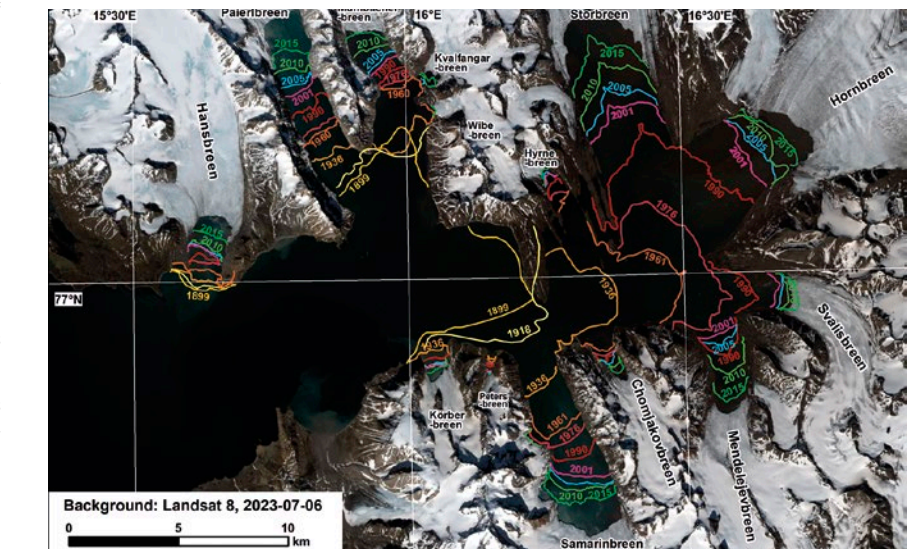
Geological Description

Two fjords in south Spitsbergen represent the diversity of glacial and periglacial environments, including glaciers behaving in different ways. In the southerly Hornsund fjord numerous secondary inlets are steadily expanding as tidewater glaciers continue to retreat, whereas moraine ridges inland indicate much larger past extent of glaciation. The inner part of Van Mijenfjord consists of two branches, with one ending in a large glacial complex with several surging glaciers. One surge some 600 years ago formed a large moraine along the shores, partly ice-cored and partly consisting of marine clays. A large glaciolacustrine lake existed for a short time. Scheelebreen, another part of the complex, is presently surging and advanced some two kilometres over the summer and winter 2021/2022. In both areas landforms produced by meltwater are abundant, including large outwash plains. The ground is permanently frozen at depth, but summer thaw in the active layer gives rise to diverse periglacial landforms such as patterned (sorted) ground, frost fissures, solifluction features and rock glaciers. Raised marine terraces and relict cliffs provide evidence

of glaci-isostatic uplift. These two localities show complementary bedrock topography. High-mountain scenery dominates around Hornsund, while the inner Van Mijenfjorden is surrounded by plateau mountains on sedimentary rocks.

Scientific research and tradition

Scientific activities have been conducted since 1900 and are currently based on permanent research facilities established in both areas. Numerous benchmark studies of periglacial processes, glacier behaviour, post-glacial uplift and landscape restoration have been published. Ongoing research focuses on geomorphic response to climate change.



Post-LIA retreat of tidewater glaciers in Hornsund Fjord (acc. to Błaszczyk et al. 2013, supplemented by M.Błaszczyk for 2015; Background: Landsat 8, 6.07.2023).

VATNAJÖKULL

ICELAND



UNESCO World Heritage Site

Subglacial eruption of Gjálp volcano in northwestern part of the Vatnajökull glacier (3 October 1996).
Copyright Oddur Sigurðsson, Icelandic Meteorological Office.

UNIQUE LANDSCAPE FORGED BY THE CONSTANT CONFLICT BETWEEN FIRE AND ICE IN THE RIFT ZONE AT THE DIVERGENT PLATE TECTONICS.

Vatnajökull is an outstanding example representing interactions between volcanism and glaciation (Baldursson *et al.*, 2018). The most spectacular are the jökulhlaups – sudden floods caused by glacier margin breaches during an eruption with a huge water discharges. This recurrent phenomenon has led to the formation of unique sandur plains, among the best of their kind

in the world (Magilligan *et al.*, 2002; Thórhallsdóttir and Svavarsson, 2022), braided channel systems and rapidly evolving canyons. Vatnajökull also illustrates different types of glaciation, from ice cap to outlet glaciers, and glacial landforms around the ice cap provide evidence of ice advance and retreat.

SITE 195

GEOLOGICAL PERIOD	Quaternary
LOCATION	Vatnajökull, Iceland 64°34'39"N 016°52'54"W
MAIN GEOLOGICAL INTEREST	Geomorphology and active geological processes Volcanology

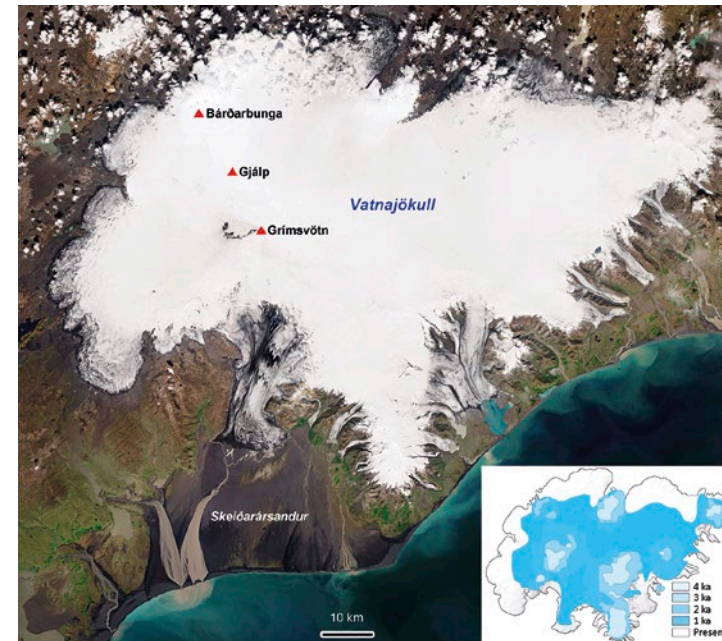


Waving front of Fláajökull - one of the 40 outflow glaciers in the south-eastern part of Vatnajökull ice cap.
Photo by Zbigniew Zwoliński.

Geological Description

This area covers almost 10% of Iceland's territory and is characterised by the coexistence and ongoing interaction of an active oceanic rift on land, a mantle plume, and an ice cap that have varied in size and extent over the past 2.8 million years. Earth system interactions are constantly modifying this area, cre-

ating remarkably diverse landscapes and a wide variety of plate-tectonic, volcanic and glaciovolcanic features. There are eight subglacial volcanoes. Some of them are among the most active in Iceland (e.g. Grímsvötn, Bárðarbunga; Gudmundsson, 2004). Particulary interesting and unique in this regard



Vatnajökull is the greatest mass of ice in Europe with 40 outlet glaciers, 8 active volcanoes and vast outwash plain of the Skeiðarársandur (1300 km²).

are the basaltic lava shields, volcanic fissures and cone rows, vast flood lavas, and features of ice-dominated glacio-volcanism, such as tuyas and tindars. Geothermal heat and subglacial eruptions produce meltwater and jökulhlaups that maintain globally unique sandur plains, to the north and south of the Vatnajökull ice cap (~8000 km²), as well as rapidly evolving canyons. In addition, the area contains a dynamic set of glaciological and geomorphological features, created by 40 expanding or retreating outlet glaciers in response to climate change. These features can be easily accessed and explored at the snouts of Vatnajökull's many glaciers and their forelands, especially in the southern lowlands (e.g. Skeiðarársandur).

Scientific research and tradition

The pioneering descriptions of the Vatnajökull glacier were made by the Finnish geologist Jöns Svanberg in 1794. In the late 19th century, interest began to focus on the relationship between the geology and dynamics of the Vatnajökull glacier in an attempt to understand how the glacier responds to climate change.

YOSEMITÉ VALLEY

UNITED STATES OF AMERICA



UNESCO World Heritage Site

Yosemite Valley from Tunnel View. (Will Parrinello, Mill Valley Film Group).

ARCHETYPAL GLACIAL LANDFORMS INSET INTO SPECTACULAR MOUNTAINOUS GRANITE TOPOGRAPHY.

Yosemite Valley is a classic, most impressive example of glacial landforms resulting from mountain glaciation, as well as of granite landforms, with relationships between joint patterns and landform shapes clearly exposed (Matthes, 1930; Graham, 2012). The Half Dome, Royal Arches and El Capitan are reference structural granite landforms, shown in many textbooks. Pio-

neering studies of linkages between uplift and erosion (Stock *et al.*, 2005), factors influencing the magnitude of glaciation, and rockfall-triggering mechanisms (Collins and Stock, 2016) were executed in Yosemite. The sheer scale of landforms can be appreciated from numerous vantage points, including the globally famous Glacier Point.

SITE 196

GEOLOGICAL PERIOD	Neogene to Quaternary
LOCATION	Sierra Nevada, United States of America 37°44'30"N 119°34'12"W
MAIN GEOLOGICAL INTEREST	Geomorphology and active geological processes

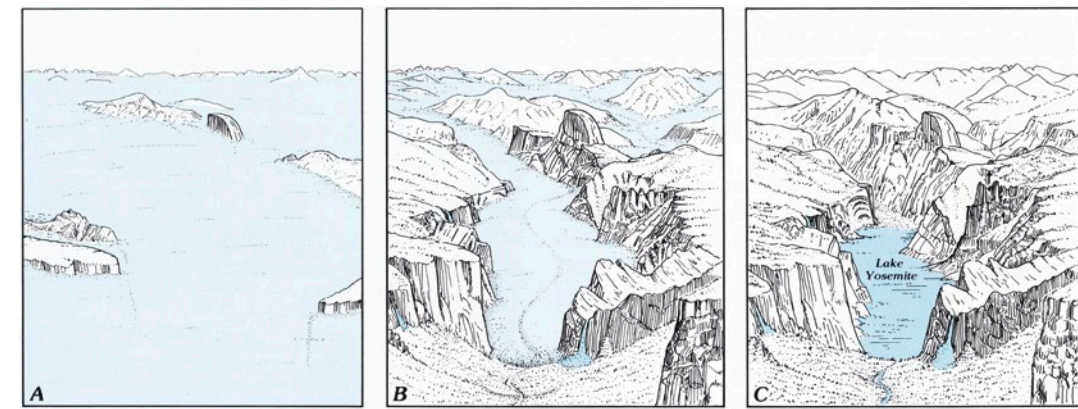


Upper and Lower Yosemite Falls. (Photo: National Park Service)

Geological Description

Yosemite Valley is located within the western slope of the Sierra Nevada range, which was subject to considerable asymmetric uplift in the Neogene and Quaternary. Uplift triggered massive erosion, resulting in the origin of valleys several kilometres deep, but undulating surfaces survived along water divides, creating spectacular landscape contrast. Geologically, Yosemite Valley is carved in granites and granodiorites of Cretaceous age, cut by numerous dikes. Jointing exerts evident control on the shape of many landforms, including the famous domes and blind arches. In the Quaternary, high elevation coupled with the location on the windward side, exposed to moist air masses arriving from the Pacific, allowed for the development of extensive mountain glaciation. An ice cap formed over the plateau, carving cirques, whereas long ice tongues descended into the valleys, transforming them into impressive U-shaped glacial

troughs. Different intensity of glacial erosion between the trunk and tributary valleys resulted in the origin of hanging valleys and spectacular waterfalls, among the highest on Earth. Evidence of glaciation also includes ice-polished surfaces, roche-moutonnées, moraines and lake basins. Yosemite Valley remains geomorphologically very active, with rockfalls and rockslides being the most visible processes transforming glacial morphology complemented by bedrock abrasion and gravel-bed river erosion.



Evolution of the Yosemite Valley from the times of major glaciation to the early Holocene (after Huber, 1989).

Scientific research and tradition

The history of coordinated geological research in Yosemite goes back to 1913 (Huber, 1989), and the area has become a natural laboratory to investigate granite geology, granite landforms, uplift-erosion interactions and glacial landforms (Graham, 2012). It yielded many landmark studies and research continues, benefitting from excellent exposures and great landforms.

IMPACT STRUCTURES AND EXTRATERRESTRIAL ROCKS



Photo: Bernhard Edmaier

Impact craters are geological structures created when extraterrestrial objects such as asteroids and comets impact Earth's surface. Impact structures range from small craters (just a few meters in diameter) to massive basins hundreds of kilometres across. On Earth their rapid formation can produce dramatic effects on the environment and life. Major impacts, such as the one that led to the extinction of the dinosaurs 66 million years ago, highlight the profound consequences impact events can have on biological evolution. The field of impact cratering originated with studies of circular features on the Moon and Earth before the recognition that rocks from space collided with planets and has advanced significantly over the last seventy-five years. The study of impact cratering now encompasses field geology, geophysics, geochemistry, mineralogy, experimental petrology, remote sensing, and planetary science. Modern technologies such as geophysical surveys and drilling programs allow terrestrial impact structures to be examined and sampled in incredible detail. Advances in isotopic dating have made possible accurate dating of impacts, allowing them to be linked to past geological and biological events. The study of impact structures is a dynamic and interdisciplinary field. Academic researchers, international organizations such as the International Continental Drilling Program (ICDP), professional societies (Meteoritical Society Impact Cratering Committee), public databases (e.g., Impact Earth & Earth Impact Database), and members of the public all play critical roles in increasing understanding about impact craters. At present, more than 200 impact structures on Earth have been identified and confirmed, and ongoing research continues to discover new sites and expand our knowledge of known impact craters.

This chapter presents an overview of four important impact craters, each demonstrating its unique characteristics and contributions to the field of impact studies.

1. Vredefort Dome (South Africa): Vredefort Dome is the eroded remains of the largest known impact structure on Earth. This site is important for the study of the effects of large-scale impacts on Earth's crust and the preservation of impact sites over 'deep time'.

2. Ries Crater (Germany): One of the best-preserved craters in the world, Ries Crater displays well-exposed impact features that are easy to access and study. Its accessibility makes it an ideal natural laboratory for understanding the formation of complex impact craters.

3. Lake Bosumtwi Impact Crater (Ghana): Bosumtwi is the youngest and best-preserved complex impact crater on Earth and the source of Ivory Coast tektites. This site has been drilled and provides a unique opportunity to study a relatively recent large impact event.

4. The Barringer Meteorite Crater (USA): Also known as Meteor Crater, it is one of the longest studied and best-preserved meteorite craters on Earth. This exceptional example of a simple impact structure provides valuable information about the mechanics and effects of the impact event.

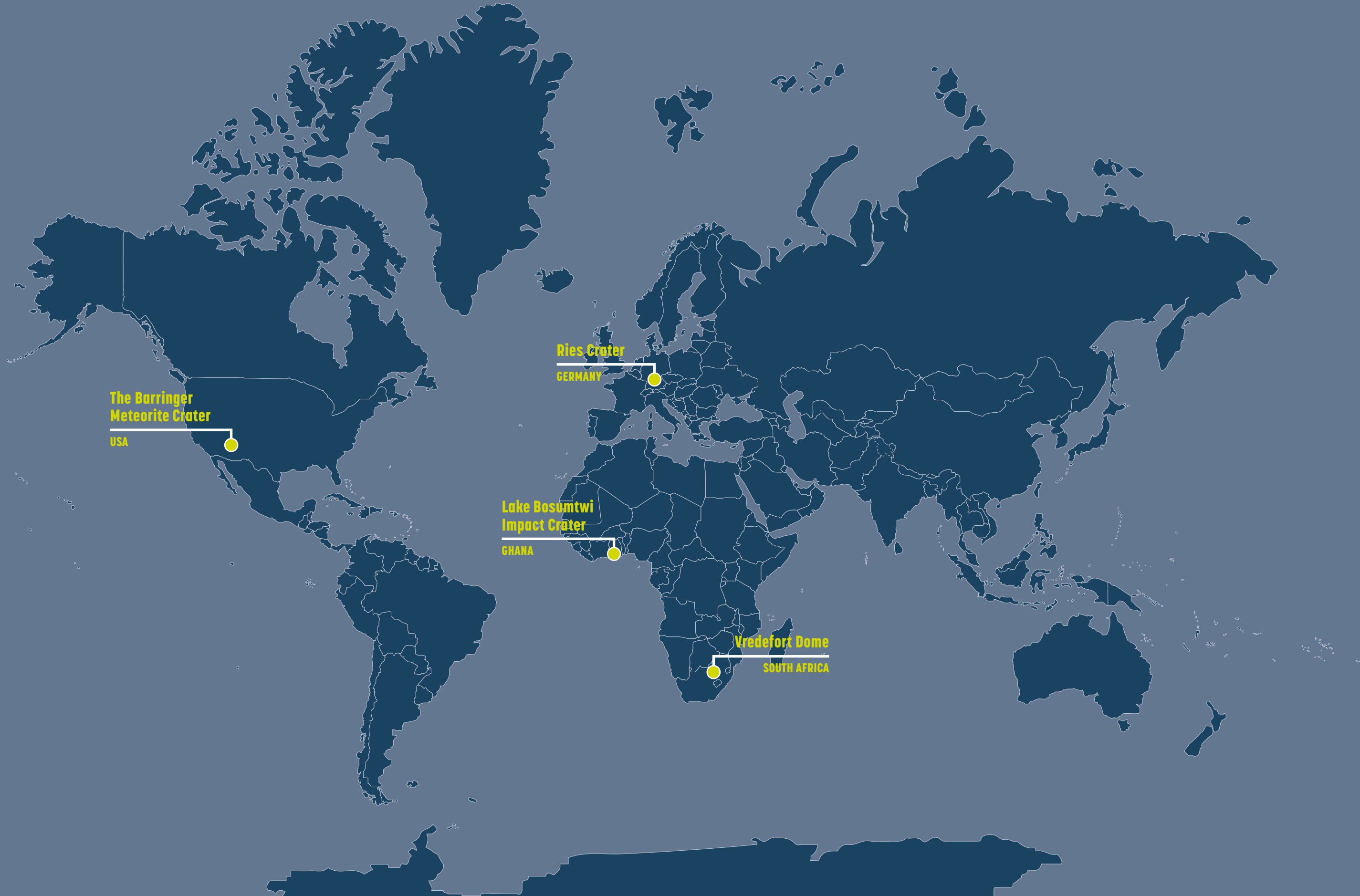
These sites represent a variety of impact structures, each adding a unique contribution to our understanding of meteorite impacts and their impact on Earth's geology and life. This chapter examines the importance of these structures and highlights their scientific value.

Daniel Asiedu

Department of Earth Sciences.
University of Ghana. Ghana.

Aaron J. Cavosie

School of Earth and Planetary Sciences (EPS).
Curtin University. Australia.
Chair, ICC - Impact Cratering Committee of the
Meteoritical Society, ICC.
IUGS Geological Heritage Sites referee.



VREDEFORT DOME

SOUTH AFRICA



UNESCO World Heritage Site

ERODED REMNANT OF EARTH'S LARGEST IMPACT STRUCTURE, EXPOSING VARIED IMPACT-RELATED DEFORMATION AND MELT ROCKS AND A DEEPLY EXHUMED CRUSTAL PROFILE.

As the heart of the largest confirmed hypervelocity impact structure on Earth, the Vredefort Dome provides a unique perspective into the only planetary process that has affected the surfaces of all rocky bodies in our Solar System. Its deep level of exhumation allows an unprecedented view of the catastrophic processes accompanying impact into crustal rocks.

Understanding these processes extends beyond these geological phenomena to include planetary-scale environmental consequences of giant impacts and the implications for Life on Earth. This significance was acknowledged by declaration of part of the Vredefort Dome as a UNESCO World Heritage Site in 2005.

VREDEFORT DOME

SOUTH AFRICA

GEOLOGICAL PERIOD	Paleoproterozoic
LOCATION	North-central South Africa / centered ca. 120 km southwest of Johannesburg, South Africa 27°00'00"S 027°18'00"E
MAIN GEOLOGICAL INTEREST	Impact structures and extraterrestrial rocks Tectonics

Geological Description

The 90-kilometer-diameter Vredefort Dome is the deeply eroded remnant of the central uplift of the world's largest (>250 kilometer diameter) known impact structure. It exposes macroscopic structural evidence (shatter cones, intense fracture patterns, faults, folds) and large dikes of impact melt rock (Vredefort Granophyre) and pseudotachylitic breccia, and rocks containing a range of micro-scale shock metamorphic features, that are all related to the 2.02 Ga impact event. Unusual thermal-metamorphic phenomena attributed to residual heat from the impact are also found in the rocks of the Dome. With an age of 2.02 Ga, the Vredefort Dome is also the second-oldest of the known terrestrial impact structures.

The combination of exceptional differential uplift and rotation that formed the dome and subsequent erosional exhumation by ~10 kilometers has exposed a 20-25 kilometer section through upper and mid-crustal levels of the Archean Kaapvaal craton. Rocks spanning ~1.4 billion years of Earth history, from a >3.1 Ga granite-greenstone Archean Basement Complex to a near-continuous record of Neoarchean to Paleoproterozoic sedimentation and volcanism between 3 and 2.1 Ga

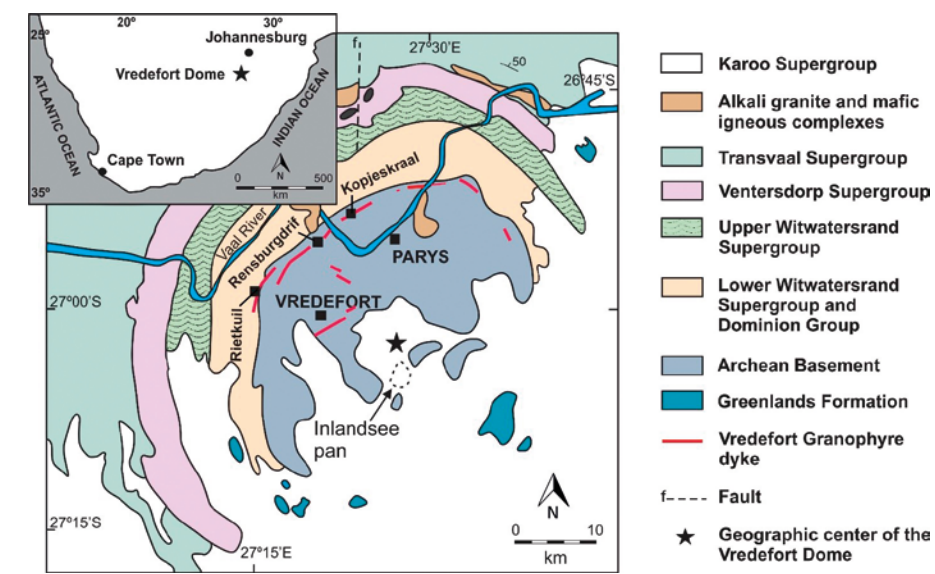


Large impact-induced pseudotachylitic breccia in Archean granitoid gneisses in Leeukop quarry (northern core, Vredefort Dome). Outcrop width: ca. 25 meters. Photo: W.U. Reimold.

Scientific research and tradition

(Dominion Group and Witwatersrand, Ventersdorp and Transvaal supergroups) provide an exceptional record of early crustal evolution.

The Vredefort impact structure extends over much of the gold-bearing Witwatersrand Basin, and the impact event was integral to the preservation of this exceptional resource.



Schematic geological map of the Vredefort Dome. Source: W.U. Reimold.

RIES CRATER

GERMANY



UNESCO Global Geopark

Panoramic view of the Ries crater with the town of Nördlingen in the central part (Geopark Ries, Photographer Fotostudio Herzig).

ONE OF THE BEST PRESERVED CRATERS WORLDWIDE DISPLAYING MANY IMPACT FEATURES, WHICH CAN BE STUDIED IN AN EASILY ACCESSIBLE REGION.

The Ries Crater is very well preserved and displays the different rock types in numerous outcrops. Excursion guides (e.g. Chao *et al.*, 1978; Geopark Ries, 2019), maps and geotouristic infrastructure (trails, guided tours, Rieskrater-Museum) are excellent. The Crater is an important training area for space missions. In 1970 NASA conducted

field exercises in rock identification for the astronauts of Apollo 14 and 17 missions. To this day, the Ries is a port of call for the astronauts of the European Space Agency (ESA). Results of recent investigations are important for the interpretation of extraterrestrial impact craters, especially on Mars.

SITE 198

GEOLOGICAL PERIOD	Miocene
LOCATION	Nördlinger Ries, Bavaria / Baden-Württemberg, Germany 48°53'03"N 010°33'25"E
MAIN GEOLOGICAL INTEREST	Impact structures and extraterrestrial rocks History of geosciences



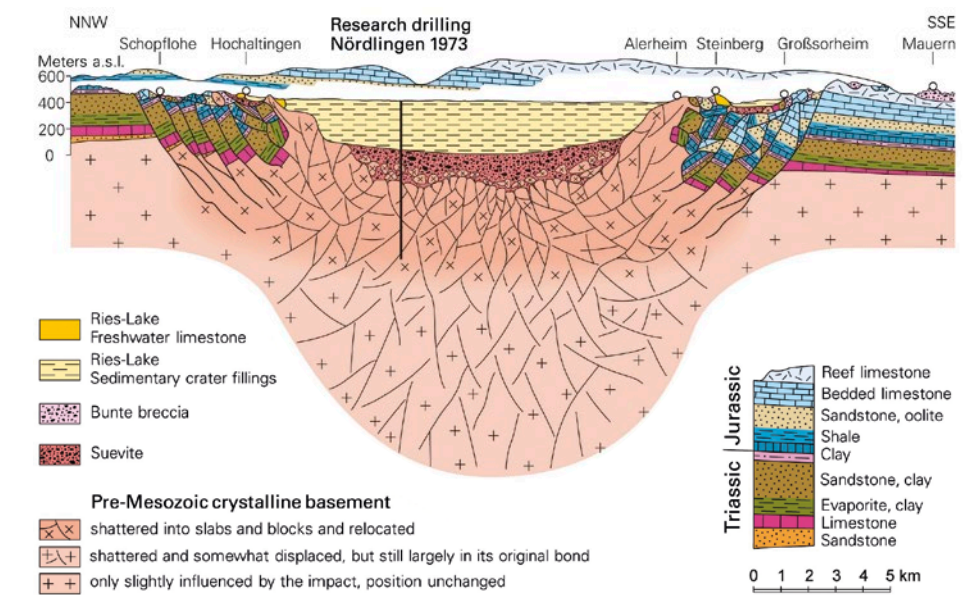
Suevite with degassing-pipe (left) in contact with banked upper jurassic limestones (right) in the quarry Altenbürg (Geopark Ries, Photographer Fabian Weiß).

Geological Description

The Nördlinger Ries is a depression 25 meters wide and up to 150 meters deep embedded in the Swabian-Franconian Cuesta Landscape. The bottom today is a plain created by post-impact Ries-Lake sediments and a Pleistocene loess veneer. The structure belongs to the class of "complex" impact craters in which uplifts form an inner ring (Stöffler *et al.*, 2013). Originally the impact of a 1 kilometer asteroid created a primary crater 11 kilometers wide that subsequently was modified by crater floor uplift and marginal collapse ("megablock zone"), which enlarged the crater. As in very few cases on Earth, most of the blanket of ejected masses is preserved. Different rock types are existent, which have been modified or created by the impact. "Bunte breccia" is a polymict breccia with fragments of all stratigraphic, predominantly Mesozoic, units. Polymict crystalline breccias consist of fragments of the crystalline basement. Most characteristic is the iconic "suevite", an impact breccia composed of rock and mineral fragments with "glass bombs" of crystalline basement melt. It was deposited from the ejecta plume, a hot, glowing cloud. Because of its similarity

with volcanic tuff, the Ries structure formerly was interpreted to have been formed by a kind of volcanic explosion.

Geological Cross section of the Ries crater with reconstructed pre-impact landsurface (Bavarian Environment Agency (LfU)).



Scientific research and tradition

There are hundreds of publications about the Ries. Gümbel (1870) provided the first detailed study. The impact origin was demonstrated by Chao and Shoemaker (1961). Research drilling was conducted in 1973. The crater filling was studied by Arp *et al.* (2021). The city of Nördlingen operates an Impact Research Center.

LAKE BOSUMTWI IMPACT CRATER

GHANA



Aerial overview of the Bosumtwi impact structure, Ghana.

BOSUMTWI IS THE YOUNGEST WELL PRESERVED COMPLEX IMPACT STRUCTURE KNOWN ON EARTH AND THE SOURCE OF THE IVORY COAST TEKTITES.

The Bosumtwi impact crater in Ghana is arguably the best-preserved complex young impact structure known on Earth. It displays a pronounced rim and is almost completely filled by Lake Bosumtwi, a hydrologically closed basin. It is the source crater of one of the four traditional tektite strewn fields, the Ivory Coast field. Besides

being of local spiritual interest, the crater lake contains sediments that document the regional paleoclimate of the last million years, and it is a economic source of fish and tourism. It is a striking geographical feature with potential for outreach and education.

SITE 199

GEOLOGICAL PERIOD	Pleistocene
LOCATION	Ashanti Province, Ghana 06°32'00"N 001°25'00"W
MAIN GEOLOGICAL INTEREST	Impact structures and extraterrestrial rocks History of geosciences



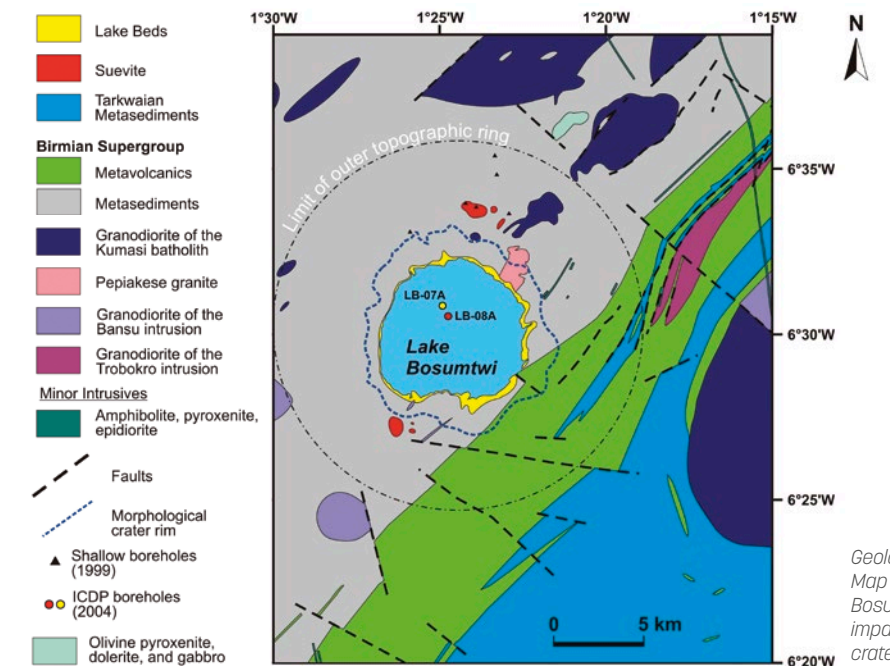
Outcrop of polymict impact breccia (suevite) north of crater rim at Bosumtwi.

Geological Description

Bosumtwi is the largest young impact structure currently known on Earth and is associated with one of only four known tektite strewn fields, the Ivory Coast field. It has an age of 1.07 Ma and a rim to rim diameter of about 10.5 kilometers. Bosumtwi is located in

the Ashanti Region of Ghana. The Ivory Coast tektite strewn field extends beyond the land, as microtektites have been found in deep-sea cores off the coast of West Africa. Age and geochemical data confirm that these tektites were generated in the Bosumtwi impact event.

The well-preserved complex impact structure displays a pronounced rim, is almost completely filled by the Lake Bosumtwi, which has a diameter of ca. 8.5 kilometer. It is surrounded by a slight near-circular depression and an outer ring of minor topographic highs about 20 kilometers in diameter. The crater is excavated in 2 Ga old metamorphosed crystalline rocks. The first suggestion that Bosumtwi might be of impact origin came in 1931, and confirming evidence has been described from the 1960s in studies of high-temperature minerals, shock metamorphism, and meteoritic components in impact rocks and tektites. The lake sediments contain an important 1-Myr paleoclimatic record. The crater was extensively drilled in 2004.



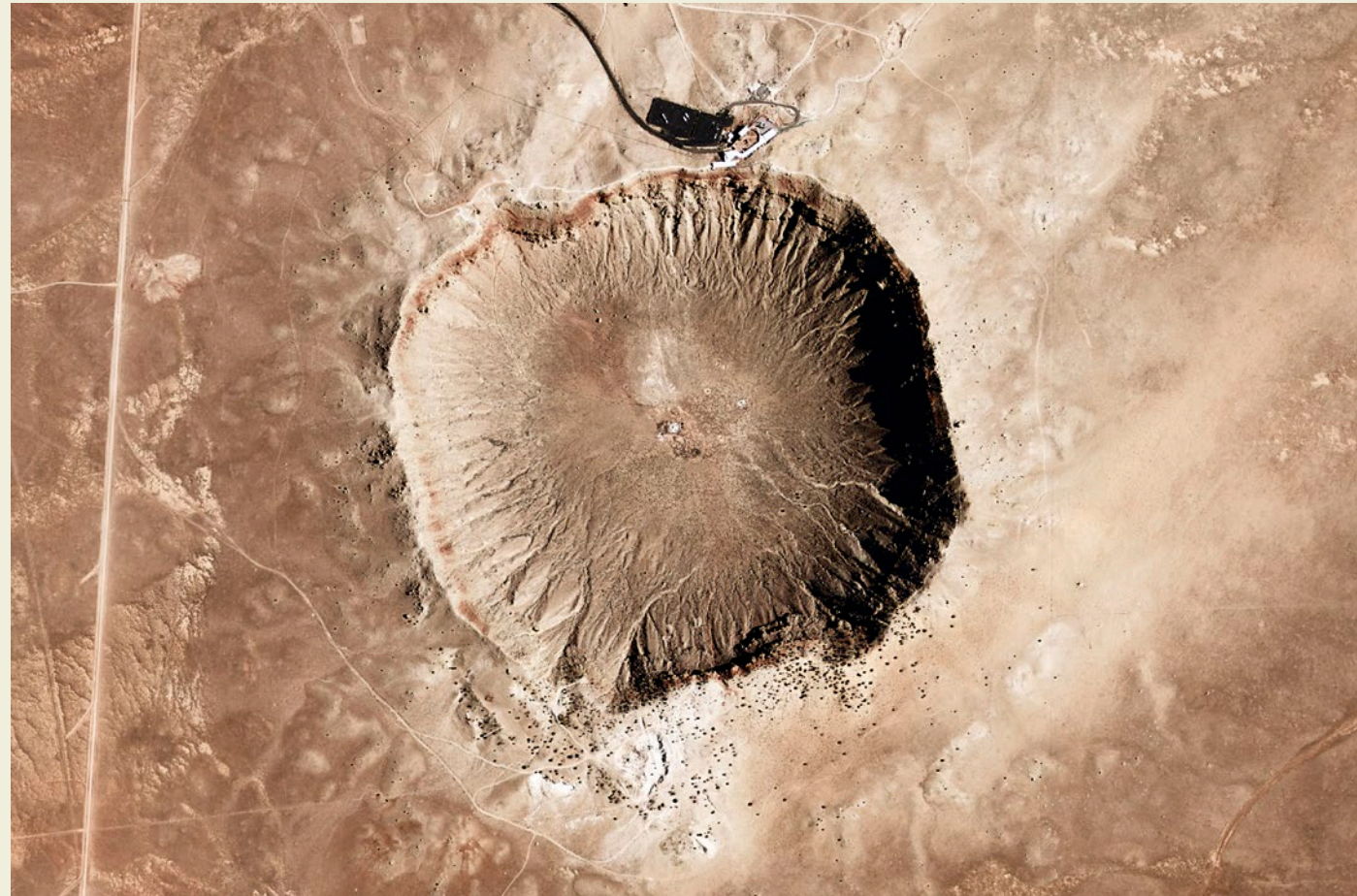
Geological Map of the Bosumtwi impact crater area.

Scientific research and tradition

Bosumtwi has been scientifically studied for almost a century and was the location of a major International Continental Scientific Drilling Program (ICDP) drilling project in 2004, for sediment (paleoclimate) and impact research. It is one of only 20 confirmed impact structures in Africa, and one of the best preserved.

THE BARRINGER METEORITE CRATER

UNITED STATES OF AMERICA



Satellite image of Meteor Crater. Credit: NASA Earth Observatory.

THE BARRINGER METEORITE CRATER AKA "METEOR CRATER" IS ONE OF THE BEST PRESERVED AND EXPOSED METEORITE IMPACT CRATERS ON EARTH.

Barringer Crater, also known as Meteor Crater, is located in northern Arizona 60 kilometers east of Flagstaff. This is arguably the best-preserved and best-exposed meteorite impact crater on Earth and is considered the type locality on Earth of a simple impact crater. It was one of the first geological structures to be proposed as

having been formed by the impact of an extraterrestrial object with the Earth - by Daniel M. Barringer in 1903. Subsequent studies of Meteor Crater played an important role in the recognition of shock metamorphism and our understanding of impact melting.

GEOLOGICAL PERIOD

Holocene

LOCATION

Arizona, United States of America
35°01'41"N
111°01'24"W

MAIN GEOLOGICAL INTEREST

Impact structures and extraterrestrial rocks
History of geosciences

SITE 200



A panorama looking in to the interior of Meteor Crater. Credit: G. Osinski.

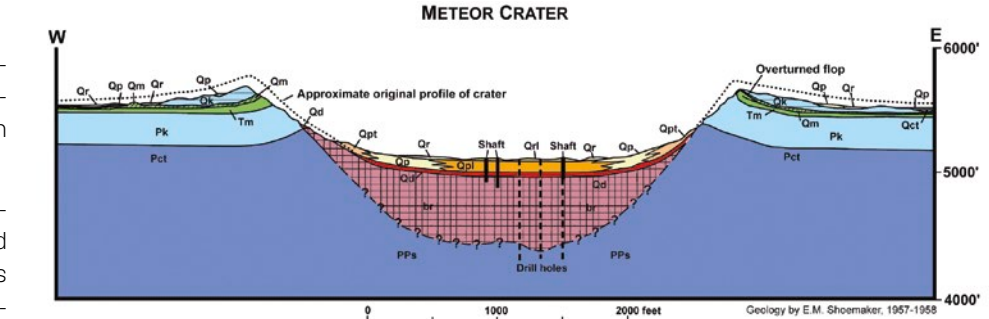
Geological Description

Meteor Crater formed ~50,000 years ago from the collision of an iron asteroid ~30-50 meters in diameter into flat-lying sedimentary rocks of the Colorado Plateau. These target rocks were, from oldest to youngest, the Coconino Sandstone (sandstone), the Toroweap Formation (limestone), and the Kaibab Formation (dolostone), all of Permian age, and the youngest rocks exposed at the surface - then and today - the Triassic Moenkopi Formation.

Fragments of the projectile have been discovered and are known as the Canyon Diablo Meteorite, named after the nearby Cañon Diablo.

Meteor Crater is classed as a simple impact crater. It possesses a bowl-shaped crater 1,200 meters across and 170 meters deep. Its rim rises 45 meters above the surrounding plains. Buried beneath a few tens of meters of sediment is a lens of crater-fill impactites, comprising impact breccias with minor amounts of admixed shock-melted materials; these melts are typically mixtures of the sedimentary target rocks and the iron meteorite projectile. The rim of Meteor Crater is composed of uplifted and overturned target rocks overlain by blocks and breccias that together constitute the impact ejecta blanket.

Geological cross-section of Meteor Crater. Credit: Kring (2017).



Qr - Recent alluvium

Qrl - Recent playa beds

Qp - Pleistocene alluvium

Qpl - Pleistocene lake beds

Qpt - Pleistocene talus

Qm - mixed debris from Coconino, Toroweap, Kaibab, and Moenkopi formations; includes lechatelierite and meteoritic material

Qd - debris from Coconino and Toroweap formations

Qk - debris from Kaibab limestone

Qct - debris from Moenkopi formation

br - breccia (includes lechatelierite and meteoritic material)

Tm - Moenkopi formation (Triassic)

Pk - Kaibab limestone (Permian)

Pct - Coconino and Toroweap formations (Permian)

PPs - Supai formation (Permian and Pennsylvanian)

REFERENCES

I. HISTORY OF GEOSCIENCES

101. Arduino's lithostratigraphical sequence of the Agno Valley

Arduino, G. (1758) 'Representation of the strata of different species of rocks, observed on right and left of river Agno, from Montecchio Maggiore as far as the highest summits of the Alps above Recoaro, in my journey of 19.20.21.22 and 23. October 1758 - of which strata hills, mounts and mountains are composed'. manuscript in Biblioteca Civica (Public Library) of Verona (Italy), Fondo G.Arduino, b.760, IV.c.11 [45 x 30 cm / 18 x 12 in].

Barbieri, G. et al. (1980) 'Note illustrative della carta geologica dell'area di Recoaro alla scala 1:20.000', *Memorie di scienze geologiche*, pp. 23-52 (with 1 geological map and 1 table of cross sections).

De Zanche, V. and Mietto, P. (1981) 'Review of the Triassic sequence of Recoaro (Italy) and related problems', *Rendiconti della Società Geologica Italiana*, 4, pp. 25-28.

Ell, T. (2011) 'Two Letters of Signor Giovanni Arduino, Concerning His Natural Observations: First Full English Translation. Part 1', *Earth Sciences History*. Edited by D. Oldroyd, 30(2), pp. 267-286. Available at: <https://doi.org/10.17704/eshi.31.2.c2q4076006wn7751>.

Ell, T. (2012) 'Two Letters of Signor Giovanni Arduino, Concerning His Natural Observations: First Full English Translation. Part 2', *Earth Sciences History*. Edited by D. Oldroyd, 31(2), pp. 168-192. Available at: <https://doi.org/10.17704/eshi.31.2.c2q4076006wn7751>.

Gibbard, P.L. (2019) 'Giovanni Arduino - the man who invented the Quaternary', *Quaternary International*, 500, pp. 11-19. Available at: <https://doi.org/10.1016/j.quaint.2019.04.021>.

Vaccari, E. (2006) 'The "classification" of mountains in eighteenth century Italy and the lithostratigraphic theory of Giovanni Arduino (1714-1795)', in G.B. Vai, W. Glen, and E. Caldwell (eds) *The Origins of Geology in Italy*. Geological Society of America, p. 0. Available at: [https://doi.org/10.1130/2006.2411\(10\)](https://doi.org/10.1130/2006.2411(10)).

102. Cavanham Ferry and Llanstephan Quarries

Geikie, S.A. (1875) *Life of Sir Roderick I. Murchison, Bart., K. C. B., F. R. S.; Sometime Director-general of the Geological Survey of the United Kingdom. Based on his Journals and Letters with Notices of his Scientific Contemporaries and a Sketch of the Rise and Growth of Palaeozoic Geology in Britain (2 vols)*. London: John Murray.

Hawley, D. (1997) "The first true Silurian": an evaluation of the site of Murchison's discovery of the Silurian', *Proceedings of the Geologists' Association*, 108(2), pp. 131-140. Available at: [https://doi.org/10.1016/S0016-7878\(97\)80035-1](https://doi.org/10.1016/S0016-7878(97)80035-1).

Murchison, R.I. (1831) *Field Notebook. No. 2, Murchison papers*. LDGSL/839/58, Geological Society of London Archives. (Murchison's field section, extracted from page 7 is © Geological Society of London, reproduced with permission).

Murchison, R.I. (1839) *The Silurian System (2 vols)*. London: John Murray.

Secord, J.A. (1986) *Controversy in Victorian Geology: The Cambrian-Silurian Dispute*. Princeton University Press. Available at: <https://www.jstor.org/stable/j.ctt7zv9kj>.

Thackray, J.C. (1978) 'R. I. Murchison's Silurian System (1839)', *Journal of the Society for the Bibliography of Natural History*, 9(1), pp. 61-73. Available at: <https://doi.org/10.3366/jsbnh.1978.9.1.61>.

103. Jurassic Coast: Lyme Regis

Callomon, J.H. and Cope, J.C.W. (1995) 'The Jurassic Geology of Dorset.', in P.D. Taylor (ed.) *Field Geology of the British Jurassic*. Geological Society, London, pp. 51-103.

Gallois, R. (2019) 'The stratigraphy of the Permo-Triassic rocks of the Dorset and East Devon Coast World Heritage Site, U.K.', *Proceedings of the Geologists' Association*, 130(3), pp. 274-293. Available at: <https://doi.org/10.1016/j.pgeola.2018.01.006>.

Jurassic Coast Trust (2021) *The Jurassic Coast Collection: year 1 report*, p. 135. Available at: <https://indd.adobe.com/view/06b9ab57-534b-4997-89b3-2d7c1d3cb27b>.

Mortimore, R.N. (2019) 'Late Cretaceous stratigraphy, sediments and structure: Gems of the Dorset and East Devon Coast World Heritage Site (Jurassic Coast), England', *Proceedings of the Geologists' Association*, 130(3), pp. 406-450. Available at: <https://doi.org/10.1016/j.pgeola.2018.05.008>.

Simms, M.J. et al. (2004) *British Lower Jurassic Stratigraphy*. Peterborough: Joint Nature Conservation Committee (Geological conservation review series, 30).

104. Metamorphic Barrow Zones in Scottish Highlands

Barrow, G. (1912) 'On the geology of lower dee-side and the southern highland border', *Proceedings of the Geologists' Association*, 23(5), pp. 274-311. Available at: [https://doi.org/10.1016/S0016-7878\(12\)80018-6](https://doi.org/10.1016/S0016-7878(12)80018-6).

Evans, B.W. (ed.) (2007) *Landmark Papers 3: Metamorphic Petrology*. Twickenham, UK: Mineralogical Society of Great Britain and Ireland.

Tilley, C.E. (1925) 'A Preliminary Survey of Metamorphic Zones in the Southern Highlands of Scotland', *Quarterly Journal of the Geological Society of London*, 81(1-4), pp. 100-112. Available at: <https://doi.org/10.1144/GSL.JGS.1925.081.01-04.05>.

Viate, D.R. et al. (2013) 'Timing and heat sources for the Barrovian metamorphism, Scotland', *Lithos*, 177, pp. 148-163. Available at: <https://doi.org/10.1016/j.lithos.2013.06.009>.

Vorhies, S.H. and Ague, J.J. (2011) 'Pressure-temperature evolution and thermal regimes in the Barrovian zones, Scotland', *Journal of the Geological Society*, 168, pp. 1147-1166. Available at: <https://doi.org/10.1144/0016-76492010-073>.

Weller, O.M. et al. (2013) 'Quantifying Barrovian metamorphism in the Danba Structural Culmination of eastern Tibet', *Journal of Metamorphic Geology*, 31(9), pp. 909-935. Available at: <https://doi.org/10.1111/jmg.12050>.

105. Contact metamorphic rocks of Orijärvi

Eskola, P. (1914) 'On the petrology of the Orijärvi region in southwestern Finland', *Bulletin de la Commission géologique de Finlande*, 40, p. 277.

Eskola, P. (1915) 'On the relations between the chemical and mineralogical composition in the metamorphic rocks of the Orijärvi region', *Bulletin de la Commission géologique de Finlande*, 44, pp. 109-145.

Eskola, P. (1920) 'The mineral facies of rocks', *Norsk Geologisk Tidsskrift*, 6, pp. 143-194.

Evans, B.W. (ed.) (2007) *Landmark Papers 3: Metamorphic Petrology*. Twickenham, UK: Mineralogical Society of Great Britain and Ireland.

Goldschmidt, V.M. (1911) *Die kontaktmetamorphose im Kristianiagebiet*. Kristiania: In kommission bei J. Dybwad (Videnskapselskapets skrifter. I. Mat.-naturv. klasse 1911, no. 1).

Kara, J. et al. (2018) '190-188 Ga arc magmatism of central Fennoscandia: geochemistry, U-Pb geochronology, Sm-Nd and Lu-Hf isotope systematics of plutonic-volcanic rocks from southern Finland', *Geological Acta*, 16(1), pp. 1-XIV.

Schneiderman, J.S. and Tracy, R.J. (1991) 'Petrology of orthoamphibole-cordierite gneisses from the Orijärvi area, southwest Finland', *American Mineralogist*, 76(5-6), pp. 942-955.

106. Durbuy Anticline

Dejonghe, L. and Jumeau, F. (2007) *Les plus beaux rochers de Wallonie - Géologie et Petite histoire*. (Collection Geosciences du Service Géologique de Belgique). Available at: <https://www.naturalsciences.be/fr/science/do/94/page/1494>.

D'Omalius d'Halloy, J.B.J. (1807) 'Notice sur la disposition des couches du coteau de Durbuy', *Journal des Mines*, 21, pp. 475-480.

Groessens, E. and Groessens-Van Dyck, M.-C. (2007) 'Two Hundred Years of Geological Mapping in Belgium, From D'Omalius D'halloy to the Belgian Federal State', *Earth Sciences History*, 26(1), pp. 75-84. Available at: <https://doi.org/10.17704/eshi.26.1.80j02357x222n732>.

107. Vesuvius volcano

Arrighi, S., Principe, C. and Rosi, M. (2001) 'Violent strombolian and subplinian eruptions at Vesuvius during post-1631 activity', *Bulletin of Volcanology*, 63(2), pp. 126-150. Available at: <https://doi.org/10.1007/s004450100130>.

Consiglio Nazionale delle Ricerche (no date) 'Historical Bibliography of Italian Active Volcanoes - BIBV', *BIBV*. Available at: http://geca-cnr.ge.imati.cnr.it/pisa/vulcani/make_home_page.php?status=startd.

Principe, C. et al. (2004) 'Chronology of Vesuvius' activity from A.D. 79 to 1631 based on archeomagnetism of lavas and historical sources', *Bulletin of Volcanology*, 66(8), pp. 703-724. Available at: <https://doi.org/10.1007/s00445-004-0348-8>.

Rosi, M., Principe, C. and Vecchi, R. (1993) 'The 1631 Vesuvius eruption. A reconstruction based on historical and stratigraphical data', *Journal of Volcanology and Geothermal Research*, 58(1), pp. 151-182. Available at: [https://doi.org/10.1016/0377-0273\(93\)90106-2](https://doi.org/10.1016/0377-0273(93)90106-2).

Sbrana, A. et al. (2020) 'Volcanic evolution of the Somma-Vesuvius Complex (Italy)', *Journal of Maps*, 16(2), pp. 137-147. Available at: <https://doi.org/10.1080/17445647.2019.1706653>.

Sigurdsson, H. et al. (1985) 'The eruption of Vesuvius in AD 79', *National Geographic Research*, 1, pp. 332-387.

108. Scheibenberg lava flow

Deutsche Geologische Gesellschaft Geologische Vereinigung DGGV (2023) 'Der Scheibenberg - Digital Geology', 15 May. Available at: <https://digitalgeology.de/der-scheibenberg>.

Fritscher, B. (1991) *Vulkanismusstreit und Geochemie: die Bedeutung der Chemie und des Experiments in der Vulkanismus-Neptunismus-Kontroverse*. Stuttgart: F. Steiner.

Guntau, M. (1984) *Abraham Gottlob Werner. Biographien hervorragender Naturwissenschaftler, Techniker und Mediziner*. B. G. Teubner Leipzig 1984 (Bd. 75).

Kölbl-Ebert, M. (2001) 'Abraham Gottlob Werner's conflicting images: thoughts inspired by special exhibitions for his 250th anniversary', *Neues Jahrbuch für Geologie und Paläontologie - Monatshefte*, pp. 277-297. Available at: <https://doi.org/10.1127/njpm/2001/2001/277>.

Sebastian, U. (2013) *Die Geologie des Erzgebirges*. Berlin, Heidelberg: Springer. Available at: <https://doi.org/10.1007/978-3-8274-2977-3>.

Werner, A.G. (1788) 'Bekanntmachung einer am Scheibenberg-Hügel über die Entstehung des Basalts gemachten Entdeckung', *Bergmännisches Journal*, 2(1), pp. 845-907.

109. Montagne Pelée volcano

Boudon, G. and Balcone-Boissard, H. (2021) 'Volcanological evolution of Montagne Pelée (Martinique): A textbook case of alternating Plinian and dome-forming eruptions', *Earth-Science Reviews*, 221, p. 103754. Available at: <https://doi.org/10.1016/j.earscirev.2021.103754>.

Germa, A., Lahitte, P. and Quidelleur, X. (2015) 'Construction and destruction of Mont Pelée volcano: Volumes and rates constrained from a geomorphological model of evolution', *Journal of Geophysical Research: Earth Surface*, 120(7), pp. 1206-1226. Available at: <https://doi.org/10.1002/2014JF003355>.

Lacroix, A. (1904) *La Montagne Pelée et ses éruptions*. Paris: Masson.

Le Friant, A. et al. (2003) 'Large-scale flank collapse events during the activity of Montagne Pelée, Martinique, Lesser Antilles', *Journal of Geophysical Research: Solid Earth*, 108(B1). Available at: <https://doi.org/10.1029/2001JB001624>.

Westercamp, D. et al. (1989) 'Carte géologique à 1/50 000 de la Martinique'. BRGM, 246 p.

110. Oligocene Laccoliths and Sedimentary Rock Domes of the Henry Mountains

Gilbert, G.K. (1877) *Report on the geology of the Henry Mountains, Monograph*. U.S. Government Printing Office. Available at: <https://doi.org/10.3133/70039916>.

Hunt, C.B. (1988) *Geology of the Henry Mountains, Utah, as recorded in the notebooks of G. K. Gilbert, 1875–76*. Geological Society of America. Available at: <https://doi.org/10.1130/MEM167>.

Jackson, M.D. and Pollard, D.D. (1988) 'The laccolith-stock controversy: New results from the southern Henry Mountains, Utah', *GSA Bulletin*, 100(1), pp. 117–139. Available at: [https://doi.org/10.1130/0016-7606\(1988\)100<0117:TLSCNR>2.3.CO;2](https://doi.org/10.1130/0016-7606(1988)100<0117:TLSCNR>2.3.CO;2).

Jackson, M.D. and Pollard, D.D. (1990) 'Flexure and faulting of sedimentary host rocks during growth of igneous domes, Henry Mountains, Utah', *Journal of Structural Geology*, 12(2), pp. 185–206.

Pollard, D.D. and Johnson, A.M. (1973) 'Mechanics of growth of some laccolithic intrusions in the Henry mountains, Utah, II: Bending and failure of overburden layers and sill formation', *Tectonophysics*, 18(3), pp. 311–354. Available at: [https://doi.org/10.1016/0040-1951\(73\)90051-6](https://doi.org/10.1016/0040-1951(73)90051-6).

Pollard, D.D. and Martel, S.J. (2020) *Structural Geology: A Quantitative Introduction*. Cambridge University Press.

111. Marua Falls

Bolt, B.A. (1987) '50 years of studies on the inner core', *Eos, Transactions American Geophysical Union*, 68(6), pp. 73–81. Available at: <https://doi.org/10.1029/E0068i006p00073-01>.

Bolt, B.A. and Hjortenberg, E. (1994) 'Memorial essay: Inge Lehmann (1888–1993)', *Bulletin of the Seismological Society of America*, 84(1), pp. 229–233. Available at: <https://doi.org/10.1785/BSSA0840010229>.

Brush, S.G. (1980) 'Discovery of the Earth's core', *American Journal of Physics*, 48(9), pp. 705–724. Available at: <https://doi.org/10.1119/1.12026>.

Hancox, G.T. et al. (2016) *Landslides caused by the MS 7.8 Murchison earthquake of 17 June 1929 in northwest South Island, New Zealand. Lower Hutt, N.Z. GNS Science report 2015/42*. GNS Science, p. 131 pp. + 4 maps.

Kölbl-Ebert, M. (2001) 'Inge Lehmann's paper: "P"'(1936)', *Episodes Journal of International Geoscience*, 24(4), pp. 262–267. Available at: <https://doi.org/10.18814/epiugs/2001/v24i4/007>.

Lehmann, I. (1936) 'P', *Bureau Central Séismologique International Strasbourg: Publications du Bureau Central Scientifiques*, 14, pp. 87–115.

112. Mer de Glace

Deline, P. (2005) 'Change in surface debris cover on Mont Blanc massif glaciers after the "Little Ice Age" termination', *The Holocene*, 15(2), pp. 302–309. Available at: <https://doi.org/10.1191/0959683605hl809rr>.

Le Roy, M. et al. (2015) 'Calendar-dated glacier variations in the western European Alps during the Neoglacial: the Mer de Glace record, Mont Blanc massif', *Quaternary Science Reviews*, 108, pp. 1–22. Available at: <https://doi.org/10.1016/j.quascirev.2014.10.033>.

Nussbaumer, S., Zumbühl, H. and Steiner, D. (2007) 'Fluctuations of the Mer de Glace (Mont Blanc area, France) AD 1500–2050: an interdisciplinary approach using new historical data and neural network simulations', *Zeitschrift für Gletscherkunde und Glazialgeologie*, 40, pp. 1–183.

Nussbaumer, S.U. et al. (2012) *Mer de Glace. Art et science, Mer de Glace. Art et science*. Edited by: Nussbaumer, Samuel U; Deline, Philip; Vincent, Christian; Zumbühl, Heinz J (2012). *Chamonix: Atelier Esope*. Chamonix: Atelier Esope. Available at: <https://www.zora.uzh.ch/id/eprint/85505/>.

Peyaud, V. et al. (2020) 'Numerical modeling of the dynamics of the Mer de Glace glacier, French Alps: comparison with past observations and forecasting of near-future evolution', *The Cryosphere*, 14(11), pp. 3979–3994. Available at: <https://doi.org/10.5194/tc-14-3979-2020>.

Vincent, C. et al. (2019) 'Déclin des deux plus grands glaciers des Alpes françaises au cours du XXI^e siècle : Argentière et Mer de Glace', *La Météorologie*, 106, pp. 49–58. Available at: <https://doi.org/10.4267/2042/70369>.

113. Esmark Moraine and Otto Tank's Moraine

Esmark, J. (1824) 'Bidrag til vor Jordklodes Historie', *Magazin for Naturvidenskaberne (Anden Aargangs første Bind, Første Heft)*, 3, pp. 28–49.

Esmark, J. (1826) 'Remarks tending to explain the Geological History of the Earth', *The Edinburgh New Philosophical Journal*, 2 [First part October–December 1826], pp. 107–121.

Hestmark, G. (2017) *Istdagens Oppdager. Jens Esmark, pioneren i Norges fjellverden*. Oslo: Kagge Forlag.

Hestmark, G. (2018) 'Jens Esmark's mountain glacier traverse 1823 – the key to his discovery of Ice Ages', *Boreas*, 47(1), pp. 1–10. Available at: <https://doi.org/10.1111/bor.12260>.

Krüger, T. (2013) *Discovering the Ice Ages: International Reception and Consequences for a Historical Understanding of Climate*. Leiden, Brill. Available at: <https://brill.com/display/title/22701>.

Worsley, P. (2006) 'Jens Esmark, Vassryggen and early glacial theory in Britain', *Mercian Geologist*, 16, pp. 161–172.

114. The Parallel Roads of Glen Roy

Agassiz, L. (1840) 'On glaciers, and the evidence of their having once existed in Scotland, Ireland, and England', in *Proceedings of the Geological Society of London*, pp. 327–332.

Brazier, V. et al. (2017) 'The Parallel Roads of Glen Roy, Scotland: geoconservation history and challenges', *Proceedings of the Geologists' Association*, 128(1), pp. 151–162. Available at: <https://doi.org/10.1016/j.pgeola.2016.11.008>.

Palmer, A.P. et al. (2020) 'A revised chronology for the growth and demise of Loch Lomond Readvance ("Younger Dryas") ice lobes in the Lochaber area, Scotland', *Quaternary Science Reviews*, 248, p. 106548. Available at: <https://doi.org/10.1016/j.quascirev.2020.106548>.

Palmer, A.P. (2021) 'Glen Roy and Glen Spean', in C.K. Ballantyne and J.E. Gordon (eds) *Landscapes and Landforms of Scotland*. Cham: Springer International Publishing (World Geomorphological Landscapes), pp. 299–315. Available at: https://doi.org/10.1007/978-3-030-71246-4_16.

Palmer, A.P. and Lowe, J.J. (eds) (2017) 'The Lateglacial and early Holocene of Glen Roy, Lochaber western Scottish Highlands. Dynamic responses to rapid climate change in a sensitive Highland landscape', *Special Issue. Proceedings of the Geologists' Association*, 128(1), p. 162. Available at: [https://doi.org/10.1016/S0016-7878\(17\)30010-X](https://doi.org/10.1016/S0016-7878(17)30010-X).

Rudwick, M.J.S. (2017) 'The origin of the Parallel Roads of Glen Roy: a review of 19th Century research', *Proceedings of the Geologists' Association*, 128(1), pp. 26–31. Available at: <https://doi.org/10.1016/j.pgeola.2016.04.001>.

Sissons, J.B. (2017) 'The lateglacial lakes of Glens Roy, Spean and vicinity (Lochaber district, Scottish Highlands)', *Proceedings of the Geologists' Association*, 128(1), pp. 32–41. Available at: <https://doi.org/10.1016/j.pgeola.2015.12.004>.

II. STRATIGRAPHY AND SEDIMENTOLOGY

115. The Mesoproterozoic Belt-Purcell Supergroup

Henderson, T. et al. (2020) *National Park Service geologic type section inventory: Rocky Mountain Inventory & Monitoring Network*. NPS/ROMN/NRR–2020/2215. Fort Collins, Colorado: National Park Service. Available at: <https://doi.org/10.36967/nrr-2283702>.

Lonn, J.D. et al. (2020) 'The Mesoproterozoic Belt Supergroup', *Montana Bureau of Mines Special Publication*, 120, p. 38.

Pratt, B.R. and Rule, R.G. (2021) 'A Mesoproterozoic carbonate platform (lower Belt Supergroup of western North America): Sediments, facies, tides, tsunamis and earthquakes in a tectonically active intracratonic basin', *Earth-Science Reviews*, 217, p. 103626. Available at: <https://doi.org/10.1016/j.earscirev.2021.103626>.

Thornberry-Ehrlich, T.L. (2004) *Glacier National Park: geologic resource evaluation report*. Denver, Colorado : Washington, D.C.: Geologic Resources Division, Natural Resource Program Center ; U.S. Department of the Interior (Natural resource report, NPS/NRPC/GRD/NRR 2004/001). Available at: <http://www.npshistory.com/publications/glac/nrr-2004-001.pdf>.

Walcott, C.D. (1899) 'Pre-Cambrian fossiliferous formations', *GSA Bulletin*, 10(1), pp. 199–244. Available at: <https://doi.org/10.1130/GSAB-10-199>.

Winston, D. and Link, P.K. (1993) 'Middle Proterozoic rocks of Montana, Idaho and eastern Washington: The Belt Supergroup', in J.C. Reed et al. (eds) *The Geology of North America, Precambrian: Conterminous US*. Geological Society of America, Boulder, Colorado, pp. 487–517.

116. The Ordovician section of the Hällekis Quarry

Lindskog, A. et al. (2019) 'Lower–Middle Ordovician carbon and oxygen isotope chemostratigraphy at Hällekis, Sweden: implications for regional to global correlation and palaeoenvironmental development', *Lethaia*, 52(2), pp. 204–219. Available at: <https://doi.org/10.1111/let.12307>.

Lindskog, A. and Eriksson, M.E. (2017) 'Megascopic processes reflected in the microscopic realm: sedimentary and biotic dynamics of the Middle Ordovician "orthoceratite limestone" at Kinnekulle, Sweden', *GFF*, 139(3), pp. 163–183. Available at: <https://doi.org/10.1080/11035897.2017.1291538>.

Schmitz, B. et al. (2019) 'An extraterrestrial trigger for the mid-Ordovician ice age: Dust from the breakup of the L-chondrite parent body', *Science Advances*, 5(9), p. eaax4184. Available at: <https://doi.org/10.1126/sciadv.aax4184>.

Schmitz, B. and Häggström, T. (2006) 'Extraterrestrial chromite in Middle Ordovician marine limestone at Kinnekulle, southern Sweden—Traces of a major asteroid breakup event', *Meteoritics & Planetary Science*, 41(3), pp. 455–466. Available at: <https://doi.org/10.1111/j.1945-5100.2006.tb00473.x>.

Strong, M. et al. (2023) *The Ordovician of Västergötland and Dalarna, Sweden*. (Field guide for the ISOS 14 post-conference excursion. Geologiska Föreningen Specialpublikation, 3).

117. The Ordovician glacial pavements of the Tassili n'Ajjer

Beuf, S. et al. (1971) *Les gres du paleozoïque inférieur au sahara : sedimentation et discontinuités, évolution structurale d'un craton*. Paris: Technip (Science et Technique du Pétrole, 18).

Denis, M. et al. (2010) 'Subglacial deformation and water-pressure cycles as a key for understanding ice stream dynamics: evidence from the Late Ordovician succession of the Djado Basin (Niger)', *International Journal of Earth Sciences*, 99(6), pp. 1399–1425. Available at: <https://doi.org/10.1007/s00531-009-0455-z>.

Deschamps, R., Eschard, R. and Roussé, S. (2013) 'Architecture of Late Ordovician glacial valleys in the Tassili N'Ajjer area (Algeria)', *Sedimentary Geology*, 289, pp. 124–147. Available at: <https://doi.org/10.1016/j.sedgeo.2013.02.012>.

Ghienne, J.-F. et al. (2023) 'The Ordovician record of North and West Africa: unravelling sea-level variations, Gondwana tectonics, and the glacial impact', *Geological Society of London Special Publications*, 533, pp. SP533-2022-213. Available at: <https://doi.org/10.1144/SP533-2022-213>.

Le Heron, D.P. et al. (2022) 'New Perspectives on Glacial Geomorphology in Earth's Deep Time Record', *Frontiers in Earth Science*, 10, p. 870359. Available at: <https://doi.org/10.3389/feart.2022.870359>.

Moreau, J. et al. (2005) '440 Ma ice stream in North Africa', *Geology*, 33(9), pp. 753–756. Available at: <https://doi.org/10.1130/G21782.1>.

118. Carboniferous evolution of The Burren and Cliffs of Moher

Barham, M. et al. (2015) 'Conodonts of the genus *Lochriea* in Ireland and the recognition of the Viséan–Serpukhovian (Carboniferous) boundary', *Lethaia*, 48(2), pp. 151–171. Available at: <https://doi.org/10.1111/let.12096>.

Best, J. and Wignall, P.B. (2016) 'Introduction to the Field Guide', in J. Best and P.B. Wignall (eds) *A Field Guide to the Carboniferous Sediments of the Shannon Basin, Western Ireland*. John Wiley & Sons, Ltd, pp. 1–15. Available at: <https://doi.org/10.1002/9781119257141.ch1>.

Gallagher, S.J. et al. (2006) 'Biostratigraphy, microfacies and depositional environments of upper Viséan limestones from the Burren region, County Clare, Ireland', *Geological Journal*, 41(1), pp. 61–91. Available at: <https://doi.org/10.1002/gj.1033>.

Gill, W.D. (1979) *Syndepositional sliding and slumping in the West Clare Namurian Basin, Ireland*. Dublin: Geological Survey of Ireland (Special paper (Geological Survey of Ireland), 4).

Hodson, F. and Lewarne, G.C. (1961) 'A mid-Carboniferous (namurian) basin in parts of the counties of Limerick and Clare, Ireland', *Quarterly Journal of the Geological Society of London*, 117(1–4), pp. 307–333. Available at: <https://doi.org/10.1144/gsjgs.117.1.0307>.

Wignall, P.B. and Best, J.L. (2004) 'Sedimentology and kinematics of a large, retrogressive growth-fault system in Upper Carboniferous deltaic sediments, western Ireland', *Sedimentology*,

51(6), pp. 1343–1358. Available at: <https://doi.org/10.1111/j.1365-3091.2004.00673.x>.

119. Permian reef complex of the Guadalupe Mountains

Beaubouef, R.T. et al. (1999) *Deep-Water Sandstones, Brushy Canyon Formation, West Texas*. American Association of Petroleum Geologists. Available at: <https://doi.org/10.1306/CE40695>.

Bebout, D.G. and Kerans, C. (eds) (1993) *Guide to the Permian Reef Geology Trail: McKittrick Canyon, Guadalupe Mountains National Park, west Texas*. Austin, Tex: Bureau of Economic Geology, University of Texas at Austin (Guidebook, 26).

Glenister, B.F. et al. (1992) 'The Guadalupian: Proposed International Standard for a Middle Permian Series', *International Geology Review*, 34(9), pp. 857–888. Available at: <https://doi.org/10.1080/00206819209465642>.

Kerans, C. et al. (2021) 'Natural laboratory for studying stratigraphic architecture, facies tract distribution and syndepositional deformation in carbonate ramps and steep-rimmed platforms: Guadalupe Mountains, West Texas and New Mexico', in, pp. 129–178. Available at: <https://doi.org/10.54780/IASFG3/03>.

King, P.B. (1948) *Geology of the Southern Guadalupe Mountains, Texas*. Professional Paper. 215. U.S. Geological Survey. Available at: <https://doi.org/10.3133/pp215>.

Newell, N.D. et al. (1953) *The Permian Reef Complex of the Guadalupe Mountains Region, Texas and New Mexico*. W.H. Freeman, San Francisco. Republished 1973, Hafner Pub. Co. NY.

120. Latemar Triassic carbonate platform

Gaetani, M. et al. (1981) 'Nature and evolution of Middle Triassic carbonate buildups in the Dolomites (Italy)', *Marine Geology*, 44(1), pp. 25–57. Available at: [https://doi.org/10.1016/0025-3227\(81\)90112-2](https://doi.org/10.1016/0025-3227(81)90112-2).

Gianolla, P. et al. (2009) *Nomination of the Dolomites for inscription on the World Natural Heritage List*. UNESCO WHS Nomination. Available at: <http://whc.unesco.org/en/list/1237>.

Goldhammer, R.K., Dunn, P.A. and Hardie, L.A. (1987) 'High frequency glacio-eustatic sealevel oscillations with Milankovitch characteristics recorded in Middle Triassic platform carbonates in northern Italy', *American Journal of Science*, 287(9), pp. 853–892. Available at: <https://doi.org/10.2475/ajs.287.9.853>.

Jacquemyn, C. et al. (2014) 'Dolomitization of the Latemar platform: Fluid flow and dolomite evolution', *Marine and Petroleum Geology*, 55, pp. 43–67. Available at: <https://doi.org/10.1016/j.marpetgeo.2014.01.017>.

Preto, N. et al. (2021) 'The depositional architecture of Latemar and Sella, isolated Triassic microbial platforms of the Dolomites, NE Italy', in V.P. Wright and G. Della Porta (eds) *Field guides to exceptionally exposed carbonate outcrops*. International Association of Sedimentologists, pp. 209–263. Available at: <https://doi.org/10.54780/IASFG3/05>.

121. End-Triassic Flood Basalts at the Old Wife

Blackburn, T.J. et al. (2013) 'Zircon U-Pb geochronology links the end-Triassic extinction with the Central Atlantic Magmatic Province', *Science (New York, N.Y.)*, 340(6135), pp. 941–945. Available at: <https://doi.org/10.1126/science.1234204>.

Olsen, P.E. (1999) 'Giant Lava Flows, Mass Extinctions, and Mantle Plumes', *Science*, 284(5414), pp. 604–605. Available at: <https://doi.org/10.1126/science.284.5414.604>.

Whiteside, J.H. et al. (2007) 'Synchrony between the Central Atlantic magmatic province and the Triassic–Jurassic mass-extinction event?', *Palaeogeography, Palaeoclimatology, Palaeoecology*, 244(1), pp. 345–367. Available at: <https://doi.org/10.1016/j.palaeo.2006.06.035>.

Withjack, M.O., Olsen, P.E. and Schlische, R.W. (1995) 'Tectonic evolution of the Fundy rift basin, Canada: Evidence of extension and shortening during passive margin development', *Tectonics*, 14(2), pp. 390–405. Available at: <https://doi.org/10.1029/94TC03087>.

122. The Jurassic Navajo Sandstone at Coyote Buttes and The Wave

Chan, M.A. et al. (2008) 'Polygonal cracks in bedrock on Earth and Mars: Implications for weathering', *Icarus*, 194(1), pp. 65–71. Available at: <https://doi.org/10.1016/j.icarus.2007.09.026>.

Chan, M.A. and Bruhn, R.L. (2014) 'Dynamic liquefaction of Jurassic sand dunes: processes, Origins, and implications', *Earth Surface Processes and Landforms*, 39(11), pp. 1478–1491. Available at: <https://doi.org/10.1002/esp.3539>.

Loope, D.B. et al. (2008) 'Wind Scour of Navajo Sandstone at the Wave (Central Colorado Plateau, U.S.A.)', *The Journal of Geology*, 116(2), pp. 173–183. Available at: <https://doi.org/10.1086/528902>.

Loope, D.B. and Rowe, C.M. (2003) 'Long-Lived Pluvial Episodes during Deposition of the Navajo Sandstone', *The Journal of Geology*, 111(2), pp. 223–232. Available at: <https://doi.org/10.1086/345843>.

Seiler, W.M. and Chan, M.A. (2014) 'Coloration and Diagenetic History of the Jurassic Navajo Sandstone at Coyote Buttes, Paria Canyon–Vermilion Cliffs Wilderness, Utah and Arizona', in J.S. MacLean, R.F. Biek, and J.E. Huntoon (eds) *Utah's Far South: Utah Geological Association Publication*, pp. 237–257.

123. The Oligocene-Miocene molassic and rock pinacles of Meteora

Desprairies, A. (1979) 'Etude sedimentologique des formations à caractère flysch et molasse, Macédoine, Épire (Grèce)', *Mémoires de la Société géologique de France*, 136, pp. 1–80.

Freriere, J. et al. (2011) 'Tectonic control of the Meteora conglomeratic formations (Mesohellenic basin, Greece)', *Bulletin de la Société Géologique de France*, 182(5), pp. 437–450. Available at: <https://doi.org/10.2113/gssgbull.182.5.437>.

Migón, P. (2020) 'Geomorphology of conglomerate terrains – Global overview', *Earth-Science Reviews*, 208, p. 103302. Available at: <https://doi.org/10.1016/j.earscirev.2020.103302>.

Ori, G.G. and Roveri, M. (1987) 'Geometries of Gilbert-type deltas and large channels in the Meteora Conglomerate, Meso-Hellenic basin (Oligo-Miocene), central Greece', *Sedimentology*, 34(5), pp. 845–859. Available at: <https://doi.org/10.1111/j.1365-3091.1987.tb00808.x>.

Vamvaka, A. et al. (2006) 'Geometry and structural evolution of the Mesohellenic Trough (Greece): a new approach', *Geological Society, London, Special Publications*, 260(1), pp. 521–538. Available at: <https://doi.org/10.1144/GSL.SP.2006.260.01.22>.

Zelilidis, A., Piper, D.J.W. and Kontopoulos, N. (2002) 'Sedimentation and Basin Evolution of the Oligocene-Miocene Mesohellenic Basin,

Greece', *AAPG Bulletin*, 86(1), pp. 161–182. Available at: <https://doi.org/10.1306/61EEDA6C-173E-11D7-8645000102C1865D>.

124. Pliocene cyclostratigraphy of Scala dei Turchi

Beltran, C. et al. (2011) 'Long chain alkenones in the Early Pliocene Sicilian sediments (Trubì Formation – Punta di Maiata section): Implications for the alkenone paleothermometry', *Palaeogeography, Palaeoclimatology, Palaeoecology*, 308(3–4), pp. 253–263. Available at: <https://doi.org/10.1016/j.palaeo.2011.03.017>.

Cita, M.B. and Gartner, S. (1973) 'The stratotype Zanclean foraminiferal and nannofossil biostratigraphy', *Rivista Italiana Paleontologia e Stratigrafia*, 79, pp. 503–558.

Foucault, A. and Mélières, F. (2000) 'Palaeoclimatic cyclicity in central Mediterranean Pliocene sediments: the mineralogical signal', *Palaeogeography, Palaeoclimatology, Palaeoecology*, 158(3), pp. 311–323. Available at: [https://doi.org/10.1016/S0031-0182\(00\)00056-0](https://doi.org/10.1016/S0031-0182(00)00056-0).

Hilgen, F.J. (1991a) 'Astronomical calibration of Gauss to Matuyama sapropels in the Mediterranean and implication for the Geomagnetic Polarity Time Scale', *Earth and Planetary Science Letters*, 104(2), pp. 226–244. Available at: [https://doi.org/10.1016/0012-821X\(91\)90206-W](https://doi.org/10.1016/0012-821X(91)90206-W).

Hilgen, F.J. (1991b) 'Extension of the astronomically calibrated (polarity) time scale to the Miocene/Pliocene boundary', *Earth and Planetary Science Letters*, 107(2), pp. 349–368. Available at: [https://doi.org/10.1016/0012-821X\(91\)90082-S](https://doi.org/10.1016/0012-821X(91)90082-S).

Lourens, L.J. et al. (1996) 'Evaluation of the Plio-Pleistocene astronomical timescale', *Paleoceanography*, 11(4), pp. 391–413. Available at: <https://doi.org/10.1029/96PA01125>.

Sgarrella, F. et al. (1997) 'Paleoceanographic conditions at the base of the Pliocene in the Southern Mediterranean Basin', *Rivista Italiana di Paleontologia e Stratigrafia*, 103. Available at: <https://doi.org/10.13130/2039-4942/5291>.

125. Etosha Pan

Buch, M.W. and Rose, D. (1996) 'Mineralogy and geochemistry of the sediments of the Etosha Pan Region in northern Namibia: a reconstruction of the depositional environment', *Journal of African Earth Sciences*, 22(3), pp. 355–378. Available at: [https://doi.org/10.1016/0899-5362\(96\)00020-6](https://doi.org/10.1016/0899-5362(96)00020-6).

Buch, M.W., Rose, D. and Zöller, L. (1992) 'A TL-calibrated pedostratigraphy of the western lunette dunes of Etosha Pan/ northern Namibia: Palaeoenvironmental implications for the last 140 ka', in K. Heine (ed.) *Palaeoecology of Africa and the surrounding islands*, pp. 129–147.

deMenocal, P.B. (2004) 'African climate change and faunal evolution during the Pliocene–Pleistocene', *Earth and Planetary Science Letters*, 220(1), pp. 3–24. Available at: [https://doi.org/10.1016/S0012-821X\(04\)00003-2](https://doi.org/10.1016/S0012-821X(04)00003-2).

Hipondoka, M. (2005) *The development and evolution of Etosha Pan, Namibia*, [https://opus.bibliothek.uni-wuerzburg/frontdoor/index/index/docId/1195](https://opus.bibliothek.uni-wuerzburg.de/opus4-wuerzburg/frontdoor/index/index/docId/1195). Thesis. University of Wurzburg. Available at: <https://repository.unam.edu.na/handle/11070/1784>.

Miller, R.M., Pickford, M. and Senut, B. (2010) 'The geology, palaeontology and evolution of the Etosha Pan, Namibia: implications for terminal Kalahari deposition.', *South African*

Journal of Geology, 113(3), pp. 307–334. Available at: <https://doi.org/10.2113/gssajg.113.3.307>.

Pickford, M. et al. (2019) 'Update of the Pliocene fauna of the Ekuma Valley, Etosha, Namibia.', *Communications of the Geological Survey of Namibia*, 17, pp. 113–142.

126. Pliocene to Holocene records from Raciška Pećina Cave

Horáček, I. et al. (2007) 'Fossil Vertebrates and Paleomagnetism Update of One of the Earlier Stages of Cave Evolution in the Classical Karst, Slovenia: Pliocene of Črnotiče II Site and Raciška Pećina Cave', *Acta Carsologica*, 36(3). Available at: <https://doi.org/10.3986/ac.v36.i3.179>.

Pruner, P. et al. (2010) 'Magnetostratigraphy and fold tests from Raciška pećina and Pećina v Borštu caves (Classical Karst, Slovenia)', *Studia Geophysica et Geodaetica*, 54(1), pp. 27–48. Available at: <https://doi.org/10.1007/s11200-010-0002-1>.

Sierpień, P. et al. (2021) 'Flowstones from the Raciška Pećina Cave (SW Slovenia) Record 3.2-Ma-Long History', *Geochronometria*, 48, pp. 31–45. Available at: <https://doi.org/10.2478/geochr-2021-0004>.

Zupan Hajna, N. et al. (2020) 'Karst sediments in Slovenia: Plio-Quaternary multi-proxy records', *Quaternary International*, 546, pp. 4–19. Available at: <https://doi.org/10.1016/j.quaint.2019.11.010>.

Zupan Hajna, N. et al. (2021) 'Pliocene to Holocene chronostratigraphy and palaeoenvironmental records from cave sediments: Račiška pećina section (SW Slovenia)', *Quaternary International*, 605–606, pp. 5–24. Available at: <https://doi.org/10.1016/j.quaint.2021.02.035>.

127. Holocene coral reef terraces of Kikaijima Island

Abram, N. et al. (2001) 'Biological response of coral reefs to sea surface temperature variation: evidence from the raised Holocene reefs of Kikai-jima (Ryukyu Islands, Japan)', *Coral Reefs*, 20(3), pp. 221–234. Available at: <https://doi.org/10.1007/s003380100163>.

Garas, K.L., Watanabe, T. and Yamazaki, A. (2023) 'Hydroclimate seasonality from paired coral Sr/Ca and δ¹⁸O records of Kikai Island, Southern Japan: Evidence of East Asian monsoon during mid-to late Holocene', *Quaternary Science Reviews*, 301, p. 107926. Available at: [https://doi.org/](https://doi.org/10.1016/j.quascirev.2022.107926)

128. Shark Bay

Berry, P.F., Bradshaw, S.D. and Wilson, B.R. (eds) (1990) *Research in Shark Bay: report of the France-Australe Bicentenary expedition committee*. Perth, W.A.: Western Australian Museum.

Brocx, M. and Semeniuk, V. (2007) 'Geoheritage and geoconservation - History, definition, scope and scale', *Journal of the Royal Society of Western Australia*, 90, pp. 53–87.

Brocx, M. and Semeniuk, V. (2010) 'Coastal geoheritage: A hierarchical approach to classifying coastal types as a basis for identifying geodiversity and sites of significance in Western Australia', *Journal of the Royal Society of Western Australia*, 93, pp. 81–113.

Logan, B.W. et al. (1970) *Carbonate Sedimentation and Environments, Shark Bay, Western Australia*. Tulsa, Oklahoma: American Association of Petroleum Geologists (Memoir 13). Available at: <https://doi.org/10.1306/M13369>.

Logan, B.W. et al. (1974) *Evolution and Diagenesis of Quaternary Carbonate Sequences, Shark Bay, Western Australia*. Tulsa, Oklahoma: American Association of Petroleum Geologists (Memoir 22). Available at: <https://doi.org/10.1306/M22379>.

Logan, B.W., Read, J.F. and Davies, G.R. (1970) 'History of Carbonate Sedimentation, Quaternary Epoch, Shark Bay, Western Australia', in B.W. Logan et al. (eds) *Carbonate Sedimentation and Environments, Shark Bay, Western Australia*. American Association of Petroleum Geologists, p. 0. Available at: <https://doi.org/10.1306/M13369C2>.

129. Uyuni salt flat

Quezada Cortez, G. and Carvajal Velasco, N. (2022) *El Salar de Uyuni: El depósito evaporítico más grande del mundo*. Available at: <https://gmga.com.br/06-salar-de-uyuni-el-deposito-evaporitico-mas-grande-del-mundo/>.

Risacher, F. and Fritz, B. (1991) 'Quaternary geochemical evolution of the salars of Uyuni and Coipasa, Central Altiplano, Bolivia', *Chemical Geology*, 90(3), pp. 211–231. Available at: [https://doi.org/10.1016/0009-2541\(91\)90101-V](https://doi.org/10.1016/0009-2541(91)90101-V).

Risacher, F. and Fritz, B. (1995) 'Evolucion cuaternaria del salar de Uyuni, Altiplano central, Bolivia.', in P. Ribstein and B. Francou (eds) *Aguas, glaciares y cambios climáticos en los Andes tropicales: conferencias y posters. Aguas, Glaciares y Cambios Climáticos en los Andes Tropicales; Seminario Internacional, La Paz, Bolivia: ORSTOM*, pp. 281–282.

Servant, M. and Fontes, J. (1978) 'Les lacs quaternaires des hauts plateaux des Andes boliviennes: Premières interpretation paleoclimatiques', *Cahiers ORSTOM. Serie Géologie*, 10(1), pp. 9–23.

Sieland, R. (2014) *Hydraulic Investigations of the Salar de Uyuni, Bolivia, FOG - Freiberg Online Geoscience*. Thesis. FOG - Freiberg Online Geoscience. Available at: https://www.researchgate.net/publication/281061345_Hydraulic_Investigations_of_the_Salar_de_Uyuni_Bolivia.

U.S. Geological Survey (2020) *Mineral Commodity Summaries*. U.S. Geological Survey, p. 200. Available at: <https://doi.org/10.3133/mcs2020>.

130. The Dead Sea

Ben-Avraham, Z., Gat, J. and Niemi, T.M. (eds) (1997) *The Dead Sea: the lake and its setting*. Oxford University Press (Oxford)

Monographs on Geology and Geophysics, 36). Available at: <https://cris.tau.ac.il/en/publications/the-dead-sea-the-lake-and-its-setting>.

Enzel, Y., Agnon, A. and Stein, M. (eds) (2006) *New Frontiers in Dead Sea Paleoenvironmental Research*. Geological Society of America (Geological Society of America Special Paper, 401). Available at: <https://doi.org/10.1130/SPE401>.

Lynch, W.F. (1849) *Narrative of the United States' expedition to the river Jordan and the Dead Sea*. Philadelphia: Lea and Blanchard publishing. Available at: <http://archive.org/details/narrativeofunite00lyncrich>.

Stein, M. and Goldstein, S.L. (2020) 'The ICDP Dead Sea deep drilling project – introduction', *Quaternary Science Reviews*, 249, p. 106639. Available at: <https://doi.org/10.1016/j.quascirev.2020.106639>.

131. Mars analog of Lake Salda

Balci, N. et al. (2020) 'Biotic and Abiotic Imprints on Mg-Rich Stromatolites: Lessons from Lake Salda, SW Turkey', *Geomicrobiology Journal*, 37(5), pp. 401–425. Available at: <https://doi.org/10.1080/01490451.2019.1710784>.

Braithwaite, C.J.R. and Zedef, V. (1996) 'Hydromagnesite stromatolites and sediments in an alkaline lake, Salda Golu, Turkey', *Journal of Sedimentary Research*, 66(5), pp. 991–1002. Available at: <https://doi.org/10.1306/D426845F-2B26-11D7-8648000102C1865D>.

Garczynski, B.J. et al. (2019) 'Searching for Potential Biosignatures in Jezero Crater with Mars 2020 – A Spectral Investigation of Terrestrial Lacustrine Carbonate Analogs', in *Ninth International Conference on Mars. LPI Contributions. Ninth International Conference on Mars*, California, p. 6302. Available at: <https://ui.adsabs.harvard.edu/abs/2019LPICo2089.6302G>.

Garczynski, B.J. et al. (2020) 'Investigating the Origin of Carbonate Deposits in Jezero Crater: Mineralogy of a Fluviolacustrine Analog at Lake Salda, Turkey', in *51st Lunar and Planetary Science Conference, held 16–20 March, 2020 at The Woodlands, Texas. LPI Contribution. 51st Annual Lunar and Planetary Science Conference*, p. 2128. Available at: <https://ui.adsabs.harvard.edu/abs/2020LPI....51.2128G>.

Kaiser, J. et al. (2016) 'Sedimentary lipid biomarkers in the magnesium rich and highly alkaline Lake Salda (south-western Anatolia)', *Journal of Limnology*, 75(3), pp. 581–596. Available at: <https://doi.org/10.4081/jlimnol.2016.1337>.

Kazancı, N., Girgin, S. and Dügel, M. (2004) 'On the limnology of Salda Lake, a large and deep soda lake in southwestern Turkey: future management proposals', *Aquatic Conservation: Marine and Freshwater Ecosystems*, 14(2), pp. 151–162. Available at: <https://doi.org/10.1002/aqc.609>.

Russell, M.J. et al. (1999) 'Search for signs of ancient life on Mars: expectations from hydromagnesite microbialites, Salda Lake, Turkey', *Journal of the Geological Society*, 156(5), pp. 869–888. Available at: <https://doi.org/10.1144/gsjgs.156.5.0869>.

III. PALEONTOLOGY

132. Ediacaran fauna of the Nama Group

Germs, G.J.B. (1983) 'Implications of a sedimentary facies and depositional environmental analysis of the Nama Group in South West Africa/Namibia', *Evolution of the Damara Orogen. Special Publication of the Geological Society of South Africa*. Edited by R.M. Miller, [1], pp. 89–114.

Linnemann, U. et al. (2019) 'New high-resolution age data from the Ediacaran–Cambrian boundary indicate rapid, ecologically driven onset of the Cambrian explosion', *Terra Nova*, 31(1), pp. 49–58. Available at: <https://doi.org/10.1111/ter.12368>.

Narbonne, G.M., Saylor, B.Z. and Grotzinger, J.P. (1997) 'The youngest Ediacaran fossils from southern Africa', *Journal of Paleontology*, 71(6), pp. 953–967. Available at: <https://doi.org/10.1017/s002233600035940>.

Penny, A.M. et al. (2014) 'Ediacaran metazoan reefs from the Nama Group, Namibia', *Science*, 344(6191), pp. 1504–1506.

133. The Late Devonian fossil-fish Lagerstätte of Miguasha

Chevrinakis, M., Sire, J.-Y. and Cloutier, R. (2017) 'Unravelling the ontogeny of a Devonian early gnathostome, the "acanthodian" *Triazeugacanthus affinis* (eastern Canada)', *PeerJ*, 5, p. e3969. Available at: <https://doi.org/10.7717/peerj.3969>.

Cloutier, R. (2013) 'Great Canadian Lagerstätten 4. The Devonian Miguasha Biota (Québec): UNESCO World Heritage Site and a Time Capsule in the Early History of Vertebrates', *Geoscience Canada*, pp. 149–163. Available at: <https://doi.org/10.12789/geocanj.2013.40.008>.

Cloutier, R. et al. (2020) 'Elpistostege and the origin of the vertebrate hand', *Nature*, 579(7800), pp. 549–554. Available at: <https://doi.org/10.1038/s41586-020-2100-8>.

Cloutier, R., Proust, J.-N. and Tessier, B. (2011) 'The Miguasha Fossil-Fish-Lagerstätte: A consequence of the Devonian land-sea interactions', *Palaeobiodiversity and Palaeoenvironments*, 91, pp. 293–323. Available at: <https://doi.org/10.1007/s12549-011-0058-0>.

Klug, C. et al. (2021) 'A late-surviving stem-ctenophore from the Late Devonian of Miguasha (Canada)', *Scientific Reports*, 11(1), pp. 1–9. Available at: <https://doi.org/10.1038/s41598-021-98362-5>.

Schultze, H.-P. and Cloutier, R. (eds) (1996) *Devonian Fishes and Plants of Miguasha, Quebec, Canada*. München: Verlag Dr. Friedrich Pfeil.

134. Permian vegetation of the Wuda Fossil Site

Bashforth, A.R. and DiMichele, W.A. (2012) 'Permian Coal Forest offers a glimpse of late Paleozoic ecology', *Proceedings of the National Academy of Sciences*, 109(13), pp. 4717–4718. Available at: <https://doi.org/10.1073/pnas.1203261109>.

Hvistendahl, M. (2012) 'Primeval Land Rises From the Ashes', *Science*, 336, p. 662.

Schmitz, M.D. et al. (2021) 'A volcanic tuff near the Carboniferous–Permian boundary, Taiyuan Formation, North China: Radioisotopic dating and global correlation', *Review of Palaeobotany and Palynology*, 294, p. 104244. Available at: <https://doi.org/10.1016/j.repalbo.2020.104244>.

Wang, J. et al. (2012) 'Permian vegetational Pompeii from Inner Mongolia and its implications for landscape paleoecology and paleobiogeography of Cathaysia', *Proceedings of the National Academy of Sciences*, 109(13), pp. 4927–4932. Available at: <https://doi.org/10.1073/pnas.1115076109>.

Wang, J. et al. (2021) 'Ancient noeggerathialean reveals the seed plant sister group diversified alongside the primary seed plant radiation', *Proceedings of the National Academy of Sciences*, 118(11), p. e2013442118. Available at: <https://doi.org/10.1073/pnas.2013442118>.

Zhou, W. et al. (2019) 'A left-handed fern twiner in a Permian swamp forest', *Current Biology*, 29(22), pp. R1172–R1173. Available at: <https://doi.org/10.1016/j.cub.2019.10.005>.

135. Triassic Dinosaurs and mammalian reptiles from Ischigualasto

Benton, M.J. (1993) 'Late Triassic Extinctions and the Origin of the Dinosaurs', *Science*, 260(5109), pp. 769–770. Available at: <https://doi.org/10.1126/science.260.5109.769>.

Dingwall, P. (2000) *World Heritage Nomination IUCN Technical Evaluation. Ischigualasto Provincial Park-Talampaya National Park (Argentina)*. IUCN, Gland, Switzerland.

Milana, J. and Alcober, O. (1994) 'Modelo tectosedimentario de la cuenca triásica de Ischigualasto (San Juan, Argentina)', *Revista de la Asociación Geológica Argentina*, 49, pp. 217–235.

Sereno, P.C. and Novas, F.E. (1992) 'The Complete Skull and Skeleton of an Early Dinosaur', *Science*, 258(5085), pp. 1137–1140. Available at: <https://doi.org/10.1126/science.258.5085.1137>.

Stipanicic, P. and Bonaparte, J. (1972) 'Cuenca triásica de Ischigualasto-Villa Unión (provincias de San Juan y La Rioja).', in A. Leanza (ed.) *Geología Regional Argentina*. Córdoba: Academia Nacional Ciencias, pp. 507–536.

136. Middle Jurassic dinosaur footprints from the Serras de Aire and Candeeiros

Azeredo, A. (2007) 'Formalização da litostratigrafia do Jurássico Inferior e Médio do Maciço Calcário Estremenho (Bacia Lusitânica)', *Comunicações Geológicas*, 94, pp. 29–51.

Castanera, D. et al. (2016) 'Iberian sauropod tracks through time: Variations in sauropod manus and pes track morphologies', in P. Falkingham, D. Marty, and A. Richter (eds) *Dinosaur tracks - The next steps*. Bloomington, Indiana University Press, pp. 121–137. Available at: https://www.researchgate.net/publication/316516090_Iberian_sauropod_tracks_through_time_Variations_in_sauropod_manus_and_pes_track_morphologies.

Razzolini, N.L. et al. (2016) 'Ichnological evidence of Megalosaurid Dinosaurs Crossing Middle Jurassic Tidal Flats', *Scientific Reports*, 6(1), p. 31494. Available at: <https://doi.org/10.1038/srep31494>.

Santos, V.F. (2016) 'Dinosaur tracksites in the Middle Jurassic of Maciço Calcário Estremenho (west-central Portugal): A geoheritage to be enhanced', 103, pp. 55–58.

Santos, V.F. dos, Moratalla, J.J. and Royo-Torres, R. (2009) 'New Sauropod Trackways from the Middle Jurassic of Portugal', *Acta Palaeontologica Polonica*, 54, pp. 409–422. Available at: <https://doi.org/10.4202/app.2008.0049>.

137. Dashanpu Middle Jurassic Dinosaur Fossils Site

Barrett, P.M., Butler, R.J. and Knoll, F. (2005) 'Small-bodied ornithischian dinosaurs from the Middle Jurassic of Sichuan, China'. Available at: <https://digital.csic.es/handle/10261/12933>.

Chatterjee, S. and Zheng, Z. (2002) 'Cranial anatomy of *Shunosaurus*, a basal sauropod dinosaur from the Middle Jurassic of China', *Zoological Journal of the Linnean Society*, 136(1), pp. 145–169. Available at: <https://doi.org/10.1046/j.1096-3642.2002.00037.x>.

Peng, G.Z. *et al.* (2005) *Jurassic dinosaur faunas in Zigong*. Chengdu: Sichuan People's Publishing house.

Sereno, P.C. and Zhimin, D. (1992) 'The skull of the basal stegosaur *Huayangosaurus taibaii* and a cladistic diagnosis of stegosauria', *Journal of Vertebrate Paleontology*, 12(3), pp. 318–343. Available at: <https://doi.org/10.1080/02724634.1992.10011463>.

Tong, H. *et al.* (2011) 'Middle Jurassic turtles from the Sichuan Basin, China: a review', *Geological Magazine*, 149(4), pp. 675–695. Available at: <https://doi.org/10.1017/S0016756811000859>.

Wang, J. *et al.* (2018) 'Age of Jurassic basal sauropods in Sichuan, China: A reappraisal of basal sauropod evolution', *GSA Bulletin*, 130(9–10), pp. 1493–1500. Available at: <https://doi.org/10.1130/B31910.1>.

138. Upper Jurassic Carnegie Quarry Dinosaur Bone Site

Bilbey, S.A., Kerns, R.L. and Bowman, J.T. (1974) *Petrology of the Morrison Formation, Dinosaur Quarry Quadrangle, Utah*. Salt Lake City: Utah Geological and Mineral Survey, Utah Dept. of Natural Resources (Utah Geological and Mineral Survey Special Studies, 48).

Carpenter, K. (2013) 'History, Sedimentology, and Taphonomy of the Carnegie Quarry, Dinosaur National Monument, Utah', *Annals of Carnegie Museum*, 81(3), pp. 153–232. Available at: <https://doi.org/10.2992/007.081.0301>.

Carpenter, K. (2018) 'Rocky Start of Dinosaur National Monument (USA), The World's First Dinosaur Geoconservation Site', *Geoconservation Research*, 1(1), pp. 1–20. Available at: <https://doi.org/10.30486/gcr.2018.539322>.

Carpenter, K. (2020) 'Hydraulic modeling and computational fluid dynamics of bone burial in a sandy river channel', *Geology of the Intermountain West*, 7, pp. 97–120. Available at: <https://doi.org/10.31711/giw.v7.pp97-120>.

Carpenter, K. (2023) 'Reconstructing the floodplain paleogeography associated with the Quarry River, Dinosaur National Monument, Utah, USA', in J.J. Kirkland, R. Hunt-Foster, and M. Loewen (eds) *The Anatomical Record. 14th Symposium on Mesozoic Terrestrial Ecosystems and Biota*, Salt Lake City, Utah: Utah Department of Natural Resources, pp. 65–67.

Lawton, R. (1977) 'Taphonomy of the dinosaur quarry, Dinosaur National Monument', *Rocky Mountain Geology*, 15(2), pp. 119–126.

139. Early Cretaceous wetland of Las Hoyas

Fregenal Martínez, M.A. and Meléndez Hevia, M.N. (2016) 'Environmental reconstruction: a historical review.', in F.J. Poyato Ariza and Á.D. Buscalioni (eds) *Las Hoyas: A Cretaceous Wetland: A multidisciplinary synthesis after 25 years of research on an exceptional fossil Lagerstätte from Spain*. Friedrich Verlag,

pp. 14–28. Available at: <https://dialnet.unirioja.es/servlet/articulo?codigo=5757674>.

Iniesto, M. *et al.* (2015) 'The Impact of Microbial Mats and Their Microenvironmental Conditions in Early Decay of Fish', *Palaeos*, 30, pp. 792–801. Available at: <https://doi.org/10.2110/palo.2014.086>.

Martin, T. *et al.* (2015) 'A Cretaceous eutrichodont and integument evolution in early mammals', *Nature*, 526(7573), pp. 380–384. Available at: <https://doi.org/10.1038/nature14905>.

Marugán-Lobón, J., Martín-Abad, H. and Buscalioni, Á.D. (2023) 'The Las Hoyas Lagerstätte: a palaeontological view of an Early Cretaceous wetland', *Journal of the Geological Society*, 180(3), pp. jgs2022-079. Available at: <https://doi.org/10.1144/jgs2022-079>.

Navalón, G. *et al.* (2015) 'Soft-tissue and dermal arrangement in the wing of an Early Cretaceous bird: Implications for the evolution of avian flight', *Scientific Reports*, 5(1), p. 14864. Available at: <https://doi.org/10.1038/srep14864>.

Sanz, J.L. *et al.* (1996) 'An Early Cretaceous bird from Spain and its implications for the evolution of avian flight', *Nature*, 382(6590), pp. 442–445. Available at: <https://doi.org/10.1038/382442a0>.

140. Cretaceous Lagerstätten of Cariri Stone

Assine, M. *et al.* (2014) 'Sequências Deposicionais do Andar Alagoas (Aptiano superior) da Bacia do Araripe, Nordeste do Brasil', *Boletim de Geociências - Petrobras*, 22, pp. 3–28.

Kunzmann, L. *et al.* (2022) 'Crato Flora: A 115-Million-Year-Old Window into the Cretaceous World of Brazil', in R. Iannuzzi, R. Rößler, and L. Kunzmann (eds) *Brazilian Paleofloras: From Paleozoic to Holocene*. Cham: Springer International Publishing, pp. 1–40. Available at: https://doi.org/10.1007/978-3-319-90913-4_27.1.

do Nascimento, D.R., da Silva Filho, W.F. and Erthal, F. (2023) 'Crato Lake Deposits. Rocks to Preserve an Extraordinary Fossil Lagerstätte', in R. Iannuzzi, R. Rößler, and L. Kunzmann (eds) *Brazilian Paleofloras: From Paleozoic to Holocene*. Cham: Springer International Publishing, pp. 1–53. Available at: https://doi.org/10.1007/978-3-319-90913-4_28.2.

Neumann, V.H. *et al.* (2003) 'Organic matter composition and distribution through the Aptian–Albian lacustrine sequences of the Araripe Basin, northeastern Brazil', *International Journal of Coal Geology*, 54(1), pp. 21–40. Available at: [https://doi.org/10.1016/S0166-5162\(03\)00018-1](https://doi.org/10.1016/S0166-5162(03)00018-1).

Ponte, F.C. and Ponte Filho, F. (1996) 'Evolução tectônica e classificação da Bacia do Araripe', *Boletim do 4º Simpósio sobre o Cretáceo do Brasil UNESP, Campus de Rio Claro, São Paulo*, pp. 123–133.

Viana, M. and Neumann, V. (2002) 'Membro Crato da Formação Santana, Chapada do Araripe, CE', in C. Schobbenhaus *et al.* (eds) *Sítios Geológicos e Paleontológicos do Brasil*. Brasília: DNPM/CPMR – Comissão Brasileira de Sítios Geológicos e Paleobiológicos (SIGEP), pp. 113–120.

141. The Cretaceous Dinosaur Nesting Grounds of the Willow Creek Anticline

Chin, K. (2007) 'The paleobiological implications of herbivorous dinosaur coprolites from the Upper Cretaceous Two Medicine formation of Montana: Why eat wood?', *PALAIOS*, 22(5), pp. 554–566. Available at: <https://doi.org/10.2110/palo.2006.p06-087r>.

Horner, J.R. and Makela, R. (1979) 'Nest of juveniles provides evidence of family structure among dinosaurs', *Nature*, 282(5736), pp. 296–298. Available at: <https://doi.org/10.1038/282296a0>.

Horner, J.R. and Weishampel, D.B. (1988) 'A comparative embryological study of two ornithischian dinosaurs', *Nature*, 332(6161), pp. 256–257. Available at: <https://doi.org/10.1038/332256a0>.

Varrichio, D.J. *et al.* (1997) 'Nest and egg clutches of the dinosaur *Troodon formosus* and the evolution of avian reproductive traits', *Nature*, 385, pp. 247–250. Available at: <https://doi.org/10.1038/385247a0>.

Weaver, L.N. *et al.* (2021) 'Early mammalian social behaviour revealed by multituberculates from a dinosaur nesting site', *Nature Ecology & Evolution*, 5(1), pp. 32–37. Available at: <https://doi.org/10.1038/s41559-020-01325-8>.

Woodward, H.N. *et al.* (2015) 'Maiasaura, a model organism for extinct vertebrate population biology: A large sample statistical assessment of growth dynamics and survivorship', *Paleobiology*, 41(4), pp. 503–527. Available at: <https://doi.org/10.1017/pab.2015.19>.

142. Whale Valley, Cetacea and Sirenia Eocene fossils of Wadi Al-Hita

Ahmed, E.A. (2006) *Vertebrate paleontological studies on some paleogene outcrops in fayum area, Egypt*. M.Sc. Thesis, Mansoura university, faculty of science, department of geology. Available at: http://srv3.eulc.edu.eg/eulc_v5/Libraries/Thesis/BrowseThesisPages.aspx?fn=PublicDrawThesis&BibID=263758.

Andrews, C.W. (1906) *A descriptive catalogue of the Tertiary Vertebrata of the Fayûm, Egypt*. London: British Museum (Natural hist.). Available at: <http://archive.org/details/descriptivecatal00andr>.

Gingerich, P.D. (1992) 'Marine Mammals (Cetacea and Sirenia) from the Eocene of Gebel Mokattam and Fayum, Egypt: Stratigraphy, Age and Paleoenvironments'. Available at: <http://deepblue.lib.umich.edu/handle/2027.42/48630>.

Gingerich, P.D. *et al.* (1994) 'Cranial Morphology of *Protosiren fraasi* (Mammalia, Sirenia) from the Middle Eocene of Egypt: A New Study Using Computed Tomography'. Available at: <http://deepblue.lib.umich.edu/handle/2027.42/48641>.

King, C., Underwood, C. and Steurbaut, E. (2014) 'Eocene stratigraphy of the Wadi Al-Hitan World Heritage Site and adjacent areas (Fayum, Egypt)', *Stratigraphy*, 11, pp. 185–234.

Uhen, M.D. (2004) *Form, function, and anatomy of *Dorudon atrox* (Mammalia, Cetacea): an archaeocete from the middle to late Eocene of Egypt*. Ann Arbor, Mich: University of Michigan (Papers on paleontology, no. 34).

Zalmout, I. and Gingerich, P. (2012) 'Late Eocene Sea Cows (Mammalia, Sirenia) From Wadi Al Hitan In The Western Desert of Fayum, Egypt', *University of Michigan Papers on Paleontology*, 37, pp. 1–158.

143. The La Venta middle Miocene neotropical biome

Carrillo, J.D. (ed.) (2023) 'Neotropical palaeontology: the Miocene La Venta biome.', *Geodiversitas*, 45(2), p. Articles 3, 6, 10, 12, 13, 15, 18, 25, and 26.

Defler, T. (2019) 'La Venta: A Miocene Mammalian Community from Colombia', in T. Defler (ed.) *History of Terrestrial Mammals in South*

America: How South American Mammalian Fauna Changed from the Mesozoic to Recent Times

Cham: Springer International Publishing (Topics in Geobiology), pp. 199–219. Available at: https://doi.org/10.1007/978-3-319-98449-0_10.

Dill, H.G. *et al.* (2020) 'The "badland trilogy" of the Desierto de la Tatacoa, upper Magdalena Valley, Colombia, a result of geodynamics and climate: With a review of badland landscapes', *CATENA*, 194, p. 104696. Available at: <https://doi.org/10.1016/j.catena.2020.104696>.

Kay, R. *et al.* (1997) *Vertebrate Paleontology in the Neotropics. The Miocene Fauna of La Venta, Colombia*. Washington D.C.: Smithsonian Institution Press.

Montes, C. *et al.* (2021) 'A Middle to Late Miocene Trans-Andean Portal: Geologic Record in the Tatacoa Desert', *Frontiers in Earth Science*, 8. Available at: <https://www.frontiersin.org/articles/10.3389/feart.2020.587022>.

Spradley, J.P., Glazer, B.J. and Kay, R.F. (2019) 'Mammalian faunas, ecological indices, and machine-learning regression for the purpose of paleoenvironment reconstruction in the Miocene of South America', *Palaeogeography, Palaeoclimatology, Palaeoecology*, 518, pp. 155–171. Available at: <https://doi.org/10.1016/j.palaeo.2019.01.014>.

144. The modern human fossils of the Kibish Formation

Brown, F.H. and Fuller, C.R. (2008) 'Stratigraphy and tephra of the Kibish Formation, southwestern Ethiopia', *Journal of Human Evolution*, 55(3), pp. 366–403. Available at: <https://doi.org/10.1016/j.jhevol.2008.05.009>.

Butzer, K.W. and Thurber, D.L. (1969) 'Some Late Cenozoic Sedimentary Formations of the Lower Omo Basin', *Nature*, 222, pp. 1138–1143. Available at: <https://doi.org/10.1038/2221138a0>.

Fleagle, J.G. *et al.* (2008) 'Paleoanthropology of the Kibish Formation, southern Ethiopia: Introduction', *Journal of Human Evolution*, 55(3), pp. 360–365. Available at: <https://doi.org/10.1016/j.jhevol.2008.05.007>.

McDougall, I., Brown, F.H. and Fleagle, J.G. (2005) 'Stratigraphic placement and age of modern humans from Kibish, Ethiopia', *Nature*, 433(7027), pp. 733–736. Available at: <https://doi.org/10.1038/nature03258>.

Vidal, C.M. *et al.* (2022) 'Age of the oldest known *Homo sapiens* from eastern Africa', *Nature*, 601(7894), pp. 579–583. Available at: <https://doi.org/10.1038/s41586-021-04275-8>.

145. The Human Footprints of Acahualinca

Brown, R.W. (1947) 'Fossil Plants and Human Footprints in Nicaragua',

Schmincke, H.-U. *et al.* (2010) 'Walking through volcanic mud: the 2,100 year-old Acahualinca footprints (Nicaragua) II: the Acahualinca people, environmental conditions and motivation', *International Journal of Earth Sciences*, 99(1), pp. 279–292. Available at: <https://doi.org/10.1007/s00531-009-0438-0>.

IV. IGNEOUS AND METAMORPHIC PETROLOGY

146. The larvikite plutonic rocks of the Oslo Rift

Brøgger, W.C. (1891) 'Die Mineralien der Syentipemmatitgänge der südnorwegischen Augit- und Nephelinsyenite', *Geologiska Föreningen i Stockholm Förhandlingar*, 13(2), pp. 128–131. Available at: <https://doi.org/10.1080/11035899109446866>.

Buch, L. von (1810) *Reise durch Norwegen und Lappland*. Berlin: G. C. Nauck (Ordentlichen Mitgliede der Königlichen Academie der Wissenschaften zu). Available at: <http://archive.org/details/reisedurchnorw00buch>.

Dahlgren, S., Corfu, F. and Heaman, L. (1998) 'Datering av plutoner og pegmatitter i Larvik pluton-kompleks, sydlige Oslo Grøben, ved hjelp av U-Pb isotoper i zirkon og baddeleyitt.', in *Norsk Bergverksmuseum Skrift. Kongsberg mineral symposium 1998*, pp. 32–39.

Heldal, T., Meyer, G.B. and Dahl, R. (2015) 'Global stone heritage: Larvikite, Norway', in D. Pereira (ed.) *Global Heritage Stone: Towards International Recognition of Building and Ornamental Stones*. Geological Society of London Special PublicationGeological Society, London, Special Publications 407, pp. 21–34. Available at: <https://doi.org/10.1144/SP407.14>.

Neuman, E.-R. (1980) 'Petrogenesis of the Oslo Region Larvikites and Associated Rocks', *Journal of Petrology*, 21(3), pp. 499–531. Available at: <https://doi.org/10.1093/petrology/21.3.499>.

Petersen, J.S. (1978) 'Structure of the larvikite-lardalite complex, Oslo-region, Norway, and its evolution', *Geologische Rundschau*, 67(1), pp. 330–342. Available at: <https://doi.org/10.1007/BF01803271>.

147. The Rum Igneous Complex

Emeleus, C.H. and Troll, V.R. (2014) 'The Rum Igneous Centre, Scotland', *Mineralogical Magazine*, 78(4), pp. 805–839. Available at: <https://doi.org/10.1180/minmag.2014.078.4.04>.

Geikie, A. (1897) *The ancient volcanoes of Great Britain* (2 vol.). London, Macmillan. Available at: <http://archive.org/details/ancientvolcanoe02geikgoog>.

Goodenough, K. *et al.* (2008) *The Geological Society of London - Golden Rum!* Available at: <https://www.geolsoc.org.uk/Geoscientist/Archive/March-2008/Golden-Rum>.

Judd, J.W. (1874) 'The Secondary Rocks of Scotland. Second Paper. On the Ancient Volcanoes of the Highlands and the Relations of their Products to the Mesozoic Strata', *Quarterly Journal of the Geological Society of London*, 30(1–4), pp. 220–302. Available at: <https://doi.org/10.1144/GSL.JGS.1874.030.01-04.37>.

Upton, B.G.J. *et al.* (2023) 'The Central Series of the Rum Igneous Complex, NW Scotland: the rises and falls of magma in a large mafic-ultramafic volcano', *Geology Today*, 39(4), pp. 130–143. Available at: <https://doi.org/10.1111/gto.12441>.

Wager, L.R. and Brown, G.M. (1968) *Layered Igneous Rocks*. Oliver and Boyd, Edinburgh and London. Available at: <https://www.semanticscholar.org/paper/Layered-Igneous-Rocks-Wager-Brown/9e0ef3a52eead4278a836cd12641c1adea6b2f0e>.

148. Devils Tower

Bassett, W.A. (1961) 'Potassium-Argon Age of Devils Tower, Wyoming', *Science*, 134, p. 1373. Available at: <https://doi.org/10.1126/science.134.3487.1373>.

Brady, J. (1999) "'Land Is Itself a Sacred, Living Being": Native American Sacred Site Protection on Federal Public Lands Amidst the Shadows of Bear Lodge', *American Indian Law Review*, 24(1), p. 153.

Dutton, C.E. and Schwartz, G.M. (1936) 'Notes on the Jointing of the Devil's Tower, Wyoming', *The Journal of Geology*, 44(6), pp. 717–728. Available at: <https://doi.org/10.1086/624472>.

Hanson, J.R. and Moore, D. (1999) 'Applied Anthropology at Devils Tower National Monument', *Plains Anthropologist*, 44(170), pp. 53–60. Available at: <https://doi.org/10.1080/2052546.1999.11931965>.

Jenkins, M. (2013) 'Devils Tower, Sacred Space', *Virginia Quarterly Review*, 89(1), pp. 232–237.

Robinson, C.S. (1956) *Geology of Devils Tower National Monument, Wyoming*. 1021–I. U.S. Geological Survey, pp. 289–302. Available at: <https://doi.org/10.3133/b1021l>.

Závada, P. *et al.* (2015) 'Devils Tower (Wyoming, USA): A lava coulée emplaced into a maar-diatreme volcano?', *Geosphere*, 11(2), pp. 354–375. Available at: <https://doi.org/10.1130/GES01166.1>.

149. The Mohorovicic discontinuity in the Ivrea-Verbano Zone

Boriani, A. and Rivalenti, G. (1984) 'Crusta profonda e significato delle rocce basiche e ultrabasiche dell'Ivrea-Verbano in un secolo di studi', in *Cento anni di geologia Italiana*, pp. 113–131.

Brack, P., Ulmer, P. and Schmid, S.M. (2010) 'A crustal-scale magmatic system from the Earth's mantle to the Permian surface: Field trip to the area of lower Valsesia and Val d'Ossola (Massiccio dei Laghi, Southern Alps, Northern Italy)', *Swiss Bulletin für angewandte Geologie*, 15(2), pp. 3–21.

Quick, J.E., Sinigoi, S. and Mayer, A. (1994) 'Emplacement dynamics of a large mafic intrusion in the lower crust, Ivrea-Verbano Zone, northern Italy', *Journal of Geophysical Research: Solid Earth*, 99(B11), pp. 21559–21573. Available at: <https://doi.org/10.1029/94JB00113>.

Quick, J.E., Sinigoi, S. and Mayer, A. (1995) 'Emplacement of mantle peridotite in the lower continental crust, Ivrea-Verbano zone, northwest Italy', *Geology*, 23(8), pp. 739–742. Available at: [https://doi.org/10.1130/0091-7613\(1995\)023<0739:EMOPIT>2.3.CO;2](https://doi.org/10.1130/0091-7613(1995)023<0739:EMOPIT>2.3.CO;2).

Schmid, S.M. (1993) 'Ivrea Zone and Adjacent Southern Alpine Basement', in J.F. von Raumer and F. Neubauer (eds) *Pre-Mesozoic Geology in the Alps*. Berlin, Heidelberg: Springer, pp. 567–583. Available at: https://doi.org/10.1007/978-3-642-84640-3_33.

150. The Cambrian Leka Ophiolite

Carter, E.J. *et al.* (2021) 'Multi-stage fluid infiltration and metasomatism in supra-subduction zone mantle: evidence from halogens and noble gases in the Leka Ophiolite Complex, Norway',

Geochimica et Cosmochimica Acta, 307, pp. 258–280. Available at: <https://doi.org/10.1016/j.gca.2021.04.028>.

Dunkel, K.G. *et al.* (2017) 'Localized slip controlled by dehydration embrittlement of partly serpentinized dunites, Leka Ophiolite Complex, Norway', *Earth and Planetary Science Letters*, 463, pp. 277–285. Available at: <https://doi.org/10.1016/j.epsl.2017.01.047>.

Dunning, G.R. and Pedersen, R.B. (1988) 'U/Pb ages of ophiolites and arc-related plutons of the Norwegian Caledonides: implications for the development of Iapetus', *Contributions to Mineralogy and Petrology*, 98(1), pp. 13–23. Available at: <https://doi.org/10.1007/BF00371904>.

Furnes, H. *et al.* (1991) 'Magma development of the Leka Ophiolite Complex, central Norwegian Caledonides', *Lithos*, 27(4), pp. 259–277. Available at: [https://doi.org/10.1016/0024-4937\(91\)90003-4](https://doi.org/10.1016/0024-4937(91)90003-4).

Furnes, H., Pedersen, R.B. and Stillman, C.J. (1988) 'The Leka Ophiolite Complex, central Norwegian Caledonides: field characteristics and geotectonic significance', *Journal of the Geological Society*, 145(3), pp. 401–412. Available at: <https://doi.org/10.1144/gsjgs.145.3.0401>.

Pedersen, R.-B., Johannessen, G.M. and Boyd, R. (1993) 'Stratiform platinum-group element mineralizations in the ultramafic cumulates of the Leka ophiolite complex, central Norway', *Economic Geology*, 88(4), pp. 782–803. Available at: <https://doi.org/10.2113/gsecongeo.88.4.782>.

Prestvik, T. and Roaldset, E. (1978) 'Rare earth element abundances in Caledonian metavolcanics from the island of Leka, Norway', *Geochemical Journal*, 12(2), pp. 89–100. Available at: <https://doi.org/10.2343/geochemj.12.89>.

151. Late Cretaceous Samail Ophiolite

Allemann, F. and Peters, T. (1972) 'The Ophiolite-Radiolarite Belt of the North-Oman Mountains', *Eclogae Geologicae Helvetiae*, 65(3), pp. 657–697.

Glennie, K.W. *et al.* (1974) *Geology of the Oman Mountains*. Delft: Koninklyk Nederlands Geologisch Mynbouwkundig Genootschap (Nederlands Geologisch Mynbouwkundig Genootschap, Transactions, 31).

Hansman, R.J. *et al.* (2021) 'Structural architecture and Late Cretaceous exhumation history of the Saih Hatat Dome (Oman), a review based on existing data and semi-restorable cross-sections', *Earth-Science Reviews*, 217, p. 103595. Available at: <https://doi.org/10.1016/j.earscirev.2021.103595>.

Lippard, S.J., Shelton, A.W. and Gass, I.G. (1986) *The ophiolite of northern Oman*. Geological Society of London (Memoir, 11).

Nicolas, A. *et al.* (2000) 'Accretion of Oman and United Arab Emirates ophiolite – Discussion of a new structural map', *Marine Geophysical Researches*, 21(3), pp. 147–180. Available at: <https://doi.org/10.1023/A:1026769727917>.

Reinhardt, B.M. (1969) 'On the genesis and emplacement of ophiolites in the Oman Mountains geosyncline', *Schweizerische Mineralogische und Petrographische Mitteilungen*, 49(1), pp. 1–30.

Tilton, G.R., Hopson, C.A. and Wright, J.E. (1981) 'Uranium-lead isotopic ages of the Samail Ophiolite, Oman, with applications to Tethyan ocean ridge tectonics', *Journal of Geophysical Research: Solid Earth*, 86(B4), pp. 2763–2775. Available at: <https://doi.org/10.1029/JB086iB04p02763>.

152. Lower Pillow Lavas of Troodos Ophiolite

Bear, L.M. (1960) *The geology and mineral resources of the Akaki-Lythrodondha area*. Nicosia: Government of Cyprus (Memoir / Geological Survey Department, Cyprus, no. 3).

Coogan, L.A. *et al.* (2017) 'The role of low-temperature (off-axis) alteration of the oceanic crust in the global Li-cycle: Insights from the Troodos ophiolite', *Geochimica et Cosmochimica Acta*, 203, pp. 201–215. Available at: <https://doi.org/10.1016/j.gca.2017.01.002>.

Coogan, L.A. and Gillis, K.M. (2018) 'Temperature dependence of chemical exchange during seafloor weathering: Insights from the Troodos ophiolite', *Geochimica et Cosmochimica Acta*, 243, pp. 24–41. Available at: <https://doi.org/10.1016/j.gca.2018.09.025>.

Edwards, S. *et al.* (2010) *Cyprus*. illustrated edition. Harpenden: Terra Publishing (Classic Geology in Europe, 7).

Morris, A. (1990) *Palaeomagnetic studies of the Mesozoic-Tertiary tectonic evolution of Cyprus, Turkey and Greece*. PhD Thesis. The University of Edinburgh. Available at: <https://era.ed.ac.uk/handle/1842/12687>.

Morris, A. (1996) 'A review of palaeomagnetic research in the Troodos ophiolite, Cyprus', *Geological Society, London, Special Publications*, 105(1), pp. 311–324. Available at: <https://doi.org/10.1144/GSL.SP.1996.105.01.27>.

Schouten, H. and Kelemen, P.B. (2002) 'Melt viscosity, temperature and transport processes, Troodos ophiolite, Cyprus', *Earth and Planetary Science Letters*, 201(2), pp. 337–352. Available at: [https://doi.org/10.1016/S0012-821X\(02\)00709-4](https://doi.org/10.1016/S0012-821X(02)00709-4).

153. The ultrahigh-pressure unit of the Dora-Maira Massif

Chopin, C. (1984) 'Coesite and pure pyrope in high-grade blueschists of the Western Alps: a first record and some consequences', *Contributions to Mineralogy and Petrology*, 86(2), pp. 107–118. Available at: <https://doi.org/10.1007/BF00381838>.

Chopin, C., Henry, C. and Michard, A. (1991) 'Geology and petrology of the coesite-bearing terrain, Dora Maira massif, Western Alps.', *European Journal of Mineralogy*, pp. 263–292. Available at: <https://doi.org/10.1127/ejm/3/2/0263>.

Compagnoni, R. *et al.* (2012) 'Geological map of the ultra-high pressure Brossasco-Isasca unit (Western Alps, Italy)', *Journal of Maps*, 8(4), pp. 465–472. Available at: <https://doi.org/10.1080/17446247.2012.744367>.

V. VOLCANOLOGY

154. Deccan Traps

Bodas, M.S. and Sen, B. (2014) 'The Lonar Crater: The Best Preserved Impact Crater in the Basaltic Terrain', in V.S. Kale (ed.) *Landscapes and Landforms of India*. Dordrecht: Springer Netherlands (World Geomorphological Landscapes), pp. 223–230. Available at: https://doi.org/10.1007/978-94-017-8029-2_24.

Kaur, G. et al. (2019) 'The Late Cretaceous-Paleogene Deccan Traps: a Potential Global Heritage Stone Province from India', *Geoheritage*, 11(3), pp. 973–989. Available at: <https://doi.org/10.1007/s12371-018-00342-1>.

Ollier, C.D. and Sheth, H.C. (2008) 'The High Deccan duricrusts of India and their significance for the "laterite" issue', *Journal of Earth System Science*, 117(5), pp. 537–551. Available at: <https://doi.org/10.1007/s12040-008-0051-9>.

Ottens, B. (2003) 'Minerals of the Deccan Traps, India', *Indian zeolites and related species, The Mineralogical Record*, 34(1), pp. 5–83.

Sheth, H. (2023) 'The Volcanic Geoheritage of the Ajanta and Ellora Caves, Central Deccan Traps, India', *Geoheritage*, 15(1), p. 39. Available at: <https://doi.org/10.1007/s12371-023-00809-w>.

Sheth, H.C. (2014) 'Mahabaleshwar, Deccan Traps, India', *International Journal of Earth Sciences*, 103(3), pp. 799–799. Available at: <https://doi.org/10.1007/s00531-013-0943-z>.

155. Muriwai megapillow lava flows

Allen, S.R., Hayward, B.W. and Mathews, E.J. (2006) 'A facies model for a submarine volcanoclastic apron: the Miocene Manukau volcanic complex, Northland, New Zealand', *ASEG Extended Abstracts*, 2006(1), pp. 1–2. Available at: <https://doi.org/10.1071/ASEG2006ab107>.

Bartrum, J.A. (1930) 'Pillow-Lavas and Columnar Fan-Structures at Muriwai, Auckland, New Zealand', *The Journal of Geology*, 38(5), pp. 447–455.

Bear, A.N. and Cas, R.A.F. (2007) 'The complex facies architecture and emplacement sequence of a Miocene submarine mega-pillow lava flow system, Muriwai, North Island, New Zealand', *Journal of Volcanology and Geothermal Research*, 160(1), pp. 1–22. Available at: <https://doi.org/10.1016/j.jvolgeores.2006.09.002>.

Hayward, B.W. (1976) 'Lower Miocene geology and sedimentary history of the Muriwai-Te Waharoa coastline, North Auckland, New Zealand', *New Zealand Journal of Geology and Geophysics*, 19(5), pp. 639–662. Available at: <https://doi.org/10.1080/00288306.1976.10426312>.

Hayward, B.W. (1979) *Ancient Undersea Volcanoes: A guide to the geological formations at Muriwai, west Auckland*. Wellington: Geological Society of New Zealand ([Guidebook 3]).

Hayward, B.W. (2022) 'Muriwai pillow lava: undersea flows with globally-rare fans of huge columnar joints', in *Mountains, Volcanoes, Coasts and Caves: Origins of Aotearoa New Zealand's natural wonders*. Auckland University Press, p. 384.

156. The Pleistocene Al Wahbah dry maar crater

Abdel Wahab, A. et al. (2014) 'The geology and geochronology of Al Wahbah maar crater, Harrat Kishb, Saudi Arabia', *Quaternary*

Geochronology, 21, pp. 70–76. Available at: <https://doi.org/10.1016/j.quageo.2013.01.008>.

Abdel Wahab, A., Ghoneim, M.F. and Abu-Alam, T. (2017) 'Isotopic, mineralogical, and thermobarometric variations of Al-Wahbah crater (Maklaa Tameya), Kishb area, Saudi Arabia', *Arabian Journal of Geosciences*, 10(2), p. 30. Available at: <https://doi.org/10.1007/s12517-016-2804-0>.

Daoudi, M.A.-A., Al-Doaan, M.I. and Jamil, A. (2018) 'Geomorphology of the Al Wahbah crater at Harrat Kishb west of the Kingdom of Saudi Arabia', *Arabian Journal of Geosciences*, 11(12), p. 297. Available at: <https://doi.org/10.1007/s12517-018-3567-6>.

Grainger, D.J. (1996) 'Al Wahbah volcanic explosion crater, Saudi Arabia', *Geology Today*, 12(1), pp. 27–30. Available at: <https://doi.org/10.1046/j.1365-2451.1996.00006.x>.

Moufti, M.R. et al. (2013) 'Geoheritage values of one of the largest maar craters in the Arabian Peninsula: The Al Wahbah Crater and other volcanoes (Harrat Kishb, Saudi Arabia)', *Central European Journal of Geosciences*, 5(2), pp. 254–271. Available at: <https://doi.org/10.2478/s13533-012-0125-8>.

Moufti, M.R. and Németh, K. (2016) *Geoheritage of Volcanic Harrats in Saudi Arabia*. Cham: Springer International Publishing (Geoheritage, Geoparks and Geotourism). Available at: <https://doi.org/10.1007/978-3-319-33015-0>.

157. El Laco iron lavas

Alva-Valdivia, L.M. et al. (2003) 'Rock-Magnetic and Oxide Microscopic Studies of the El Laco Iron Ore Deposits, Chilean Andes, and Implications for Magnetic Anomaly Modeling', *International Geology Review*, 45(6), pp. 533–547. Available at: <https://doi.org/10.2747/0020-6814.45.6.533>.

Broman, C. et al. (1999) 'Fluid inclusions in magnetite-apatite ore from a cooling magmatic system at El Laco, Chile', *GFF*, 121(3), pp. 253–267. Available at: <https://doi.org/10.1080/1103589901213253>.

Guijón, R., Henríquez, F. and Naranjo, J.A. (2011) 'Geological, Geographical and Legal Considerations for the Conservation of Unique Iron Oxide and Sulphur Flows at El Laco and Lastarria Volcanic Complexes, Central Andes, Northern Chile', *Geoheritage*, 3(4), pp. 299–315. Available at: <https://doi.org/10.1007/s12371-011-0045-x>.

Henriquez, F. and Martin, R.F. (1978) 'Crystal-growth textures in magnetite flows and feeder dykes, El Laco, Chile', *The Canadian Mineralogist*, 16(4), pp. 581–589.

Naranjo Soza, J.A., Henríquez Barrientos, F. and Nystrom, J.O. (2010) 'Subvolcanic contact metasomatism at El Laco Volcanic Complex, Central Andes', *Andean geology: Formerly Revista geológica de Chile*, 37(1), pp. 110–120.

Park, C.F. (1961) 'A magnetite "flow" in northern Chile', *Economic Geology*, 56(2), pp. 431–436. Available at: <https://doi.org/10.2113/gsecongeo.56.2.431>.

158. Ngorongoro Crater

Dawson, J.B. (1997) 'Neogene; recent rifting and volcanism in northern Tanzania; relevance for comparisons between the Gardar Province and the East African Rift valley', *Mineralogical Magazine*, 61(4), pp. 543–548.

Dawson, J.B. (2008) *The Gregory Rift Valley and Neogene–Recent Volcanoes of Northern Tanzania*. Geological Society of London. Available at: <https://doi.org/10.1144/M33>.

Mollel, G.F. et al. (2008) 'Geochemical evolution of Ngorongoro Caldera, Northern Tanzania: Implications for crust–magma interaction', *Earth and Planetary Science Letters*, 271(1), pp. 337–347. Available at: <https://doi.org/10.1016/j.epsl.2008.04.014>.

Mollel, G.F. and Swisher, C.C. (2012) 'The Ngorongoro Volcanic Highland and its relationships to volcanic deposits at Olduvai Gorge and East African Rift volcanism', *Journal of Human Evolution*, 63(2), pp. 274–283. Available at: <https://doi.org/10.1016/j.jhevol.2011.09.001>.

Scoon, R. (2018) *Geology of National Parks of Central/Southern Kenya and Northern Tanzania*. Available at: <https://doi.org/10.1007/978-3-319-73785-0>.

Scoon, R.N. (2021) 'Lake Natron and the Ngorongoro Conservation Area, Northern Tanzania', in R.N. Scoon (ed.) *The Geotraveller: Geology of Famous Geosites and Areas of Historical Interest*. Cham: Springer International Publishing, pp. 117–137. Available at: https://doi.org/10.1007/978-3-030-54693-9_7.

159. Ruapehu Volcano

Cronin, S.J. et al. (1999) 'Dynamic interactions between lahars and stream flow: A case study from Ruapehu volcano, New Zealand', *GSA Bulletin*, 111(1), pp. 28–38. Available at: [https://doi.org/10.1130/0016-7606\(1999\)111<0028:DIBLAS>2.3.CO;2](https://doi.org/10.1130/0016-7606(1999)111<0028:DIBLAS>2.3.CO;2).

Gamble, J.A. et al. (1999) 'A fifty year perspective of magmatic evolution on Ruapehu Volcano, New Zealand: verification of open system behaviour in an arc volcano', *Earth and Planetary Science Letters*, 170(3), pp. 301–314. Available at: [https://doi.org/10.1016/S0012-821X\(99\)00106-5](https://doi.org/10.1016/S0012-821X(99)00106-5).

Leonard, G.S. et al. (2021) 'Ruapehu and Tongariro stratovolcanoes: a review of current understanding', *New Zealand Journal of Geology and Geophysics*, 64(2–3), pp. 389–420. Available at: <https://doi.org/10.1080/00288306.2021.1909080>.

Price, R.C. et al. (2012) 'The Anatomy of an Andesite Volcano: a Time-Stratigraphic Study of Andesite Petrogenesis and Crustal Evolution at Ruapehu Volcano, New Zealand', *Journal of Petrology*, 53, pp. 2139–2189. Available at: <https://doi.org/10.1093/petrology/egs050>.

Procter, J. et al. (2010) 'Quantifying the geomorphic impacts of a lake-breakout lahar, Mount Ruapehu, New Zealand', *Geology*, 38(1), pp. 67–70. Available at: <https://doi.org/10.1130/G30129.1>.

Voloschina, M. et al. (2020) 'Lithosedimentological and tephrostratigraphical characterisation of small-volume, low-intensity eruptions: The 1800 years Tufa Trig Formation, Mt. Ruapehu (New Zealand)', *Journal of Volcanology and Geothermal Research*, 402, p. 106987. Available at: <https://doi.org/10.1016/j.jvolgeores.2020.106987>.

160. Parícutin Volcano

Cebriá, J.M. et al. (2011) 'The Parícutin calc-alkaline lavas: New geochemical and petrogenetic modelling constraints on the crustal assimilation process', *Journal of Volcanology and Geothermal Research*, 201(1), pp. 113–125. Available at: <https://doi.org/10.1016/j.jvolgeores.2010.11.011>.

Hasenaka, T. and Carmichael, I.S.E. (1985) 'The cinder cones of Michoacán-Guanajuato, central Mexico: their age, volume and

distribution, and magma discharge rate', *Journal of Volcanology and Geothermal Research*, 25(1), pp. 105–124. Available at: [https://doi.org/10.1016/0377-0273\(85\)90007-1](https://doi.org/10.1016/0377-0273(85)90007-1).

Larrea, P. et al. (2019) 'A re-interpretation of the petrogenesis of Parícutin volcano: Distinguishing crustal contamination from mantle heterogeneity', *Chemical Geology*, 504, pp. 66–82. Available at: <https://doi.org/10.1016/j.chemgeo.2018.10.026>.

Luhr, J.F., Simkin, T. and Smithsonian Institution (eds) (1993) *Parícutin: the volcano born in a Mexican cornfield*. Phoenix, Ariz: Geoscience Press, Inc.

McBirney, A.R., Taylor, H.P. and Armstrong, R.L. (1987) 'Parícutin re-examined: a classic example of crustal assimilation in calc-alkaline magma', *Contributions to Mineralogy and Petrology*, 95(1), pp. 4–20. Available at: <https://doi.org/10.1007/BF00518026>.

161. Heisei Shinzan Lava Dome

Nakada, S. et al. (1995) 'Endogenous growth of dacite dome at Unzen volcano (Japan), 1993–1994', *Geology*, 23(2), pp. 157–160. Available at: [https://doi.org/10.1130/0091-7613\(1995\)023<0157:DDA>2.3.CO;2](https://doi.org/10.1130/0091-7613(1995)023<0157:DDA>2.3.CO;2).

Nakada, S. and Fujii, T. (1993) 'Preliminary report on the activity at Unzen Volcano (Japan), November 1990–November 1991: Dacite lava domes and pyroclastic flows', *Journal of Volcanology and Geothermal Research*, 54(3), pp. 319–333. Available at: [https://doi.org/10.1016/0377-0273\(93\)90070-8](https://doi.org/10.1016/0377-0273(93)90070-8).

Nakada, S., Shimizu, H. and Ohta, K. (1999) 'Overview of the 1990–1995 eruption at Unzen Volcano', *Journal of Volcanology and Geothermal Research*, 89(1), pp. 1–22. Available at: [https://doi.org/10.1016/S0377-0273\(98\)00118-8](https://doi.org/10.1016/S0377-0273(98)00118-8).

Sakuma, S. et al. (2008) 'Drilling and logging results of USDP-4 – Penetration into the volcanic conduit of Unzen Volcano, Japan', *Journal of Volcanology and Geothermal Research*, 175(1), pp. 1–12. Available at: <https://doi.org/10.1016/j.jvolgeores.2008.03.039>.

Umakoshi, K., Itasaka, N. and Shimizu, H. (2011) 'High-frequency earthquake swarm associated with the May 1991 dome extrusion at Unzen Volcano, Japan', *Journal of Volcanology and Geothermal Research*, 206(3), pp. 70–79. Available at: [https://doi.org/10.1016/j.jvolgeores.2011.07.00](https://doi.org/10.1016/j.jvolgeores.2011.07.004)

Lane, E.M. (2022) 'Atmospheric waves reinforced tsunami after Tongan eruption', *Nature*, 609(7928), pp. 677–678. Available at: <https://doi.org/10.1038/d41586-022-01855-0>.

Németh, K. (2022) 'Geoheritage and geodiversity aspects of catastrophic volcanic eruptions: Lessons from the 15th of January 2022 Hunga Tonga - Hunga Ha'apai eruption, SW Pacific', *International Journal of Geoheritage and Parks*, 10(4), pp. 546–568. Available at: <https://doi.org/10.1016/j.ijgeop.2022.08.003>.

Purkis, S.J. et al. (2023) 'The 2022 Hunga-Tonga megatsunami: Near-field simulation of a once-in-a-century event', *Science Advances*, 9(15), p. eadfd5493. Available at: <https://doi.org/10.1126/sciadv.adf5493>.

163. Rotorua's geothermal fields (Ahi-Tupua)

Chambefort, I. and Bignall, G. (eds) (2016) *Taupo Volcanic Zone geothermal systems, New Zealand: Exploration, science and development*. Elsevier (Geothermics, 59B).

Hayward, B.W. (2022) 'Pohutu Geyser, Whakarewarewa, Rotorua: New Zealand's largest and most regular geyser, and Waiotapu, Rotorua: Most colourful geothermal area in New Zealand', in *Mountains, Volcanoes, Coasts and Caves: Origins of Aotearoa New Zealand's natural wonders*. Auckland University Press, p. 384.

Hunt, T., Glover, R. and Wood, C. (1994) 'Waimangu, Waiotapu, and Waikite geothermal systems, New Zealand: Background and history', *Geothermics*, 23(5), pp. 379–400. Available at: [https://doi.org/10.1016/0375-6505\(94\)90010-8](https://doi.org/10.1016/0375-6505(94)90010-8).

Lloyd, E.F. (1959) 'The hot springs and hydrothermal eruptions of Waiotapu', *New Zealand Journal of Geology and Geophysics*, 2(1), pp. 141–176. Available at: <https://doi.org/10.1080/00288306.1959.1043131>.

Power, J.F. et al. (2023) 'Temporal dynamics of geothermal microbial communities in Aotearoa-New Zealand', *Frontiers in Microbiology*, 14. Available at: <https://www.frontiersin.org/articles/10.3389/fmicb.2023.1094311>.

Scott, B.J. et al. (2016) 'The Rotorua Geothermal Field: An experiment in environmental management', *Geothermics*, 59, pp. 294–310. Available at: <https://doi.org/10.1016/j.geothermics.2015.09.004>.

VI. TECTONICS

164. The Mid-Atlantic ridge on Reykjanes

Friðleifsson, G.Ó. et al. (2020) 'The Iceland Deep Drilling Project at Reykjanes: Drilling into the root zone of a black smoker analog', *Journal of Volcanology and Geothermal Research*, 391, p. 106435. Available at: <https://doi.org/10.1016/j.jvolgeores.2018.08.013>.

Icelandic Met Office (2023) 'Skjálfala-Lísa'. Available at: <https://skjalfala.vedur.is/#/page/map>.

Khodayar, M. et al. (2018) 'Tectonic Control of the Reykjanes Geothermal Field in the Oblique Rift of SW Iceland: From Regional to Reservoir Scales', *Open Journal of Geology*, 08(03), pp. 333–382. Available at: <https://doi.org/10.4236/ojg.2018.83021>.

Sæmundsson, K., Sigurgeirsson, M.Á. and Friðleifsson, G.Ó. (2020) 'Geology and structure of the Reykjanes volcanic system, Iceland', *Journal of Volcanology and Geothermal Research*, 391, p. 106501. Available at: <https://doi.org/10.1016/j.jvolgeores.2018.11.022>.

165. The evolution of the Andes in Colca Canyon

Paulo, A. (2008) 'Geology of the Western Cordillera in Southern Peru – an outline', in *Polskie badania w Kanie Colca i Dolinie Wulkanów*. Cracovia (English and Polish), pp. 35–53.

Schildgen, T.F. et al. (2007) 'Uplift of the western margin of the Andean plateau revealed from canyon incision history, southern Peru', *Geology*, 35(6), pp. 523–526. Available at: <https://doi.org/10.1130/G23532A.1>.

Schildgen, T.F. et al. (2009) 'Late Cenozoic structural and tectonic development of the western margin of the central andean plateau in southwest Peru', *Tectonics*, 28(4). Available at: <https://doi.org/10.1029/2008TC002403>.

Thouret, J.-C. et al. (2007) 'Geochronologic and stratigraphic constraints on canyon incision and Miocene uplift of the Central Andes in Peru', *Earth and Planetary Science Letters*, 263(3), pp. 151–166. Available at: <https://doi.org/10.1016/j.epsl.2007.07.023>.

166. Salt domes and glaciers of the Zagros Fold and Thrust Belt

Faramarzi, N.S. et al. (2015) 'Geochronology and geochemistry of rhyolites from Hormuz Island, southern Iran: A new record of Cadomian arc magmatism in the Hormuz Formation', *Lithos*, 236–237, pp. 203–211. Available at: <https://doi.org/10.1016/j.lithos.2015.08.017>.

Ghassemi, M.R. and Roustaei, M. (2021) 'Salt extrusion kinematics: insights from existing data, morphology and InSAR modelling of the active emergent Angur diapir in the Zagros fold and thrust belt, Iran', *Journal of the Geological Society*, 178(6), pp. jgs2020-136. Available at: <https://doi.org/10.1144/jgs2020-136>.

Jahani, S. et al. (2007) 'The Salt Diapirs of the Eastern Fars Province (Zagros, Iran): A Brief Outline of their Past and Present', in O. Lacombe et al. (eds) *Thrust Belts and Foreland Basins*. Berlin, Heidelberg: Springer (Frontiers in Earth Sciences), pp. 289–308. Available at: https://doi.org/10.1007/978-3-540-69426-7_15.

Jahani, S. (2008) *Tectonique salifère, plissement et fracturation dans les provinces du Fars Oriental et le domaine marin adjacent du Golfe Persique (Iran)*. Ph.D. Thesis. Cergy-Pontoise University.

Smith, A.G. (2012) 'A review of the Ediacaran to Early Cambrian ("Infra-Cambrian") evaporites and associated sediments of the Middle East', *Geological Society, London, Special Publications*, 366(1), pp. 229–250. Available at: <https://doi.org/10.1144/SP366.12>.

Talbot, C.J. (1979) 'Fold trains in a glacier of salt in southern Iran', *Journal of Structural Geology*, 1(1), pp. 5–18. Available at: [https://doi.org/10.1016/0191-8141\(79\)90017-8](https://doi.org/10.1016/0191-8141(79)90017-8).

167. The Patos Shear Zone

Archango, C.J., Hollanda, M.H.B.M.D. and Viegas, L.G.F. (2021) 'Late Ediacaran lateral-escape tectonics as recorded by the Patos shear zone (Borborema Province, NE Brazil)', *Brazilian Journal of Geology*, 51(2), p. e20200132. Available at: <https://doi.org/10.1590/2317-4889202120200132>.

Cavalcante, C. et al. (2022) 'TitaniQ temperatures and textural analysis as a record of the deformation history in a major continental shear zone system, Borborema Province, Brazil', *Tectonophysics*, 841, p. 229548. Available at: <https://doi.org/10.1016/j.tecto.2022.229548>.

Cavalcante, G.C.G. et al. (2016) 'The influence of partial melting and melt migration on the rheology of the continental crust', *Journal of*

Geodynamics, 101, pp. 186–199. Available at: <https://doi.org/10.1016/j.jog.2016.06.002>.

Corsini, M., Vauchez, A. and Caby, R. (1996) 'Ductile duplexing at a bend of a continental-scale strike-slip shear zone: example from NE Brazil', *Journal of Structural Geology*, 18(4), pp. 385–394. Available at: [https://doi.org/10.1016/0191-8141\(95\)00102-J](https://doi.org/10.1016/0191-8141(95)00102-J).

Fossen, H. et al. (2022) 'The Patos-Pernambuco shear system of NE Brazil: Partitioned intracontinental transcurrent deformation revealed by enhanced aeromagnetic data', *Journal of Structural Geology*, 158, p. 104573. Available at: <https://doi.org/10.1016/j.jsg.2022.104573>.

168. Esia Unit thrust system

Alonso, J.L. (1987) 'Sequences of thrusts and displacement transfer in the superposed duplexes of the Esia Nappe Region (cantabrian zone, nw spain)', *Journal of Structural Geology*, 9(8), pp. 969–983. Available at: [https://doi.org/10.1016/0191-8141\(87\)90005-8](https://doi.org/10.1016/0191-8141(87)90005-8).

Alonso, J.L. (1989) 'Fold reactivation involving angular unconformable sequences: theoretical analysis and natural examples from the Cantabrian Zone (Northwest Spain)', *Tectonophysics*, 170(1), pp. 57–77. Available at: [https://doi.org/10.1016/0040-1951\(89\)90103-0](https://doi.org/10.1016/0040-1951(89)90103-0).

Arboleya, M.L. (1989) 'Fault Rocks of the Esia Thrust (Cantabrian Mountains, N Spain) an Example of Foliatec Cataclasites', *Annales Tectonicae*, III(2), pp. 99–109.

Comte, P. (1959) *Recherches sur les terrains anciens de la Cordillère cantabrique*. Madrid: Tip.-Lit. Coullaut (Memorias del Instituto Geológico y Minero de España, 60).

IGME (2014) 'Spanish digital Geological Map. Cantabrian Zone'. Madrid (GEODE). Available at: <http://info.igme.es/cartografiadigital/geologica/geodezona.aspx?Id=Z1000>.

de Paz-Álvarez, M.I., Llana-Fúnez, S. and Alonso, J.L. (2021) 'Intrusion fracturing and quartz sand-rich injections in thrust-related fault rocks within the basal shear zone of the Esia Nappe (Cantabrian Zone, NW Iberia)', *Journal of Structural Geology*, 142, p. 104230. Available at: <https://doi.org/10.1016/j.jsg.2020.104230>.

169. Glarus Thrust

Herwegh, M. et al. (2008) 'The Glarus thrust: Excursion guide and report of a field trip of the Swiss Tectonic Studies Group (Swiss Geological Society, 14–16. 09. 2006)', *Swiss Journal of Geosciences*, 101, pp. 323–340. Available at: <https://doi.org/10.1007/s00015-008-1259-z>.

Pfiffner, O.A., Burkhard, M. and Schmid, S.M. (2006) *Comparative study on thrust faults*. UNESCO-World Heritage TektonicArena Sardona, p.129. Available at: <https://data.unesco-sardona.ch/forschen/wissenschaftliche-publikationen/>.

Pfiffner, O.A. and Schmid, S.M. (2008) *Supplement to the Comparative study on thrust faults: The Glarus overthrust*. UNESCO-World Heritage TektonicArena Sardona. Available at: <https://data.unesco-sardona.ch/forschen/wissenschaftliche-publikationen/>.

Schmid, S. (1975) 'The Glarus overthrust: field evidence and mechanical model The Glarus Overthrust: Field Evidence and Mechanical Model', *Eclogae Geologicae Helvetiae*, 68, pp. 247–280. Available at: <https://doi.org/10.5169/seals-164386>.

Westermann, A. (2009) 'Inherited Territories: The Glarus Alps, Knowledge Validation, and the Genealogical Organization of Nineteenth-Century Swiss Alpine Geognosy', *Science in Context*, 22(3), pp. 439–461. Available at: <https://doi.org/10.1017/S0269889709990081>.

170. Monte Perdido massif tectonic structure

Labalme, P. et al. (2016) 'Tectonothermal history of an exhumed thrust-sheets-top basin: An example from the south Pyrenean thrust belt: JACA THRUST-SHEET-TOP BASIN', *Tectonics*, 35(5), pp. 1280–1313. Available at: <https://doi.org/10.1002/2016TC004192>.

Muñoz, J.-A. et al. (2013) 'The Ainsa Fold and thrust oblique zone of the central Pyrenees: Kinematics of a curved contractional system from paleomagnetic and structural data', *Tectonics*, 32(5), pp. 1142–1175. Available at: <https://doi.org/10.1002/tect.20070>.

Pujalte, V. et al. (2016) 'A siliciclastic braid delta within a lower Paleogene carbonate platform (Ordesa-Monte Perdido National Park, southern Pyrenees, Spain): Record of the Paleocene-Eocene Thermal Maximum perturbation', *Palaeogeography, Palaeoclimatology, Palaeoecology*, 459, pp. 453–470. Available at: <https://doi.org/10.1016/j.palaeo.2016.07.029>.

Roussel, J. (1904) 'Tableau Stratigraphique des Pyrénées', *Bulletin Géologique de France*, 1(97), pp. 1–119.

Seguret, M. (1972) *Etude tectonique des nappes et séries décollées de la partie centrale du versant sud des Pyrénées: caractère synsédimentaire, rôle de la compression et de la gravité*. Montpellier: Université des Sciences et Techniques du Languedoc (Publication Ustela).

Van de Velde, E.J. (1968) 'Geology of the Ordesa overthrust mass, Spanish Pyrenees, Province of Huesca', *Estudios Geológicos*, 23(3–4), pp. 163–201.

171. Brittle structures of the Somerset Coast

Dart, C.J., McClay, K. and Hollings, P.N. (1995) '3D analysis of inverted extensional fault systems, southern Bristol Channel basin, UK', *Geological Society, London, Special Publications*, 88(1), pp. 393–413. Available at: <https://doi.org/10.1144/GSL.SP.1995.088.01.21>.

Hancock, P.L. (1985) 'Brittle microtectonics: principles and practice', *Journal of Structural Geology*, 7(3), pp. 437–457. Available at: [https://doi.org/10.1016/0191-8141\(85\)90048-3](https://doi.org/10.1016/0191-8141(85)90048-3).

McGrath, A.G. and Davison, I. (1995) 'Damage zone geometry around fault tips', *Journal of Structural Geology*, 17(7), pp. 1011–1024. Available at: <a href="https://doi.org/10.1016/019

Italy', *Memorie della Società Geologica Italiana*, 48, Part 2, pp. 541–548.

Civico, R. et al. (2018) 'Surface ruptures following the 30 October 2016 Mw 6.5 Norcia earthquake, central Italy', *Journal of Maps*, 14(2), pp. 151–160.

Livio, F.A. et al. (2016) 'Surface faulting during the August 24, 2016, central Italy earthquake (Mw 6.0): preliminary results', *Annals of Geophysics*, 59. Available at: <https://doi.org/10.4401/ag-7197>.

Pierantoni, P., Deiana, G. and Galderini, S. (2013) 'Stratigraphic and structural features of the Sibillini Mountains (Umbria–Marche Apennines, Italy)', *Italian Journal of Geosciences*, 132 (2013) f.3. Available at: <https://doi.org/10.3301/IJG.2013.08>.

Villani, F. et al. (2018) 'A database of the coseismic effects following the 30 October 2016 Norcia earthquake in Central Italy', *Scientific Data*, 5. Available at: <http://dx.doi.org/10.1038/sdata.2018.49>.

173. Alpine superposed buckle folds in Aliaga

Arenas, C. et al. (1998) *Guía del Parque Geológico de Aliaga*. Edited by J.L. Simón. Ayto. de Aliaga - CEDEMADE - Dpto. de Geología, Universidad de Zaragoza.

Lisle, R.J. (2020) *Geological Structures and Maps: A Practical Guide*. Fourth Edition. Oxford, United Kingdom ; Cambridge, MA.

Simón, J.L. (1980) 'Estructuras de superposición de plegamientos en el borde NE de la cadena Ibérica', *Acta geológica hispánica*, 15(5), pp. 137–140.

Simón, J.L. (2004) 'Superposed buckle folding in the eastern Iberian Chain, Spain', *Journal of Structural Geology*, 26(8), pp. 1447–1464. Available at: <https://doi.org/10.1016/j.jsg.2003.11.026>.

Simón, J.L. (2005) 'Erosion-controlled geometry of buckle fold interference', *Geology*, 33(7), pp. 561–564. Available at: <https://doi.org/10.1130/G21468.1>.

174. Marine terraces of San Juan de Marcona

Broggi, J.A. (1946) 'Las terrazas marinas de la bahía de San Juan en Ica', *Boletín de la Sociedad Geológica del Perú*, 19, pp. 21–33.

Freisleben, R. et al. (2021) 'Marine terraces of the last interglacial period along the Pacific coast of South America (1°N–40°S)', *Earth System Science Data*, 13(6), pp. 2487–2513. Available at: <https://doi.org/10.5194/essd-13-2487-2021>.

Hsu, J.T.J. (1988) *Emerged quaternary marine terraces in southern Peru: Sea level changes and continental margin tectonics over the subducting Nazca Ridge*. Ph.D. Thesis. Ithaca, NY (US); Cornell Univ. Available at: <https://www.osti.gov/biblio/7164193>.

Macharé, J. and Ortílieb, L. (1992) 'Plio-Quaternary vertical motions and the subduction of the Nazca Ridge, central coast of Peru', *Tectonophysics*, 205(1), pp. 97–108. Available at: [https://doi.org/10.1016/0040-1951\(92\)90420-B](https://doi.org/10.1016/0040-1951(92)90420-B).

Ortílieb, L. and Macharé, J. (1990) 'Geocronología y morfoestratigrafía de terrazas marinas del Pleistoceno superior: el caso de San Juan–Marcona, Perú', *Boletín de la Sociedad Geológica del Perú*, 81, pp. 87–106.

Saillard, M. et al. (2011) 'Andean coastal uplift and active tectonics in southern Peru: 10Be surface exposure dating of differentially uplifted marine terrace sequences (San Juan de Marcona,

~15.4°S)', *Geomorphology*, 128(3), pp. 178–190. Available at: <https://doi.org/10.1016/j.geomorph.2011.01.004>.

VII. MINERALOGY

175. The Sar-e-Sang Lapis Lazuli Deposit

Kulke, H. (1976) 'Die Lapislazuli-Lagerstätte Sare Sang (Badakhshan)', *Geologie, Entstehung, Kulturgeschichte und Bergbau. Afghanistan Journal*, 3, pp. 43–56.

Schreyer, W. and Abraham, K. (1976) 'Three-stage metamorphic history of a whiteschist from Sar e Sang, Afghanistan, as part of a former evaporite deposit', *Contributions to Mineralogy and Petrology*, 59(2), pp. 111–130. Available at: <https://doi.org/10.1007/s00269-016-0860-3>.

Wali Faryad, S. (2002) 'Metamorphic Conditions and Fluid Compositions of Scapolite-Bearing Rocks from the Lapis Lazuli Deposit at Sare Sang, Afghanistan', *Journal of Petrology*, 43(4), pp. 725–747. Available at: <https://doi.org/10.1093/petrology/43.4.725>.

Yurgenson, G.A. and Sukharev, B.P. (1985) 'Localization of Lapis Lazuli Bodies of Badakhshan and Their Mineral Zonation', *International Geology Review*, 27, pp. 230–237. Available at: <https://doi.org/10.1080/00206818509466410>.

176. The Kalahari Manganese Field

Cairncross, B. and Beukes, N.J. (2013) *The Kalahari Manganese Field: the adventure continues*. Struik Nature (an imprint of Penguin Random House (Pty) Ltd), Cape Town.

Gutzmer, J. and Beukes, N.J. (1995) 'Fault-controlled metasomatic alteration of early Proterozoic sedimentary manganese ores in the Kalahari manganese field, South Africa', *Economic Geology*, 90(4), pp. 823–844. Available at: <https://doi.org/10.2113/gsecongeo.90.4.823>.

Gutzmer, J. and Beukes, N.J. (1996) 'Mineral paragenesis of the Kalahari manganese field, South Africa', *Ore Geology Reviews*, 11(6), pp. 405–428. Available at: [https://doi.org/10.1016/S0169-1368\(96\)00011-X](https://doi.org/10.1016/S0169-1368(96)00011-X).

Kleyenstein, A.S.E. (1984) 'The mineralogy of the manganese-bearing Hotazel Formation, of the Proterozoic Transvaal Sequence in Griqualand West, South Africa', *South African Journal of Geology*, 87(3), pp. 257–272.

Tsikos, H. et al. (2003) 'Deposition, Diagenesis, and Secondary Enrichment of Metals in the Paleoproterozoic Hotazel Iron Formation, Kalahari Manganese Field, South Africa', *Economic Geology*, 98(7), pp. 1449–1462. Available at: <https://doi.org/10.2113/gsecongeo.98.7.1449>.

Wilson, W.E. et al. (2017) 'The N'Chwaning mines, Kalahari Manganese Field, Northern Cape Province, South Africa', *The Mineralogical Record*, pp. 13–114.

177. The Broken Hill Pb-Zn-Ag deposit

Birch, W.D. (1999) *Minerals of Broken Hill*. Broken Hill City Council in conjunction with Museum Victoria.

Birch, W.D. and van der Heyden, A. (1997) 'Minerals of the Kintore and Block 14 open cuts at Broken Hill, New South Wales', *Australian Journal of Mineralogy*, 3(1), pp. 23–72.

Elliott, P. (2021) 'Cardite, Zn5.5[AsO4]2[AsO3OH](OH)3·3H2O, a new zinc arsenate mineral from Broken Hill, New South Wales, Australia', *Mineralogy and Petrology*, 115(4), pp. 467–475. Available at: <https://doi.org/10.1007/s00710-021-00750-2>.

Frost, B.R., Swapp, S.M. and Gregory, R.W. (2005) 'Prolonged existence of sulfide melt in the Broken Hill orebody, New South Wales, Australia', *The Canadian Mineralogist*, 43(1), pp. 479–493. Available at: <https://doi.org/10.2113/gscanmin.43.1.479>.

Shchipalkina, N.V. et al. (2017) 'Ferrorhodonite, CaMn3Fe[Si5O15], a new mineral species from Broken Hill, New South Wales, Australia', *Physics and Chemistry of Minerals*, 44(5), pp. 323–334. Available at: <https://doi.org/10.1007/s00269-016-0860-3>.

Stevens, B.P.J., Page, R.W. and Crook, A. (2008) 'Geochronology of Willyama Supergroup metavolcanics, metasediments and contemporaneous intrusions, Broken Hill, Australia', *Australian Journal of Earth Sciences*, 55(3), pp. 301–330. Available at: <https://doi.org/10.1080/08120090701769456>.

178. Mineral site of Mont Saint-Hilaire

Currie, K.L., Eby, G.N. and Gittins, J. (1986) 'The petrology of the Mont Saint Hilaire complex, southern Quebec: An alkaline gabbro-peralkaline syenite association', *Lithos*, 19(1), pp. 65–81. Available at: [https://doi.org/10.1016/0024-4937\(86\)90016-2](https://doi.org/10.1016/0024-4937(86)90016-2).

Feininger, T. and Goodacre, A.K. (1995) 'The eight classical Monteregian hills at depth and the mechanism of their intrusion', *Canadian Journal of Earth Sciences*, 32(9), pp. 1350–1364. Available at: <https://doi.org/10.1139/e95-109>.

Foland, K.A. et al. (1986) '40Ar/39Ar ages for plutons of the Monteregian Hills, Quebec: Evidence for a single episode of Cretaceous magmatism', *GSA Bulletin*, 97(8), pp. 966–974. Available at: [https://doi.org/10.1130/0016-7606\(1986\)97<966:AAFPOT>2.0.CO;2](https://doi.org/10.1130/0016-7606(1986)97<966:AAFPOT>2.0.CO;2).

Horváth, L. et al. (2019) *Mont Saint-Hilaire: History, Geology, Mineralogy*. (The Canadian Mineralogist, Special Publication, 14).

179. The Muzo emerald deposit

Branquet, Y. et al. (1999) 'Emeralds in the Eastern Cordillera of Colombia: Two tectonic settings for one mineralization', *Geology*, 27(7), pp. 597–600. Available at: [https://doi.org/10.1130/0091-7613\(1999\)027<0597:EITECO>2.3.CO;2](https://doi.org/10.1130/0091-7613(1999)027<0597:EITECO>2.3.CO;2).

Giuliani, G. (2022) *Émeraudes, tout un Monde ! Les Éditions du Piat*, Saint-Julien-du-Pinet, France.

Laumonier, B. et al. (1996) 'Mise en évidence d'une tectonique compressive Éocène-Oligocène dans l'Ouest de la Cordillère orientale de Colombie, d'après la structure en duplex des gisements d'émeraude de Muzo et de Coscuez (Évidence for an Eocene-Oligocene compressive tectonics in the western part of Eastern Cordillera of Colombia, from the duplex structure of the Muzo and Coscuez emerald deposits)', *Comptes rendus de l'Académie des sciences*, 323, pp. 705–712.

Ottaway, T.L. et al. (1994) 'Formation of the Muzo hydrothermal emerald deposit in Colombia', *Nature*, 369, pp. 552–554. Available at: <https://doi.org/10.1038/369552a0>.

Pignatelli, I. et al. (2015) 'Colombian Trapiche Emeralds: Recent Advances in Understanding Their Formation', *Gems & Gemology*, pp. 222–259. Available at: <https://doi.org/10.5741/GEMS.51.3.222>.

Pogue, J. (1916) 'The emerald deposits of Muzo, Colombia', *Transactions of the American Institute of Mining and Metallurgical Engineers*, 55, pp. 810–834.

VIII. GEOMORPHOLOGY AND ACTIVE GEOLOGICAL PROCESS

180. Granite landforms of Dartmoor

Eden, M.J. and Green, C.P. (1971) 'Some Aspects of Granite Weathering and Tor Formation on Dartmoor, England', *Geografiska Annaler: Series A, Physical Geography*, 53(2), pp. 92–99. Available at: <https://doi.org/10.1080/04353676.1971.11879838>.

Gerrard, J. (1988) 'Periglacial Modification of the Cox Tor–Staple Tors Area of Western Dartmoor, England', *Physical Geography*, 9(3), pp. 280–300. Available at: <https://doi.org/10.1080/02723646.1988.10642355>.

Gunnell, Y. et al. (2013) 'The granite tors of Dartmoor, Southwest England: rapid and recent emergence revealed by Late Pleistocene cosmogenic apparent exposure ages', *Quaternary Science Reviews*, 61, pp. 62–76. Available at: <https://doi.org/10.1016/j.quascirev.2012.11.005>.

Gunnell, Y. (2020) 'Landscape evolution of Dartmoor, SW England: A review of evidence-based controversies and their wider implications for geoscience', *Proceedings of the Geologists' Association*, 131(2), pp. 187–226. Available at: <https://doi.org/10.1016/j.pgeola.2020.04.003>.

Gunnell, Y. and Jarman, D. (2020) 'Dartmoor', in A. Goudie and P. Migoñ (eds) *Landscapes and Landforms of England and Wales*. Cham: Springer International Publishing (World Geomorphological Landscapes), pp. 239–255. Available at: https://doi.org/10.1007/978-3-030-38957-4_13.

Linton, D.L. (1955) 'The Problem of Tors', *The Geographical Journal*, 121(4), pp. 470–487. Available at: <https://doi.org/10.2307/1791756>.

181. Inverted landscape of a Plio-Pleistocene phreatomagmatic monogenetic volcanic field in the Bakony-Balaton Upland

Kereszturi, G. et al. (2011) 'The role of external environmental factors in changing eruption styles of monogenetic volcanoes in a Mio/Pleistocene continental volcanic field in western Hungary', *Journal of Volcanology and Geothermal Research*, 201(1), pp. 227–240. Available at: <https://doi.org/10.1016/j.jvolgeores.2010.08.018>.

Kereszturi, G. and Németh, K. (2012) 'Structural and morphometric irregularities of eroded Pliocene scoria cones at the Bakony–Balaton Highland Volcanic Field, Hungary', *Geomorphology*, 136(1), pp. 45–58. Available at: <https://doi.org/10.1016/j.geomorph.2011.08.005>.

Martin, U. and Németh, K. (2004) *Mio/Pliocene phreatomagmatic volcanism in the western Pannonian Basin*. International Maar Conference, Budapest: Geological Institute of Hungary (Geologica Hungarica. Series geologica, t. 26).

(Hungary) using physical volcanology data', *Zeitschrift für Geomorphologie*, 43(4), pp. 417–438. Available at: <https://doi.org/10.1127/zfg/43/1999/417>.

Wijbrans, J. *et al.* (2007) '40Ar/39Ar geochronology of Neogene phreatomagmatic volcanism in the western Pannonian Basin, Hungary', *Journal of Volcanology and Geothermal Research*, 164(4), pp. 193–204. Available at: <https://doi.org/10.1016/j.jvolgeores.2007.05.009>.

182. Great Salt Lake

Chan, M. *et al.* (2024) 'The Holocene Great Salt Lake and Pleistocene Lake Bonneville System: Conserving our Geoheritage for Future Generations', *Geosites*, 51, pp. 1–13. Available at: <https://doi.org/10.3171/ugap.v51i1.132>.

Gilbert, G.K. (1886) 'The inculcation of scientific method by example, with an illustration drawn from the Quaternary geology of Utah', *American Journal of Science*, s3-31(184), pp. 284–299. Available at: <https://doi.org/10.2475/ajs.s3-31.184.284>.

Gilbert, G.K. (1890) *Lake Bonneville, Lake Bonneville*. USGS Numbered Series 1. Washington, D.C.: U.S. Government Printing Office, p. 562. Available at: <https://doi.org/10.3133/ml>.

Gwynn, J.W. (2002) *Great Salt Lake: an overview of change*. Utah Geological Survey, Salt Lake City, Utah. Available at: <https://www.utahmapstore.com/products/great-salt-lake-an-overview-of-change>.

Oviatt, C.G. and Shroder, J.F. (eds) (2016) *Lake Bonneville: A Scientific Update*. New York, N.Y: Elsevier.

183. Mackenzie Delta

Burn, C.R. (2010) 'The Mackenzie Delta: An Archetypal Permafrost Landscape', in P. Migan (ed.) *Geomorphological Landscapes of the World*. Dordrecht: Springer Netherlands, pp. 1–12. Available at: https://doi.org/10.1007/978-90-481-3055-9_1.

Burn, C.R. (2017) 'Mackenzie Delta: Canada's Principal Arctic Delta', in O. Slaymaker (ed.) *Landscapes and Landforms of Western Canada*. Cham: Springer International Publishing (World Geomorphological Landscapes), pp. 321–334. Available at: https://doi.org/10.1007/978-3-319-44595-3_23.

Carson, M.A., Jasper, J.N. and Conly, F.M. (1998) 'Magnitude and Sources of Sediment Input to the Mackenzie Delta, Northwest Territories, 1974–94', *ARCTIC*, 51(2), pp. 116–124. Available at: <https://doi.org/10.14430/arctic1053>.

Mackay, J. (1998) 'Pingo Growth and collapse, Tuktoyaktuk Peninsula Area, Western Arctic Coast, Canada: a long-term field study', *Géographie physique et Quaternaire*, 52(3), pp. 271–323. Available at: <https://doi.org/10.7202/004847ar>.

Vesakoski, J.-M. *et al.* (2017) 'Arctic Mackenzie Delta channel planform evolution during 1983–2013 utilising Landsat data and hydrological time series', *Hydrological Processes*, 31(22), pp. 3979–3995. Available at: <https://doi.org/10.1002/hyp.11315>.

184. Getbol Tidal Flats

Chun, S.S. *et al.* (2015) 'Sedimentation and Holocene evolution of archipelago tidal flats in SW Korea', in *Extended Abstracts. 9th international conference on tidal sedimentology (Tidalites 2015)*, pp. 35–37.

Chun, S.S. (2018) 'The macrotidal flats in the southwestern coast of Korea: classification, characteristics and uniqueness', in *Western Pacific sedimentology meeting proceedings*, pp. 1–8.

Crofts, R. *et al.* (2020) *Guidelines for geoconservation in protected and conserved areas*. IUCN. Available at: <https://doi.org/10.2305/IUCN.CH.2020.PAG.31.en>.

UNESCO (2021) *A nomination of the World Heritage, Getbol, Korean Tidal Flats*. UNESCO World Heritage Center.

Woo, K.S., Chun, S.S. and Moon, K.O. (2020) 'Outstanding Geoheritage Values of the Island-Type Tidal Flats in Korea', *Geoheritage*, 12(1), p. 8. Available at: <https://doi.org/10.1007/s12371-020-00445-8>.

185. Fontaine de Vaucluse

Audra, P. *et al.* (2004) 'The effect of the Messinian Deep Stage on karst development around the Mediterranean Sea. Examples from Southern France', *Geodinamica Acta - GEODIN ACTA*, 17, pp. 389–400. Available at: <https://doi.org/10.3166/ga.17.389-400>.

Blavoux, B., Mudry, J. and Puig, J.-M. (1992) 'The karst system of the Fontaine de Vaucluse (Southeastern France)', *Environmental Geology and Water Sciences*, 19(3), pp. 215–225. Available at: <https://doi.org/10.1007/BF01704088>.

Bonacci, O. (2007) 'Analysis of Long-Term (1878–2004) Mean Annual Discharges of the Karst Spring Fontaine de Vaucluse (France)', *Acta Carsologica*, 36(1). Available at: <https://doi.org/10.3986/ac.v36i1.217>.

Cognard-Plancq, A.-L., Gévaudan, C. and Emblanch, C. (2006) 'Historical monthly rainfall-runoff database on Fontaine de Vaucluse karst system: review and lessons', in *Karst, cambio climático y aguas subterráneas*. Geological and Mining Institute of Spain (Hidrogeología y Aguas Subterráneas), 18, pp. 465–475.

Gaubert, G. and Le Falher, B. (1990) *Les cavernes d'Albion. Hydrologie et spéléologie des territoires alimentant en eau la Fontaine de Vaucluse. Association de recherches et d'études hydrologiques du Plateau d'Albion (AREHPA)*.

Puig, J.-M. (1987) *Le système karstique de la Fontaine de Vaucluse*. These de doctorat. Avignon. Available at: <https://theses.fr/1987AVIG0004>.

186. Wakulla spring

Glowacki, M. (2019) 'Illicit Digging, Illicit Collecting, and Archaeology: A Perspective from Florida', in D.K. Thulman and E.G. Garrison (eds) *New Directions in the Search for the First Floridians*. University Press of Florida, p. 0. Available at: <https://doi.org/10.5744/florida/9781683400738.003.0009>.

Kincaid, T. (1999) *Morphologic and Fractal Characterization of Saturated Karstic Caves*. Ph.D. Geohydrology. The University of Wyoming. Available at: <https://doi.org/10.13140/RG.2.1.2523.9448>.

Kincaid, T. (2006) 'Karst Hydrogeology of the Woodville Karst Plain - Wakulla & St. Marks River Basins', in *Field trip guide book including full page maps. American Society of Civil Engineers Conference, SEGS • FAPG • GUE • HC • HKI*. (Field trip guide book), p. 9. Available at: <http://wakullaspringsalliance.org/wp-content/uploads/2020/04/Kincaid.2006.Karst-Hydrogeology-of-the-Woodville-Karst-Plain.sans-maps.pdf>.

Northwest Florida Water Management District (NFWFMD) (2021) *Recommended Minimum Flows for Wakulla and Sally Ward Springs*,

187. Vrelo Bune Spring

Ford, D. and Williams, P.W. (2007) *Karst Hydrogeology and Geomorphology*. Wiley.

Milanović, P. (2023) *Karst of East Herzegovina and Dubrovnik Littoral*. Springer. Available at: <https://link.springer.com/book/10.1007/978-3-031-28120-4>.

Milanović, P., Stevanović, Z. and Čokorilo Ilić, M. (eds) (2014) 'Field Trip Guide', in *DIKTAS International conference „Karst Without Boundaries“ and the International course and seminar „Characterization and Engineering of Karst Aquifers“*, Trebinje, p. 69.

Stevanović, Z. (2010) 'Major springs of southeastern Europe and their Utilization', in N. Kresic and Z. Stevanović (eds) *Groundwater Hydrology of Springs*. Boston: Butterworth-Heinemann, pp. 389–410. Available at: <https://doi.org/10.1016/B978-1-85617-502-9.00010-4>.

Touloumdjian, C. (2005) 'The Springs of Montenegro and Dinaric karst', in Z. Stevanović and P. Milanović (eds) *Proceedings of the IAH International conference KARST 2005*. University of Belgrade, Institute of Hydrogeology, Belgrade: Nat.Com. of the IAH Serb. & Monten., pp. 443–458.

188. Mammoth Cave

Bledsoe, L.A., Groves, C. and Toomey, R. (2021) 'The Mammoth Cave National Park World Heritage Site', *Zeitschrift für Geomorphologie, Supplementary Issues*, pp. 145–193. Available at: https://doi.org/10.1127/zfg_suppl/2021/0694.

Granger, D.E., Fabel, D. and Palmer, A.N. (2001) 'Pliocene–Pleistocene incision of the Green River, Kentucky, determined from radioactive decay of cosmogenic ^{26}Al and ^{10}Be in Mammoth Cave sediments', *GSABulletin*, 113(7), pp. 825–836. Available at: [https://doi.org/10.1130/0016-7606\(2001\)113<0825:PPIOTG>2.0.CO;2](https://doi.org/10.1130/0016-7606(2001)113<0825:PPIOTG>2.0.CO;2).

Groves, C. *et al.* (2021) *Mammoth Cave National Park*. Natural Resource Report NPS/MACA/NRR 2021/2258. Fort Collins, Colorado: National Park Service, p. 585.

Hobbs III, H.H. *et al.* (eds) (2017) *Mammoth Cave: A Human and Natural History*. Cham: Springer International Publishing (Cave and Karst Systems of the World). Available at: <https://doi.org/10.1007/978-3-319-53718-4>.

189. The White Limestone Karst of Cockpit Country

Dwyer, S. and Smickle, D. (2004) *Cockpit Country hydrological assessment: A Desk Study of the Hydrological and Hydrogeological Regime Governing Flow in the Cockpit Country of Jamaica*. Water Resources Authority & The Nature Conservancy.

Miller, D.J. (2003) 'Karst geomorphology of the White Limestone Group', *Cainozoic research*, 3(1/2), pp. 189–219.

Mitchell, S., Miller, D.J. and Maharaj, R. (2003) 'Field guide to the geology and geomorphology of the Tertiary limestones of the Central Inlier and Cockpit Country', *Caribbean Journal of Earth Science*, 37, pp. 39–48.

Mitchell, S.F. (2013) 'Stratigraphy of the White Limestone of Jamaica', *Bulletin de la Société Géologique de France*, 184(1–2), pp. 111–118. Available at: <https://doi.org/10.2113/gssgbull.184.1-2.111>.

Sawkins, J.G. (1869) *Reports on the Geology of Jamaica; Or, Part II. of the West Indian Survey*. Printed for H.M. Stationery Off., Longmans, Green, and Co. (Memoirs of the Geological Survey). Available at: <http://archive.org/details/reportsongeolog00hoffgoog>.

Sweeting, M.M. (1958) 'The Karstlands of Jamaica', *The Geographical Journal*, 124(2), pp. 184–199. Available at: <https://doi.org/10.2307/1790245>.

190. Guilin Karst

Tang Xireng, Y.W. (1987) *Xu Xiake and His Travels*. China Social Science Press.

Yuan, D.X. (ed.) (1991) *Karst of China*. Geological Publishing House, Beijing.

Zhu, X.W. (1991a) 'New Considerations on the Characteristics and Evolution of Tower Karst (Part 1)', *Carsologica Sinica*, 10(1), pp. 51–62.

Zhu, X.W. (1991b) 'New Considerations on the Characteristics and Evolution of Tower Karst (Part 2)', *Carsologica Sinica*, 10(2), pp. 137–150.

Zhu, X.W. (1991c) 'New Considerations on the Characteristics and Evolution of Tower Karst (Part 3)', *Carsologica Sinica*, 10(3), pp. 171–182.

Zhu, X.W., Wang, X.Y. and Zhu, D.H. (1988) *Research on Guilin Karst Geomorphology and Caves*. Geological Publishing House, Beijing.

191. Ha Long Bay-Cat Ba Archipelago

Tran Duc Thanh (1998) *Geological history of Ha Long Bay*. Hai Phong Institute of Oceanology, National Centre for Natural Science and Technology of Vietnam.

Tran Duc Thanh and Waltham, T. (2000) *The outstanding value of geology of Ha Long Bay. Proceedings of workshop on "Five years of Ha Long Bay World Heritage"*. Ha Long City: Quang Ninh Provincial People's Committee, Ministry of Culture and Information, and Vietnam National Commission for UNESCO.

Tran Van Tri *et al.* (2003) 'The Ha Long Bay World Heritage: Outstanding Geological Values', *Journal of Geology*, 22, pp. 1–18.

Tran Van Tri and Dang Vu Khuc (eds) (2011) *Geology and Earth Resources of Viet Nam*. Ha Noi: Natural Science and Technology Publishing House.

UNESCO (no date) 'UNESCO World Heritage page for Ha Long Bay'. Available at: <https://whc.unesco.org/en/list/672>.

Waltham, T. (1998) *Limestone karst of Ha Long Bay, Vietnam. An assessment of the karst geomorphology of the World Heritage Site for the World Conservation Union and The Management Department of Ha Long Bay*. Engineering Geology Report 806. Nottingham Trent University, UK.

192. Tepuis and quartzite karst of Gran Sabana

Briceño, H.O. and Schubert, C. (1990) 'Geomorphology of the Gran Sabana, Guayana Shield, southeastern Venezuela', *Geomorphology*, 3(2), pp. 125–141. Available at: [https://doi.org/10.1016/0169-555X\(90\)90041-N](https://doi.org/10.1016/0169-555X(90)90041-N).

Galan, C. and Lagarde, J. (1988) 'Morphologie et évolution des cavernes et formes superficielles dans les quartzites du Roraima', *Karstologia : revue de karstologie et de spéléologie physique*, 11(1), pp. 49–60. Available at: <https://doi.org/10.3406/karst.1988.2190>.

Piccini, L. and Mecchia, M. (2009) 'Solution weathering rate and origin of karst landforms and caves in the quartzite of Auyan-tepui (Gran Sabana, Venezuela)', *Geomorphology*, 106(1), pp. 15–25. Available at: <https://doi.org/10.1016/j.geomorph.2008.09.019>.

Sauro, F. (2014) 'Structural and lithological guidance on speleogenesis in quartz–sandstone: Evidence of the arenisation process', *Geomorphology*, 226, pp. 106–123. Available at: <https://doi.org/10.1016/j.geomorph.2014.07.033>.

Urbani, F. and Szczepan, E. (1974) 'Venezuelan caves in non-carbonate rocks: a new field in karst research', *NSS News*, 32, pp. 233–235.

Wray, R.A.L. (2010) 'The Gran Sabana: The World's Finest Quartzite Karst?', in P. Migon (ed.) *Geomorphological Landscapes of the World*. Dordrecht: Springer Netherlands, pp. 79–88. Available at: https://doi.org/10.1007/978-90-481-3055-9_9.

Wray, R.A.L. and Sauro, F. (2017) 'An updated global review of solutional weathering processes and forms in quartz sandstones and quartzites', *Earth-Science Reviews*, 171, pp. 520–557. Available at: <https://doi.org/10.1016/j.earscirev.2017.06.008>.

193. Fjords and towering sea cliffs of Fiordland

Dlabola, E.K. et al. (2015) 'A post-glacial relative sea-level curve from Fiordland, New Zealand', *Global and Planetary Change*, 131, pp. 104–114. Available at: <https://doi.org/10.1016/j.gloplacha.2015.05.010>.

Dykstra, J.L. (2012) *The Post-LGM Evolution of Milford Sound, Fiordland, New Zealand: Timing of Ice Retreat, the Role of Mass Wasting & Implications for Hazards*. PhD thesis. University of Canterbury. Geological Sciences. Available at: <https://ir.canterbury.ac.nz/handle/10092/9282>.

Hayward, B.W. (2022) 'Piopiotahi / Milford Sound; Deep glacier-carved valley drowned by sea level rise after the Last Ice Age', in *Mountains, Volcanoes, Coasts and Caves: Origins of Aotearoa New Zealand's natural wonders*. Auckland University Press, p. 384.

Klepeis, K.A. et al. (2019) 'The Age and Origin of Miocene-Pliocene Fault Reactivations in the Upper Plate of an Incipient Subduction Zone, Puysegur Margin, New Zealand', *Tectonics*, 38(8). Available at: <https://doi.org/10.1029/2019TC005674>.

Strachan, L.J. et al. (2016) 'Non-cohesive silt turbidity current flow processes; insights from proximal sandy-silt and silty-sand turbidites, Fiordland, New Zealand', *Sedimentary Geology*, 342, pp. 118–132. Available at: <https://doi.org/10.1016/j.sedgeo.2016.06.017>.

Turnbull, I.M., Allibone, A.H. and Jongens, R. (2010) *Geology of the Fiordland area, 1:250,000 geological map 17*. Institute of Geological and Nuclear Sciences. Available at: <https://natlib.govt.nz/records/30190164>.

194. Fjords and glaciers in Hornsund and Van Mijenfjorden, Svalbard

Błaszczyk, M., Jania, J.A. and Kolondra, L. (2013) 'Fluctuations of tidewater glaciers in Hornsund Fjord (Southern Svalbard) since the beginning of the 20th century', *Polish Polar Research*, 34(4), pp. 327–352. Available at: <https://doi.org/10.2478/popore-2013-0024>.

Erikstad, L., Hagen, D. and Simensen, T. (2023) 'Working with Natural Processes: Restoring a Mining Landscape in the High Arctic, Svalbard, Norway', *Geoheritage*, 15(3), p. 87. Available at: <https://doi.org/10.1007/s12371-023-00855-4>.

Jahn, A. (1975) *Problems of the periglacial zone*. Warsaw: Państwowe Wydawnictwo Naukowe. Available at: <http://archive.org/details/problemsofperigl0000alfr>.

Kristensen, L. et al. (2009) 'Mud aprons in front of Svalbard surge moraines: Evidence of subglacial deforming layers or proglacial glaciotectonics?', *Geomorphology*, 111(3), pp. 206–221. Available at: <https://doi.org/10.1016/j.geomorph.2009.04.022>.

Larsen, E. et al. (2018) 'Lateglacial and Holocene glacier activity in the Van Mijenfjorden area, western Svalbard', *arktos*, 4(1), pp. 1–21. Available at: <https://doi.org/10.1007/s41063-018-0042-2>.

Lyså, A. et al. (2018) 'A temporary glacier-surge ice-dammed lake, Braganzavågen, Svalbard', *Boreas*, 47(3), pp. 837–854. Available at: <https://doi.org/10.1111/bor.12302>.

Zwolinski, Z., Kostrzewski, A. and Pulina, M. (eds) (2013) *Ancient and modern geocosystems of Spitsbergen*. Poznań: Bogucki Wyd Nauk.

195. Vatnajökull

Baldursson, S. et al. (2018) *Nomination of Vatnajökull National Park for inclusion in the World Heritage List*. Reykjavík: Vatnajökull National Park.

Gudmundsson, M.T. et al. (2004) 'The 1996 eruption at Gjálp, Vatnajökull ice cap, Iceland: efficiency of heat transfer, ice deformation and subglacial water pressure', *Bulletin of Volcanology*, 66(1), pp. 46–65. Available at: <https://doi.org/10.1007/s00445-003-0295-9>.

Thórhallsdóttir, T.E. and Svavarssdóttir, K. (2022) 'The Environmental History of Skeiðarársandur Outwash Plain, Iceland', *Journal of the North Atlantic*, 2022(43), pp. 1–21. Available at: <https://doi.org/10.3721/037.006.4303>.

196. Yosemite Valley

Collins, B.D. and Stock, G.M. (2016) 'Rockfall triggering by cyclic thermal stressing of exfoliation fractures', *Nature Geoscience*, 9(5), pp. 395–400. Available at: <https://doi.org/10.1038/ngeo2686>.

Graham, J.P. (2012) *Yosemite National Park: geologic resources inventory report*. NPS/NRSS/GRD/NRR--2012/560. Denver, CO : Fort Collins, Colorado: National Park Service, Geologic Resources Division ; U.S. Department of the Interior, National Park Service, Natural Resource Stewardship and Science, p. 70. Available at: <https://irma.nps.gov/DataStore/DownloadFile/453731>.

Huber, N.K. (1987) *The geologic story of Yosemite National Park*, Bulletin. 1595. U.S. Government Printing Office. Available at: <https://doi.org/10.3133/b1595>.

Matthes, F.E. (1930) *Geologic history of the Yosemite Valley*, Professional Paper. 160. U.S. Geological Survey. Available at: <https://doi.org/10.3133/pp160>.

Stock, G.M., Anderson, R.S. and Finkel, R.C. (2005) 'Rates of erosion and topographic evolution of the Sierra Nevada, California, inferred from cosmogenic ^{26}Al and ^{10}Be concentrations', *Earth Surface Processes and Landforms*, 30(8), pp. 985–1006. Available at: <https://doi.org/10.1002/esp.1258>.

IX. IMPACT STRUCTURES AND EXTRATERRESTRIAL ROCKS

197. Vredefort Dome

Allen, N.H. et al. (2022) 'A Revision of the Formation Conditions of the Vredefort Crater', *Journal of Geophysical Research: Planets*, 127(8), p. e2022JE007186. Available at: <https://doi.org/10.1029/2022JE007186>.

Gibson, R.L. (2019) 'The Mesoarchaean Basement Complex of the Vredefort Dome—A Mid-Crustal Section Through the Central Kaapvaal Craton Exposed by Impact', in A. Kröner and A. Hofmann (eds) *The Archaean Geology of the Kaapvaal Craton, Southern Africa*. Cham: Springer International Publishing (Regional Geology Reviews), pp. 109–132. Available at: https://doi.org/10.1007/978-3-319-78652-0_5.

Gibson, R.L. and Reimold, W.U. (2008) *Geology of the Vredefort impact structure: a guide to sites of interest*. Pretoria: Council for Geoscience (Memoir, 97).

Gottwald, M., Kenkmann, T. and Reimold, W.U. (2020) *Terrestrial impact structures: the TanDEM-X Atlas*. München, Germany: Verlag Dr. Friedrich Pfeil.

Grieve, R.A.F. et al. (2008) 'Observations and interpretations at Vredefort, Sudbury, and Chicxulub: Towards an empirical model of terrestrial impact basin formation', *Meteoritics & Planetary Science*, 43(5), pp. 855–882. Available at: <https://doi.org/10.1111/j.1945-5100.2008.tb01086.x>.

Reimold, W.U. and Gibson, R.L. (2010) *Meteorite Impact!: The Danger from Space and South Africa's Mega-Impact The Vredefort Structure*. Berlin, Heidelberg: Springer. Available at: <https://doi.org/10.1007/978-3-642-10464-0>.

198. Ries Crater

Arp, G. et al. (2021) 'A Volcanic Ash Layer in the Nördlinger Ries Impact Structure (Miocene, Germany): Indication of Crater Fill Geometry and Origins of Long-Term Crater Floor Sagging', *Journal of Geophysical Research: Planets*, 126(4), p. e2020JE006764. Available at: <https://doi.org/10.1029/2020JE006764>.

Chao, E.C.T., Hüttner, R. and Schmidt-Kaler, H. (1978) *Principal exposures of the Ries meteorite crater in Southern Germany. Description, photographic documentation and interpretation*. Munich: Bayerisches Geologisches Landesamt.

Geopark Ries (ed.) (2019) *Windows into the Earth with excursion tips. Adventure geotopes*.

Gümbel, C.W. von (1870) *Ueber den Riesvulkan und über vulkanische Erscheinungen im Rieskessel*. München (Sitzungsberichte der mathematisch-physikalischen Klasse der Bayerischen Akademie der Wissenschaften.). Available at: <https://publikationen.bwdw.de/de/003392895>.

Shoemaker, E.M. and Chao, E.C.T. (1961) 'New evidence for the impact origin of the Ries Basin, Bavaria, Germany', *Journal of Geophysical Research (1896–1977)*, 66(10), pp. 3371–3378. Available at: <https://doi.org/10.1029/JZ066i010p03371>.

Stöffler, D. et al. (2013) 'Ries crater and suevite revisited—Observations and modeling Part I: Observations', *Meteoritics & Planetary Science*, 48(4), pp. 515–589. Available at: <https://doi.org/10.1111/maps.12086>.

199. Lake Bosumtwi Impact Crater

Ferrière, L. et al. (2008) 'Shock metamorphism of Bosumtwi impact crater rocks, shock attenuation, and uplift formation', *Science*, 322(5908), pp. 1678–1681. Available at: <https://doi.org/10.1126/science.1166283>.

Jones, W.B., Bacon, M. and Hastings, D.A. (1981) 'The Lake Bosumtwi Impact Crater, Ghana', *Geological Society of America Bulletin*, 92, pp. 342–349. Available at: [https://doi.org/10.1130/0016-7606\(1981\)92<342:TLBICG>2.0.CO;2](https://doi.org/10.1130/0016-7606(1981)92<342:TLBICG>2.0.CO;2).

Koeberl, C. et al. (1998) 'Petrology and geochemistry of target rocks from the Bosumtwi impact structure, Ghana, and comparison with Ivory Coast tektites', *Geochimica et Cosmochimica Acta*, 62(12), pp. 2179–2196. Available at: [https://doi.org/10.1016/S0016-7037\(98\)00137-9](https://doi.org/10.1016/S0016-7037(98)00137-9).

Koeberl, C. et al. (2007) 'An international and multidisciplinary drilling project into a young complex impact structure: The 2004 ICDP Bosumtwi Crater Drilling Project - An overview', *Meteoritics and Planetary Science*, 42(4–5), pp. 483–511. Available at: <https://doi.org/10.1111/j.1945-5100.2007.tb01057.x>.

MacLaren, M. (1931) 'Lake Bosumtwi, Ashanti', *The Geographical Journal*, 78(3), pp. 270–276. Available at: <https://doi.org/10.2307/1784899>.

Talbot, M.R. and Johannessen, T. (1992) 'A high resolution palaeoclimatic record for the last 27,500 years in tropical West Africa from the carbon and nitrogen isotopic composition of lacustrine organic matter', *Earth and Planetary Science Letters*, 110(1), pp. 23–37. Available at: [https://doi.org/10.1016/0012-821X\(92\)90036-U](https://doi.org/10.1016/0012-821X(92)90036-U).

200. The Barringer Meteorite Crater

Barringer, D.M. (1905) 'Coon Mountain and Its Crater', *Proceedings of the Academy of Natural Sciences of Philadelphia*, 57. Available at: <https://scholar.archive.org/work/mmostybzvffnl77cc4ibnrhpq>.

Chao, E.C.T., Shoemaker, E.M. and Madsen, B.M. (1960) 'First Natural Occurrence of Coesite', *Science*, 132(3421), pp. 220–222. Available at: <https://doi.org/10.1126/science.132.3421.220>.

Foote, A.E. (1891) 'A new locality for meteoric iron with a preliminary notice of the discovery of diamonds in the iron', *American Journal of Science*, s3-42(251), pp. 413–417. Available at: <a href="https

AUTHORS

I. HISTORY OF GEOSCIENCES

101. Arduino's lithostratigraphical sequence of the Agno Valley

Ezio Vaccari. *International Commission on the History of Geological Sciences (INHIGEO) / Università degli Studi dell'Insubria. Italy.*

102. Cavanisham Ferry and Llanstephan Quarries

Duncan Hawley. *History of Geology Group, Geological Society of London and INHIGEO. United Kingdom.*

103. Jurassic Coast: Lyme Regis

Jonathan Larwood. *Natural England. United Kingdom.*

104. Metamorphic Barrow Zones in Scottish Highlands

Owen Weller. *University of Cambridge. United Kingdom.*

Richard Palin. *University of Oxford. United Kingdom.*

Richard White. *University of St Andrews. United Kingdom.*

105. Contact metamorphic rocks of Orijärvi

Owen Weller. *University of Cambridge. United Kingdom.*

Richard White. *University of St Andrews. United Kingdom.*

Richard Palin. *University of Oxford. United Kingdom.*

106. Durbuy Anticline

Sophie Verheyden. *Royal Belgian Institute of Natural Sciences - RBINS.*

Serge Delaby. *UGGp Famenne-Ardenne, Belgium.*

Léon Dejonghe. *Royal Belgian Institute of Natural Sciences - RBINS.*

Xavier Devleeschouwer. *Royal Belgian Institute of Natural Sciences - RBINS.*

Michiel Dusar. *Royal Belgian Institute of Natural Sciences - RBINS.*

Robert Speijer. *KU Leuven, Belgium.*

107. Vesuvius volcano

Claudia Principe. *Istituto di Geoscienze e Georisorse, CNR, Pisa and INHIGEO - IUGS International Commission on the History of Geological Sciences. Italy.*

108. Scheibenberg lava flow

Martina Kölbl-Ebert. *International Commission on the History of Geological Sciences (INHIGEO) & Department of Earth and Environmental Sciences University of Munich, Germany.*

109. Montagne Pelée volcano

Nicolas CHARLES. *PhD – BRGM / French Geological Survey.*

110. Oligocene Laccoliths and Sedimentary Rock Domes of the Henry Mountains

Marie D. Jackson. *Department of Geology and Geophysics, University of Utah, USA.*

David D. Pollard. *Department of Earth and Planetary Sciences, Stanford University, USA.*

111. Marua Falls

Martina Kölbl-Ebert. *International Commission on the History of Geological Sciences (INHIGEO) & Department of Earth and Environmental Sciences University of Munich, Germany.*

112. Mer de Glace

Philip Deline. *Laboratoire EDYTEM, Université Savoie Mont Blanc – CNRS, Chambéry, France.*

Ludovic Ravanel. *Laboratoire EDYTEM, Université Savoie Mont Blanc – CNRS, Chambéry, France.*

113. Esmark Moraine and Otto Tank's Moraine

Geir Hestmark. *CEES, Department of Biosciences, University of Oslo and INHIGEO. Norway.*

114. The Parallel Roads of Glen Roy

John E. Gordon. *University of St Andrews, Scotland, UK.*

Adrian P. Palmer. *Royal Holloway University of London, England, UK.*

J. John Lowe. *Royal Holloway University of London, England, UK.*

Colin K. Ballantyne. *University of St Andrews, Scotland, UK.*

James Rose. *Royal Holloway University of London, England, UK.*

II. STRATIGRAPHY AND SEDIMENTOLOGY

115. The Mesoproterozoic Belt-Purcell Supergroup

Kylie Caesar. *National Park Service, Glacier National Park. USA.*

Tara Carolin. *National Park Service, Glacier National Park. USA.*

Teagan Tomlin. *National Park Service, Glacier National Park. USA.*

Richard Menicke. *National Park Service, Glacier National Park. USA.*

Locke Marshall. *Parks Canada, Waterton Lakes National Park. USA.*

116. The Ordovician section of the Hällekis Quarry

Per Ahlberg. *Lund University, Sweden.*

David A.T. Harper. *Department of Earth Sciences, Durham University, Durham, UK.*

Lars Holmer. *Uppsala University, Sweden.*

Anders Lindskog. *Lund University, Sweden.*

Birger Schmitz. *Lund University, Sweden.*

117. The Ordovician glacial pavements of the Tassili n'Ajjer

Ghienne Jean-François. *Institut Terre et Environnement de Strasbourg, France.*

Abdallah Hussein. *Alicante, Spain.*

Buoncristiani Jean-François. *Biogéosciences, Université de Bourgogne, France.*

Deschamps Rémi. *IFPEN, Rueil-Malmaison, France.*

Le Heron Daniel. *Department of Geology, Universität Wien, Austria.*

Moreau Julien. *NW Edge, Isle of Lewis, HS2 9AJ United Kingdom.*

118. Carboniferous evolution of The Burren and Cliffs of Moher

Eamon Doyle. *Burren and Cliffs of Moher UNESCO Global Geopark, Ireland.*

Clare Glanville. *Geoheritage Division, Geological Survey Ireland, Ireland.*

Patrick N. Wyse Jackson. *International Commission on the History of Geological Sciences (INHIGEO) & Trinity College Dublin, Ireland.*

David A.T. Harper. *Department of Earth Sciences, Durham University, Durham, UK.*

119. Permian reef complex of the Guadalupe Mountains

Charles Kerans. *University of Texas at Austin. USA.*

Lance L. Lambert. *University of Texas at San Antonio. USA.*

120. Latemar Triassic carbonate platform

Nereo Preto. *Department of Geosciences, University of Padova, Padova, Italy.*

121. End-Triassic Flood Basalts at the Old Wife

John H. Calder. *Cliffs of Fundy UGGp, Canadian Geoparks Network and Saint Mary's University, NS, Canada.*

122. The Jurassic Navajo Sandstone at Coyote Buttes and The Wave

Winston Seiler. *University of Utah. USA.*

Marjorie A. Chan. *University of Utah. USA.*

123. The Oligocene-Miocene molassic and rock pinnacles of Meteora

Nikolaos Zouros. *Director of the Natural History Museum of the Lesvos Petrified Forest, Professor in the Department of Geography, University of the Aegean. Greece.*

124. Pliocene cyclostratigraphy of Scala dei Turchi

Antonio Caruso. *Università degli studi di Palermo - Dipartimento di Scienze e Tecnologie Biologiche Chimiche e Farmaceutiche. Italy.*

125. Etosha Pan

Helke Mocke. *Geological Survey of Namibia, Namibia.*

Roy McG. Miller. *Consulting Geologist.*

Martin Hipondoka. *University of Namibia.*

Martin Pickford. *Muséum National d'Histoire Naturelle. France.*

Brigitte Senut. *Natural History Museum, Paris. France.*

Loïc Ségalen. *Sorbonne University, Paris. France.*

126. Pliocene to Holocene records from Raciška Pecina Cave

Nadja Zupan Hajna. *ZRC SAZU Karst Research Institute. Slovenia.*

Astrid Švara. *Karst Research Institute ZRC SAZU. Slovenia.*

127. Holocene coral reef terraces of Kikajima Island

Taro Komagoe. *KIKAI institute for Coral Reef Sciences. Japan.*

Atsuko Yamazaki. *Nagoya University /KIKAI institute for Coral Reef Sciences. Japan.*

Takayasu Amano. *Kikai Town Office. Japan.*

Rintaro Suzuki. *KIKAI institute for Coral Reef Sciences. Japan.*

Yoshitaka Uechi. *Kikai Town Office. Japan.*

Tsuyoshi Watanabe. *Hokkaido University / Research Institute for Humanity and Nature / KIKAI institute for Coral Reef Sciences. Japan.*

128. Shark Bay

Margaret Brocx. *Adjunct Professor of Research/College of Science, Health, Engineering and Education, Discipline Environmental and Conservation Sciences. Murdoch University, Western Australia, Australia.*

Vic Semeniuk. *Adjunct Professor of Research/College of Science, Health, Engineering and Education, Discipline Environmental and Conservation Sciences. Murdoch University, Western Australia, Australia.*

129. Uyuni salt flat

Wilfredo Ramos Collorana. *Universidad Mayor de San Andrés, Ingeniería Geológica, IGEMA. Bolivia.*

Nelson Roman Carvajal Velasco. *YLB. Bolivia.*

Luis Mario Jimenez Huanca. *Independiente. Bolivia.*

130. The Dead Sea

Amit G Reiss. *Rice University. USA.*

Uri Schatnner. *University of Haifa. Israel.*

Ran N Nof. *Geological Survey of Israel.*

Michael Lazar. *University of Haifa. Israel.*

Nurit Shtober-Zisu. *University of Haifa. Israel.*

Michal Rosenthal. *Israel Geological Society.*

Lior Kamhaji. *Israel Geological Society.*

Yoav Nahmias. *Geological Survey of Israel.*

131. Mars analog of Lake Salda

Nizamettin Kazancı. *Ankara University, Ankara, Turkey.*

Nurgül Balci. *Istanbul Technical University Geological Engineering Dept, Geomicrobiology & Biogeochemistry Laboratory, Istanbul, Türkiye.*

III. PALEONTOLOGY

132. Ediacaran fauna of the Nama Group

Helke Mocke. *Geological Survey of Namibia, Namibia.*

Rachel Wood. *University of Edinburgh, Scotland.*

Patricia Vickers-Rich. *Swinburne University of Technology, and Monash University, Australia.*

Ulf Linnemann. *Senckenberg Research Institute, Germany.*

Simon Darroch. *Senckenberg Institute and Museum of Natural History, Germany.*

Mike Hall. *Monash University, Australia.*

Guy M. Narbonne. *Department of Geological Sciences and Geological Engineering, Queen's University, Kingston, ON Canada.*

Alan Jay Kaufman. *University of Maryland, USA.*

Marc Laflamme. *University of Toronto, Canada.*

Alexander G. Liu. *University of Cambridge, United Kingdom.*

Fred Bowyer. *University of Edinburgh, Scotland.*

Mandy Zieger-Hofmann. *Senckenberg Research Institute, Germany.*

Karl-Heinz Hoffmann. *Private Consultant, Windhoek, Namibia.*

Gabi Schneider. *Namibia Uranium Institute, Namibia.*

Peter Swinkels. *Private Consultant, Australia.*

Kombada Mhopjeni. *Geological Survey of Namibia, Namibia.*

Freddy Muyamba. *Geological Survey of Namibia, Namibia.*

133. The Late Devonian fossil-fish Lagerstätte of Miguasha

Godfrey Nowlan. *Geological Survey of Canada (retired), Calgary, Alberta, Canada.*

Richard Cloutier. *Université du Québec à Rimouski, Canada.*

134. Permian vegetation of the Wuda Fossil Site

Jun Wang. *Nanjing Institute of Geology and Palaeontology, Chinese Academy of Sciences.*

Renbin Zhan. *Nanjing Institute of Geology and Palaeontology, Chinese Academy of Sciences.*

Hermann W. Pfefferkorn. *University of Pennsylvania, USA.*

135. Triassic Dinosaurs and mammalian reptiles from Ischigualasto

Carlos Nelson Dal Molin. *Geological and Mining Survey of Argentina (SEGEPLAN).*

Fernando Miranda. *Geological and Mining Survey of Argentina (SEGEPLAN).*

136. Middle Jurassic dinosaur footprints from the Serras de Aire and Candeeiros

Luís Lopes. *University of Évora / ICT-Earth Sciences Institute, Portugal.*

Artur Abreu Sá. *Department of Geology, University of Trás-os-Montes e Alto Douro, 5000-801 Vila Real, Portugal.*

Jorge Carvalho. *LNEG - National Laboratory of Energy and Geology, Portugal.*

Lia Mergulhão. *ICNF - Institute of Nature and Forest Conservation, Portugal.*

Mário Cachão. *University of Lisbon / IDL - Dom Luiz Institute, Portugal.*

António Galopim de Carvalho. *University of Lisbon, Portugal.*

137. Dashanpu Middle Jurassic Dinosaur Fossils Site

PENG Guanzhao. *Zigong Dinosaur Museum, China.*

YE Yong. *Zigong Dinosaur Museum, China.*

JIANG Shan. *Zigong Dinosaur Museum, China.*

LI Biao. *Zigong Dinosaur Museum, China.*

LI Yi. *Zigong Dinosaur Museum, China.*

WANG Wenwei. *The Management Center for Zigong UGGp, China.*

WANG Lingling. *The Management Center for Zigong UGGp, China.*

138. Upper Jurassic Carnegie Quarry Dinosaur Bone Site

Kenneth Carpenter. *University of Colorado Museum, Boulder, Colorado USA.*

John Foster. *Utah Field House of Natural History State Park Museum, Vernal, Utah USA.*

ReBecca Hunt-Foster. *National Park Service, Dinosaur National Monument, Jensen, Utah USA.*

139. Early Cretaceous wetland of Las Hoyas

Angela D. Buscalioni. *Universidad Autónoma de Madrid, Centro para la Integración en Paleobiología, Spain.*

Jesús Marugán-Lobón. *Universidad Autónoma de Madrid, Spain.*

Hugo Martín Abad. *Universidad Autónoma de Madrid, Spain.*

José Luis Sanz García. *Universidad Autónoma de Madrid, Real Academia de Ciencias, Spain.*

José Joaquín Moratalla. *Geological and Mining Institute of Spain (IGME, CSIC).*

Romain Vullo. *Université Rennes 1, France.*

Candela Blanco Moreno. *Universidad Autónoma de Madrid.*

Jerónimo López-Martínez. *Universidad Autónoma de Madrid, Spain.*

140. Cretaceous Lagerstätten of Cariri Stone

Maria Somália Sales Viana. *Federal University of Ceará, ProGEO, Brazil.*

Virginio Henrique de Miranda Lopes Neumann. *Federal University of Pernambuco, Brazil.*

Allysson Pontes Pinheiro. *Regional University of Cariri, Brazil.*

Maria Edenilce Peixoto Batista. *Regional University of Cariri, Brazil.*

Wellington Ferreira da Silva Filho. *Federal University of Ceará, Brazil.*

Olga Alcântara Barros. *Regional University of Cariri, Brazil.*

Maria da Glória Motta Garcia. *University of São Paulo, Brazil.*

141. The Cretaceous Dinosaur Nesting Grounds of the Willow Creek Anticline

John B. Scannella. *Museum of the Rockies and Department of Earth Sciences, Montana State University, USA.*

David J. Varricchio. *Department of Earth Sciences, Montana State University, USA.*

Lee E. Hall. *Museum of the Rockies, Montana State University, USA.*

Scott A. Williams. *Museum of the Rockies, Montana State University, USA.*

Holly N. Woodward. *Department of Anatomy and Cell Biology, Oklahoma State University Center for Health Sciences, USA.*

142. Whale Valley, Cetacea and Sirenia Eocene fossils of Wadi Al-Hita

Enas Abd Elhady Ahmed. *Faculty of Petroleum and Mining Science, University of Matrouh, Egypt.*

143. The La Venta middle Miocene neotropical biome

Marianela Vargas Anaya. *Servicio Geológico Colombiano.*

José Enrique Arenas. *Servicio Geológico Colombiano.*

Laura Mora Rojas. *Servicio Geológico Colombiano.*

Manuel Gómez Guerrero. *Servicio Geológico Colombiano.*

Luis Francisco Melo Rojas. *Servicio Geológico Colombiano.*

Victoria Elena Corredor Bohórquez. *Servicio Geológico Colombiano.*

Catalina Suárez Gómez. *Instituto Argentino de Nivología, Glaciología y Ciencias Ambientales (IANIGLA).*

Carlos Jaramillo. *Smithsonian Tropical Research Institute, USA.*

Edwin Cadena. *Universidad del Rosario, Colombia.*

Susana Salazar Jaramillo. *Universidad Nacional de Colombia.*

144. The modern human fossils of the Kibish Formation

Afawossen Asrat. *Botswana International University of Science and Technology, Palapye, Botswana.*

145. The Human Footprints of Acahuilinca

Everling Espinoza. *Dirección de Vulcanología, Dirección General de Geología y Geofísica - INETER, Instituto Nicaragüense de Estudios Territoriales, Managua, Nicaragua.*

William Martinez. *INETER, Instituto Nicaragüense de Estudios Territoriales, Managua, Nicaragua.*

Benjamin van Wyk de Vries. *Université Clermont Auvergne, Laboratoire Magmas et Volcans, OPGC, CNRS et IRD, Clermont Ferrand, France.*

IV. IGNEOUS AND METAMORPHIC PETROLOGY

146. The larvikite plutonic rocks of the Oslo Rift

Tom Heldal. *Scientist, Geological Survey of Norway.*

Kristin Rangnes. *General manager/Geologist, Gea Norvegica UNESCO Global Geopark, Norway.*

147. The Rum Igneous Complex

James Day. *Scripps Institution of Oceanography, University of California San Diego, USA.*

Michele Lustrino. *Sapienza Università di Roma, Italy.*

Sebastian Tappe. *Arctic University of Norway.*

Roger Mitchell. *Lakehead University, Thunder Bay, Ontario, Canada.*

Georg Zellmer. *Massey University, Palmerston North, New Zealand.*

Andrew Kerr. *Department of Earth Sciences, Memorial University, St. John's NL Canada.*

Monica Heilbron. *Universidade do Estado do Rio de Janeiro, Brazil.*

James Natland. *University of Miami, USA.*

Alexei Ivanov. *Institute of the Earth's Crust, Siberian Branch of the Russian Academy of Sciences, Irkutsk, Russia.*

Rajesh Kumar Srivastava. *Baranasi Hindu University, Varanasi, India.*

Barbara Scott Smith. *Scott-Smith Petrology Inc., Vancouver, Canada.*

Mitsuhiro Nakagawa. *Hokkaido University, Japan.*

Zhengfu Guo. *Chinese Academy of Science, Beijing, China.*

Anna Doroshkevich. *Sobolev Institute of Geology and Mineralogy, Siberian Branch of the Russian Academy of Sciences Novosibirsk, Russia.*

Marjorie Wilson. *Leeds University, UK.*

Bernard Bonin. *Université Paris-Sud, Orsay Cedex, France.*

Julian Pearce. *Cardiff University, UK.*

148. Devils Tower

Richard Stoffle. *University of Arizona, USA.*

Kathleen van Vlack. *Northern Arizona University, USA.*

Vic Semeniuk. *Adjunct Professor of Research/College of Science, Health, Engineering and Education, Discipline Environmental and Conservation Sciences, Murdoch University, Western Australia, Australia.*

Margaret Brocx. *Adjunct Professor of Research/College of Science, Health, Engineering and Education, Discipline Environmental and Conservation Sciences, Murdoch University, Western Australia, Australia.*

149. The Mohorovicic discontinuity in the Ivrea-Verbano Zone

Paolo Falletti. *ARPA Piemonte, Biella, Italy.*

150. The Cambrian Leka Ophiolite

Bergliot Kulsrud Storruste. *Trollfjell UNESCO Global Geopark, Norway.*

Rolf Birger Pedersen. *University of Bergen, Norway.*

Tom Heldal. *Scientist, Geological Survey of Norway.*

151. Late Cretaceous Samail Ophiolite

Andreas Scharf. *Department of Earth Sciences, Sultan Qaboos University, Sultanate of Oman.*

Frank Mattern. *14532 Stahnsdorf, Germany.*

Bernhard Pracejus. *04887 Lúcar (prov. Almería), Spain.*

152. Lower Pillow Lava of Troodos Ophiolite

Efthymios Tsialakis. *Geological Survey Department, Cyprus.*
 Christodoulos Hadjigeorgiou. *Geological Survey Department, Cyprus.*
 Vasilis Symeou. *Geological Survey Department, Cyprus.*

153. The ultrahigh-pressure unit of the Dora-Maira Massif

Hans-Peter Schertl. *Ruhr-University Bochum, Germany.*
 Christian Chopin. *Ecole Normale Supérieure de Paris - CNRS -PSL, France.*

V. VOLCANOLOGY**154. Deccan Traps**

Hetu Sheth. *Indian Institute of Technology Bombay.*
 Satish C. Tripathi. *The Society of Earth Scientists, Lucknow, India.*

155. Muriwai megapillow lava flows

Bruce W Hayward. *Geoscience Society of New Zealand.*

156. The Pleistocene Al Wahbah dry maar crater

Mohammed Rashad Moufti. *King Abdulaziz University, Jeddah, Kingdom of Saudi Arabia.*
 Károly Németh. *Saudi Geological Survey, Kingdom of Saudi Arabia.*

157. El Laco iron lavas

José Antonio Naranjo. *Servicio Nacional de Geología y Minería, Chile.*
 Fernando Henríquez. *Departamento de Ingeniería en Minas, Universidad de Santiago de Chile.*
 Jan Olov Nyström. *Swedish Museum of Natural History, Stockholm, Sweden.*
 Richard Naslund. *Department of Geological Sciences, SUNY, Binghamton, USA.*

158. Ngorongoro Crater

Ramadhani Khatibu. *Senior Geologist/Ngorongoro Lengai UGGp/ Ngorongoro Conservation Area Authority, Tanzania.*
 Lightness S. Kyambile. *Cultural Heritage Officer/Ngorongoro Lengai UGGp/ Ngorongoro Conservation Area Authority, Tanzania.*

159. Ruapehu Volcano

Jonathan Procter. *Massey University, New Zealand.*
 Gabor Keresztsuri. *Massey University, New Zealand.*
 Anke Zernack. *Massey University, New Zealand.*
 Károly Németh. *Saudi Geological Survey, Kingdom of Saudi Arabia.*
 Gert Lube. *Massey University, New Zealand.*

160. Parícutin Volcano

Dante Jaime Morán-Zenteno. *Institute of Geology, Universidad Nacional Autónoma de México.*
 Barbara Martiny. *Institute of Geology, Universidad Nacional Autónoma de México.*

Marie-Noelle Guibaud. *Institute of Geophysics, Universidad Nacional Autónoma de México.*

Lucero Morelos Rodríguez. *Instituto de Geología, Universidad Nacional Autónoma de México.*

Laura Luna González. *Institute of Geology, Universidad Nacional Autónoma de México.*

Hermes Martín García Rodríguez. *School of Engineering, Universidad Nacional Autónoma de México.*

Claus Siebe. *Institute of Geophysics, Universidad Nacional Autónoma de México.*

Denis Ramón Avellán López. *Institute of Geophysics, Universidad Nacional Autónoma de México.*

Guillermo Cisneros Máximo. *Institute of Geophysics, Universidad Nacional Autónoma de México.*

161. Heisei Shinzan Lava Dome

Setsuya Nakada. *The University of Tokyo (presently NIED), Japan.*
 Marekazu Ohno. *Unzen Volcanic Area UNESCO Global Geopark (presently, Mt. Chokai & Tobishima Island National Geopark), Japan.*

162. The Active Hunga Volcano

Taaniela Kula. *Ministry of Lands, Survey, Planning and Natural Resources, Kingdom of Tonga.*

Shane Cronin. *University of Auckland, New Zealand.*

Gary Lee. *The Pacific Community (SPC), Fiji.*

James Garvin. *NASA (Goddard Space Flight Center), USA.*

Paul Taylor. *Australian Volcanological Investigations, Australia.*

Mike Williams. *National Institute of Water and Atmospheric Research (NIWA), New Zealand.*

Károly Németh. *Saudi Geological Survey, Kingdom of Saudi Arabia.*

Sung-Hyun Park. *Korea Polar Research Institute, Korea.*

Isobel Yeo. *National Oceanography Centre Southampton, UK.*

Mike Clare. *National Oceanography Centre Southampton, UK.*

Emily Lane. *National Institute of Water and Atmospheric Research (NIWA), New Zealand.*

Sarah Seabrook. *National Institute of Water and Atmospheric Research (NIWA), New Zealand.*

163. Rotorua's geothermal fields (Ahi-Tupua)

Bruce W Hayward. *Geoscience Society of New Zealand.*

Brad J. Scott. *GNZ Science, Wairakei, New Zealand.*

VI. TECTONICS**164. The Mid-Atlantic ridge on Reykjanes**

Robert A. Askew. *Icelandic Institute of Natural History.*
 Lovísa Ásbjörnsdóttir. *Icelandic Institute of Natural History.*
 Ingvar Atlí Sigurðsson. *Icelandic Institute of Natural History.*

165. The evolution of the Andes in Colca Canyon

Bilverto Zavala Carrión. *Instituto Geológico Minero y Metalúrgico - INGEMMET, Perú.*
 Carlos Benavente Escobar. *Instituto Geológico Minero y Metalúrgico, Perú.*
 Igor Astete Farfán. *Instituto Geológico Minero y Metalúrgico - INGEMMET, Perú.*

166. Salt domes and glaciers of the Zagros Fold and Thrust Belt

Mohammad R. Ghassemi. *Research Institute of Earth Sciences, Geological Survey of Iran.*
 Jafar Omrani. *Deputy of Geology, Geological Survey of Iran.*

Alireza Amirkazemi. *Director of Qeshm Island UNESCO Global Geopark & Member of the Scientific Committee of Lut Desert World Heritage Base, Iran.*

167. The Patos Shear Zone

Carolina Cavalcante. *Departamento de Geología, Universidad Federal do Paraná, Av. Cel. Francisco Heráclito dos Santos, 100, Centro Politécnico, Curitiba (PR), 81531-980, Brazil.*

Haakon Fossen. *Museum of Natural History/Department of Earth Science, University of Bergen, Allégaten 41, 5007 Bergen, Norway.*

168. Esla Unit thrust system

Manuel Ignacio de Paz Álvarez. *Departamento de Geología, Universidad de Oviedo, C/ Jesús Arias de Velasco s/n, 33005 Oviedo, Spain.*
 Juan Luis Alonso. *Departamento de Geología, Universidad de Oviedo, C/ Jesús Arias de Velasco s/n, 33005 Oviedo, Spain.*
 Sergio Llana Fúnez. *Departamento de Geología, Universidad de Oviedo, C/ Jesús Arias de Velasco s/n, 33005 Oviedo, Spain.*
 María Luisa Arboleja. *Departamento de Geología, Universitat Autònoma de Barcelona, 08193, Bellaterra, Barcelona, Spain.*

Thomas G. Blenkinsop. *School of Earth and Environmental Sciences, Cardiff University, Main Building, Park Place, CF10 3AT, Cardiff, UK.*

Ernest Rutter. *Department of Earth and Environmental Sciences, University of Manchester, 5 Manchester M13 9PL, UK.*

David Buchs. *School of Earth & Environmental Sciences, Cardiff University, Cardiff, CF10 3AT, UK.*

Lesley Cherns. *School of Earth and Environmental Sciences, Cardiff University, Main Building, Park Place, CF10 3AT, Cardiff, UK.*

Adriana Georgina Flórez Rodríguez. *Departamento de Geología, Universidad de Oviedo, C/ Jesús Arias de Velasco s/n, 33005 Oviedo, Spain.*

169. Glarus Thrust

Thomas Buckingham. *UNESCO-World Heritage Swiss Tectonic Arena Sardona, Switzerland.*
 Adrian O. Pfiffner. *Professor Emeritus at Universität Bern, Switzerland.*

170. Monte Perdido massif tectonic structure

Ruth Soto Marín. *Geological and Mining Institute of Spain (IGME, CSIC).*
 Oriol Oms Llobet. *Universitat Autònoma de Barcelona, Spain.*
 Ánchel Belmonte Ribas. *Sobrarbe-Pirineos UNESCO Global Geopark, Spain.*

171. Brittle structures of the Somerset Coast

David Peacock. *University of Göttingen, Germany.*

172. Surface faulting of a seismic sequence in Mt. Vettore

Elisa Brustia. *ISPRA-Italian Geological Survey, Rome, Italy.*
 M. Cristina Giovagnoli. *ISPRA-Italian Geological Survey, Rome, Italy.*
 Roberto Pompili. *ISPRA-Italian Geological Survey, Rome, Italy.*
 Paolo Primerano. *ISPRA-Italian Geological Survey, Rome, Italy.*

173. Alpine superposed buckle folds in Aliaga

José Luis Simón Gómez. *Department of Earth Sciences, Zaragoza University, Spain.*
 Luis Alcalá Martínez. *Parque de las Ciencias de Andalucía, Granada, Spain.*

174. Marine terraces of San Juan de Marcona

Carlos Benavente Escobar. *Instituto Geológico Minero y Metalúrgico - INGEMMET, Perú.*
 Bilverto Zavala Carrión. *Instituto Geológico Minero y Metalúrgico - INGEMMET, Perú.*
 Igor Astete Farfán. *Instituto Geológico Minero y Metalúrgico - INGEMMET, Perú.*
 Laurence Audin. *Instituto de Investigación para el Desarrollo - IRD, Perú.*
 Marianne Saillard. *Instituto de Investigación para el Desarrollo - IRD, Perú.*

VII. MINERALOGY**175. The Sar-e-Sang Lapis Lazuli Deposit**

Hans-Peter Schertl. *Ruhr-University Bochum, Germany.*
 Andreas Massanek. *TU Bergakademie Freiberg, Germany.*

176. The Kalahari Manganese Field

Bruce Cairncross. *University of Johannesburg, South Africa.*
 Craig Smith. *Geological Society of South Africa.*

Deshenthree Chetty. *Mintek, South Africa.*

Petra Dinham. *Mineralogical Association of South Africa (MINSA).*

177. The Broken Hill Pb-Zn-Ag deposit

William Birch. *Museums Victoria, Australia.*

178. Mineral site of Mont Saint-Hilaire

Robert A. Gault. *Research Associate (retired), Canada.*

László Hórvath.

179. The Muzo emerald deposit

Gaston Giuliani. *Université Paul Sabatier, GET/IRD and Université de Lorraine, France.*

VIII. GEOMORPHOLOGY AND ACTIVE GEOLOGICAL PROCESS

180. Granite landforms of Dartmoor

Piotr Migoń. *Institute of Geography and Regional Development, University of Wrocław, Wrocław, Poland.*

181. Inverted landscape of a Plio-Pleistocene phreatomagmatic monogenetic volcanic field in the Bakony-Balaton Upland

Barnabás Korbély. *Bakony-Balaton Geopark Group, Balaton Uplands National Park Directorate, Csopak, Hungary.*

Károly Németh. *Saudi Geological Survey, Kingdom of Saudi Arabia.*

182. Great Salt Lake

Marjorie A. Chan. *University of Utah, USA.*

Charles G. Oviatt. *Kansas State University, USA.*

Basil Tikoff. *University of Wisconsin, USA.*

Bonnie K. Baxter. *Westminster College, UK.*

Genevieve Atwood. *Earth Science Education.*

183. Mackenzie Delta

Zbigniew Zwoliński. *Institute of Geoeocology and Geoinformation, Adam Mickiewicz University in Poznań, Poland.*

184. Getbol Tidal Flats

Kyung Sik, Woo. *Kangwon National University, South Korea.*

Seung Soo, Chun. *Jeonnam National University, South Korea.*

Kyong O, Moon. *World Heritage Promotion Team of Korean Tidal Flats, South Korea.*

185. Fontaine de Vaucluse

Zoran Stevanovic. *(Past-Chair) The Karst Commission of the International Association of Hydrogeologists, Univ. Belgrade, Serbia.*

Michel Bakalowicz. *The Karst Commission of the International Association of Hydrogeologists, BRGM, France.*

Hervé Jourde. *The Karst Commission of the International Association of Hydrogeologists, Univ. Montpellier, France.*

Jacques Mudry. *The Karst Commission of the International Association of Hydrogeologists, Univ. Besançon, France.*

Naomi Mazzilli. *Univ. Avignon, France.*

Christophe Emblanch. *Univ. Avignon, France.*

186. Wakulla spring

Zoran Stevanovic. *(Past-Chair) The Karst Commission of the International Association of Hydrogeologists, Univ. Belgrade, Serbia.*

Neven Kresic. *(Past Co-Chair) The Karst Commission of the International Association of Hydrogeologists.*

187. Vrelo Bune Spring

Zoran Stevanovic. *(Past-Chair) The Karst Commission of the International Association of Hydrogeologists, Univ. Belgrade, Serbia.*

Petar Milanovic. *The Karst Commission of the International Association of Hydrogeologists.*

Ferid Skopljak. *Federal Geological Survey, Sarajevo, Bosnia & Herzegovina.*

188. Mammoth Cave

Chris Groves. *Crawford Hydrology Laboratory, Western Kentucky University, Bowling Green Kentucky, USA.*

Zhong Liang. *International Research Centre on Karst under the auspices of UNESCO, Guilin, China.*

Rick Toomey. *Mammoth Cave National Park, Mammoth Cave, Kentucky, USA.*

Luo Qukan. *International Research Center on Karst under the auspices of UNESCO, Guilin, China.*

189. The White Limestone Karst of Cockpit Country

Simon F. Mitchell. *University of the West Indies, Mona, Kingston, Jamaica.*

Sherene James-Williamson. *University of the West Indies, Mona, Kingston, Jamaica.*

David Miller. *University of the West Indies, Jamaica.*

190. Guilin Karst

Zhong Liang. *International Research Centre on Karst under the auspices of UNESCO, Guilin, China.*

Zhang Yuanhai. *International Research Centre on Karst under the auspices of UNESCO, Guilin, China.*

Chen Weihai. *International Research Centre on Karst under the auspices of UNESCO, Guilin, China.*

191. Ha Long Bay-Cat Ba Archipelago

Tran Tan Van. *Vietnam Institute of Geosciences and Mineral Resources.*

Do Thi Yen Ngoc. *Vietnam Institute of Geosciences and Mineral Resources.*

Pham Thi Thuy. *Vietnam Institute of Geosciences and Mineral Resources.*

Tran Duc Thanh. *Institute of Marine Environment and Resources, Vietnam.*

Tran Van Tri. *Vietnam Union of Geological Sciences.*

Vu Kien Cuong. *Ha Long Bay Management Department, Vietnam.*

192. Tepuis and quartzite karst of Gran Sabana

Piotr Migoń. *Institute of Geography and Regional Development, University of Wrocław, Wrocław, Poland.*

Francesco Sauro. *Italian Institute of Speleology, University of Bologna, Italy.*

193. Fjords and towering sea cliffs of Fiordland

Bruce W Hayward. *Geoscience Society of New Zealand.*

Jill A Kenny. *Geoheritage Subcommittee, Geoscience Society of New Zealand.*

194. Fjords and glaciers in Hornsund and Van Mijenfjorden, Svalbard

Piotr Migoń. *Institute of Geography and Regional Development, University of Wrocław, Wrocław, Poland.*

Zbigniew Zwoliński. *Institute of Geoeocology and Geoinformation, Adam Mickiewicz University in Poznań, Poland.*

Lars Erikstad. *ProGEO, Norway.*

Astrid Lyså. *Geological Survey of Norway.*

195. Vatnajökull

Zbigniew Zwoliński. *Institute of Geoeocology and Geoinformation, Adam Mickiewicz University in Poznań, Poland.*

Małgorzata Mazurek. *Institute of Geoeocology and Geoinformation, Adam Mickiewicz University, Poznań, Poland.*

196. Yosemite Valley

Piotr Migoń. *Institute of Geography and Regional Development, University of Wrocław, Wrocław, Poland.*

Olav Slaymaker. *Department of Geography, University of British Columbia, Vancouver, Canada.*

IX. IMPACT STRUCTURES AND EXTRATERRESTRIAL ROCKS

197. Vredefort Dome

W. Uwe Reimold. *University of Brasília, Brazil.*

Roger L. Gibson. *University of the Witwatersrand, Johannesburg, South Africa.*

198. Ries Crater

Georg Loth. *Bavarian Environment Agency (LfU), Department Geological Survey, 95030 Hof, Germany.*

Dieter Stöfler (+). *former: Natural History Museum, Berlin, Germany.*

Heike Burkhardt. *UNESCO Global Geopark Ries, Donauwörth, Germany.*

Gisela Pösges. *UNESCO Global Geopark Ries, Donauwörth, Germany.*

Günther Zwerger. *UNESCO Global Geopark Ries, Donauwörth, Germany.*

Cindy Cooper. *Freelance translator.*

Fabian Weiß. *UNESCO Global Geopark Ries, Donauwörth, Germany.*

Dietmar Jung. *Bavarian Environment Agency (LfU), Department Geological Survey, Hof, Germany.*

Heinz-Gerd Röhling. *German Geological Society (DGGV), Germany.*

Marie-Luise Frey. *Welterbe Grube Messel gGmbH, Rossdörferstr. 108, 64409 Messel, www.grube-messel.de, Germany.*

199. Lake Bosumtwi Impact Crater

Christian Koeberl. *University of Vienna, Austria.*

Aaron Cavosie. *Curtin University, Australia.*

David Baratoux. *Research Institute for Development, Geosciences Environment, Toulouse, France.*

Daniel Kwadwo Asiedu. *University of Ghana.*

Marian Selorm Sapah. *University of Ghana.*

Yvonne Sena Akosua Loh. *University of Ghana.*

Daniel Kwaku Boamah. *Ghana Institution of Geoscientists.*

Prosper Mackenzie Nude. *University of Ghana.*

Samuel Boakye Dampare. *Ghana Atomic Energy Commission.*

Emmanuel Atuobi Agyekum. *Ghana Institution of Geoscientists.*

200. The Barringer Meteorite Crater

Gordon Osinski. *University of Western Ontario, Canada.*

Aaron Cavosie. *Curtin University, Australia.*

Drew Barringer. *Barringer Crater Company, USA.*

Alexandra Hart. *Barringer Crater Company, USA.*

Matt Kent. *Meteor Crater Enterprises, USA.*

Christian Koeberl. *University of Vienna, Austria.*

Jennifer Wadsworth. *Barringer Crater Company, USA.*

Thank you

The IUGS wants to express its most sincere gratitude to all participants and authors that have contributed to this unique announcement.

IUGS recognition identifies these sites as being of the highest scientific value. They are sites that served to develop the science of geology. They are the world's best demonstrations of geologic features and processes. They are the sites of fabulous discoveries of the Earth and its history. Recognition and visibility of the "Second 100" IUGS Geological Heritage Sites can lead to their further appreciation, to their use as educational resources, and, most importantly, to their preservation.

Please, do not hesitate to contact us in case you see any error or misspelling. We will be happy to improve future editions.

Contact: iugs.globalgeosites@igme.es